MINERALOGICAL SOCIETY OF POLAND

Vol. 28, 2006

MINERALOGIA POLONICA

Special Papers

Geochemical
Mineralogical
Petrological
Research

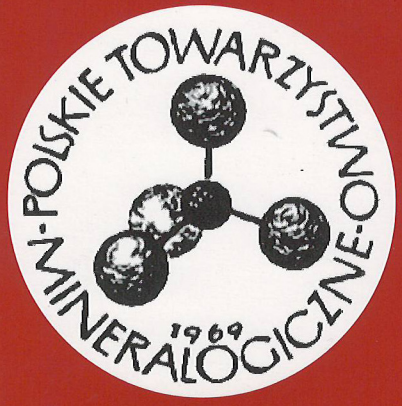

MINERALOGIA POLONICA
SPECIAL PAPERS
Volume 28, 2006

1st Central European Mineralogical Conference

Extended Abstracts

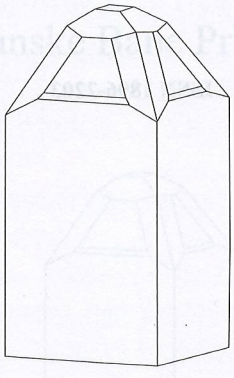

Vyšná Boca, Slovak Republic, 12-14 September 2006

Mineralogia Polonica – Special Papers - continuation of *Polskie Towarzystwo Mineralogiczne – Prace Specjalne*

Editor of the series: Jacek Puziewicz (University of Wrocław, Institute of Geological Sciences, 50-204 Wrocław, Pl. M. Borna 9; e-mail jpuz@ing.uni.wroc.pl)

Editors of Volume 28:
Daniel OZDÍN & Pavel UHER (Faculty of Natural Sciences, Comenius University, Mlynská dolina, 84215 Bratislava, Slovak Republic)

ISSN 1896-2203

Wydawnictwo Naukowe „Akapit", Kraków
tel./fax 608 024 572 / (012) 280-71-51; www.akapit.krakow.pl
e-mail: wn@akapit.krakow.pl

1st Central European Mineralogical Conference

organised by

Faculty of Natural Science, Comenius University, Bratislava

Slovak Geological Society

Mineralogical Society of Poland

Czech Geological Society

Geological Institute, Slovak Academy of Sciences, Bratislava

State Geological Institute of Dionýz Štúr, Bratislava

Hornonitrianske Bane Prievidza, Ltd.

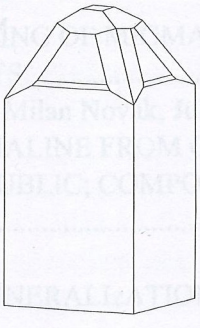

Vyšná Boca, Slovak Republic, 12-14 September 2006

Organising Committee:

Daniel OZDÍN, PhD. – Department of Mineralogy and Petrology, Faculty of Natural Science, Comenius University, Bratislava, Slovak Republic

Assoc. Prof. Pavel UHER, PhD. – Department of Mineral Deposits, Faculty of Natural Science, Comenius University, Bratislava, Slovak Republic

Juraj MAJZLAN, PhD. – Institute of Mineralogy and Geochemistry, Albert-Ludwig-University, Freiburg, Germany

Scientific Guarantees of Conference:

Prof. Emil MAKOVICKÝ, Copenhagen University
Prof. Martin CHOVAN, Comenius University, Bratislava
Prof. Milan NOVÁK, Masaryk University, Brno
Assoc. Prof. Adam PIECZKA, AGH – University of Science and Technology, Kraków
Dr. Jiří SEJKORA, National Museum, Praha
Dr. Igor BROSKA, Geological Institute, Slovak Academy of Sciences, Bratislava

Reviewers of extended abstracts submitted to Volume 28:

Peter ANDRÁŠ
Igor BROSKA
Jiří ČEJKA
Miloš GREGOR
Juraj MAJZLAN
Daniel OZDÍN
Jaroslav PRŠEK
Pavel UHER
Marián URBAN

CONTENTS

MINERALOGIA POLONICA - SPECIAL PAPERS
Volume 28 - 2006

Peter BAČÍK[1], Daniel OZDÍN[2,3], Pavel UHER[1], František BAKOS[3], Jarmila LUPTÁKOVÁ[4]

CHEMICAL COMPOSITION OF TOURMALINES FROM HYDROTHERMAL VEINS IN METAMORPHIC ROCKS OF TATRIC AND VEPORIC CRYSTALLINE BASEMENT OF THE WESTERN CARPATHIANS

INTRODUCTION

Tourmaline group minerals (TGM) occur in hydrothermal veins from several localities in Western Carpathians. The veins, commonly brecciated, occur in gneisses and phyllites, they are usually <50 cm thick. We studied occurrences in Tatric Unit: Brezno - Koleso (BK); Jasenie - Soviansko (JS); Čavoj (CA); Jamnická dolina (JD) and Jamnické plesá (JP); as well as localities from Veporic Unit: Ľubietová - Predsvätodušná (LP); Ľubietová - Včelínec (LV), Hnúšťa - Mútnik (HM) and Jedľové Kostoľany (JK). TGM are part of alpine-type assemblage stage present in carbonate veins (mainly siderite, besides magnesite in Hnúšťa, Mútnik) of Cretaceous age. TGM associate with albite, muscovite, chamosite, clinochlore, quartz and accessory monazite-(Ce), xenotime-(Y), fluorapatite, rutile and zircon.

METHODS

Chemical composition of tourmalines was analyzed on CAMECA SX100 electron-microprobe in WDS mode (Dionýz Štúr State Geological Institute, Bratislava), under following conditions: accelerating voltage 15 kV, current 20 nA, diameter beam 2 to 5 μm.

RESULTS AND DISCUSSION

TGM show schorl to dravite compositions, characteristic for each studied locality (Fig. 1).

Contents of *X*-site cations are strongly influenced by chemical attributes of surrounding rocks. Content of ^{X}Ca is just below 0.5 apfu for dravite in samples from magnesite-talc deposit in Hnúšťa, Mútnik (Uher et al. 2002). Content of ^{X}Ca in remaining samples is usually below 0.1 apfu. There is notable correlation between *X*-site vacancy amount and Fe/Mg ratios. Proportion of *X*-site vacancy

[1] *Comenius University, Faculty of Natural Sciences, Department of Geology of Mineral Deposits, Mlynská dolina, 842 15 Bratislava, Slovak Republic; bacikp@fns.uniba.sk*
[2] *Comenius University, Faculty of Natural Sciences, Department of Mineralogy and Petrology, Mlynská dolina, 842 15 Bratislava, Slovak Republic*
[3] *State Geological Institute of Dionýz Štúr, Mlynská dolina 1, 817 04 Bratislava, Slovak Republic*
[4] *Geological Institute of Slovak Academy of Sciences, Severná 5, 974 01 Banská Bystrica, Slovak Republic*

may decrease with increasing temperature and pressure (Henry, Dutrow 1996). Also Fe/Mg ratio in tourmaline, which decreases with increasing temperature, could indicate P-T conditions (Henry, Guidotti 1985), but it can be also affected by chemical properties of the adjacent mineral association and the host rock.

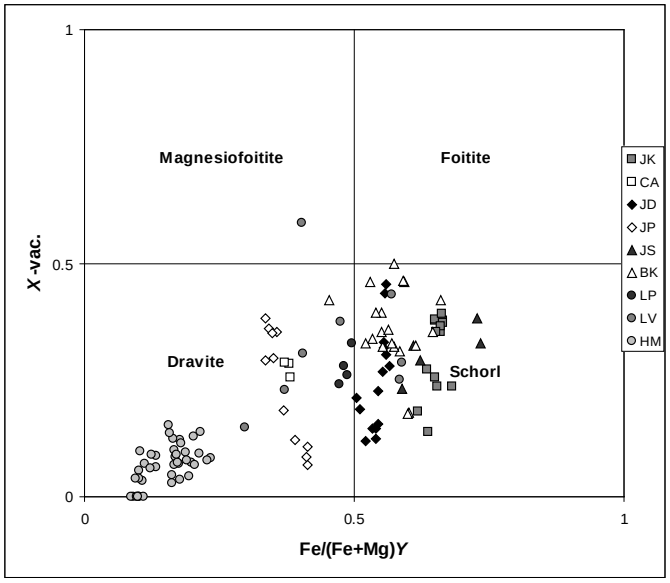

Fig. 1. *X*-site vacancy vs. Fe/Mg ratio in *Y*-site diagram of the studied tourmaline group minerals.

Y-site is dominantly occupied by Fe and Mg, which is characteristic for hydrothermal TGM. The majority of studied TGM show Fe-rich dravite to Mg-rich schorl compositions (Fig. 1). Fe/Mg ratio is probably related to chemical composition of source fluids. There could be possible comparison to the host carbonate vein filling; Fe-rich members occur in siderite veins, whereas dravite with the highest Mg contents was found in the Hnúšťa, Mútnik magnesite-talc deposit.

TGM composition is influenced by several cation and anion substitutions. In brief description, uvite, alkali-deficient and proton-deficient along with Fe-Mg substitution are the most important trends with the strongest impact on tourmaline crystal chemistry (Trumbull, Chaussidon 1999). The major trend for hydrothermal tourmalines from studied samples is alkali-deficient locally verging to proton-deficient substitution (Fig. 2). Trend of proton-deficient substitution could indicate presence of ferric iron in schorl. There are exceptional trends in Hnúšťa, Mútnik and Koleso TGM with trend to uvite substitution.

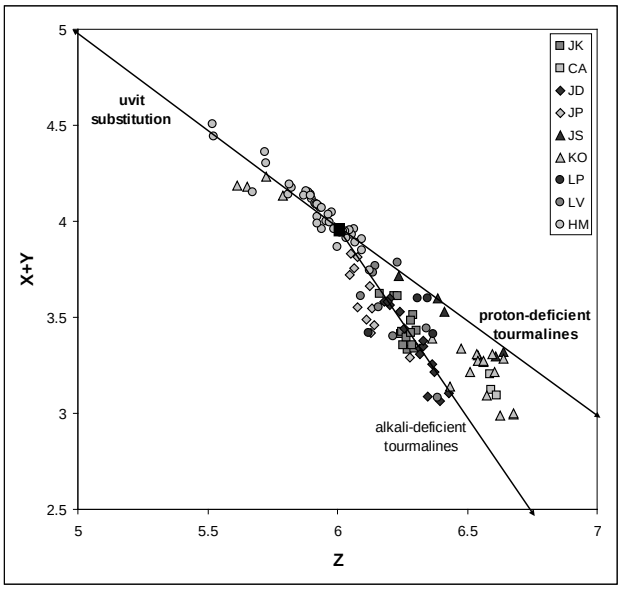

Fig. 2: (X+Y) vs. Z diagram where Z = Al + 1.33 Ti; X = Ca + Na; Y = Fe + Mg + Mn. Vectors represents common substitution trends in TGM (Trumbull, Chaussidon 1999).

CONCLUSIONS

Chemical composition of hydrothermal TGM from studied occurrences varies in range of schorl-dravite series. Fe/Mg and Ca/Na in TGM ratios similarly as in the host carbonate (siderite or magnesite) strongly depend on chemical composition of source fluids on the each locality, whereas proportion of *X*-site vacancy probably depends also on the temperature of TGM origin.

REFERENCES

HENRY D.J., DUTROW B.L., 1996: Metamorphic tourmaline and its petrologic applications. In: Grew E. S., Anowitz L. M. (eds.): Boron. Mineralogy, petrology and geochemistry. Rev. Mineral., 33: 503-557.

HENRY D.J., GUIDOTTI C.V., 1985: Tourmaline as a petrogenetic idicator mineral: an example from the staurolite-grade metapelites of NW Maine. Am. Mineral., 70: 1-15.

TRUMBULL R.B., CHAUSSIDON M., 1999: Chemical and boron isotopic composition of magmatic and hydrothermal tourmalines from the Sinceni granite-pegmatite system in Swaziland. Chem. Geol., 153: 125-137.

UHER P., JANÁK M., OZDÍN D., 2002: Calcian dravite from metacarbonate rocks of the Mútnik magnesite-talc deposit, Hnúšťa, Slovakia. N. Jb. Miner. Mh., 2: 68-84.

MINERALOGIA POLONICA - SPECIAL PAPERS
Volume 28 - 2006

Tomasz BAJDA[1], Maciej MANECKI[1], Ewelina SZMIT[1], Justyna FLIS[1]

THERMODYNAMIC STABILITY OF MIMETITE $Pb_5(AsO_4)_3Cl$ AT 5-35°C

INTRODUCTION

A remediation method for As removal from polluted waste waters and soils by inducing precipitation of crystalline mimetite was proposed by Comba (1987). However, the changes in temperature and pH of percolating solutions might significantly influence the stability of formatting solid phases. Therefore, accurate values for solubility of mimetite at different temperatures are necessary. Though thermodynamic data for this mineral are established, almost no experimental results for its solubility are recorded in the literature (see for example Bajda et al., 2005). The purpose of this study was to measure the solubility of mimetite at the temperatures ranging from 5 °C to 35 °C and initial pH=2, the conditions potentially similar to ones in contaminated soils or waste waters.

METHODS

To synthesize 13 g of mimetite, 8.33 g $Na_2HAsO_4 \cdot 7H_2O$, 20.63 g $Pb(NO_3)_2$ and 0.52 g NaCl were weighted to separate 500 cm^3 beakers and diluted in 300 cm^3 of redistill water at 20 °C. With the use of peristaltic pump, solutions were gradually mixed into large 3 dm^3 beaker filled with 1.5 dm^3 of continuously stirred redistill water at 20 °C. After the solutions were exhausted, suspension was left still for aging for 24 hours, decanted, filtered, washed with redistill water until no Cl^- was detected, and washed three times with acetone.

This synthesis results in the formation of fine white precipitate. The precipitate was examined with X-ray diffraction, scanning microscopy SEM/EDS, and infra-red spectroscopy FTIR (data not shown). The only crystalline phase identified within the detection limits of methods used was mimetite $Pb_5(AsO_4)_3Cl$.

The dissolution experiments were carried out at 5±1 °C, 20±1 °C, and 35±1 °C at initial pH value of 2.0±0.05 adjusted with 0.1 M HNO_3 and 0.1 M NaOH. A weight of 500±10 mg of dry mimetite was added to 0.5 dm^3 polypropylene bottles filled with the solution of pH=2. 10 cm^3 of solution was syringe sampled periodically for up to 2 months and analyzed for Pb, As, and pH. Cl was analyzed only in equilibrium solutions. Pb was determined with AAS, As with the use of colorimetry (molybdene blue method), and Cl by titration (Mohr's method). All experiments were run in triplicates.

RESULTS

The bulk of the dissolution occurred within the first two weeks of the experiment with rates declined with time. The evolution of solution composition over time in the dissolution experiment at initial pH=2 and various temperatures is shown in Fig. 1. Equilibrium was attained after two weeks. There is a general

[1] *Department of Mineralogy, Petrography, and Geochemistry, AGH-University of Science and Technology, 30-059 Krakow, Poland; bajda@geolog.geol.agh.edu.pl*

increase in the concentrations of Pb and As with increasing temperature. Based on averaged experimental triplicates of measured equilibrium Pb_{aq} and As_{aq} concentrations, and calculated respective Cl concentrations (based on molar ratio

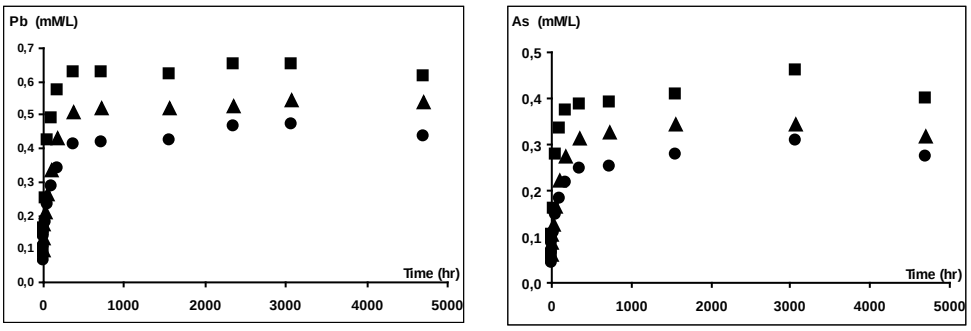

Fig. 1. Concentrations of Pb (left) and As (right) in the dissolution experiments with initial pH=2.0 at 5 °C (circles), 20 °C (triangles), and 35 °C (squares).

As:Cl=3:1 from the stoichiometry of mimetite), equilibrium aqueous activities were calculated using the geochemical speciation model PHREEQC (Parkhurst 1995) with thermodynamic database from MINTEQA2. Activity corrections were made using the Davies equation. The equilibrium ion activity products (IAP) were calculated for dissolution reaction of mimetite:

$$Pb_5(AsO_4)_3Cl \leftrightarrow 5Pb^{2+} + 3AsO_4^{-} + Cl^{-} \quad (1)$$

for 5 °C, 20 °C, and 35 °C. At equilibrium, the solubility product, K_{sp}, is equal the IAP, which for the reaction (1) is given by:

$$IAP = [Pb^{2+}]^5 + [AsO_4^{-}]^3 + [Cl^{-}] \quad (2)$$

where brackets denote aqueous activity. The $\log K_{sp}$ determined from the experiments show a clear decrease with the increase of temperature, ranging from –75.6 at 5 °C, through –74.39 at 20 °C, to –73.1 at 35 °C. The dependence of $\log K_{sp}$ on the inverse of the temperature (Fig. 2) appears to be linear (r^2=0.9988) suggesting that the enthalpy of dissolution reaction is constant over the temperature range used in the experiments.

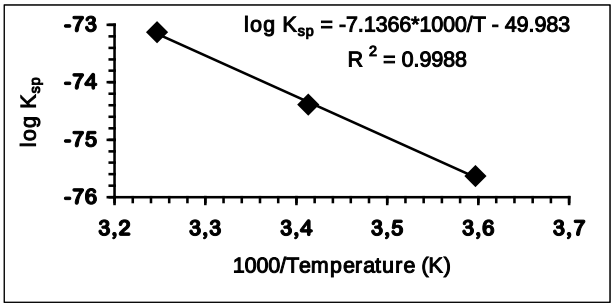

Fig. 2. Calculated mimetite $\log K_{sp}$ values versus inverse temperature.

The function $K_{sp}(T)$ can be written as:

$$\log(K_{sp}) = A * 1/T + B \quad (3)$$

where $A = -\Delta H_r^o/\ln(10)R$ and $B = \Delta S_r^o/\ln(10)R$, ($R = 8.3143$ J.mol^{-1}.K^{-1}, gas constant). Using equation (3), and the slope of the fitted data, the enthalpy of dissolution reaction (1) was calculated to be 136.6 kJ·mol^{-1} and the entropy calculated from the intercept equals – 956.9 J.mol^{-1}. Using the data in Table 1 we calculated the enthalpy of formation for mimetite to be $\Delta H_{f\ mimetite}^o$ = -273.5kJ.mol^{-1}.

Table 1. Relevant thermodynamic data (Robie et al. 1978) .

Species	$-\Delta H_f^o$ kJ·mol^{-1}
Pb^{2+}	-1.7
AsO_4^{3-}	12.9
Cl^-	-167.08

CONCLUSIONS

To our knowledge for the first time the temperature dependence of the solubility of mimetite was determined in the direct experiment. Solubility of mimetite increases with temperature. Dissolution of mimetite is endothermic with the enthalpy of the reaction ΔH_r°=136.6 kJ.mol^{-1}, constant in the range of 5 to 35 °C.

ACKNOWLEDGEMENTS: This research was partially financed by MEN grant No. 2 PO4D 01329.

REFERENCES

BAJDA T., SZMIT E., MANECKI M., SIKORA M., 2005: Solubility of Mimetite $Pb_5(AsO_4)_3Cl$ at 20 °C and pH from 2.0 to 12.0. Pol. Tow. Mineral. Prace Spec., 25: 27-30.

COMBA P.G., 1987: Removal of arsenic from process and wastewater solutions. M.S. Thesis, Montana College of Mineral Science and Technology, Butte, MT, 137.

PARKHURST D.L., 1995: User's guide to PHREEQC – a computer program for speciation, reaction-path, advective-transport, and inverse geochemical calculations. U.S. Geological Survey Water-Resources Investigations Report, 95-4227, 1-143.

ROBIE R.A., HEMINGWAY B.S., FISHER J.R., 1978: Thermodynamic properties of minerals and related substances at 298.15 K and 1 bar (10^5 Pascal) pressure and at higher temperatures. US Geological Survey Bulletin, 1-1452.

MINERALOGIA POLONICA - SPECIAL PAPERS
Volume 28 - 2006

Tímea BÁLINTOVÁ[1], Martin ŠTEVKO[1], Daniel OZDÍN[1]

SULPHOSALTS OF LILLIANITE HOMOLOGOUS SERIES FROM CHYŽNÉ OCCURRENCE (SLOVAKIA)

INTRODUCTION

We carried research on the Herichová occurrence that found ~3 km NNE from the village Chyžné (County Revúca) in the central part of the Slovakia. Locality is situated in western part of Spišsko-gemerské rudohorie Mts. near contact zone two significant tectonic units in the Western Carpathians – Gemericum and Veporicum Unit. Sulphosalts occurs in hydrothermally quartz-stibnite veins with sulphides and hübnerite in S-type leucocratic granites of mostly carboniferous Age (350 ± 5 Ma; Bibikova et al. 1988).

Hydrothermal mineralization were studied by Bálintová (2006) which from Chyžné described following primary minerals: native bismuth, arsenopyrite, pyrite, chalcopyrite, galena, bismuthinite, sphalerite, berthierite, stibnite, joseite-A, joseite-B, baksanite, tetrahedrite, chalcostibite, kermesite, jamesonite, zinkenite, plagionite, pellouxite, boulangerite, geocronite, andorite, ramdohrite, gustavite, heyrovskyite, robinsonite, quartz, rutile, hübnerite, calcite, rodochrosite, kutnohorite, monazite-(Ce), xenotime-(Y), fluorapatite, muscovite, ortoclase and titanite. More informations about andorite publish Ozdín, Bálintová (2003) and about sulphosalts Bálintová et al. (2006).

METHODS

The chemical analyses were carried on the CAMECA SX100 microprobe in Geological Institute of Dionýz Štúr in Bratislava, with synthetic and natural standards: PbS (Pb Mα), $CuFeS_2$ (S Kα, Fe Kα, Cu Kα), Sb_2S_3 (Sb Lβ), Bi_2Se_3 (Bi Lα), NaCl (Cl Kα), FeAsS (As Kβ), Ag (Ag Lα), Cd (Cd Lα), Mn (Mn Kα), HgS (Hg Lα), ZnS (Zn Kα). Operating conditions were follow: accelerating voltage 20 kV , beam current 15-20 nA and diameter of beam 1-5 μm.

RESULTS

We are described following mineral assemblages: 1. Carbonate, 2. Alpine paragenesis stage, 3. Arsenopyrite-pyrite, 4. Hübnerite, 5. Stibnite; 6. Pb-Bi-Te, 7. Hypergenne. Sulphosalts of lillianite homologous series are mainly represented by Ag-Pb-Sb (andorite, ramdohrite) and Ag-Pb-Bi (gustavite, heyrovskyite) phases.

In studing locality Ag-Pb-Sb (andorite, ramdohrite and an unnamed member $Pb_{22}Ag_{13}Sb_{45}S_{96}$) sulphosalts make sequential transition into Ag-Pb-Bi (heyrovskyite, gustavite) members of lillianite homologous series. On this suggest extremely increased concentration of Bi in Ag-Pb-Sb (ramdohrite and an unnamed member $Pb_{22}Ag_{13}Sb_{45}S_{96}$) sulphosalts.

Ramdohrite and an unnamed member of the series “81.25” (with the theoretical

[1] *Department of Mineralogy and Petrology, Faculty of Natural Sciences, Comenius University, Mlynská dolina, 842 15 Bratislava, Slovak Republic; timea.balintova@post.sk*

formula of $Pb_{22}Ag_{13}Sb_{45}S_{96}$) occurs associated with Ag-Pb-Bi sulphosalts, native bismuth, bismuthinite and Bi-Te minerals in galena. These sulphosalts have an increased content of Cd (up to 0.22 *apfu*). Content of Bi in ramdohrite is varies about 4.18 *apfu* and in unnamed member is it about 1.38 *apfu*.

Andorite forms tiny needles and inclusions in stibnite together with robinsonite and jamesonite. Rarely is occurs in association with hübnerite. It contains 97.76–101.38 % molecule of andorite and according to Moëlo et al. (1989) it is senandorite (andorite VI). This andorite have an increased content of Cu (up to 0.22 *apfu*), Fe (up to 0.02 *apfu*), Cd (up to 0.02 *apfu*) and sometimes Bi (up to 0.01 *apfu*), too.

Ag-Pb-Bi sulphosalts are represented by *heyrovskyite* and *gustavite* (Fig. 1). These sulphosalts occurs in association together with native bismuth, bismuthinite, Bi-Te minerals and Ag-Sb-Bi sulphosalts (ramdohrite, unnamed member) in galena. Gustavite is represented by two forms. The first type of gustavite forms darker (in BSE) exsolutions, that rarely occur in lighter gustavite or included with heyrovskyite forms idiomorphous crystals. The darker parts of gustavite they have toward lighter parts higher content of Ag. The darker parts have content of Ag average 8,96 wt. % and lighter parts average 6,17 wt. %. Analyses of gustavite from Chyžné occurrence could be separate to the two fields. The first field is represented by analyses with low substitution values from 54,84 to 71,97 mol. % of

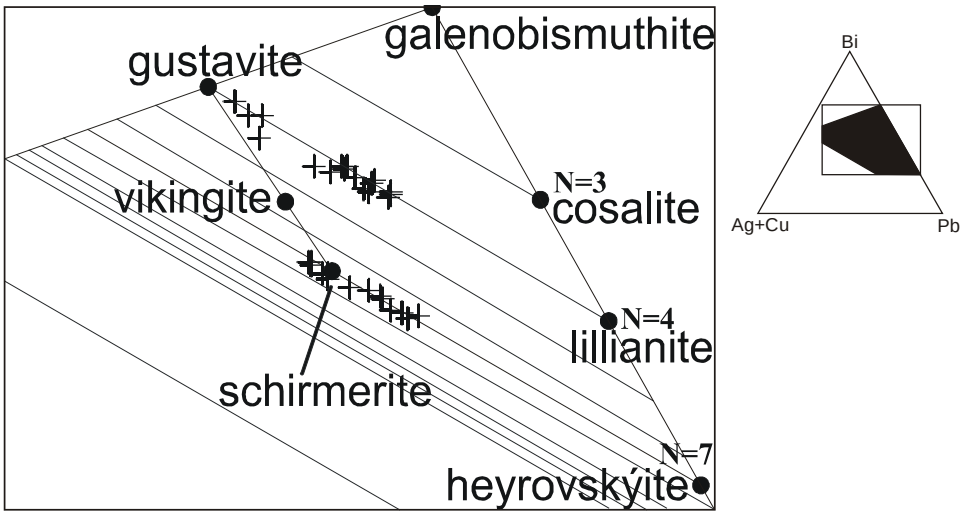

Fig. 1. Chemical composition of lillianite homologous from Chyžné.

AgBi member and the second field is represented by analyses with higher substitution values from 79,57 to 93,99 mol. % of AgBi member. In Chyžné-Herichová occurrence was determined "La Roche Balue" trend, wich was named according to La Roche Balue occurrence in France (Moëlo et al. 1987). Is concerned reduction content of AgBi members from gustavite over vikingite till about AgBi heyrovskyite. Gustavite and heyrovskyite have an increased content of

Sb (up to 1.42 *apfu*) and Cd (up to 0.16 *apfu*), Bi is replaced by Sb and Pb is replaced by Cd.

CONCLUSIONS

In the Chyžné-Herichová occurrence Ag-Pb-Sb sulphosalts of lillianite homologous series sequential transition into Ag-Pb-Bi sulphosalts. Ramdohrite and an unnamed member are characteristic increased contents of Cd (up to 0.22 *apfu*) and Bi (up to 4.18 *apfu*). Andorite is a typical by increased content of Cu (up to 0.22 *apfu*), Fe (up to 0.02 *apfu*) and Cd (up to 0.02 *apfu*). Content of Cu is probably highest determined in the world. Heyrovskyite and gustavite are characteristic by increased content of Sb (up to 1.42 *apfu*) and Cd (up to 0.16 *apfu*).

ACKNOWLEDGEMENTS: This study has been carried with contributing to project VEGA No. V-374-05-00 of Ministry of education of the Slovak Republic.

REFERENCES

BÁLINTOVÁ, T., OZDÍN, D., ŠTEVKO, M., 2006: Chemical composition of sulphosalts on locality Chyžné - Herichová. Miner. Slov., 38, 2: (in press). (in Slovak)

BIBIKOVA E.V., CAMBEL B., KORIKOVSKY S.P., BROSKA I., GRACHEVA T.V., MAKAROV V.A., ARAKELIANTS M. M.: U-Pb and K-Ar isotopic dating of Sinec (Rimavica) granites (Kohút zone of Veporides). Geol. Zbor. Geol. Carpath., 39, 2: 147-157.

MOËLO Y., MARCOUX E., MAKOVICKÝ E., KARUP-MØLLER S., LEGENDRE O., 1987: Homologues de la lillianite (gustavite, vikingite, heyrovskyite riche en Ag et Bi) de l'indice a W-As-(Pb, Bi, Ag) de La Roche-Balue (Loire Atlantique, France). Bull. Mineral., 110: 43-64.

MOËLO Y., MAKOVICKY E., KARUP-MØLLER S., 1989: Sulfures complexes plombo-argentiferes: minéralogie et cristallochimie de la série andorite-fizelyite. Documents du BRGM, 167: 1-107.

OZDÍN D., BÁLINTOVÁ T., 2004: New find of andorite ($PbAgSb_3S_6$) on the locality Chyžné (Slovakia). Bull. mineral.-petrolog. Odd. Nár. Muz. (Praha), 12: 147-152. (in Czech)

MINERALOGIA POLONICA - SPECIAL PAPERS
Volume 28 - 2006

Anikó BATKI[1], Elemér PÁL-MOLNÁR[1]

ROCK-FORMING MINERALS OF LAMPROPHYRES FROM THE DITRĂU ALKALINE MASSIF, ROMANIA

INTRODUCTION

Lamprophyres are a group of alkali-rich igneous rocks containing essential amphibole and/or phlogopite with no feldspar or quartz phenocrysts. They typically form subvolcanic dykes, sills, plugs, stocks or vents (Rock 1991).

This paper reports new results on the mineralogy of lamprophyres, which were slightly discussed in former works of the Ditrău Alkaline Massif, Romania.

GEOLOGICAL SETTINGS

The Ditrău Alkaline Massif (DAM) is a Mesozoic alkaline igneous complex and situated in the S-SW part of the Giurgeu Alps belonging to the Eastern Carpathians (Romania). This body intruded into the pre-Alpine metamorphic basement complexes of the Bucovinian Nappe Complex located on the east side of the Culimani-Gurghiu-Harghita Neogene-Quarternary calc-alkaline volcanic arc, and took part in the Alpine tectonic events together with these metamorphic rocks (Pál-Molnár 2000). The centre of the DAM was formed by nepheline syenite, which is surrounded by syenite and monzonite. The northwestern and northeastern parts are composed of hornblendite, diorite (called Tarncia Complex, Pál-Molnár 2000), monzonite and alkali granite. The whole complex is cut by late-stage lamprophyre, alkali feldspar syenite and tinguaite dykes.

METHODS

Mineral compositions for six selected samples were determined by Cameca SX-50 electron microprobe at the Department of Earth Sciences, University of Uppsala, Sweden. Operating conditions were probe current of 15 nA and acceleration voltage of 20 kV. Representative results can be seen in Table 1.

RESULTS

The studied area is the northern part of the Orotva Creek, Ditrău Alkaline Massif. Samples were collected from nine natural outcrops of six creeks. Lamprophyres collected from Tarnica Complex (Orotva, Tászok, Fülöp and Gudu Creeks) crosscut hornblendites, diorites and syenitoids. Other lamprophyres from Török and Nagyág Creeks intersect granitoids. The dykes are 20cm to 2m wide. Contacts of the dykes with the wall rock are sharp. The lamprophyre dykes show felsic globular structures up to 11 mm in size. Their texture is typically panidiomorphic, porphyritic and at some places vitrous in contact zones.

Petrographic investigations show that DAM lamprophyres can be divided into two main groups: (1) Dark-grey, greenish-grey mafic (melanocratic) rocks, which

[1] *Department of Mineralogy, Geochemistry and Petrology, PO Box 651, University of Szeged, 6701 Hungary; e-mail: batki@geo.u-szeged.hu*

are amphibole rich and plagioclase-bearing called camtonites (in all the studied creeks).

Table 1. Representative diopside, amphibole and phlogopite compositions from the DAM lamprophyres.

Mineral	diopside	diopside	krs	hs	eck	phl	phl	phl
Rock-type	campt.	vog.	campt.	campt.	vog.	campt.	campt.	minette
Locality	Tarncia Complex	Nagyág Creek	Tarncia Complex	Török Creek	Nagyág Creek	Tarncia Complex	Török Creek	Török Creek
SiO_2	46.12	47.21	38.49	39.44	52.89	35.70	34.99	38.08
TiO_2	2.14	1.97	6.67	1.89	0.00	1.66	2.44	0.27
Al_2O_3	7.05	6.49	13.55	12.11	1.73	14.69	15.53	16.62
FeO^t	7.19	7.68	10.46	19.48	22.99	17.05	20.51	9.59
MnO	0.09	0.15	0.11	0.41	0.92	0.14	0.27	0.66
MgO	12.91	13.13	12.02	8.69	3.34	13.71	11.61	16.77
CaO	21.85	22.19	11.87	11.79	6.79	0.30	0.00	0.00
Na_2O	0.73	0.60	2.55	1.98	9.59	0.00	0.06	0.03
K_2O	0.00	0.00	1.01	1.75	0.00	9.40	9.59	10.08
Total	98.12	99.45	96.79	97.57	98.29	92.76	95.02	92.13
mg#	-	-	0.67	0.49	0.20	0.60	0.50	0.76

t – total Fe as FeO; mg# - Mg/(Mg+Fe); krs – kaersutite, eck – eckermannite, hs – hastingsite, phl – phlogopite, campt. – camptonite, vog. – vogesite

(2) Two varieties of less mafic, light-grey, intermediate (mesocratic) rocks: *(a)* phlogopite and K-feldspar rich minettes (Török Creek); *(b)* amphibole and K-feldspar rich vogesites (Nagyág Creek).

Camptonites from Tarnica Complex carry aluminian subsilicic ferroan diopside ($Ca_{0.9}Mg_{0.7}Fe_{0.2}Al_{0.26}Si_{1.73}O_6$) phenocrysts (Fig. 1A), reddish-brown kaersutite, subordinate strongly magnesian annite to phlogopite microphenocrysts up to mg# = 0.73 (Fig. 1B) and interstitial plagioclase (An_{04-34}). Kaersutites occur as euhedral groundmass minerals with up to 6.6 wt.% TiO_2 (Table 1). Camptonites from Török and Nagyág Creek have only groundmass minerals with no phenocrysts. The groundmass consist of elongated magnesian hastingsite crystals (mg# = 0.49-0.55) displaying preferred orientation due to magma flow, annite (Fig. 1B) represented by small crystals with moderate mg# (0.47-0.50) and interstitial plagioclase (An_{05-16}). Apatite, titanite and magnetite are common minor phases in the studied camptonites. Secondary phases are tremolite to actinolite, pycnochlorite, muscovite and allanite-(Ce).

Minettes from Török Creek contain andradite phenocrysts, phlogopite (mg# = 0.70-0.76) (Table 1; Fig. 1B), nearly pure albite (An_{01}), K-feldspar (Or_{97}) and haüyne in the groundmass. The Ti-bearing andradites are surrounded by secondary phlogopite, pycnochlorite and magnetite. Feldspars are strongly sericitized. Other secondary phases are calcite and epidote.

Vogesites from Nagyág Creek carry diopside phenocrysts (Fig. 1A), ferro-eckermanite (FeO^t 21-26 wt.%), ferrorichterite (FeO^t 20.5 wt.%), small amount of phlogopite (mg# = 0.50-0.67), pure albite (An_{00}), K-feldspar (Or_{96}) and haüyne in the groundmass. Accessory minerals are apatite, titanite, magnetite and zircon in vogezites and minettes as well.

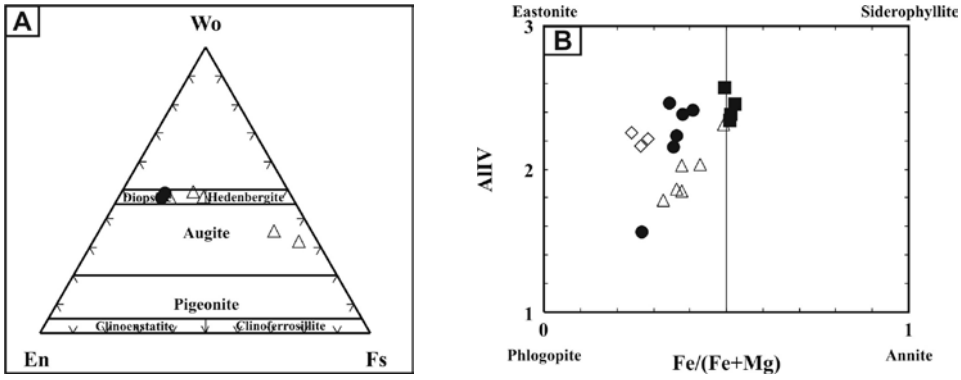

Fig. 1 Variations in composition of (A) clinopyroxenes and (B) dark micas from the DAM lamprophyres; ● camptonites – Tarnica Complex, ■ camptonites – Török and Nagyág Creeks; ◇ minettes – Török Creek; △ vogesites – Nagyág Creek

CONCLUSIONS

The main rock-forming minerals in the studied camptonites, minettes and vogesites which are considered to be primary are dark micas close to phlogopite composition, kaersutites rich in Ti, magnesian hastingsites, eckermanites and richterites rich in Fe, Al-, Fe-bearing diopsides, Ti-bearing andradites, intermediate plagioclases and alkali feldspars. The mineral compositions show similarities from individual rock types within the whole area with only weak regional differences.

ACKNOWLEDGEMENTS: The financial background for this work was provided by the Hungarian National Science Found (OTKA, Grant No. T 046736) and the Department of Geology and Geochemistry, Stockholm University, Sweden.

REFERENCES

PÁL-MOLNÁR E., 2000: Hornblendites and diorites of the Ditró Syenite Massif. Department of Mineralogy, Geochemistry and Petrology, University of Szeged, 1-172.

ROCK N.M.S., 1991: Lamprophyres. Blackie, Glasgow, 1-285.

MINERALOGIA POLONICA - SPECIAL PAPERS
Volume 28 - 2006

Slavica BLAGOJEVIĆ-BABIĆ[1], Nada VASKOVIĆ[1], Ljubomir CVETKOVIĆ[1], Danilo BABIĆ[1]

MINERAL COLLECTIONS FROM SLOVAKIA

The Institute of Mineralogy, Crystallography, Petrology and Geochemistry of the Faculty of Mining and Geology (Belgrade University) owns Museum of minerals and stones. It is founded in 1884 under the name Chair of Minerals at the High Education School (HES). The oldest mineral collection dates from 1835 and represents a gift of Baron von Herder to prince Milos. This collection has initiated gathering of minerals in Serbia and founding of Geology and Mineralogy at the HES. A great number of collections from abroad testify about tradition of our Museum, which from its foundation till now has been used as a means of student's education. Some of previously mentioned collections are very precious to us as for example: Collection of Queen Katherine II form Petersburg, Collection of marquis de Mauroy from Paris, Collection of Royal Ontario Museum and many others. For this occasion we want to present only two collections of a few from Slovakia.

The first collection, dating from 1963, was brought by professor of mineralogy and ore microscopy S. Rakić during his study journey across Slovakia. Specimens are from Rožňava and Banská Štiavnica and represent gift of the "Ustřední ústav geologický" to Professor S. Rakić who donated it to the Museum. Collection comprises 40 specimens and among them we have to mention hematite, siderite, barite, annabergite, pyrite, schwazite, tetrahedrite and pyrhotite from Rožňava as well as barite, galena, sphalerite and chalcopyrite from Banská Štiavnica (Fig. 1a, b). All specimens have labels with number and location (Fig. 1e). The Collection is in use for students' education because of its mineral-rich content and beauty also.

The second collection is from Bratislava and comprises 33 specimens. As in the first collection, specimens have labels with number and location (Fig 1f). Besides specimens from Slovakia this collection comprises specimens from Romania, Czech Republic, Germany, Sweden, Switzerland as well as form Africa, India and Bolivia (Fig. 1c, d). We don't know when and on which way this collection arrived to Museum? We just ask ourselves, is this occasion a right place for finding answer on our question and for establishing future collaboration.

[1] *Faculty of Mining and Geology, Djušina 7, 110 00 Beograd, Serbia; danislav@mkpg.rgf.bg.ac.yu*

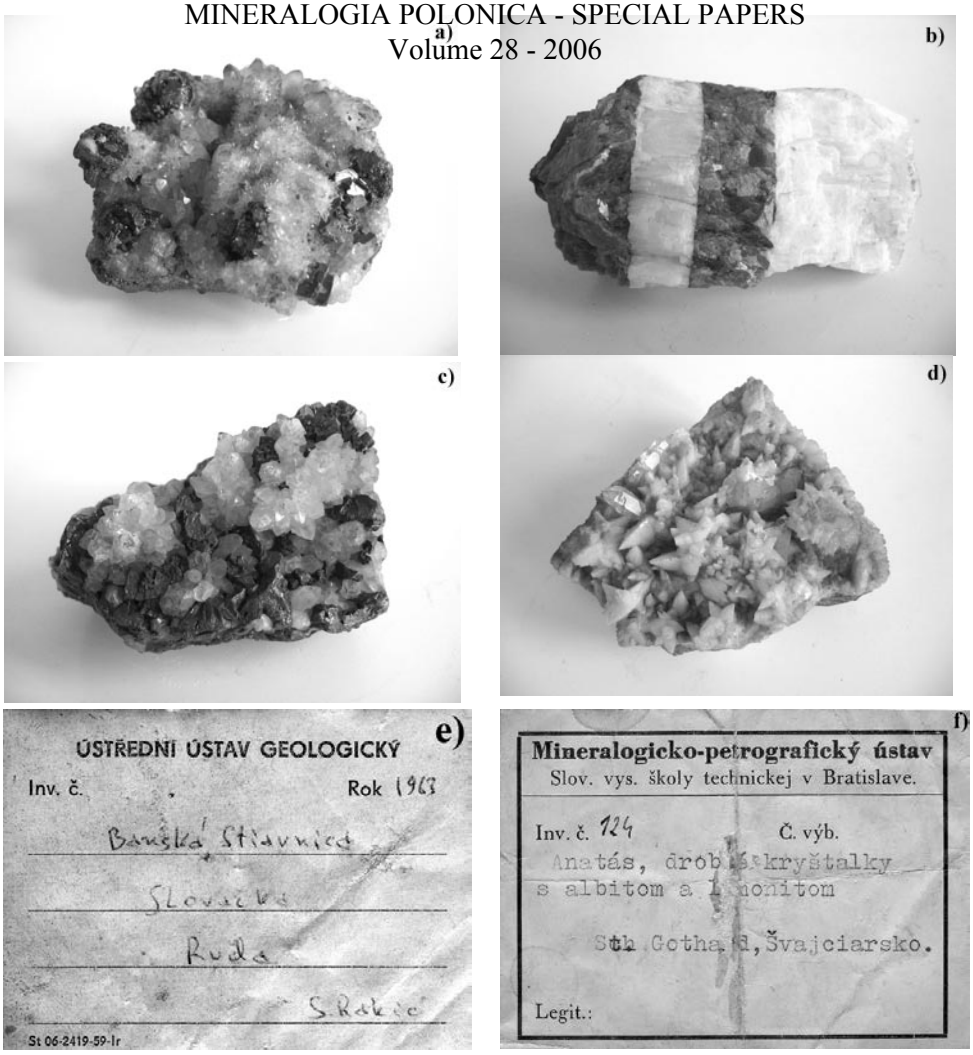

Fig. 1. Some minerals and labels from the Slovakia and Bratislava Collection: a) Sphalerite, galena and quartz. B. Štiavnica, Slovakia (from the collection of prof. S. Rakić); b) Barite and siderite. Rožňava, Slovakia (from the collection of prof. S. Rakić); c) Chalcopyrite and quartz. B. Štiavnica, Bratislava; d) Calcite and quartz. B. Štiavnica, Bratislava, e) Label from gift Collection of prof. S. Rakić; f) Label from the Bratislava Collection.

MINERALOGIA POLONICA - SPECIAL PAPERS
Volume 28 - 2006

Martin BOHÁČ[1], *Miroslava GREGEROVÁ*[1]

HYDRATION PRODUCTS OF GGBS IN PORTLAND CEMENT CONCRETE

INTRODUCTION

New hydration products of ground granulated blast-furnace slag (GGBS) are formed during the hydration process of Portland slag cement concrete (Richardson et al. 1994; Števula et al. 1994; Brough, Atkinson 2002; Hill, Sharp 2002). Richardson, Cabrera (2000) revealed that hydration of slag in concrete is accompanied by morphological changes and decrease of capillary porosity of C-S-H products. Spatial distribution of microcracks in concrete is related to chemical composition of new-formed slag hydrates. The permeability of concrete is one of the most important factors that influence the final durability of concrete.

METHODS

The examined concrete samples were represented by dry drilled cores or knocked off fragments of reinforced concrete highway bridges. The structures comprise four bridges from Brno or its vicinity. Polished thin sections of selected samples were analyzed by optical polarization microscopy (Olympus BX51) and scanning electron microscopy (Cameca SX100); chemical composition of slag grains and its hydration products was studied in thin sections by WDX analyses, line scans (15 kV, 10 nA) and X-ray maps.

RESULTS

The hydration products of ground granulated blast-furnace slag in Portland cement concrete are formed against the blast-furnace slag-hydrated cement paste interface. This interaction changes chemical composition and morphology of C-S-H products. Aluminium substitutes for silicon in the central tetrahedron of pentameric silicate chains or in every third tetrahedron in longer chains. The alumino-silicate chains get on average longer, and its morphology changes from fibrillar to foil-like. The change in C-S-H morphology results in a less well-interconnected capillary pore

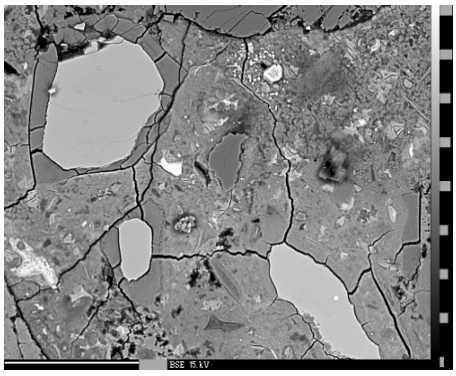

Fig. 1. Rims of hydration products around blast-furnace slag in Portland cement concrete.

[1] *Institute of Geology, Kotlářská 2, Faculty of Science, Masaryk University, 611 37 Brno, Czech Republic; e-mail: bohy@mail.muni.cz*

structure (Richardson 2000). Just a small increase of Al content in few µm around original grains of slag was observed in the examined samples. The electron microscope images show that hydration products of slag form rims around an unhydrated slag core (Fig. 1). The rims are within the boundaries of the original grain. These rims are often segmented into two or more layers.

To understand the process of hydration the X-ray maps and the line scans (Fig. 2) on electron microscope were used. The lines were directed from C-S-H products through the hydration products of slag to the unhydrated slag core. Ca, Si, Mg and Al were analyzed. There are considerable differences of chemical composition of used slag in each concrete bridge. The morphology and chemical composition of slag hydration products differs in each structure as well. The chemical composition of hydration products is very variable and unstable. Stable mineral phases are present rarely. The Si/Ca ratios rise in hydration products near the unhydrated slag core significantly. There is also a certain increase of Mg and Al content in the central parts of hydration rims. Mg and Al were probably present as hydroxides interacting with C-S-H products to form new phases of variable chemical composition. Some of them are close to hydrotalcite-like phase $Mg_6Al_2(CO_3)(OH)_{16}\cdot 4(H_2O)$.

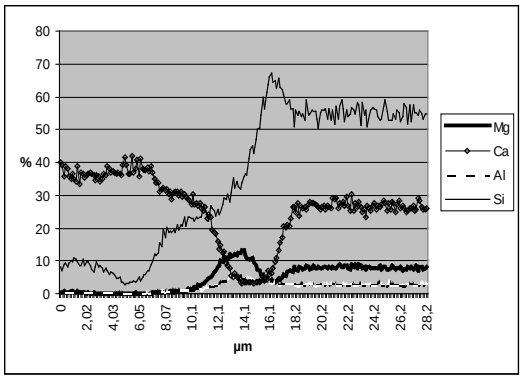

Fig. 2. Line scan – chemical composition of major elements from C-S-H products through the hydration.

Carrasquillo et al. in Häkkinen (1993) published that microcracks in concrete may be formed as a result of volume changes during setting and hardening and segregation and bleeding. One of the important factors causing internal stresses and microcracks in concrete is drying shrinkage. The formation of combined cracks containing two or more cracks connected to each other leads to failure of concrete (Häkkinen 1993). Considerable microcracking is observed a) against the hydrated slag grains-paste interface, b) between hydration rims or c) against the hydration products-unhydrated core interface. There were detected bond and mortar microcracks communicating with each other during the analyses on electron microscope. The high

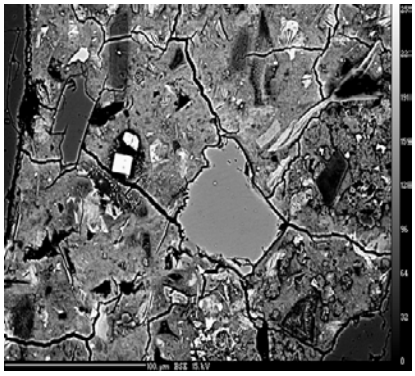

Fig. 3. System of combined microcracks in concrete. Cubes of NaCl in cement paste and void.

permeability of concrete was demonstrated by cubic and acicular crystals of NaCl in microcracks and voids filled with alkali-silica gel (Fig. 3). The amount of microcracks was reduced in samples of concrete with a lower content of vitreous fraction where the slag basicity was high. The Ca/Si ratio in these slag grains was approximately 2:1. The microcracks play an important role in the samples where the Ca/Si ratio was much lower - approximately 1:2.

CONCLUSIONS

New-formed hydration products are accompanied by volume changes, which can lead to the process of microcracking. The chemical composition of blast-furnace slag especially its basicity is another important factor that influence the microcracking in concrete and the final durability of concrete.

ACKNOWLEDGEMENTS: Thanks are due to the Research Grant MSM 0021622418 “Dynamic Geovisualisation in Crisis Management” and GACR n. 103/06/1801, to RNDr. Petr Sulovský, Ph.D., Mgr. Radek Škoda and Mgr. Renata Čopjaková for great help with SEM analyses.

REFERENCES

BROUGH A.R., ATKINSON A., 2002: Sodium silicate-based, alkali-activated slag mortars. Cement and Concrete Res., 32: 865-879.

HÄKKINEN, T. 1993: The influence of slag content on the microstructure, permeability and mechanical properties of concrete. Cement and Concrete Res., 23: 518-530.

HILL J., SHARP, J.H., 2002: The mineralogy and microstructure of three composite cements with high replacement levels. Cement and Concrete Comp., 24: 191-199.

RICHARDSON I.G. 2000: The nature of hydration product in hardened cement pastes. Cement and Concrete Composites, 22, 97-113.

RICHARDSON, I. G., CABRERA, J. G. 2000: The nature of C-S-H in model slag cement. Cement and Concrete Composites, 22, 259-266. RICHARDSON I.G., BROUGH A.R., GROVES G.W., DOBSON C.M., 1994: The characterization of hardened alkali-activated blast-furnace slag pastes and the nature of calcium silicate hydrate (C-S-H) phase. Cement and Concrete Res., 24: 813-829.

ŠTEVULA L., MADEJ J., KOZÁNKOVÁ J., MADEJOVÁ J., 1994: Hydration products at the blast-furnace slag aggregate-cement paste interface. Cement and Concrete Res., 24: 413-423.

MINERALOGIA POLONICA - SPECIAL PAPERS
Volume 28 - 2006

Igor BROSKA[1], C. Terry WILLIAMS[2], Martin HRDLIČKA[1]

BEHAVIOUR OF PRINCIPAL ACCESSORY PHOSPHATE MINERALS IN THE SILICIC MELT OF THE WESTERN CARPATHIANS

INTRODUCTION

The paragenesis of accessory minerals in granitic rocks depends strongly on water and/or volatile contents, as well as on the aluminosity and alkalinity of the primary melt. The distribution of REE and P can also affect the behaviour of the melt, and influence mineral precipitation, and in this contribution we discuss the role of the REE and P in forming accessory mineral assemblages in granitic rocks. Of the typical accessory minerals present in granites, monazite-(Ce), apatite, allanite-(Ce), titanite, xenotime-(Y) and magnetite are the most important phases. These minerals, and especially monazite and apatite, are important for discrimination (by their presence or absence, or their compositional character) of the Palaeozoic orogenic I- and S- type granitic suites of the Western Carpathians.

APATITE AND MONAZITE DISTRIBUTION

Observed differences in relative abundance of monazite-(Ce), apatite and allanite-(Ce), important for distinguishing between I- and S-type granites, can be explained by their different solubilities in a peraluminous melt, where the solubility of apatite is higher than monazite. Monazite, locally occurring with xenotime, characterizes the complete differentiation range of S-type granites. However, monazite is present only in small quantities within late differentiates of the I-type granitic rocks. Early magmatic differentiates of S-type granites contain 0.0X wt.% of monazite and apatite. Apatite is relatively common in the early magmatic differentiates of I-type granites and can often reach 0.X wt.%, but its abundance rapidly decreases with differentiation.

LREE AND P DISTRIBUTION IN THE SILICIC MELT

The overall distribution of REE in a silicic melt is controlled mainly by the distribution of REE minerals such as monazite-(Ce), allanite-(Ce) and apatite. These minerals, together with titanite, zircon and xenotime, are the most common REE accessory mineral phases accounting for >90% of whole-rock REE concentration. The crystallisation of these minerals significantly decreases the REE concentration in the residual melt. Monazite-(Ce), xenotime-(Y) and to a lesser extent apatite, are characteristic accessory mineral phases in granites with S-type affinity. Abundant apatite, allanite-(Ce), magnetite and titanite are typical for the I-type granitic rocks. The presence or absence of accessory monazite, allanite and apatite depends on the P, LREE and Ca concentrations in the melt, and additionally, is influenced by magmatic differentiation and oxidation-reduction

[1] *Geological Institute, Slovak Acad. Sci., Dúbravská cesta 9, 840 05 Bratislava, Slovak Republic; igor.broska@savba.sk*
[2] *Natural History Museum London, Cromwell Road, London SW7 5BD, U.K*

stages in the silicic melt, indicated by Fe-Ti oxides, particularly by magnetite and ilmenite. Relatively high Ca activity leads to the crystallization of apatite and allanite; and in contrast, monazite indicates lower Ca activity.

Harker type diagrams show an irregular distribution of REE (or Ce) in the granites of the Western Carpathians, although in general, a negative Ce vs. Si correlation is observed (Fig. 1A-B). Irregularities in the distribution of Ce, expressed by a decrease of Ce with increase of SiO_2 to approximately 70 wt.% SiO_2, when Ce increases briefly, and then again decreases in similar manner to the earlier differentiates. This behaviour can be explained by the P distribution and Ca activity of the silicic melt. In the I-type granites the decrease in Ce is accompanied by a decrease in apatite and allanite mineral phases (Fig. 1B). After increase of Ce in the late I-type differentiates, allanite no longer crystallises because of the low Ca activity, and monazite crystallizes. A similar decrease of Ce is clearly visible in the S-type granites, but in this case, it is a function of a decrease or fractionation of monazite (Fig. 1A). When Ce increases, at approximately 70 wt.% SiO_2, the abundance of monazite appears to increase. This observation can be explained by the presence of the berlinite molecule in the system (see below).

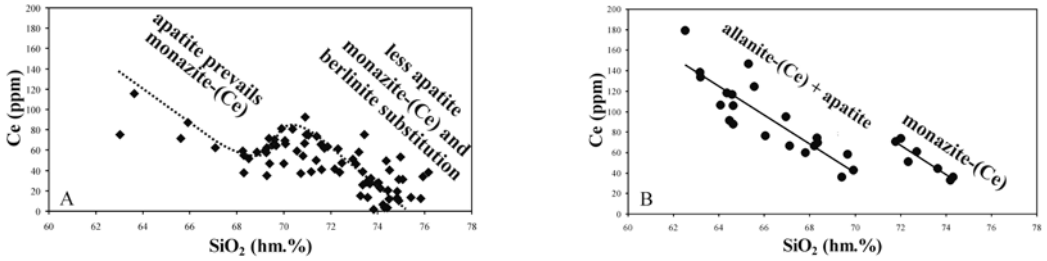

Fig. 1. Harker diagrams showing the distribution Ce (in ppm) vs. SiO_2 in granites with I and S-type affinities.

BERLINITE SUBSTITUTION AND BEHAVIOUR OF P IN THE SILICIC MELT

The berlinite substitution, based on the substitution Al + P for 2Si in feldspars, can explain the behaviour of monazite-(Ce) and apatite, both of which are significant consumers of Ce. The abundance of apatite decreases due to apatite fractionation during differentiation of I-type granite resulted in a systematic P decrease of both P and Ce in the melt. Additionally, the concentration of Ce reduced in the I-type granite melt by early precipitation of allanite-(Ce). When Ca activity becomes too low, monazite starts to crystallize instead of allanite-(Ce) and effectively takes up the bulk of the Ce and P. As the berlinite substitution is relatively low in the I-type granites, only a very small minority of P is distributed in the feldspar.

A quite different behaviour is observed for the S-type granite differentiation process. Here, initially P decreases, but subsequently, especially in high peraluminous melts, P increases. This effect was mentioned e.g. by Bea et al.

(1992) and has been explained by experimental work of London (1992, 1998) who found that the berlinite substitution starts to operate during an increase of the peraluminosity of the melt. At that time, the berlinite substitution leads to incorporation of P into the feldspar, contemporaneously apatite is soluble and monazite-(Ce) does not precipitate. Although the actual concentration of P in alkali feldspar is not particularly high (usually K-feldspar contains up to 0.5 wt. % P_2O_5), this is a significant contribution of the bulk rock P concentration. Sometimes the concentration of P in feldspars is more pronounced, and can exceed 3 wt. % (Breiter et al. 1997).

The P accommodated in the berlinite molecule of the feldspar structure can later be released to form locally secondary apatite (Broska et al. 2004). By concentrating P into early forming feldspar, P is effectively removed from the melt, a disadvantage for crystallization of accessory phosphates minerals such as monazite and apatite. At that time (the concentration of SiO_2 is approximately 70 wt.%), monazite is not able to precipitate, so that the concentration of the LREE (including Ce) in the melt increases, until such time that the activity of Ce is sufficiently high that monazite begins again to crystallize and competes for feldspar to consume the available P.

Berlinite substitution is pronounced when ACNK values are above 1.1. The behaviour of Ce influences (and mirrors that) of LREE and is reflected in the observed irregular distribution in the Harker diagrams (Fig. 1).

CONCLUDING REMARKS

The decrease in crystallization of monazite, and increase in whole rock Ce values can best be explained by the berlinite substitution mechanism occurring in feldspar. In this sense, the behaviour of accessory phosphate minerals is a complex process, and is controlled not only by physicochemical conditions, but also by crystallochemical characteristics of the whole mineral assemblage in the host rock. This process probably occurs more generally than has previously been realised.

ACKNOWLEDGEMENTS: The work was supported by grant VEGA 4097.

REFERENCES

BEA F., FERSHTATER G., CORRETGÉ L.G., 1992: The geochemistry of phosphorus in granite and the effect of aluminium. Lithos, 29: 43-45.

BROSKA I., WILLIAMS C.T., UHER P., KONEČNÝ P., LEICHMANN J., 2004: The geochemistry of phosphorus in different granite suites of the Western Carpathians, Slovakia: the role of apatite and P-bearing feldspar. Chem. Geol., 205: 1-15.

LONDON D., 1992. Phosphorus in S-type magmas: the P_2O_5 content of feldspars from peraluminious granites, pegmatites and rhyolites. Am. Mineral., 77: 126-145.

MINERALOGIA POLONICA - SPECIAL PAPERS
Volume 28 - 2006

Bartosz BUDZYŃ[1], Patrik KONEČNÝ[2], Marek MICHALIK[1]

BREAKDOWN OF PRIMARY MONAZITE AND FORMATION OF SECONDARY MONAZITE IN GNEISS CLASTS FROM GRÓDEK AT THE JEZIORO ROŻNOWSKIE LAKE (POLAND)

INTRODUCTION

Monazite is a REE phosphate commonly occurring in igneous and metamorphic rocks. Its primary formation, breakdown, and/or secondary monazite formation were studied by numerous authors (e.g. Simpson et al. 2000; Wing et al. 2003; Budzyń et al. 2005). Replacement of monazite by apatite-allanite-epidote coronas was described by e.g. Broska, Siman (1998); Finger et al. (1998); Michalik, Skublicki (1999); Majka, Budzyń (2006). In this paper we report various stages of monazite breakdown, including replacement of primary monazite by ring of apatite, and formation of secondary monazite. The process is accompanied by transformation of host mica.

STUDIED SAMPLES AND METHODS

Gravel size clasts of gneiss occurring in sedimentary rocks of the Silesian Unit were studied. Three samples that contain preserved various stages of monazite breakdown were selected for detailed investigation.

Field emission scanning electron microscope HITACHI S-4700 with NORAN Vantage energy dispersive spectrometer at the Jagiellonian University in Kraków was used for rock structure observations and determination of chemical composition of minerals. Detailed analyses were performed using Cameca SX-100 electron microprobe at the State Geological Institute of Dionýz Štur in Bratislava. Monazite U-Th-total Pb ages were calculated using method described by Montel et al. (1996) – see Konečný et al. (2004) for details and analytical methodology.

RESULTS

Studied augen gneiss clasts are coarse grained. These rocks are composed of quartz, plagioclase, K-feldspar, biotite and muscovite with accessory Fe-Ca garnet, kaolinite, zircon, apatite, monazite- (Ce), thorianite, uraninite, rutile, and chlorite.

Various stages of monazite-(Ce) breakdown were stated: 1) core of primary monazite-(Ce) successively surrounded by rings of apatite + thorianite + uraninite, kaolinite + secondary monazite-(Ce) in form of irregular veinlets or small nests (Fig. 1); 2) apatite grains with thorianite inclusions surrounded by ring of altered muscovite + secondary monazite-(Ce) in form of irregular veinlets or small nests; 3) mica + apatite grains with thorianite inclusions surrounded by secondary

[1] *Jagiellonian University, Institute of Geological Sciences; Oleandry 2a, 30-063 Kraków, Poland; e-mail: bartosz.budzyn@wp.pl*
[2] *State Geological Institute of Dionýz Štúr; Mlynská dolina 1, 817 04 Bratislava, Slovak Republic*

monazite-(Ce) in form of irregular veinlets or small nests; 4) apatite grains surrounded by ring of secondary monazite-(Ce) (Fig. 2). Other minerals (e.g. zircon) might be present within mentioned zones. Sequences of concentric rings in coronas are well preserved only in quartz (Fig. 1). Products of monazite-(Ce) breakdown and its replacement are irregular if they are in contact with biotite or muscovite flakes (Fig. 2).

Primary monazite-(Ce) contains 2.8-3.4 wt.% ThO_2 and 0.8-1.0 wt.% Y_2O_3, whereas secondary monazite-(Ce) 1.3-4.1 wt% ThO_2 and 1.7-2.5 wt.% Y_2O_3 on average. Average of Nd/Ce ratio measurements is *ca.* 0.34 and 0.36 in primary and secondary monazite-(Ce), respectively. Thorianite contains 86.98 wt% ThO_2, 5.19 wt.% UO_2 and 1.6 wt% PbO_2 with minor amounts of REE oxides.

Primary monazite-(Ce) intergrown with thorianite (Fig. 1) yielded ages of 472±49.9 Ma. "Chemical age" of thorianite (365±2.8 Ma) is difficult to interpret. Younger ages group (196±26 Ma) was obtained for secondary monazite-(Ce).

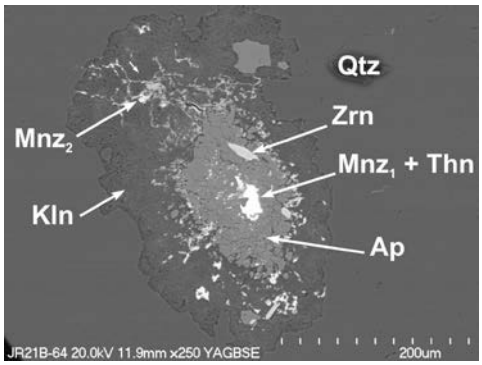

Fig. 1. Intergrowth of primary monazite (Mnz_1) and thorianite (Thn) surrounded by apatite (Ap), kaolinite (Kln) + secondary monazite (Mnz_2) corona. Qtz – quartz, Zrn – zircon. FESEM-BSE image.

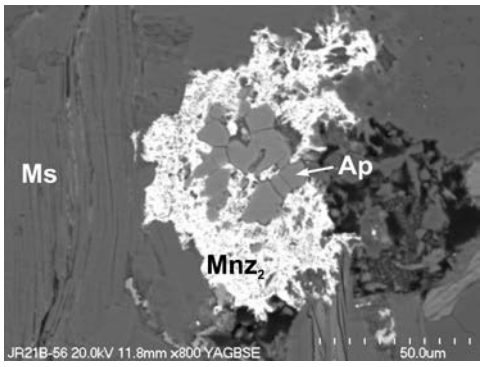

Fig. 2. Apatite (Ap) grains surrounded by secondary monazite (Mnz_2). FESEM-BSE image. Ms – muscovite.

DISCUSSION AND CONCLUSIONS

1. Formation of secondary monazite-(Ce) (both in form of dispersed veinlets or nests and as regular coronas) around the primary ones indicates a short-range transport of REE and phosphate anions.

2. Numerous tiny thorianite inclusions in primary monazite-(Ce) could influence determined Th content and shift age determination to lower ages.

3. Formation of secondary monazite-(Ce) (instead of commonly described allanite; *cf.* Finger et al. 1998) can be related to relatively high concentration of phosphorus and probably limited supply of calcium or to conditions out of stability field of epidote group minerals (e.g. lower temperature).

4. Ordovician age of primary monazite-(Ce) is related to formation of gneiss protolith. Devonian-Carboniferous ages are compatible with early stage of metamorphism (cf. e.g. Poprawa et al. 2005). Formation of secondary monazite-

(Ce) during Upper-Triassic – Early-Jurassic times was probably caused by thermal event related to rifting dated also by Michalik et al. (2004)

ACKNOWLEDGEMENTS: We thank Dr. I. Holický and Dr. V. Kollárová for their help in EMPA. Dr. I. Broska is acknowledged for his constructive comments. This study was supported by MNiSzW research grant 2P04D 041 29 (to B.B.) and Jagiellonian University research fund.

REFERENCES

BROSKA I., SIMAN P., 1998: The breakdown of monazite in the West-Carpathian Veporic orthogneisses and Tatric granites. Geol. Carpath., 49: 161-167.

BUDZYŃ B., MICHALIK M., MALATA T., POPRAWA P., 2005: Primary and secondary monazite in calcitized gneiss clast from Bukowiec (the Silesian Unit, Western Outer Carpathians). Min. Polon., 36, 2: 161-165.

FINGER F., BROSKA I., ROBERTS M.P., SCHERMAIER A., 1998: Replacement of primary monazite by apatite-allanite-epidote coronas in an amphibolite facies granite gneiss from the eastern Alps. Am. Mineral., 83: 248-258.

KONEČNÝ P., SIMAN P., HOLICKÝ I., JANÁK M., KOLLÁROVÁ V., 2004: Metodika datovania monazitu pomocou elektrónového mikroanalyzátora. Mineralia Slov., 36: 225-235.

MAJKA J., BUDZYŃ B., 2006: Monazite breakdown in metapelites from Wedel Jarlsberg Land, Svalbard. Min. Polon., 37 (1).

MICHALIK M., BROSKA I., JACHER-ŚLIWCZYŃSKA K., KONEČNÝ P., HOLICKÝ I., 2004: Dating of gneissic clasts from Gródek on the Jezioro Rożnowskie Lake (Silesian Unit). VIII Ogólnopolska Sesja Naukowa "Datowanie minerałów i skał", Kraków: 101-106.

MICHALIK M., SKUBLICKI Ł., 1999: Phosphate accessory minerals in High Tatra granitoids. Geol. Carpath., 50, Spec. Issue, 123-125.

MONTEL J. M., FORET S., VESCHAMBRE M., NICOLLET C., PROVOST A., 1996: Electron microprobe dating of monazite. Chem. Geol., 131: 37-53.

POPRAWA P., KUSIAK M.A., MALATA T., PASZKOWSKI M., PÉCSKAY Z., SKULICH J., 2005: Th-U-Pb chemical dating of monazite and K/Ar dating of mica combined: preliminary study of „exotic" crystalline clasts from the Western Outer Carpathian flysch (Poland). Pol. Tow. Mineral. Prace Spec., 25: 345-351.

SIMPSON R.K., PARRISH R.R., SEARLE M.P., WATERS D.J., 2000: Two episodes of monazite crystallization during metamorphism and crustal melting in the Everest region of the Nepalese Himalaya. Geology, 28, 5: 403-406.

WING B., FERRY J.M., HARRISON T.M., 2003: Prograde destruction and formation of monazite and allanite during contact and regional metamorphism of pelites: petrology and geochronology. Contrib. Mineral. Petrol., 145: 228-250.

MINERALOGIA POLONICA - SPECIAL PAPERS
Volume 28 - 2006

Jolanta BURDA[1]

U-Pb MONAZITE-(Ce) DATING OF MIGMATITIC GNEISS FROM THE WESTERN TATRA MTS.

INTRODUCTION

Monazite ([LREE, Th]PO_4) is used in geochronological studies because of its high U, Th concentrations and low initial Pb contents. Due to high closure temperatures (>750ºC) for the U-Th-Pb system the measured ages are likely to record the time of monazite formation during a magmatic or metamorphic events (e.g. Cherniak et al. 2004).

This study presents results of conventional U-Pb monazite-(Ce) dating from amphibolite-facies migmatitic gneiss from the Western Tatra Mts. Till now there was no directly proved age of migmatitisation for the basement rocks of the northern part of metamorphic envelope. Supposition about the age of this process is based on xenoliths of migmatites found in much younger High Tatra granite (Poller et al. 2000, 2001).

METHODS OF INVESTIGATION

The sample of migmatitic gneiss was processed using standard mineral separation techniques. Twenty to sixty grains of monazite-(Ce), 50-100μm in diameter, were mounted with standards in epoxy and polished. Microanalyses and backscattered electron (BSE) imaging were carried out using a CAMECA SX 100 microprobe analyzer equipped with 3 wavelenght-dispersive spectrometers in the Inter-Institution Laboratory of Microanalyses of Minerals and Synthetic Substances at the Warsaw University. BSE images have been used for identifying the internal structures of individual monazite grains. The operating conditions were: acceleration voltage – 20 kV, beam current – 50 nA and beam diameter-2μm.

Conventional U-Pb monazite dating were conducted on a Finnigan MAT 262 mass spectrometer, equipped with a secondary electron multiplier-ion counter system at the Geochronology Laboratory, Institute of Geology, University of Vienna. The U-Pb isotopic analyses were carried out on selected monazite grains (six fractions). The selection was based on morphology and visible corrosion (only transparent, clear, inclusion free monazite grains were selected by handpicking under a binocular microscope). The procedures applied for the conventional U-Pb dating are reported in detail by Parrish et al. (1987).

GEOLOGICAL SETTING AND SAMPLE DESCRIPTION

Western Tatra Mts. metamorphic complex is composed of schistose Lower Structural Unit (LSU) and migmatitic Upper Structural Unit (USU), forming

[1] *University of Silesia, Faculty of Earth Sciences, Będzińska 60, 41-200 Sosnowiec, Poland; e-mail: jburda@ultra.cto.us.edu.pl*

together the inverted metamorphic zonation. On the northern part (polish part) of magmatic intrusion metamorphism of Upper Unit took place in the upper amphibolite facies conditions (T = 690-780 ^{o}C, P = 7.5-10 kbar; Burda, Gawęda 1999). Sample of migmatitic gneiss from the USU was taken from Smreczyński Upłaz. The banded migmatitic gneiss is composed of quartz, plagioclase (An_{21-23}), biotite (*fm* = 0.604 - 0.612, TiO_2 = 2.7 - 3.3 wt.%), apatite, sillimanite, zircon and monazite. As the secondary minerals chlorite, epidote and sericite were stated. Migmatitic gneiss is strongly peraluminous (A/CNK = 2.37). Muscovite dehydratation-melting textures are ubiquitous in this rock. Reconnaissance thermobarometry yields P-T conditions consistent with this petrological fact: T $\geq$ 700 ^{o}C. These observations reinforce arguments that partial melting reactions are integral part of the metamorphic evolution of these rocks.

RESULTS

Monazite-(Ce) is abundant component of the analyzed rock. The crystals are almost invariably a yellow color, are usually equant and subhedral (30-140 μm in size). Monazite–(Ce) does not appear to show any notable preference for a single mineral as a host. It is present within or adjacent to biotite, plagioclase and quartz. Monazite-(Ce) crystals are homogeneous in BSE or they display only a weak zoning with no evident core-rim structure. PbO concentrations range from 0.04 to 0.13 wt.% while ThO_2 contents vary from 2 to 7.5 wt.% (typically 3-3.5 wt.%). UO_2 content in monazite-(Ce) is typically in the range of 0.2-1.5 wt.%.

The U-Pb analytical data are plotted in Fig.1. All fractions define a discordia with an upper intercept: 364. 4 ± 2.7 Ma (MSWD = 0.41). Three fractions (A,B,E) define an concordia age of 359.4 ± 0.75 Ma (MSWD = 2.9).

CONCLUSIONS

The analyzed monazite-(Ce) grains crystallized from Upper Devonian to Lower Carboniferous, contemporaneously with the emplacement of voluminous Western Tatra granite body (350-360 Ma) documented earlier by Poller et al. (2001). The metamorphism and partial melting was caused by the heat from the granite intrusion. This is confirmed by the dehydratation melting of muscovite in rocks from Upper Unit (Burda, Gawęda 1999). The crystallization of analyzed monazite-(Ce) occurred in a short period of time, most likely close to the thermal peak (~ 365 Ma) and possibly as a result of melt extraction (~360 Ma). Similar concordant ages of at 356 ± 7 Ma was detected in the migmatites found as xenolithes in granitoids from High Tatra Mts. (Poller et al. 2001). This age is interpreted as the earliest anatectical event in the High Tatra area, which as is turned out correspond to similar event in the Western Tatra Mts.

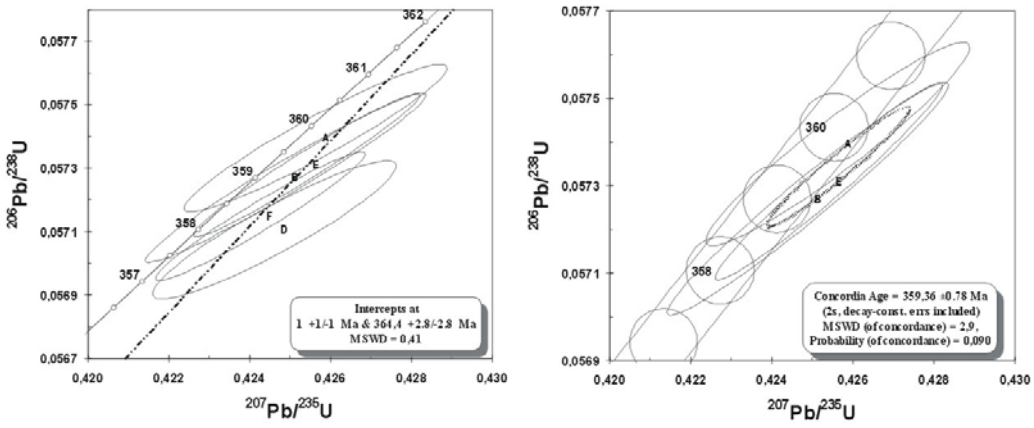

Fig.1. Concordia plot of U-Pb monazite-(Ce) data from migmatitic gneiss from the Western Tatra Mts.

ACKNOWLEDGEMENTS: This study was financially supported by Ministry of Education and Science- Project no. 2 P04D003 29.

REFERENCES

BURDA J., GAWĘDA A., 1999: Petrogeneza migmatytów z górnej części Doliny Kościeliskiej w Tatrach Zachodnich. Arch. Mineral., 52: 163-194.

CHERNIAK D. J., WATSON E.B., GROVE M., HARRISON T.M., 2004: Pb diffusion in monazite. Geochim. Cosmochim. Acta, 68: 829-840.

POLLER U., JANÁK M., KOHÚT M., TODT W., 2000: Early Variscan magmatism in the Western Carpathians: U-Pb zircon data from granitoids and ortogneisses of the Tatra Mountains (Slovakia). Int. J. Earth Sci., 89: 336-349.

POLLER U., TODT W., KOHÚT M., JANÁK M., 2001: Nd, Sr, Pb isotope study of the Western Carpathians: implications for Paleozoic evolution. Schweiz. Mineral. Petrogr.Mitt., 81: 159-174.

PARRISH P.P., RODDICK J.C., LOVERIDGE W.D., SULLIVAN R.W., 1987: Uranium-lead analytical techniques at the geochronology laboratory, Geological Survey of Canada. Geol. Surv. Canada Paper, 87/2: 3-7.

MINERALOGIA POLONICA - SPECIAL PAPERS
Volume 28 - 2006

Jan CEMPÍREK[1], Stanislav HOUZAR[1], Milan NOVÁK[2], Julie B. SELWAY[3], Vladimír ŠREIN[4]

VANADIUM-RICH TOURMALINE FROM GRAPHITIC ROCKS AT BÍTOVÁNKY, CZECH REPUBLIC; COMPOSITIONAL VARIATION, CRYSTAL STRUCTURE

INTRODUCTION

Two distinct morphological, paragenetic and compositional varieties of V-rich dravite were recognized in graphite quartzite from Bítovánky (Houzar, Šrein 1993; 2000; Houzar, Selway 1997). Green to greenish yellow V-rich dravite (GVD) forms columnar crystals to needle-like aggregates, up to l cm in size, sporadically with apparent lineation. It is associated with graphite, V-bearing muscovite I and sillimanite I and seems to be in equilibrium with the associated V-bearing muscovite I. GVD is sporadically zoned with a narrow V-enriched outer zone. Dark brown V-rich dravite (BVD) occurs as imperfectly developed columnar crystal, up to 3 cm long, broken and healed by quartz. BVD is exclusively present in rare, mobilized, ductile, quartz-rich nests and veins, locally occurring within the graphitic quartzite. It is associated with K-feldspar, green flakes of V-bearing muscovite II and sillimanite II (Houzar, Selway 1997).

METHODS

A fragment of each type of V-rich dravite was ground to a sphere and mounted on a Nicolet *R3m* automated four-circle diffractometer at the University of Manitoba, Winnipeg. The crystals (two of GVD and two of BVD) used in the collection of the X-ray intensity data were analyzed by electron microprobe using a CAMECA SX50 operating in the wavelength-dispersion mode.

Chemical variation and assemblage of several tourmaline samples was studied on electron microprobe JEOL JXA-50A at the Geological Institute of the Czech Academy of Sciences, Praha.

The structural formula of tourmaline was calculated based on 15 cations, non-analyzed oxides were calculated using following assumptions: B_2O_3 (B = 3 apfu), Li_2O (Li = 0 apfu) and H_2O (charge-balanced formula). All Fe was assumed to be divalent.

[1] *Dept. of Mineralogy and Petrography, Moravian Museum, Zelný trh 6, 659 37 Brno, Czech Republic; jcemp@sci.muni.cz*

[2] *Institute of Geological Sciences, Masaryk University, Kotlářská 2, 611 37 Brno, Czech Republic*

[3] *Precambrian Geoscience Section, Ontario Geological Survey, 933 Ramsey Lake Road, Sudbury, ON P3E 6B5, Canada*

[4] *Institute of Rock Structure and Mechanics, Academy of Sciences of the Czech Republic, V Holešovičkách 41, 182 09 Prague 8, Czech Republic*

RESULTS

Cell parameters for XRD-examined samples are listed in Table 1. In the structure, there is Al-Mg disorder in the both types of V-rich dravite, as Al and Mg occupy both the Y and Z sites. The V is assigned to both Y and Z sites and has a valence of 3+. The O(l) and O(3) sites are occupied dominantly by OH.

Table 1. Cell parameters of Bítovánky V-dravite.

	BT1	BT2	BT3	BT4
a	15.930(2)	15.917(2)	15.9412(8)	16.925(2)
c	7.184(1)	7.177(1)	7.1753(6)	7.162(1)

Green dravite (GVD) is sporadically zoned with V-enriched rims; brown dravite (BVD) is rather homogeneous. The major cations vary from 0.16 - 1.01 and 0.51 - 0.79 *apfu* V; 2.36 - 2.56 and 1.75 - 1.94 *apfu* Mg (including both ^{Y}Mg + ^{Z}Mg); 0.41 - 0.67 and 0.42 - 0.48 *apfu* Na; 0.16 - 0.31 and 0.11 - 0.22 *apfu* Ca, in the GVD and BVD, respectively. The substitutions include predominant VAl_{-1} and, in lesser extent, $[(V,Al)\square](MgNa)_{-1}$ which is a combination of the former with dravite-magnesiofoitite substitution (Fig. 1).

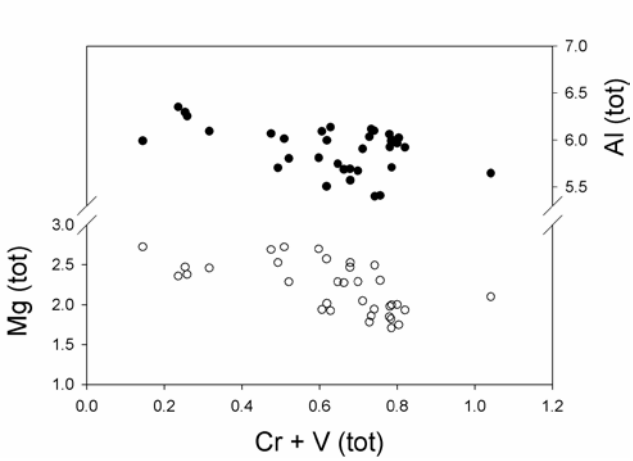

Fig.1. Variation of Cr+V with Mg and Al.

Introduction of vanadium in the structure seems to allow the increase of magnesiofoitite end-member in the solid solution (Fig. 2). The vanadiumdravite (Reznitzsky et al. 2001) component content reaches up to 30 mol. %. Compared to the world occurrences, the Bítovánky V-rich tourmaline has elevated Ca and very low Cr content.

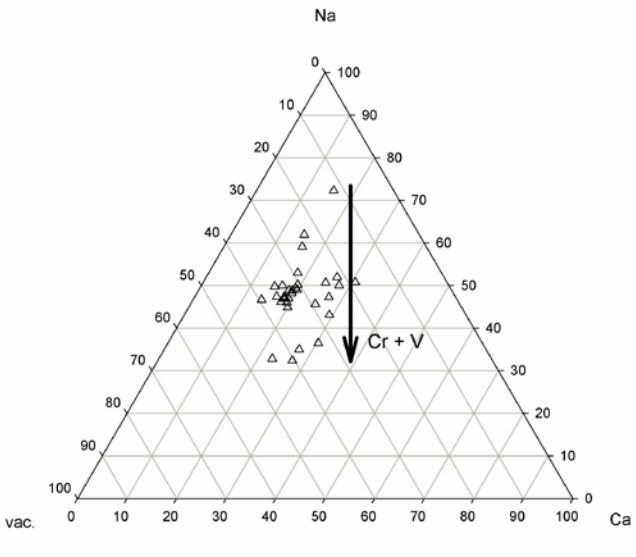

Fig. 2. X-site diagram (Ca vs. Na. vs. vacancy), with marked Cr + V increase trend.

ACKNOWLEDGEMENTS: This work was supported by the research project MK00009486201 to JC and SH, research project MSM0021622412 to MN and IRSM 340.410 to VŠ.

REFERENCES

HOUZAR S., SELWAY, J.B., 1997: Bítovánky near Třebíč. Graphite quartzite with minor V-bearing muscovite and accessory V-rich dravite. Tourmaline 1997 Field trip guidebook, 85-91.

HOUZAR S., ŠREIN V., 1993: Graphite quartzite with vanadium - bearing tourmaline from Bítovánky near Želetava, West Moravia. A preliminary report. Acta Mus. Morav. Sci. Nat, 78: 211-212.

HOUZAR S., ŠREIN V., 2000: Variation in chemical composition of V-bearing muscovite during metamorphic evolution of graphitic quartzites in the Moravian Moldanubicum. J. Czech. Geol. Soc., 45: 143-148.

REZNITSKY L.Z., SKLYAROV E.V., USHAPOVSKAYA Z.F., NARTOVA N.V., KASHAEV A.A., KARMANOV N.S., KANAKIN S.V., SMOLIN A.S., NEKRASOVA N.A., 2001: Vanadiumdravite, $NaMg_3V_6[Si_6O_{18}]$ $[BO_3]_3$ $(OH)_4$ – a new mineral of the tourmaline group. Zapisky Vseros. Miner. Obsch.., 130: 59-72 (in Russian).

MINERALOGIA POLONICA - SPECIAL PAPERS
Volume 28 - 2006

Martin CHOVAN[1]

HYDROTHERMAL ORE MINERALIZATIONS HOSTED BY VARISCAN TATRIC BASEMENT

INTRODUCTION

Tatric Unit is an extensive crustal sheet composed of the pre-Alpine (generally Variscan) crystalline basement and its sedimentary cover. The basement is mainly composed of crystalline rocks: medium- to high-grade Early Paleozoic volcano-sedimentary complexes – paragneisses, micaschits, orthogneisses ana amphibolites and phillites and several suites of Variscan granitoides (360 - 320 Ma) intruding mostly the high-grade gneiss-migmatitic complexes. The crystalline basement complexes are incorporated into several thick-skinned Variscan nappe structures. Autochthonous Mesozoic sedimentary covers as well as the crystalline complex are overthrusted by the Mesozoic nappes. Today`s horst structure of the territory was created by Paleogene and Neogene fault tectonics.

Hydrothermal ore mineralizations can be divided (Chovan et al. 1996), into several principal types: molybdenite, scheelite, arsenopyrite – pyrite and gold, stibnite and sulphosalts (Sb, Pb, Cu), carbonates – siderite and quartz vein with sulphide Cu; Pb, Sb, galena – base-metal, barite, hematite.

METHODS

Mineralogical – pragenetical study was combined by analytical metods (microprobe analysis, X-ray diffraction), fluid inclusions research and study of stable and radiogenic isotopes.

RESULTS AND DISCUSSION

Occurrences of **molybdenite** (Tab. 1) were found in the Malé Železné and Dúbrava in the Nízke Tatry Mts. Relationship to other mineralization types is unclear, however, they belong to the higher-thermal, older types. **Scheelite** (tungsten) mineralization is known in the area of Jasenie and in the Sb deposit Dúbrava in the Nízke Tatry Mts. **Arsenopyrite – pyrite** mineralization with "invisible" gold is present in almost every occurrence of stibnite ores as the older, higher thermal one. Mössbauer spectra of arsenopyrite show IS values corresponding to chemically bound gold (Dúbrava, Vyšná Boca, Pezinok) and metallic gold (Jasenie, Dúbrava). **Gold** with arsenopyrite – pyrite ores is most commonly found together with the stibnite mineralization in the deposit Magurka, Dve Vody, Mlynná dolina - Valachovo, as well as in the scheelite deposit Jasenie. Separate occurrences of quartz – gold veins are known in the Harmanec (Nízke Tatry Mts.), Pezinok – Staré mesto (Malé Karpaty Mts.) and Kriváň (Vysoké Tatry Mts.) (Bakos et al. 2002). **Stibnite** deposits Magurka, Medzibrod, Lom and Dúbrava in the Nízke Tatry Mts. were the most important ones from the viewpoint

[1] *Department of Mineralogy and Petrology, Comenius University, Mlynská dolina G, 842 15 Bratislava, Slovak Republic; chovan@fns.uniba.sk*

of exploitation. Generaly the ore mineralization is focused into hydrothermal veins, in the deposit Medzibrod is composed of bedded veins and lenses in phyllonites. Stibnite mineralization in the Malé Karpaty Mts. (Pezinok, Pernek) is located in beds of tectonically deformed black schists. Numerous occurrences and deposits of **carbonate** (siderite, ankerite) mineralizations in the area of Vyšná Boca and Ďumbier (Nízke Tatry Mts.) mostly in various types of crystalline schists, less in granitoids and also in Triasic sediments. Younger is **REE-silicate** assemblage (Ozdín 2003). In accompained **quartz veins** are accumulated Cu sulphides – tetrahedrite and chalcopyrite, galena and Cu, Sb, Pb, Bi, Ag sulphosalts (Pršek 2004). The most important galena – base metal deposit in the tatric unit is the Jasenie – Soviansko. **Barite** occurs as separate veins in the Malužiná deposit in Permian tholeitic basalts and andesites. Barite is found also in siderite, galena and less commonly stibnite deposits as a product of the youngest mineralization stage. Young **hematite** mineralization was described from many places in the Tatric tectonic Unit.

Table 1. Tectonometamorphic stages and connected mineralizations (modified by Chovan et al. 2006).

Tectonometamorphic stages	Mineralizations
Late-Variscan cooling of granodiorite to 300-400^{o}C before ~300 Ma shear zones, metamorphosis in greenschist facies, intrusions of I-type and A-type granites	molybdenite (quartz veins in granitoides) mineralizations in shear zones - in metamorphosed complexes: Sb, As, Au in black shales; in granitoides and gneisses: scheelite in quartz veins arsenopyrite-pyrite and gold in quartz veins
Jurassic continental rifting 210-170 Ma	stibnite – sfalerite, sulphosalts (Sb, Pb, Cu)
Cretaceous metamorfosis and post metamorfic cooling and extension 100–80 Ma	carbonates (siderite), REE-silicate and quartz sulphide (Cu; Sb, As, Pb), galena – base metal, barite, hematite; recrystallisation of oldest sulphides ores (stibnite)

Fluid inclusion and stable isotope data have discriminated among several contrasting types of hydrothermal mineralizations in the Variscan basement of the Western Carpathians (Chovan et al. 1995, Majzlan et al. 2001, Hurai et al. 2002, Chovan et al. 2006). High temperature assemblages with molybdenite, scheelite, arsenopyrite – pyrite and gold have been triggered by influx of low-saline CO_2 – enriched agueous fluids of magmatic or metamorphic origin. Mesothermal quartz – sulphidic (stibnite, berthierite, zinkenite, sphalerite, tetrahedrite) assemblage have precipitated from NaCl – KCl aqueous solutions, representing mostly deeply

circulating meteoric water. Microthermometry data of infrared microscopy in stibnite (Chovan et al., 1999) indicate simple NaCl – KCl solutions. $CaCl_2$ – bearing brines revealed in quartz – carbonate, carbonate – sulphide, barite and hematite assemblages correspond to formation- or halite-fractionated marine water.

CONCLUSION

The high temperature assemblages – molybdenite, scheelite, pyrite – arsenopyrite and gold, may be genetically linked to the evolution of the late Variscan granitoides and retrograde metamorfosis. Stibnite and sfalerite-Pb-Sb sulfosalts connected by Jurassic continental rifting. Carbonate – siderite and quartz – sulphide and part of older sulphide mineralization were recrystallized or they originated by mobilization during the Alpine metallogenetical cycle (Cretaceous metamorfism and post metamorfic cooling and extension).

REFERENCES

BAKOS F., PRŠEK J., TUČEK P., 2002: Variscan granitoid hosted hydrothermal gold deposit Pezinok - Staré mesto (Malé Karpaty Mts., Western Carpathians): Mineralogy, paragenesis, fluid inclusion study. Slovak Geol. Mag., 8: 37-47.

HURAI V., CHOVAN M., KRÁĽ J., LEXA J., PROCHASKA W., 2002: Origin of sulfide-bearing hydrothermal deposits hosted by Variscan basement of the Western Carpathans in light of new fluid inclusion, stable isotope and geochronological data. Geol. Carpath., Special issue, 53: 96-97.

CHOVAN M., HURAI V., SACHAN H.K., KANTOR J., 1995: Origin of the fluids associated with granodiorite-hosted, Sb-As-Au-W mineralization at Dúbrava (Nízke Tatry Mts, Western Carpathians). Min. Deposita, 30: 48-54.

CHOVAN M., SLAVKAY M., MICHÁLEK J., 1996: Ore mineralizations of the Ďumbierske Tatry Mts. (Western Carpathians, Slovakia). Geol. Carpath., 47, 6: 371-382.

CHOVAN M., LÜDERS V., HURAI V., 1999: Fluid inclusions and C, O-isotope constraints on the origin of granodiorite-hosted Sb-As-Au-W deposit at Dúbrava (Nízke Tatry Mts., Western Carpathians). Terra Nostra, 99, 6: 71-72.

CHOVAN M., HURAI V., PUTIŠ M., OZDÍN D., PRŠEK J., MORAVANSKÝ D., LUPTÁKOVÁ J., ZÁHRADNÍKOVÁ J., KRÁĽ J., KONEČNÝ P., 2006: Zdroje fluid a genéza mineralizácií tatrika a severného veporika. Manuscript, Archív ŠGÚDŠ, Bratislava, 1-250. (in Slovak)

MAJZLAN J., HURAI V., CHOVAN M., 2001: Fluid inclusion study on hydrothermal As-Au-Sb-Cu-Pb-Zn veins in the Mlynná dolina valley (Western Carpathians, Slovakia). Geol. Carpath., 52: 277-286.

OZDÍN D., 2003: Mineralogy and genese of siderite mineralization in Ďumbierske Tatry Mts. Dissertation thesis, Archive of Dpt. mineralogy and petrology, Comenius University, 1-194. (in Slovak)

PRŠEK J., 2004: Chemical composition and crystal chemistry of sulphosalts from sulphidic mineralizations of Western Carpathians. Dissertation thesis, Archive of Dpt. mineralogy and petrology, Comenius University, 1-135. (in Slovak)

MINERALOGIA POLONICA - SPECIAL PAPERS
Volume 28 - 2006

Nikita Vladimirovich CHUKANOV[1]

APPLICATION OF the IR SPECTROSCOPY IN MINERALOGY: MODERN TRENDS

INTRODUCTION

Despite the fact that IR spectroscopy is one of the most effective methods of substance investigation, its employment in mineralogy is still restricted. The main reasons of this situation are the absence of sufficiently full handbooks and prevailing tendency to deal with discrete bands, but not with a spectral curve "as a whole". In the period from 1991 to 2006 a database including about 3000 IR spectra of more than 2200 mineral species was created. In some cases IR spectrum (even in its simplified discrete form) is the most sensitive tool to detect fine features of crystal structures or specific isomorphous substitutions.

FORCE CHARACTERISTICS AND CONDENSATION OF COORDINATION POLYHEDRA

Cations in oxygen compounds can be arranged in order of decreasing force characteristics in the sequence $T \rightarrow M \rightarrow D \rightarrow A$ (where T = Si, Al, P, B, Be with the coordination number CN = 4; M = Ti, Nb, Zr, Fe^{3+}, Y, Mn^{3+}, Sn^{4+}, W^{6+} *etc*., CN = 6; D are bivalent cations Mn^{2+}, Fe^{2+}, Mg, Zn, Ca *etc*., CN = 6; A are large low-valent cations Na, K, Ca, Sr, Ba, Pb^{2+}, $(H_3O)^+$ *etc*., CN > 6). In the IR spectra of MHM, the ranges of stretching frequencies involving the H-O, T-O, M-O, D-O and A-O bonds do not overlap; in the order they are: 2000-3700, 850-1100, 550-750, 400-500 and <400 cm^{-1}. Specific values of the frequencies within each of these ranges are due to several factors, the most important being hydrogen bonding and linkage of framework-forming polyhedra. *E. g*. for aluminosilicates with the anion stoichiometry $Si_xAl_yO_z$ the following correlation has been found by Chukanov (1995): $\langle\nu_{Si\text{-}O}\rangle$ (cm^{-1}) = $(337.8t + 1827)(0.6428t + 1)^{-1}$ where $t = z(x + y/2)^{-1}$.

Condensation of MO_6 and DO_6 octahedra leads to changes of the $\langle\nu_{(M,D)\text{-}O}\rangle$ values. For manganese oxides, a linear correlation exists between wavenumbers of the strongest bands of Mn-O-stretching vibrations and the number *n* of edges shared per MnO_6 octahedron – see Potter, Rossman (1979). Similarly, linking of chains of $(Ti,Nb)O_6$ octahedra (M-octahedra) by additional D-octahedra (D = Fe, Mg, Mn or Zn) in the labuntsovite group results in a linear correlation between $\langle\nu_{M\text{-}O}\rangle$ (in the range 660-700 cm^{-1}) and the number of D atoms per formula unit – see Chukanov, Pekov (2005). On the basis of new data for gjerdingenite-Na and gjerdingenite-Ca (Pekov et

[1] *Institute of Problems of Chemical Physics, Chernogolovka, Moscow oblast, 142432, Russia; chukanov@icp.ac.ru*

al., in press), this correlation can be generalized for the case D = $(Fe,Mg,Mn,Zn)_xCa_yNa_z\square_{1-x-y-z}$: ν (cm^{-1}) = 667 + 27.02*x* +18.32*y* + 8.60*z*. The coefficients of this correlation 27.02, 18.32 and 8.60 (cm^{-1}) reflect force characteristics of the links (Ti,Nb)-O-(Fe,Mg,Mn,Zn), (Ti,Nb)-O-Ca and (Ti,Nb)-O-Na respectively.

THE ROLE OF IR SPECTROSCOPY IN THE DEFINITION OF NEW MINERAL SPECIES

In the course of the addition of new data to the database on IR spectra, we observed that in many cases two samples, formally treated as varieties of the same mineral species (on the basis of the X-ray powder diffraction data and electron microprobe analysis) give essentially different IR spectra. In most such cases, subsequent investigation of crystal structure demonstrated that we deal really with mineral species, different by symmetry, unit cell dimensions and/or site population in the unit cell. As a result, more than 70 new minerals (approved by the IMA CNMMN) have been discovered in the period 1998-2005. The examples are: shirokshinite (an analogue of tainiolite with Na instead of Li in octahedral position; the substitution of Li for heavier Na results in long-wave band-shifts); atencioite, nabalamprophyllite (additional band splitting demonstrates cation ordering accompanied by symmetry lowering in comparison with their analogues, greifensteinite and barytolamprophyllite); paratsepinite-Na (additional band splitting demonstrates unit cell doubling in comparison with tsepinite); clinobarylite (band shifts and rearrangement of band intensities due to the change of framework topology in comparison with barylite); golyshevite and mogovidite (hypercalcium eudialyte-group minerals with CO_3^{2-} substituting usual anions OH, F, Cl in the *X* site); vitimite, rudenkoite (unique IR spectra demonstrate their unique structure types).

EXPERT SYSTEM FOR THE DIAGNOSTICS OF MINERALS BY IR SPECTRA

The above examples demonstrate that even traditional variant of IR spectroscopy (dealing with discrete absorption bands) still preserves its importance for the definition of mineral species. In the new approach by Dubovitskii et al. (2004), full spectral curves of standard samples are considered as elements of a functional or as elementary units of a multidimensional space. The analysis is based on the expansion of a given spectrum over the full basis (*i. e*. full set of reference spectra) using the criteria of non-negativity, continuality and best approximation. It makes possible quantitative analysis of multiphase mixtures. On the other hand, on the basis of this approach, a quantitative IR-spectroscopic criterion of crystal-chemical affinity between different minerals can be introduced.

On the basis of this approach, expert system for a multi-step diagnostics of minerals, even that, whose spectrum is absent in the basis, has been realized. The usual procedure of such diagnostics on the example of labuntsovite-Mn is given below:

- Step 1. Expansion of the spectrum over the basis shows that 8% of the basis components (most of which are silicates, and minor part - hydroxides) give non-zero contribution. So, the analysed mineral is identified as a silicate.
- Step 2. The spectra of non-silicate minerals are deleted from the spectrum. In this case expansion of the spectrum over the basis shows that among the components with non-zero contributions titanosilicates and ring silicates prevail.
- Step 3. Expansion over the basis containing only titanosilicates and ring silicates shows that 84% of integral intensity give IR spectra of only two minerals belonging to the labuntsovite group, i. e. labuntsovite-Fe and lemmleinite-Ba. So, the analysed mineral is the member of the labuntsovite group.

This result makes clear the reason of the contribution of IR spectra of hydroxides in the expansion on the Step 1: labuntsovite-group minerals contain much OH groups connected with Ti.

REFERENCES

CHUKANOV N. V., 1995: On infrared spectra of silicates and aluminosilicates. Zapiski Vseross. Mineral. Obs., 124, 3: 80-85. (in Russian)

CHUKANOV N. V., PEKOV I. V., 2005: Heterosilicates with tetrahedral-octahedral frameworks: Mineralogical and crystal-chemical aspects. Reviews in Mineralogy and Geochemistry, Vol. 57: Micro-and mesoporous mineral phases. Editors: G.Ferraris & S.Merlino, 105-143.

DUBOVITSKII V. A., CHUKANOV N. V., VOZCHIKOVA S. A., 2004: Complex diagnostics of inorganic compounds by the IR absorption curve. Khimicheskaya Fizika, 23, 90-100.

PEKOV I.V., CHUKANOV N.V., TARESOFF P., YAMNOVA N.A., ZADOV A.E. (in press): Gjerdingenite-Na and gjerdingenite-Ca – two new minerals of the labuntsovite group. Canad. Miner.

POTTER R. M, ROSSMAN G. R., 1979: The tetravalent manganese oxides: identification, hydration, and structural relationships by infrared spectroscopy. Amer. Mineral., 64: 1199-1218.

MINERALOGIA POLONICA - SPECIAL PAPERS
Volume 28 - 2006

Renata ČOPJAKOVÁ[1], *Radek ŠKODA*[1]

MONAZITE HYDROTHERMAL ALTERATION DURING HIGH-TEMPERATURE DIAGENESIS OF THE GREYWACKES FROM THE DRAHANY UPLANDS (BOHEMIAN MASSIF, CZECH REPUBLIC)

INTRODUCTION

Monazite is a promising mineral for in-situ U-Th-Pb geochronology. Electron microprobe dating is valuable due to its spatial resolution, low matrix effects and short time of analysis. Monazite is typically present in heavy mineral assemblages from sediments and is usually considered to be stable in sedimentary environments. Suggestion that monazite may decompose during diagenesis has been debated recently (Mathieu et al. 2001). They reported monazite alteration to Th-OH silicate phase in the sandstones by saline diagenetic fluids at about 140 °C and 1 kbar.

Drahany Uplands is the southern part of the Moravo-Silesian Culm Basin. Basin sedimentation commenced about 340 Ma and finished about 325 Ma ago. Franců et al. (1999) proposed diagenetic temperature at about 130-170 °C in the southern part of the basin and at about 170-200 °C in the northwestern part of the basin. Monazite is accessory mineral in prevailing metamorphic and magmatic rock types in the conglomerates and is present in heavy mineral assemblages as well.

METHODS

Heavy mineral concentrates were separated from greywackes and mounted in the epoxy resin. The monazite and its alteration products were examined using CAMECA SX 100 electron microprobe. Operating conditions were 15 kV an accelerating voltage, a beam current of 80 nA for monazite and 10 nA for monazite alteration products and a beam diameter of <1 μm for monazite and 5-10 μm for monazite alteration products. Peak counting times were 20 s for major elements, 30-60 s for minor elements and 240 s for Pb.

RESULTS

Detrital monazite in heavy mineral assemblages is present usually as 40-100 μm, sometimes as small 10-20 μm grains enclosed in quartz or zircon. Detrital monazite is commonly homogeneous in BSE, it exceptionally shows an irregular zoning. Some monazite grains are replaced by apatite and rhabdophane propagating from rim inwards and along fractures (Fig. 1a) or by mixture of apatite and poorly defined REE minerals. Some grains from the northwestern part of the Culm basin are present as porous, corroded relicts (Fig. 1b).

Based on chondrite-normalised REE patterns were distinguished two types of detrital monazites without any significant alteration observed in BSE image (Fig. 2). Type I has common REE pattern similar to that of monazite from rock pebbles, and type II more depleted in heavier REE and Y. Detrital monazites type II usually

[1] *Joint Laboratory of Electron Microscopy and Microanalysis, Masaryk University and Czech Geological Survey, Kotlářská 2, 611 37 Brno, Czech Republic*

yield unrealistically low ages 268-318 Ma, younger than age of sedimentation. Monazite type I was found in all stratigraphic units, monazite type II was observed only in the northwestern part of the Drahany Uplands.

Porous, corroded relicts show strongly inhomogeneous composition. In the central part the composition corresponds to typical monazite with 4.5 wt. % ThO_2, 1 wt.% UO_2, 0.2 wt. % PbO and up to 2.6 wt. % Y_2O_3 and REE pattern is comparable with those from detrital monazite type I (Fig. 2b). In other parts, the analyses give low totals 96-98 wt. % and disrupted stoichiometry (excess in P-site and deficit in REE-site). Content of Th, U, Pb and Y is very low (0.1-0.8 wt. % ThO_2, 0.4-0.6 wt. % Y_2O_3, U and Pb around the detection limit) and REE patterns show two types of anomalies (Fig. 2b). The first is characterized by depletion in heavier REE (Gd, Dy, Er) and Ce remains as a dominant REE. The REE pattern of type I is similar to the REE patterns observed in detrital monazite type II. The second type is characterized by depletion of heavier REE (Dy, Er) and light REE (La, Ce) and Nd (0.33-0.37 *apfu*) predominate over Ce (0.28-0.32 *apfu*).

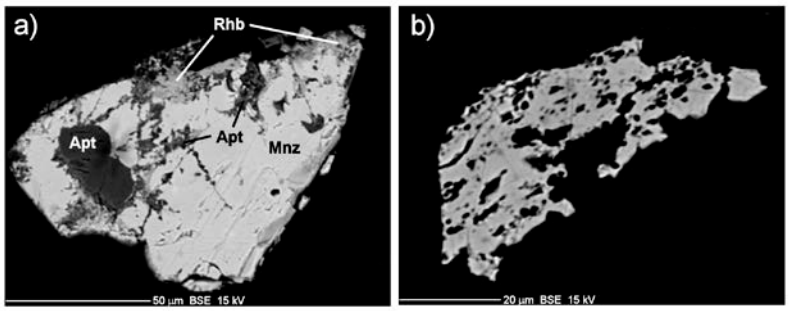

Fig. 1. BSE images of altered detrital monazites; a) altered monazite grain replaced from rim inwards and along fractures by apatite and rhabdophane; b) highly altered monazite.

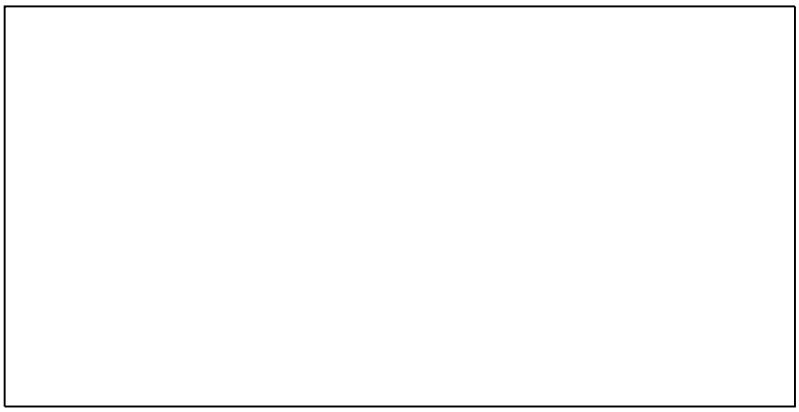

Fig. 2. Chondrite normalised REE patterns. Grey area stands for values bellow detection limit of EMP; a) detrital monazite; short dashed area – monazites of type I (this field is marked in b plot for comparison), long dashed area – monazites of type II; b) altered detrital monazite relict; cross – relict with monazite composition, square – anomalous composition type I, diamond – anomalous composition type II.

CONCLUSIONS

The grade of alteration positively correlates with intensity of diagenesis from the SSE to the NNW. We suggest that detrital monazite grains of type II, which in BSE image don't show any alteration feature, represent the first stage of monazite alteration characterized by minor depletion of heavier REE (Gd, Dy, Er), Y, Th, Pb, and in many cases by disrupted low ages. Porous corroded monazite relicts we can regard as advanced monazite alteration and/or transformation to rhabdophane. More probably it is monazite alteration, exhibiting by depletion of Gd, Dy, Er, Y, Th, U and Pb, in some cases also LREE (La,Ce), disrupted stoichiometry and decrease of totals. Rhabdophane from Culm sediments shows deficit in P-site and excess in REE-site, whereas altered parts of porous monazite grains have deficit in REE-site. Moreover, rhabdophane contains higher Pb content compared with typical monazite composition, but in altered parts of porous monazite grains Pb is very low (Škoda, Čopjaková 2006).

Based on composition of authigenic minerals replacing monazite grains and authigennic minerals from greywackes (fluorapatite, rhabdophane-(Ce), synchysite-(Ce)) (Škoda, Čopjaková 2006) we can propose, that diagenetic fluids were enriched in F, Ca, CO_2 a P. Stability and alteration features of heavy mineral assemblages testify for neutral to slightly alkaline conditions in the Culm basin. Based on Poitrasson's et al. (2004) experiments, it is evident that in neutral pH and temperature range 120-200 °C especially fluoride ions effect monazite solubility. $REEF_2^+$ and $REEF^{2+}$ complexes are the most abundant species in the solutions. At higher fluid temperature (over 250 °C) hydroxide complexes become dominant. However, such high temperatures in the Culm basin were not reached.

ACKNOWLEDGEMENTS: Financial support from the internal project of the CGS 3316 is gratefully acknowledged.

REFERENCES

FRANCŮ E., FRANCŮ J.,KALVODA J., 1999: Illite crystalinity and vitrinite reflectance in Paleozoic siliciclastics in the Bohemian Massif as evidence of thermal history. Geol. Carpath., 50: 65-71.

MATHIEU R., ZETTERSTROM L., CUNEY M., GAUTHIER-LAFAYE F., HIDAKA H., 2001: Alteration of monazite and zircon and lead migration as geochemical tracers of fluid paleocirculations around the Oklo-Okélondo and Bangombé natural nuclear reaction zones (Franceville basin, Gabon). Chem. Geol., 171: 147-171.

POITRASSON F., OELKERS E., SCHOTT J., MONTEL J.M., 2004: Experimental determination of synthetic $NdPO_4$ monazite end-member solubility in water from 21 °C to 300 °C: Implications for rare earth element mobility in crustal fluids. Geochim. Cosmochim. Acta, 68: 2207-2221.

ŠKODA R., ČOPJAKOVÁ R., 2006: Authigennic REE minerals from Culm sediments of the Drahany Uplands and their significance for diagenetic processes. Miner. Polon., this volume.

MINERALOGIA POLONICA - SPECIAL PAPERS
Volume 28 - 2006

Rastislav DEMKO[1], *Mário OLŠAVSKÝ* [1]

THE ROLE OF PLAGIOCLASE NETWORK IN CRYSTALLIZATION OF BASALTIC EFUSIVE ROCKS - IMPLICATIONS FOR AUGITE CRYSTAL GROWTH AND OPEN SYSTEM DIFFERENTIATION

INTRODUCTION

Plagioclase crystal network occurs in slowly cooled basaltic magmas of huge basalt flows and subvolcanic bodies. Formation of such a network controls further crystallization of other minerals in open to closed conditions. Various solidification processes operate in these conditions: fractional crystallization, magma mixing, floating and filter pressing (Philpotts et al. 1996; 1999). Petrographic study of Permian basaltic rocks of Hronicum unit, Western Carpathians Mts., involving chemical composition of augite, provides an evidence for catalytic behaviour of early-formed *plagioclase network* (PN) and special mode of clinopyroxene crystallization by "climbing" on plagioclase skeleton.

CRYSTALLIZATION HISTORY OF BASALTS

The aphiric parental basaltic melt had undergone early massive crystallization of plagioclase, which yielded a 3-dimensional crystal network for the sake of minimalization of free surface energy. Resulting network contains isolated intranetwork cells filled by melt. After formation of PN, crystallization continued with ilmenite and augite together with small volume of plagioclase. Process leads to decreasing of free interstitial melt volume and melt permeability. Solidification of some basalt has finished when finally the glass quenched after further chilling. Crystallization of slowly cooled basalt was accomplished by pigeonite and in the most solidified rocks by quartz. This solidification history follows ideal tholeiitic differentiation type.

Rocks of these characteristics are widespread in Lower Permian of Malužiná formations and Upper Carboniferous to Lower Permian of Nižná Boca (NB) formations of Hronicum Unit. Detailed study was focused to Slávča locality (NB), which is situated 5 km northern of Tisovec city. There are Upper Carboniferous clastic sediments cross cutted by subvolcanic dike swarms. Dikes consist of subophitic to intersertal massive basalts.

CLINOPYROXENES COMPOSITION AND SPATIAL DISTRIBUTION

Clinopyroxenes (Cpx) comprise augite and diopside. General feature of the Cpx is decrease of Al, Ti, Cr in accordance with decreased Mg. Fe_{Tot}, Mn and Na show strong negative correlation relationship with Mg. Significant relations exist between Al, Si in tetrahedral position and #Mg [$Mg/(Mg+Fe^{2+})$]. Ascent of silica activity is reverse to Al content. The Cpx composition reflects extremely low Al activity in parental melt during crystallization, due to strong Al partitioning from

[1] *State Geological Institute of Dionýz Štúr, Banská Bystrica regional centre, Kynceľovská 10, 974 01 Banská Bystrica, Slovak Republic, demko@gssrbb.sk*

percolating melt to the growing plagioclase crystal network. In several cases, strong Al deficit corresponds with entry of Fe^{3+} to the Cpx tetrahedral site.

Clinopyroxenes (augite to diopside) of subvolcanic dike basalts from the Slávča locality, which are devoid of pigeonite and quartz, may be discriminated into three main groups:

(A) Cpx with composition En(49.3-40.6)Fs(15.2-6.1)Wo(46.7-40.9) #Mg(88.6-74.2). Strong variations occur in the composition of Al_2O_3 (4-1.7 wt. %); TiO_2 (1.5-0.5 wt. %). Cpx hosts skeletal ilmenite that has probably crystallized epitaxially.

(B) Cpx En(46.1-39.5)Fs(16.3-9.2)Wo(45.6-42.2) #Mg(83.3-71). This is a transition between the groups (A) and (C).

(C) With composition En(39.8-31.9)Fs(22.5-11.3)Wo(48.9-43.8) #Mg(77.9-58.6). From the A) group differ markedly by the contents of Al_2O_3 (0.55-0.24 wt. %), TiO_2 (0.2-0.06 wt. %) and low MgO (14-11 wt. %), indicating the strong decrease of Al, Ti activities during the melt differentiation in PN.

Spatially, the Cpx A, B, C occur in intimate relation, often forming growth zones of the same Cpx crystal. Their succession in the growth zonation is however not uniform, following patterns occur (core → rim): A→B→C, A→C, but also A→C→B and C→A.

Based on chemical Cpx heterogeneities and spatial Cpx-Plg relationships (Fig. 1 and 2), following crystallization scenario of Cpx is proposed: After PN formation, Cpx starts to crystallize concurrently. Thin plagioclase (Plg) forming an early network continue in growth and increase their individual volume. Plg depleted melt fraction mixes with variably fertile melts in interstitial spaces and shifts the resulting composition to cpx phase volume. Similarly Cpx crystallization moves phase volume of residual melt along Plg-Cpx cotectic liquid line of descent. Because of low permeability of partially melted basalt, residual melt mixing and homogenization is strongly restricted. Variably mixed melt fractions located in network cells and channels essentially keep their compositional heterogenity until final quenching. Other process operated in conditions of higher melt viscosity and lower temperature on plagioclase melt interface. During transfer of plagioclase component to growing PN, neighbouring melt layer is enriched in Cpx phase, which may readily crystallize on the Plg surface. In this way plagioclase surface serves as active catalyser for Cpx nucleation. This “plagioclase-near-surface-controlled” Cpx nucleation allows crystallization of Cpx by climbing on Plg network.

Complex Cpx spatial heterogeneities in Permian subvolcanic bodies of Hronicum Unit result from crystallization from heterogeneous insufficient mixed melt fractions coupled by climbing crystallization mechanism.

REFERENCES

PHILPOTTS A.R., BRUSTMAN C.M., SHI J., CARLSON W.D., DENISON C., 1999: Plagioclase-chain networks in slowly cooled basaltic magma. Am. Mineral., 84: 1819-1829.

PHILPOTTS A.R., CARROLL M., HILL J.M., 1996: Crystal-mush compaction and the origin of pegmatitic segregation sheets in a thick flood-basalt flow in the Mesozoic Hartford basin, Connecticut. J. Petrol., 37: 811-836.

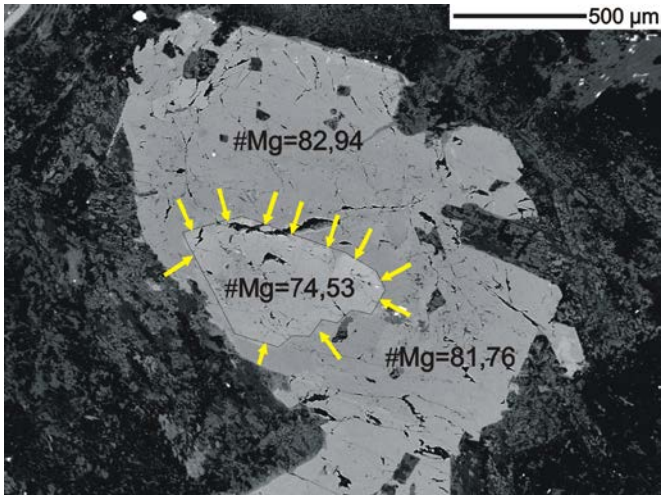

Fig. 1. Detail of subophitic Cpx in Plg network. Plagioclases are strongly saussuritized. Clinopyroxene crystallized from Plg surface towards the centre of PS cell. The light central part preserves the morphology of PS cell being dictated by Plg configuration. BSE.

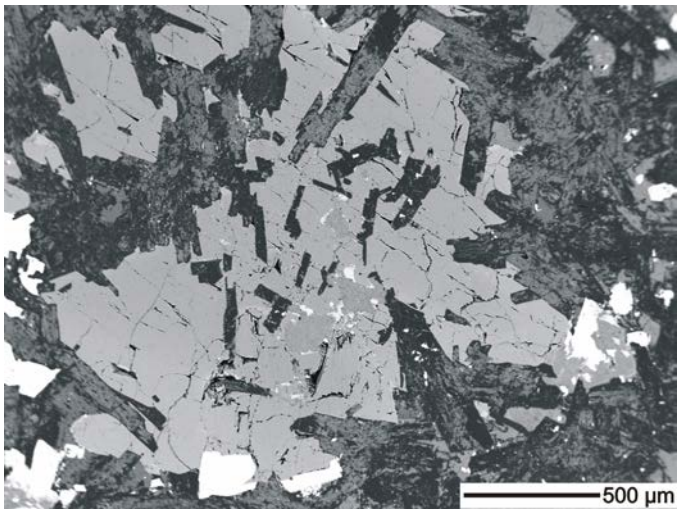

Fig. 2. Cpx crystal placed in Plg network cell. There are bright white ilmenite and spinel crystals around the cell boundary. Arm of Plg chain intergrows with Cpx. BSE.

MINERALOGIA POLONICA - SPECIAL PAPERS
Volume 28 - 2006

Petr DOBEŠ[1], Ivana JAČKOVÁ[1], Bohuslava ČEJKOVÁ[1], Josef KLOMÍNSKÝ[1]

PALEOFLUIDS IN HYDROTHERMAL VEINS IN GRANITES OF THE BEDŘICHOV WATER TUNNEL (JIZERSKÉ HORY MTS., CZECH REPUBLIC) - PRELIMINARY STABLE ISOTOPE AND FLUID INCLUSION STUDY

INTRODUCTION

Various geological, geophysical and geochemical methods were applied in the Bedřichov water tunnel (Jizerské hory Mts., cca 120 km north of Prague) to characterize fractured granite environment and its associated fossil and recent fluids. The Bedřichov tunnel was investigated as a generic analog of the underground laboratory in the state nuclear waste disposal programme (Klomínský et al. 2005).

This contribution presents the preliminary results of the fluid inclusion and stable isotope study which was carried out to estimate the temperature, composition and source of paleofluids of vein minerals (e.g. quartz, carbonates, chlorite, sulphides and epidote).

GEOLOGY

The Bedřichov water tunnel was excavated in the Jizera Granite, one of the dominant rock types of the Variscan Krkonoše-Jizera composite massif, to accommodate the water pipeline from the Josefův Důl water dam to the water treatment plant in the Bedřichov village. The 6000 m long tunnel having a diameter of 2.5 – 3.5 metres was excavated by TBM and destructive mining technologies at a depth of about 100 to 200 m.

The Jizera Granite is intersected by two almost orthogonal subvertical fracture networks with NW-SE strike or NE-SW strike. The granitic body is cut by aplopegmatite dykes mostly in NE-SW direction and numerous veins and veinlets of quartz ±carbonate ± clay minerals, chlorite or epidote. These veins are grouped into two separate sets striking to NW and NE respectively.

RESULTS

Aplopegmatite dykes

The primary aqueous inclusions with consistent liquid to vapor ratio (LVR = L/(L+V)) between 0.6 and 0.7 were found in the coarse-grained pegmatitic quartz. Homogenization temperatures (Th) were measured between 286 and 338 °C, the salinity of aqueous solution is low, from 5.3 to 7.5 wt. % NaCl equiv. (Bodnar 1993). Eutectic temperature (Te) was observed at –22 °C, indicating NaCl – H_2O composition of the solution (Borisenko 1977).

[1] *Czech Geological Survey, Klárov 3, 118 21 Praha 1, Czech Republic; dobes@cgu.cz*

NW-SE hydrothermal veins

In quartz and calcite of the NW-SE veins, several types of primary and secondary aqueous inclusions were observed. The primary inclusions have variable LVR that was probably caused by long-term maturation of the inclusions under relatively low temperature conditions (Bodnar et al. 1985). Th, measured in the groups of inclusions with consistent LVR = 0.9, range from 126 to 172 °C. Variable salinity and composition of the solution was found in the primary inclusions. Some samples contain the inclusions with relatively high salinity, between 11 and 25 wt. % NaCl equiv., and Te ranging from –50 to –56 °C, indicating Na-Ca chloride content of the solutions. The other group of samples contains the inclusions with lower salinity ranging from 0.4 to 9.5 wt. % NaCl equiv. and eutectic temperature of about –38 °C, indicating probably Na-K±Mg±Fe chloride content of the solutions.

NE-SW hydrothermal veins

Primary inclusions in quartz and calcite of the NE-SW veins have also variable LVR. Th was measured in the groups of inclusions with LVR = 0.9 and values of Th were from 135 to 184 °C. The salinity was low in all samples, between 0.5 and 4 wt. % NaCl equiv.

Stable isotopes

The isotopic composition of carbon and oxygen of calcites from the veins with both NW-SE and NE-SW strike is widely variable. The $\delta^{13}C$ values vary from –14.72 to –4.66 ‰, PDB, and $\delta^{18}O$ values range from 6.87 to 23.57 ‰, SMOW. It seems to be evident that several calcite generations were present in the veins. Some calcite samples contain carbon derived from a deep-seated source, other samples contain organic carbon probably mixed with carbon of another source.

The oxygen isotopic composition of water solution can be calculated using C and O isotopic composition and Th of fluid inclusions (Fig. 1). The $\delta^{18}O$ values of solution between +6 and +10 ‰, SMOW probably assign magmatic water as the solution source. Some samples have slightly positive $\delta^{18}O$ values, between +0.6 and +3.5 ‰, SMOW, and deep-seated brines that circulated in crystalline rocks under lower temperature are supposed to be the source solutions. Two samples of the veins with NE-SW strike reveal the $\delta^{18}O$ values of solution negative, between –1.2 and –3.1 ‰, SMOW, which probably corresponds to late meteoric waters.

CONCLUSIONS

Aqueous-only inclusions with Th lower than 200 °C were found in the quartz and quartz-carbonate hydrothermal veins in granites of the Bedřichov water tunnel. The veins with NW-SE strike contain mostly the inclusions with relatively high salinity, up to 25 wt. % NaCl equiv., and Na–Ca chloride content of the solutions. The inclusions with lower salinity and Na-K±Mg±Fe content of the solution are not

so common. On the other hand, the veins with NE-SW strike contain only the inclusions with low salinity, which does not reach 4 wt% NaCl equiv.

The isotopic composition of carbon and oxygen is variable and it is evident that the vein calcites represent various stages of fluid circulation and source solutions, probably magmatic waters, as well as deep-seated brines, and meteoric waters.

REFERENCES

BODNAR R.J., 1993: Revised equation and table for determining the freezing point depression of H_2O-NaCl solutions. Geochim. Cosmochim. Acta, 57: 683-684.

BODNAR R.J., REYNOLDS T.J., KUEHN C.A., 1985: Fluid inclusion systematics in epithermal systems. In: Berger B.R., Bethke P.M. (Eds.): Geology and geochemistry of epithermal systems. Reviews in Econ. Geology, 2. Soc. of Economic Geologists.

BORISENKO A.S., 1977: Cryotechnic methods for the determination of fluid inclusions salts in minerals. Geol. Geofiz., 8: 16–27. (in Russian).

KLOMÍNSKÝ J. et al., 2005: Geological and structural characteristics of granitoids from the water tunnels in the Jizerské hory Mts. Czech Geol. Survey, Prague, 1-182. (in Czech).

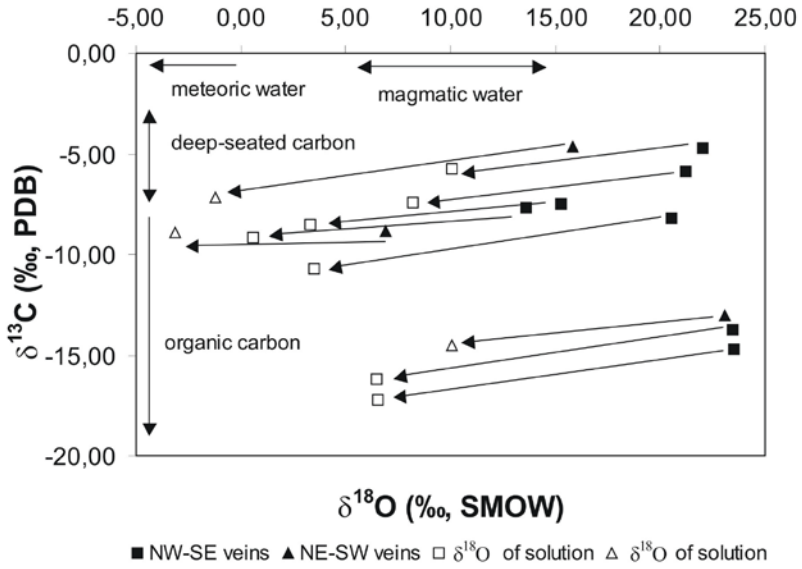

Fig.1. Isotopic composition of carbon and oxygen in vein calcites of the Bedřichov water tunnel (Jizerské hory Mts.).

MINERALOGIA POLONICA - SPECIAL PAPERS
Volume 28 - 2006

Pavla DOKOUPILOVÁ[1], Petr SULOVSKÝ[1], Zdeněk LOSOS[1]

HEMATITE, HEXAHYDRITE AND PICROMERITE GROUP FROM THE MINE WASTE OF THE COAL MINE KUKLA IN OSLAVANY

INTRODUCTION

Secondary mineralization on the waste tip of the Kukla coal mine in Oslavany was studied. Waste tip was deposited mostly between 1863 and 1973. Despite various processes running in the waste tip, its big dimension and the long time of deposition, there are only a few published studies devoted to the study of this mine tip. In 2005, sulphur, gypsum and hexahydrite were collected and verified. New phases for the locality are secondary anhydrite, aragonite, hematite, calcite, corundum, konyaite, picromerite and spinels. It is the first finding of konyaite $Na_2Mg(SO_4)_2 \cdot 5H_2O$ and picromerite $K_2Mg(SO_4)_2 \cdot 6H_2O$ in the Czech Republic.

METHODS

The XRD – analysis of the minerals was carried out with the difractometer STOE STADI-P in transmision mode; the XRD patterns were evaluated using Visual X^{Pow} software.

The chemistry of minerals was determined with electron microprobe CAMECA SX100, equipped with 5 crystal spectrometers and an EDS analyzer. The WDS analyses were performed at 15 kV accelerating voltage, probe current 10 – 20 nA, spot size 0 (oxides) to 5 μm (glass, sulfates), counting times 10 – 30 s, with natural and synthetic standards, correction procedure PAP.

RESULTS

On the dump we can see three main stages of the formation of secondary mineralization. Hematite, spinels, corundum and glass formed at high temperature during the burning of the mine waste and are the oldest secondary minerals in the dump. At the same time the sulfur sublimated (from hot gas) on cooler places near or at the surface..

Anhydrite, aragonite, calcite and gypsum represent the minerals from the waste cooling stadium. Hexahydrite, konyaite and picromerite are the youngest minerals in the dump and formed from the cool solutions.

Hematite occurs in two forms, as red disseminated powder which gives reddish color to the pile, and as a metallic gray, massive, well crystallized hematite with metal luster. In the parts more affected by temperature the second type is frequent. In some cases it makes incrustations and very rarely stalactite-looking forms. The composition of these stalactites indicates two stages of formation. The center is composed of glass, residual pyrite and relatively small (< 10 μm) hexagonal crystals of hematite (Fig. 2). Hematite in this core has increased content of Al_2O_3 - up to 8.16 % (i.e. max. 0.24 *apfu*), which according to Feenstra et al. (2005)

[1] *Institute of Geological Sciences, Faculty of Science, Masaryk University, Kotlářská 2, 611 37 Brno, Czech Republic; PavlaDokoupil@seznam.cz*

corresponds to the temperature of formation about 1100 °C. This central part also contains spinels of various composition and corundum with up to 8.07 % of Fe_2O_3 (0.11 *apfu*). The marginal part is formed by bigger hematite crystals. Macroscopically it looks like massive hematite; the grain size is > 100 μm. The marginal part consists of relatively pure hematite with some glass. The transition between these two parts is smooth. The presence of glass in both parts of stalactite indicates that both formed from melt. The presence of hematite as a primary cooling phase indicates that redox conditions were oxidizing, the melt temperature was moderate to very high and that the melt contained more than 8 wt. % of iron and crystallization temperature was as high as 900 °C (Kühnel et al. 1998).

Hematite and sulfates represent the first and the last stages of the secondary mineralization in the waste tip. While hematite is the product of coal burning in the waste, sulfates (hexahydrite, konyaite and picromerite) originated from cool aqueous solutions and according to climatic conditions they repeatedly dissolved and crystallized. All these sulfate species occur together and are stable only in dry and sheltered places. All sulfates are relatively pure phases, without any significant substitution. The average chemistry of hexahydrite is very close to ideal formula $MgSO_4 \cdot 6H_2O$. Picromerite and konyaite are also pure end-members of the picromerite group minerals, the substitution of K and Na in the position of monovalent cation is insignificant. Both have small excess of magnesium. That's why they are unstable and change in time into a mixture of hexahydrite and konyaite or picromerite. Decomposition of konyaite was described by Doesburg et al. (1982).

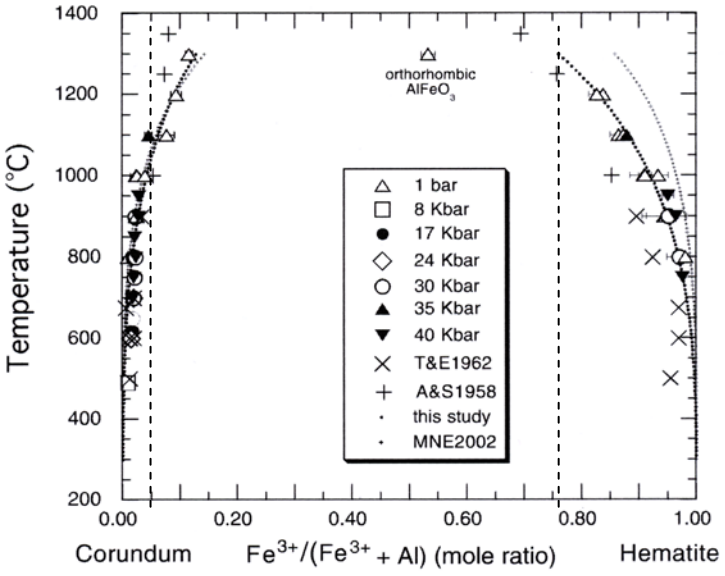

Fig. 1. Chemical compositions of Fe-corundum and Al-hematite as a function of synthesis temperature and pressure according to Feenstra et al (2005). The dashed lines show the composition of Fe-corundum and Al-hematite from the waste tip in Oslavany.

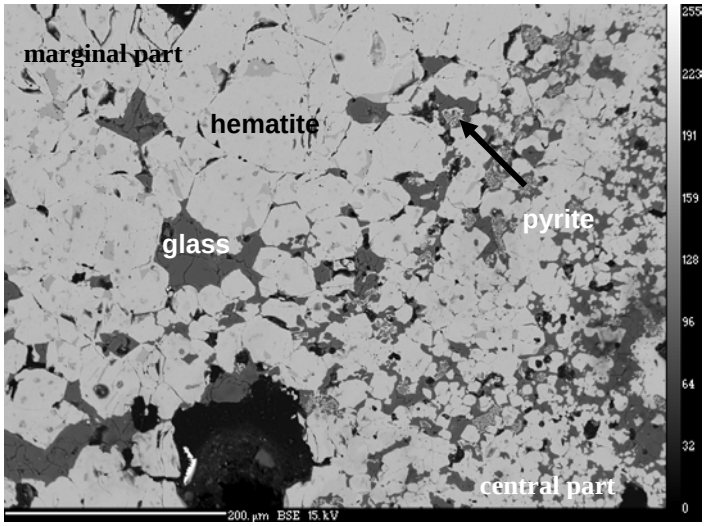

Fig. 2. Al-hematite (bright), framboidal pyrite (grey) and glass (dark) in BSE. The fine-grained hematite (central part of the stalactite) is in lower right corner, in upper left corner is coarser crystalline hematite (marginal part).

CONCLUSIONS

Chemistry of hematite and corundum indicates relatively high temperature of their formation during the burning of the mine waste, ranging from 900 to 1100 °C (Fig. 1). Hematite from the waste tip in Oslavany contains up to 8.16 % of alumina, corundum up to 8.07 % of Fe_2O_3. The higher temperature has caused easier substitution and the rapid cooling of the melt averted the unmixing. Our studies show that magnesium-bearing sulphates (especially hexahydrite) are dominant on the surface of the waste tip, especially hexahydrite. Mixed-cation sulfates (konyaite and picromerite) occur in a small amount. They are unstable and in time they change.

ACKNOWLEDGEMENTS: The study is a part of the research grant of the Ministry of Education MSM 002 1622412.

REFERENCES

DOESBURG J.D.J, VERGOUWEN L., PLAS L., 1982: Konyaite, $Na_2Mg(SO_4)_2 \cdot 5H_2O$, a new mineral from the Great Konya Basin, Turkey. Amer. Miner., 67: 1035-1038.

KÜHNEL R.A., McCARTHY G.J., EYLANDS K.E., SCHMIT C.R., WATNE-SCHUSTER T.M., 1998: Atlas of Minerals and Related Phases in Unaltered and Thermally Altered Materials from the Rocky Mountain 1 Underground Coal Gasification Field Site. – Gas Research Institute Topical Report GRI-97/0067, Chicago.

FEENSTRA A., SÄMANN S., WUNDER B., 2005: An Experimentral Study of Fe-Al Solubility in the System Corundum-Hematite up to 40 kbar and 1300 °C. Journal of Petrology, 46, 9: 1881-1892.

MINERALOGIA POLONICA - SPECIAL PAPERS
Volume 28 - 2006

Hana DOLEŽALOVÁ[1, 2], Zdeněk LOSOS[1]

GALENA AND Ag-MINERALS FROM ROŽNÁ URANIUM DEPOSIT

INTRODUCTION

The Rožná uranium deposit is located in a metamorphic complex usually assigned to the Raab subunit of the Gföhl Unit, Moldanubicum (Kříbek et al. 2005). The Gföhl Unit represents a complicated tectonic melange of upper crustal and mantle rocks, probably of Proterozoic or Lower-Palaeozoic age (Dallmaeyer et al. 1995; Finger, Steyer 1995).

In addition to the mined uranium mineralization and mineralogically interesting Se-phases, Pb-Zn ore minerals were identified in the deposit. We tried to characterise particular genetic types of galena and test the possibility if galena is a good typomorphic mineral for distinguishing these types. Presence of Ag-minerals in galena and chemical composition of the minerals were studied as well.

METHODS

The chemical analysis were performed with CAMECA SX100 microprobe at the Faculty of Science, MU Brno, in wavelength-dispersion mode. For the analysis the accelerating voltage was 25 kV, beam current 40 nA and spot size 1μm. Pure synthetic phases, metals and well defined natural sulphides were used as analytical standards. The raw data were corrected using automatic PAP routine (Pouchou, Pichoir 1985).

An average detection limit of trace elements for in galena was 820 ppm for Ag, 860 ppm for Sb and was 230 ppm for Cu, respectively.

RESULTS

Galena of Rožná uranium deposit occurs in following particular genetic types: (1) The stratidependent disseminated sulphide mineralization and skarn mineralization, (2) the pre-uranium vein siderite-sulphide mineralization including the new defined metasomatic ore mineralization in vicinity of the siderite-sulphide veins and (3) the post-uranium barite-fluorite-sulphide mineralization in veins.

We studied the distribution of elements of interest in galena for the particular genetic types, especially of Ag, Sb and Cu.

Ad (1) The oldest, mostly pre-Variscan, Pb-Zn sulphide mineralization is placed in rocks of Varied group of Moldanubicum – in marble, erlan, quartzite and gneiss. The structure of the samples is mostly disseminated or a concentration of grains is conformable with a foliation of the host rocks. Galena is in an assemblage with pyrrhotite, sphalerite ± pyrite or marcasite. Size of galena anhedral grains rarely exceeds 1 mm. This type of galena has not inclusions of Ag-minerals and its

[1] *Institute of Geological Sciences, Masaryk University, Kotlářská 2, 611 37 Brno, Czech Republic; hanadolo@email.cz*
[2] *Dept. of Mineralogy and Petrography, Moravian Museum, Zelný trh 6, 659 37 Brno, Czech Republic*

chemical composition is Ag: b. d. (below detection limit) – 0.6 wt. %, Sb: b. d. – 1.0 wt. % and Cu: b. d. – 0.04 wt. % in galena.

Ad (2) Hydrothermal galena of siderite-sulphide mineralization occurs in veins of north-east direction. Thickness of the veins is up to 4 m and their length rarely exceed 200 m (Kvaček, Novák 1974). Structure of the veins is massive, zonal or breccia type. Mostly euhedral grains of galena are enclosed in sphalerite. Contents of elements of interest for this galena type are Ag: b. d. – 0.2 wt. %, Sb: b. d. – 0.9 wt. %, Cu: b. d. – 0.3 wt. %. Inclusions of Cu and Ag-minerals (*chalcopyrite, freibergite, Ag-tetrahedrite, bournonite, pyrargyrite, stephanite*) were found in most of studied galena samples from this genetic type. Tetrahedrite coexisting with galena (28.1 – 34.4 wt. % Ag) corresponds mainly to freibergite by its chemical composition. Pyrargyrite (58.2 – 59.9 wt. % Ag) forms quite common aggregates with freibergite in galena. Inclusions of stephanite (68.4 – 67.7 wt. % Ag) in galena is very rare and sporadic in Rožná deposit.

Texturally the galena from the metasomatic ore mineralization in the vicinity of siderite-sulphide mineralization looks like disseminated galena from the first genetic type of galena. However, inclusions of freibergite were found in BSE. Galena from this subtype (Ag: 0.04 – 0.1 wt.%, Sb: b. d. – 0.1 wt.%, Cu: b. d.) has similar chemical composition as galena from hydrothermal siderite-sulphide veins.

Ad (3) The youngest type of galena has a hydrothermal origin. This type of mineralization forms vein-filling of fracture zones or small veins of north–west direction. Galena crystallises in fissures (the samples have drusy structure), occurs in an assemblage with sphalerite, barite ± fluorite ± chalcopyrite ± calcite ± quartz and forms euhedral (1 – 5 mm large) or anhedral grains in sphalerite (max. 0.5 mm). This youngest type of galena has very varying chemical composition (Ag: b. d. – 0.5 wt. %, Sb: b. d. – 0.8 wt. %, Cu: b. d. – 0.02 wt. %).

CONCLUSIONS

Contents of Ag, Sb, Cu and the other microelements are very low in all particular genetic types. The chemical composition of sphalerites from Rožná was studied in detail as well (Doležalová, Losos 2004) and therefore comparing the chemical variability of the two minerals, we can say that sphalerite is much more useful then galena for distinguishing the particular genetic type of sulphide mineralization in the Rožná uranium deposit.

Any mineral (expect of rare chalcopyrite) which contains the elements of interest (Ag, Sb, Cu) was not found in the host rocks of stratidependent disseminated sulphide mineralization. Low contents of trace elements in galena, microprobe analysis of sphalerite (high content of Mn) and stable isotopic study, published by Doležalová, Losos (2004), all together evidence the origin of the sulphides in protolith of the host metamorphic rocks.

Only galena of the vein siderite-sulphide mineralization and galena from metasomatic rocks in vicinity of the hydrothermal veins contains inclusions of Cu- and Ag-minerals. Chemical composition of sphalerite of both mineralizations is very similar. It supports the theory that Pb-Zn ores in metasomatic rocks are only subtype of the vein siderite-sulphide mineralization.

Inclusions in galena are formed by freibergite, Ag-tetrahedrite, pyrargyrite and very rarely by chalcopyrite, bournonite and stephanite. All these inclusions are of the same age as galena, which is younger then surrounding sphalerite.

The sulphur of a hydrothermal solution from which the vein siderite-sulphide mineralization crystallised can be assumed to be derived from deep-seated source (based on isotope study Žák et al. 2001; Doležalová, Losos 2004). Using isotope thermometer we estimated crystallising temperatures for this type of ore mineralization between 260 and 330 °C (Doležalová, Losos 2004). The hydrothermal mineralization have no genetic relationship neither with the oldest stratidependent sulphide mineralization nor the youngest barite-fluorite-sulphide mineralization in veins.

Genetically youngest galena type of the barite-fluorite-sulphide vein mineralization varies in chemical composition. Chemical variation of sphalerites of this type is even more remarkable (Cd content between 0.1 – 1.9 wt. %). The sulphides are probably product of few mineralization phases chronologically well separated, or the sulphides crystallised from locally circulating solutions. Sphalerite-galena thermometer yields crystallising temperatures in range of 100 - 200 °C (Žák et al. 2001).

ACKNOWLEDGEMENTS: The work was supported by grant MSM 002 1622412.

REFERENCES

DALLMAYER R.D., FRANKE W., WEBER K., 1995: Pre-Permian Geology of Central and Eastern Europe. Springer Verlag, Berlin-Heidelberg, 1-604.

FINGER F., STEYER H.P., 1995: A tectonic model for eastern Variscides: Indications from a chemical study of amphibolites in the southeastern Bohemian Massif. Geol. Carpath., 46: 137-150.

DOLEŽALOVÁ H., LOSOS Z., 2004: Sphalerite of different genetic types of sulphide ore mineralization in uranium deposit Rožná. Acta Mus. Morav. Sci. Geol., 89: 91-102 (in Czech).

KŘÍBEK B., LEICHMANN J., RENÉ M., HOLECZY D., 2005: Owerview of the geological structure of the Strážek Moldanubicum. In: Kříbek B., Hájek A. (Eds.): Uranium deposit Rožná: model of Late-Variscan and after-Variscan mineralizations. Czech Geological Survey, 8-10 (in Czech).

KVAČEK M., NOVÁK F., 1974: Manganese and iron rich sphalerites from Rožná uranium deposit, western Moravia. Čas. Mineral. Geol., 19: 175-180 (in Czech).

POUCHOU J.L., PICHOIR F., 1985: „PAP“ procedure for improved quantitative microanalysis. Microbeam Anal., 20: 104-105.

ŽÁK K., DOBEŠ P., KŘÍBEK B., PUDILOVÁ M., HÁJEK, A., HOLECZY D., 2001: Evolution of fluid type at the Rožná uranium deposits, Czech republic: Stable isotope and fluid inclusion study. In: Piestrzynski et al. (Eds.): Mineral deposit at the Beginning of the 21st Century. Lisse, Swets & Zeitlinge, 109-113.

MINERALOGIA POLONICA - SPECIAL PAPERS
Volume 28 - 2006

Krzysztof DUDEK[1], Krzysztof BUKOWSKI[1], Janusz WIEWIÓRKA[2]

MINERALOGY OF PYROCLASTIC SEDIMENTS FROM THE WIELICZKA AND BOCHNIA SALT MINES (S POLAND)

INTRODUCTION

The historical salt mines in Wieliczka and Bochnia, exploited during more than seven centuries, currently belong to the most spectacular tourist attractions of the Cracovian region. The salt deposits are situated in S part of the Carpathian Foredeep (Fig. 1), filled with Miocene sediments. In the Wieliczka–Bochnia area the middle Miocene (Badenian) sequence consists of terrigenous, argillaceous and clastic sediments at the bottom (Skawina Beds), the gypsum-anhydrite-halite evaporite series, and marly clays, siltstones and sandstones of the Chodenice Beds at the top (Garlicki 1979).

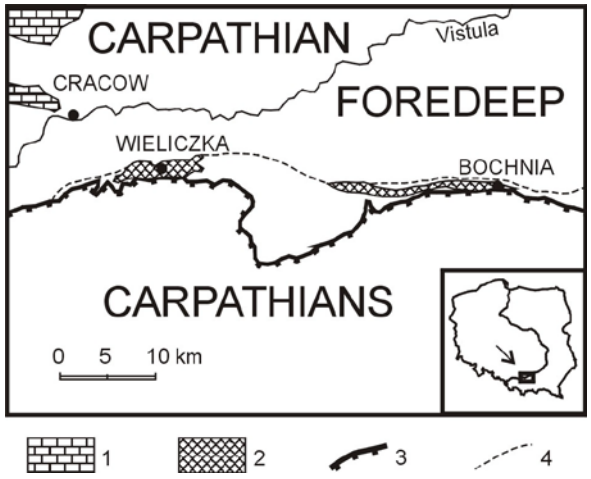

Fig. 1. Geological sketch of the Wieliczka-Bochnia area. 1 - platform Mesozoic sediments; 2 - Miocene salt deposits; 3 - Flysch Carpathians border; 4 - extent of folded Miocene sediments.

PYROCLASTIC SEDIMENTS

Several tuff levels have been reported from various parts of the Carpathian Foredeep, within the whole of the Miocene profile (see e.g. Parachoniak 1962; Alexandrowicz, Pawlikowski 1980; Alexandrowicz 1997). Four of them, labelled

[1] *AGH – University of Science and Technology, Faculty of Geology, Geophysics and Environmental Protection, Al. Mickiewicza 30, 30-059 Kraków, Poland; kadudek@uci.agh.edu.pl*
[2] *Wieliczka Salt Mine, ul. Daniłowicza 10, 32-020 Wieliczka, Poland*

from WT-1 to WT-4, were encountered in the Wieliczka and Bochnia salt mines (Wiewiórka 1979; Bukowski 1999).

The oldest of these levels, WT-1, occurs in marly clays of the Skawina Beds, a few metres below the bottom of the evaporite series. The tuff layer, 1-5 cm in thickness, distinguishes from the surrounding marly clays and siltstones by its rusty-brown colouration, due to alteration of mafic, iron-bearing minerals. The tuff WT-2 was reported only from a deep, no more accessible location in the Wieliczka salt mine (Wiewiórka 1979).

The tuff layer WT-3, encountered at the bottom of green salts in Wieliczka and within anhydrite clays, below crystalline salts in the Bochnia salt mine, seems to be of the widest extent and correlation significance (Bukowski 1999). This layer is dark, rusty-brownish, and thin; only several millimetres thick in Wieliczka, and up to 2-3 cm in Bochnia.

The tuff layer WT-4, reported only from the Wieliczka salt mine, intercalates the strongly deformed, 'lumpy' part of the deposit (Wiewiórka 1979; Parachoniak, Pawlikowski 1980).

METHODS

Thin slices of the whole-rock samples were examined with a polarizing microscope and the SEM/EDS. Separated clay fractions (below 2 μm) and weathering products were analysed with the X-ray powder diffraction method, whereas crystaloclasts of main and accessory minerals were observed under binocular microscope, in grain mounts, and analysed with the SEM/EDS.

RESULTS

Tuff WT-1. Microscope observations reveal that the main components of the rock are volcanic glass, partly bentonised, as well as euhedral and/or subhedral crystaloclasts of hornblende and zoned plagioclases, up to 0.5 mm in size. Minor components are augite, biotite and opaque minerals. Crystals are concentrated at the bottom of the layer, whereas clay matrix at the top. SEM/EDS analyses demonstrate that in plagioclases Ca prevail over Na (60-79 % An), whereas glass shards represent rather acid material (over 70 wt. % SiO_2). Accessory minerals are apatite, pyrite, ilmenite, Ti-magnetite (10-12 wt. % TiO_2) and galena (crystals below 20 μm). X-ray diffraction pattern of the distinguished clay fraction points out a mixed-layered smectite, with the main peak at 15.4 Å. Brown-yellowish weathering products proved to be a mixture of several mineral phases, including gypsum, halite and jarosite.

Tuff WT-3. The rock consists of partly altered volcanic glass and sparse, isolated crystals of plagioclase, biotite, quartz, and opaque minerals disseminated in halite matrix. The crystaloclasts are usually below 0.2 mm. In the upper part of the layer most of the glass shards are replaced by clay matrix. Opaque organic matter concentrates in numerous shear cracks, oblique to the top and bottom of the layer. SEM/EDS analyses indicate that plagioclases contain 60-76 % An and glass shards – 60-72 wt. % SiO_2. Accessory minerals are represented by euhedral crystals of ilmenite and zircon and rounded grains of apatite, generally all below

0.1 mm. Many of secondary halite crystals are coated with irregular network of aggregates of pyrite or iron sulphates, very peculiar in shapes.

CONCLUDING REMARKS

The tuff levels WT-1 and WT-3, appearing below and within the evaporite series, respectively, have already been used as significant correlation horizons for the Wieliczka and Bochnia salt deposits (Bukowski 1999). Correlation of Miocene pyroclastic levels in the whole Carpathian Foredeep is seriously hindered by relatively large distances between known occurrences (in salt mines, natural outcrops, and drillings), as well as frequent lack of lateral continuity of sediments, especially within the so-called 'folded Miocene,' at the edge of the Flysch Carpathians.

In such complicated geological conditions credible correlation of the Miocene pyroclastic levels may be facilitated by detailed mineralogical and geochemical studies of tuff samples from various localities. Such investigations, undertaken by the authors of the presented study, are also aimed at analysis of changes of volcanic processes in the neighbouring Carpathians, undoubtedly the source area for pyroclastic sediments deposited in the Carpathian Foredeep.

ACKNOWLEDGEMENTS: This study was financially supported by the AGH – UST WGGiOŚ grant no 11.11.140.158.

REFERENCES

ALEXANDROWICZ S.W., 1997: Lithostratigraphy of the Miocene Deposits in the Gliwice Area (Upper Silesia, Poland). Bull. Pol. Acad. Sci., 45: 168-179.

ALEXANDROWICZ S.W., PAWLIKOWSKI M., 1980: Policykliczny poziom tufitowy w miocenie okolic Gliwic. Kwart. Geol., 24: 663-678 (in Polish with English summary).

BUKOWSKI K., 1999: Porównanie badeńskiej serii solonośnej z Wieliczki i Bochni w świetle nowych danych. Prace PIG, 58: 43-56 (in Polish with English summary).

GARLICKI, A., 1979: Sedymentacja soli mioceńskich w Polsce. Prace Geol. Kom. Nauk Geol. PAN Oddz. w Krakowie, 119: 1-66 (in Polish with English summary).

PARACHONIAK W., 1962: Mioceńskie utwory piroklastyczne przedgórza Karpat Polskich. Prace Geol. Kom. Nauk. Geol. PAN Oddz. w Krakowie, 11: 7-77 (in Polish with English summary).

PARACHONIAK, W., PAWLIKOWSKI, M., 1980: Hornblenda z tufitu andezytowego z Wieliczki. Spraw. z Pos. Kom. Nauk. PAN Oddz. w Krakowie 21, 2: 127-128 (in Polish).

WIEWIÓRKA J., 1979: Przewodnie poziomy tufitowe w Kopalni Soli Wieliczka. Spraw. z Pos. Kom. Nauk. PAN, Oddz. w Krakowie, 21: 176-178 (in Polish).

MINERALOGIA POLONICA - SPECIAL PAPERS
Volume 28 - 2006

Suzana ERIĆ [1], Danilo BABIĆ[1], Danica SRECKOVIĆ-BATOCANIN[1]

MICAS OF STAUROLITE MICASCHIST FROM CRNI VRH (SERBIA)

INTRODUCTION

Micaschists with extremely large staurolite porphyroblasts up to 10 cm in size were noted in the Crni Vrh locality (Fig.1). They are associated with other metamorphic rocks of Proterozoic up to Lower Paleozoic in age, prevalently amphibolites and gneisses, in northwestern part of the Serbo-Macedonian Composite Terrane (Karamata, Krstic 1996).

Observed micaschists consist of quartz, micas (muscovite, biotite and paragonite), staurolite porphyroblasts, garnets, acid plagioclase and kyanite, while tourmaline, rutile and ilmenite are accessory compounds.

According to the available garnet-biotite geothermometer data, given by Eric (2005), the average metamorphic temperatures of staurolite micaschists from Crni vrh range between 550 ^{o}C (Ferry, Spear 1978) and 600 ^{o}C (Holdaway 2000). In this paper new results estimated only on Ti-apf in biotite and on muscovite component content in white micas will be presented. A comparison with the already mentioned data will be also presented.

METHODS

Mineral analyses (n = 50) were performed at the Mineralogical Institute, Hamburg, Germany with a Cameca electron microprobe. Operating conditions were 15 kV accelerating voltage and 20 nA sample current. The temperature of metamorphism was calculated according to the values of Ti-apf and Mg/(Mg+Fe) ratio in biotite (Henry et al. 2005). Equilibration temperature of coexisting paragonite and muscovite (the degree of solvus closure) has been calculated following the procedure of Blencoe et al. (1994).

RESULTS

Muscovite is the dominant mica in staurolite micaschists from Crni Vrh. It is associated with biotite and paragonite and occurs as oriented, sheet-like aggregates, defining a distinct and main rock foliation. Micas are grouped in patches or bands of few mm in thickness whose alternation with quartz accumulations resulted in banded structure. The size of sheets is up to 2 mm, commonly from 0.5 to 1 mm. Deformed or bended sheets, as well as microfolding (tightly flexed laths of microscopic size) and those developed at an angle or almost perpendicular to foliation, were recognized also (Fig. 2). These are evidence for their postkinematic development, under differential stress.

Micas with quartz and staurolite build nearly 85 volume percent of the investigated rocks. The rest is composed of garnets (almandine in composition), acid plagioclases (oligoclase) and kyanite. Accessory phases include tourmaline (dravite), rutile and

[1] *Faculty of Mining and Geology, University of Belgrade, 11000 Belgrade, Djusina 7, Serbia; suzanaeric@yahoo.com*

ilmenite. Biotites are mostly of 0.14-0.18 Ti atoms per formulae unit, while their Mg/(Mg+Fe) ratio ranges between 0.56 and 0.62. The paragonite content (X_{Pg}) in muscovite is from 0.28 to 0.33, while is content of muscovite component (X_{Ms}) in paragonite between 0.14 and 0.15 ($X_{Ms}=X_K/(X_{Na}+X_K)$; $X_{Pg}=1-X_{Ms}$, $X_K=K/(K+Na+Ca)$ i $X_{Na}=Na/(Na+K+Ca)$.

Representative analyses of biotite, muscovite and paragonite, calculated on the basis of 22 oxygens are given in Table 1. The average temperature of metamorphism was determined on the base of twenty biotite analyses, using geothermometric equations of Henry et al. (2005), while the average equilibration temperature of co-existing paragonite and muscovite was calculated applying muscovite-paragonite geothermometer of Blancoe et al. (1994). These results are given in Table 2.

Fig.1. Photomacrograph of staurolite porphyroblast.

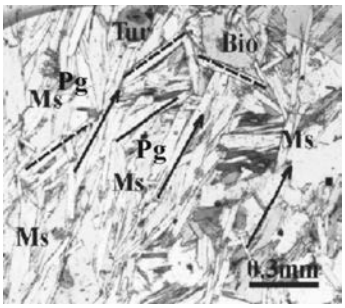

Fig. 2. Photomicrograph of micas, (II N).

Table 1. Representative analyses of micas in staurolite micaschists from Crni vrh.

	muscovite	muscovite	paragonite	paragonite	biotite	biotite
SiO_2	45.65	45.20	45.09	45.10	36.70	36.34
TiO_2	0.36	0.37	0.15	0.10	1.70	1.49
Al_2O_3	35.46	35.60	39.00	39.08	18.66	18.61
FeO	2.15	2.18	0.98	0.78	14.86	16.52
MnO	0.00	0.02	0.00	0.00	0.01	0.04
MgO	0.52	0.61	0.09	0.07	13.57	13.17
CaO	0.02	0.05	0.31	0.33	0.01	0.02
Na_2O	2.00	2.50	6.55	6.59	0.32	0.38
K_2O	7.60	7.57	1.74	1.70	9.07	8.73
Total	93.76	94.12	93.91	93.75	94.95	95.30
Si	6.125	6.064	5.900	5.905	5.464	5.429
Al^{IV}	1.875	1.936	2.100	2.095	2.536	2.571
Al^{VI}	3.755	3.694	3.915	3.936	0.738	0.706
Ti	0.036	0.037	0.015	0.010	0.190	0.167
Fe	0.241	0.245	0.107	0.085	1.850	2.064
Mn	0.000	0.002	0.000	0.000	0.001	0.005
Mg	0.104	0.122	0.018	0.014	3.012	2.933
Ca	0.003	0.007	0.043	0.046	0.002	0.003
Na	0.520	0.650	1.662	1.673	0.092	0.110
K	1.301	1.296	0.290	0.284	1.723	1.664

Table 2. Average temperatures obtained by geothermometry.

Geothermometry	Average T (^{o}C)
Ti in biotite (Henry et al. 2005)	550
T_{width} muscovite-paragonite (Blencoe et al. 1994)	620

CONCLUSIONS

The presence of extremely large staurolite porphyroblasts is not the only characteristic feature of staurolite micaschists from Crni Vrh. The presence of three different micas is of particular interest, also. Average temperatures, obtained by the value of Ti-apf in biotite are in agreement with results obtained by garnet-biotite geothermometer. The observed variations are consequences of weak chloritization (thus of lower Ti and Fe content) and of rutile and/or ilmenite presence in some biotite grains as inclusions. The final equilibration temperature between muscovite and paragonite is negligible higher than the already obtained average temperatures by other geothermometers. The observed intergranular variations on Na content in analyzed muscovites (table 1) should be taken in consideration. Common analytical errors in geothermometry are also acceptable.

REFERENCES

BLENCOE G.J., GUIDOTTI V.C., SASSI P.F., 1994: The paragonite-muscovite solvus: II Numerical geothermometrs for natural, quasibinary paragonite-muscovite pairs. Geochim. Cosmochim. Acta, 58: 2277-2288.

ERIC S., 2005: Originated of minerals of micaschists from Crni vrh and Resavski humovi (in Serbian), PhD, Fac. of Mining and Geology, Univ. of Belgrade, 1-250.

FERRY J.M., SPEAR, F.S., 1978: Experimental calibration of the partitioning of Fe and Mg between biotite and garnet. Contrib. Mineral. Petrol., 66: 113-117.

HENRY D.J., GUIDOTTI V.C., THOMSON, A.J., 2005: The Ti-saturation surface for low to medium pressure metapelitic biotites: implications for geothermometry and Ti-substitution mechanisms. Am. Mineral., 90: 316-328.

HOLDAWAY M.J., 2000: Application of new experimental and garnet Margules data to the garnet-biotite geothermometer. Am. Mineral., 85: 881-892.

KARAMATA S., KRSTIC B., 1996: Terranes of Serbia and neighbouring areas, terranes of Serbia, the formation of the geologic frame of Serbia and the adjacent Regions, 25-41.

MINERALOGIA POLONICA - SPECIAL PAPERS
Volume 28 - 2006

Štefan FERENC[1], Daniel OZDÍN[2,4], Pavol SIMAN[3], František BAKOS[4]

SIDERITE AND SULPHIDIC MINERALIZATION AT THE CINOBAŇA – JARČANISKO OCCURRENCE, SLOVENSKÉ RUDOHORIE MTS., SLOVAK REPUBLIC

INTRODUCTION

Small occurrences of siderite and sulphidic mineralization within the western domain of the Slovenské Rudohorie Mts. (Veporicum) have only mineralogical significance. These occurrences were exploited mainly for copper and silver in the Middle Ages.

The Cinobaňa – Jarčanisko is one of well known and biggest siderite and sulphidic mineralization occurrence in the Veporicum Unit. First references about exploitation of precious metals in vicinity of the Cinobaňa village were known since end of the 13th century (Žilák 1999). Based on the historical annals, discontinuous exploitation/investigation of ores (copper, silver and gold, later iron, in 19.-20th cent.) in this locality wages since the 13th to first half of the 20th century. Later, during the end of 20th and begining of the 21th century the locality again represent object for precious metal investigation, but without profound results of geological survey.

CHARACTER AND GEOLOGOCAL SETTING

The Cinobaňa – Jarčanisko occurence is situated in the south-eastern part of the Slovenské Rudohorie Mts. on the southeastern slopes of the Strieborná Mt. (719 m); circa 1 km NW from the church in Cinobaňa village. Object of exploitation was represented by subvertical siderite – quartz - sulphidic veins of NNW – SSE direction (long about 250 m), related to quartz – sericite and carbonaceous schists of the Slatviná Formation (upper Carboniferous).

Occurrence is localised in the Kohút zone of the Veporicum Unit. Wider surround is formed mainly by metasediments of the Carboniferous Slatviná Formation and garnet mica schists. Relatively small bodies of metabasics and granitoides are situated within these rocks. In the southern of the Cinobaňa - Jarčanisko locality occur metasediments of the Mesozoic cover of the Veporicum crystalline complex (Föderata Group) and nappe outliers of the Gemericum domain (Bezák et al. 1999).

[1] *State Geological Institute of Dionýz Štúr, Regional centre Banská Bystrica, Kynceľovská 10, 974 01 Banská Bystrica, Slovak Republic, ferenc@gssrbb.sk*

[2] *Department of Mineralogy and Petrology, Faculty of Natural Sciences, Comenius University, Mlynská dolina, 842 15 Bratislava, Slovak Republic*

[3] *Geological Institute of Slovak Academy of Sciences, Dúbravská cesta 9, 840 05 Bratislava, Slovak Republic*

[4] *State Geological Institute of Dionýz Štúr, Mlynská dolina 1, 817 04 Bratislava, Slovak Republic*

In the vicinity of the Cinobaňa – Jarčanisko occurrence (Lovinobaňa and Uderiná villages) are situated similar occurences of siderite–sulphidic mineralization hosted by deformed granitoides/migmatites, amphibolites, and the Carboniferous metasediments. This type of mineralization is accounted as an Alpine age.

DESCRIPTION OF MINERALOGICAL CONDITIONS

In debris material from old dumps of the Cinobaňa – Jarčanisko occurrence were found two types of mineralized gangue:

I. **Quartz** with a small amounts of pyrite and arsenopyrite; this quartz is oftenly intersected by siderite veinlets and sulphides (e. g. tetrahedrite, jamesonite, chalcopyrite).

II. **Siderite** containing veinlets, impregnations and clusters mainly of chalcopyrite, tetrahedrite and jamesonite.

The association of determined minerals (both gangue types) is relatively variegated. Siderite and quartz are main gangue minerals. Ore minerals are represented by: pyrite I, arsenopyrite, chalcopyrite, tetrahedrite I., galena, jamesonite, Pb – tetrahedrite, pyrite II (in order of precipitation). Anglesite, valentinite, bindheimite, scorodite, covellite and goethite represent minerals of supergene zone.

Mineralogical speciality of locality is occurrence of Pb-tetrahedrite (Ferenc, Maťo 2005) which, form of microscopic veinlets, irregular aggregates and grains replacing chalcopyrite, tetrahedrite I and jamesonite. Strong zonality of the Pb-tetrahedrite (BSE) is caused by the various Pb content (2.69-11.21 wt. %).

The Pb-bearing tetrahedrite demonstrates various Cu content in range of 32.74 to 38.61 at. % and Ag content is 0 to 4.15 at. %; range of Σ (Cu+Ag) is from 35.17 to 38.76 at. %.

-Σ (Cu+Ag) refers to substitution and compensation of Σ (Pb+Fe+Zn). Range of Σ (Pb+Fe+Zn) is from 3.8 to 6.52 at. % (Pb-bearing tetrahedrite).

-Σ (Cu+Ag) more than 34.48 at. % (in formula $(Cu,Ag)_{10}(Fe,Zn,Pb)_2(Sb,As)_4S_{13}$ it´s equal to 10 a.p.f.u.) indicate presence of Cu and Ag elements in tetrahedric (TET) - bivalent position. It demonstrates that Cu and Ag occupied trigonal (TRG) and tetrahedric (TET) positions according to the formula $(Cu,Ag)_6^{TRG}[Cu,Ag_{2/3}(Fe,Zn,Pb)_{1/3}]_6^{TET}(Sb,As)_4^{SM}(S)_{13}^{OCT}$.

Likewise, contents of Fe and less Zn are moderately decreasing in the Pb tetrahedrite. Data of correlation (0.872) of the Σ (Fe+Zn) vs. Pb (*apfu*) reports the compensation of increasing Pb content in the Pb-tetrahedrite, indicating higher Pb substitution by Zn. It is supported by positive correlation (0.825) of Zn vs. Pb (*apfu*).

CONCLUSIONS

The Pb-bearing tetrahedrite occurrences are relatively rarely in the world. Up to present, the max. Pb content **(**12.31 wt. %**)** is reported in the tetrahedrite from Greece (Vavelidis, Melfos 1997). The max. Pb content is **11.21 wt. %** in the Pb -

tetrahedrite of the siderite-sulphidic mineralization at the Cinobaňa-Jarčanisko occurrence.

We suggested this genetic model of mineralization of the Cinobaňa – Jarčanisko deposit:

I. **quartz veins** + pyrite I and arsenopyrite
II. **siderite** veins
III. **sulphidic mineralization** (chalcopyrite, tetrahedrite I., galena, jamesonite, Pb – tetrahedrite, pyrite II)
IV. **supergene mineralization** (anglesite, valentinite, bindheimite, scorodite, covellite, goethite).

The position of the Pb-tetrahedrite within sulphidic mineral association reflects the youngest Alpine tectonothermal event in the frame of the siderite and sulphidic mineralizations at the Cinobaňa – Jarčanisko occurrence. This event caused annealing of tetrahedrite I, jamesonite and galena, and gradually disintegration of solid phases and transfer of elements (mainly Pb). The precipitation of the Pb-bearing tetrahedrite and pyrite III was subsequent.

ACKNOWLEDGEMENTS: Financial support of research was provided by the project of the Ministry of Environment of Slovak Republic No. 2898 and VEGA grants No. V-374-05-00.

REFERENCES

BEZÁK V., HRAŠKO Ľ., KOVÁČIK M., MADARÁS J., SIMAN P., PRISTAŠ J., DUBLAN L., KONEČNÝ V., PLAŠIENKA D., VOZÁROVÁ A., KUBEŠ P., ŠVASTA J., SLAVKAY M., LIŠČÁK, P., 1999: Explanations toward geological map of western part of the Slovenské Rudohorie Mts. GSSR, Bratislava, 178. (in Slovak)

FERENC Š., MAŤO Ľ., 2005: The Pb-bearing tetrahedrite from the Cinobaňa – Jarčanisko deposit, Slovenské Rudohorie Mts., Slovak Republic. Miner. Slov., 37: 478.

VAVELIDIS M., MELFOS, V., 1997: Two plumbian tetrahedrite-tennantite occurrences from Maronia area (Thrace) and Milos Island (Aegean sea), Greece. Eur. J. Mineral., 9: 653-657.

ŽILÁK J., 1999: Occurrence and exploiting of gold ores at some localities in central Slovakia in second half of 16. century. Miner. Slov., 31: 421-424. (in Slovak)

MINERALOGIA POLONICA - SPECIAL PAPERS
Volume 28 - 2006

Bohuslav FOJT[1], *Petr SULOVSKÝ*[1]

URANIUM MINERALIZATION AT THE DEPOSIT ZÁLESÍ NEAR JAVORNÍK, SILESIA, CZECH REPUBLIC

INTRODUCTION

The deposit is located at the southern margin of the Zálesí settlement (village Travná) in Rychlebské hory Mts., about 6.5 km southwest of the town Javorník in Silesia. The area belongs to Vilémovice sector of the Stróň Group of the Orlica-Sněžník Crystalline Unit.

The ore is concentrated in irregularly developped veins of very variable thickness and also in two stratiform stockwork bodies, mostly in the so called „central fault zone". Host rocks are metasediments and basic metavolcanics; the rock complex is penetrated by lamprophyre dykes. Due to post-ore tectonic processes the content of the veins was cataclased, subsequently recrystallized and partially mobilized. From the deposit, which was mined in five horizons down to the depth of 200 m, about 400 tonnes of uranium were extracted in years 1958 to 1968.

The deposit developped in three mineralization stages: uraninite, arsenide, and the youngest sulfidic. The thorough characterization of the mineral asssemblages is given in the publication by Fojt et al. (2005).

METHODS

The samples were taken from the mine galleries during the mining period. The basic data on the mineralization were collected by the study of ore textures and by optical microscopy of polished sections. Detailed data on the chemistry of individual mineral phases were acquired by EMPA with Cameca SX100 (at Masaryk University, Brno).

RESULTS

The main mineral of the oldest mineralization stage is *uraninite* in the typical colloform development – also in stripped and massive aggregates, overgrowing comb-like (palisade) quartz. Less abundant hypogene uranium phase is a mineral with its chemistry, development and optical properties close to *coffinite*. It is considerably more common in the stratiform stockwork bodies, than in the veins. It places it obviously replaces uraninite (Fig.1). Typical phenomenon is the growth of radiate clusters of spear-shaped coffinite-like crystals on colloform uraninite. The BSE image distinctly shows the inhomogenous nature of individual crystals (Fig. 2). The combination of microscopic study and microprobe analyses indicate the oscillatory (repeated) nature uraninite and coffinite-like phase crystallization.

[1] *Institute of Geological Science, Masaryk University, Kotlářská 2, 611 37 Brno, Czech Republic; fojt@sci.muni.cz*

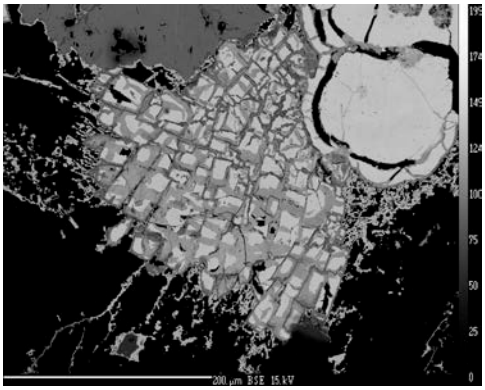

Fig.1: Replacement of uraninite (white) by coffinite-like phase (grey), calcite – black.

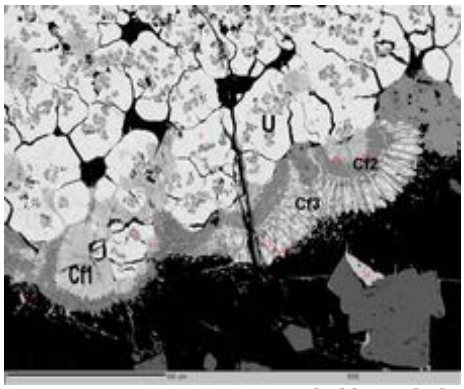

Fig.2: Uraninite (U) surrounded by radial aggregates of coffinite-like phase (Cf1,Cf2). Cf3 - crystals of the uraninitized coffinite.

The chemistry of both uranium minerals is fairly variable – more pronouncedly in case of coffinite. Uraninite contains besides uraniun oxide also SiO_2 (up to ~ 4 wt. %), further common admixtures are calcium, lead, and yttrium. The sum of lanthanides achieves up to 5 wt. % with enrichment of MREE (Fig. 4).

The mineral close to coffinite is strongly depleted in silica (SiO_2 ranges from 4 to 10 wt %). In the set of 53 spot microprobe analyses, coffinite s.s. was identified only in two cases. Recalculated on 6 oxygens, i.e. supposing two molecules of crystal water per formula, both analyses show equal quantities of Si and U, and a slight excess of cation sum. All other analyses represent transitional forms between uraninite and coffinite or rather a submicroscopic mixture of both. Compared with typical coffinite, such mineral phases are deficient in Si; the content of lanthanides is approximately by one order lower than in uraninite. These analyses show negative cerium anomaly ($Ce_N/Ce^* = 0.14$ to 0.45) and relatively high, yet strongly variable presence of arsenic (up to 10 wt. % As_2O_5), phosphorus (up to 5.5 wt. % P_2O_5), and yttrium (up to 11.8 wt. %). According to Wang and Xu (1999), coffinitization can take place most likely at temperatures below 130 °C, which is in good accordance with the results of fluid inclusion study.

The above mentioned reversible processes of uraninite to coffinite replacement are confirmed by the relations between Si^{4+} and U^{4+} in uraninite of the veins and stockworks (Fig. 3).

Uraninite is commonly accompanied by *clausthalite*, in places with rare, unnamed mineral Bi_4Se_3 phase. Very abundant component of the uraninite mineralization stage is *chalcopyrite,* while other sulfides – *sphalerite, bornite, chalcocite (anilite), marcasite* and *pyrite* (with 0.1 to 7.4 wt.% Ni) – occur only subordinately. The dominant non-ore mineral is *quartz* (rarely as amethyst or morion) and *calcite,* rarely also dark-coloured *fluorite.*

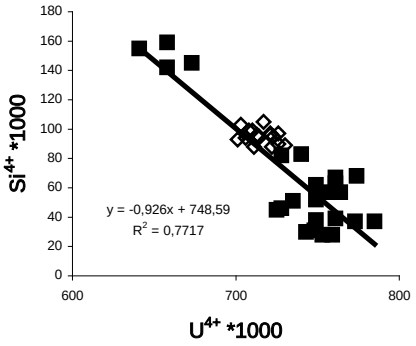

Fig. 3: Si^{4+} versus U^{4+} of the uraninite from the veins (◇) and stratiform ore body (■).

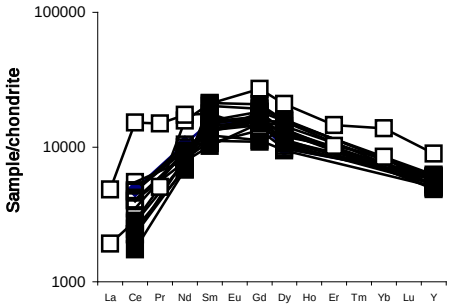

Fig. 4: C1-chondrite normalized lanthanide and yttrium abundance in uraninite. □ - veins, ■ - stratiform ore body.

CONCLUSIONS

The Zálesí deposit is a representative of the "five-element association" of the Jáchymov type with certain very distinct differences: above all the existence of stratiform stockwork mineralization, which formed probably as the result of recrystallization and subsequent mobilization of pre-existent veins as well as partial chemical changes (coffinitization) in their content. Further differences are in the fact that the assemblage of the uraninite stage includes relatively abundant clausthalite and very common chalcopyrite. The results of study of fluid inclusions in quartz, calcite and fluorite allow indicate relatively low temperature of ore-forming fluids (max. 130^{o} C) with varying salinity (0.4 to 27.5 wt. % of salts), which on their migration paths precipitated ore- and non-ore components. The isotopic composition of sulphur of chalcopyrite and sphalerite of the oldest – uraninite-stage (δ^{34} S –1.2 to –4.5 ‰ CDT) indicates it originated by the leaching in the hosted (metavolcanic) rocks (Dolníček et al. in print).

REFERENCES

DOLNÍČEK Z., FOJT B., KUČERA J., (in print): Origin of the U-Ni-Co-As-Ag/Bi depositat Zálesí near Javorník in Silesia: fluid inclusion and stable isotope study. Proceedings of the seminar "Mineralogy of the Bohemian Massif and Western Carpathians 2006", Olomouc: 6-10 (in Czech with English summary).

FOJT B., DOLNÍČEK Z., KOPA, D., SULOVSKÝ P., ŠKODA R., 2005: Paragenesis of the hypogenne associations from the uranium deposit at Zálesí near Javorník in Rychlebské hory Mts., Czech Republic. Čas. Slez. Muz. (A), 54: 223-280 (in Czech with English summary).

WANG Y., XU H., 1999: Coffinitization of uraninite: SEM/AEM investigation and chemical modelling. 1999 Proceedings 7th International Conference on Radioactive Waste Management and Environmental Remediation, ASME: 1-5, New York.

MINERALOGIA POLONICA - SPECIAL PAPERS
Volume 28 - 2006

Petr GADAS[1], *Miroslava GREGEROVÁ* [1]

MAFIC MICROGRANULAR ENCLAVES FROM GRANITOIDS OF THE BRNO MASSIF EXPOSED IN THE VICINITY OF BLANSKO

INTRODUCTION

The Brno massif is one of the exposed parts of the Brunovistulicum which constitues crystalline basement of younger sedimentary units of east margin of the Czech Massif and West Carpathians (Dudek 1980). Granitoid rocks of the Brno massif originated by the north active continental margin of Gondwana (Finger et al. 1995), about 590 Ma ago during Cadomian orogenesis (Dallmeyer et al. 1994). It is structured to the west and the east granodiorite parts, separated by the metabasite zone. Dark lens-shaped or rounded enclaves occur in some varietes of granitoids of east part of the Brno massif. They match mafic microgranullar enclaves concerning their macroscopic features.

This type of enclaves occurs often in calc-alkaline granitoids (Barbarin, Didier 1991). Their genesis is being interpreted differently (restite, autolith, xenolith or initial intrusions). Genesis by separation of globules of mafic melt followed by distribution in felsic melt of the host rock is the most accepted theory currently (Vernon 1983, Barbarin, Didier 1991). Coexistence of the two contrast magmas leads to mutual thermal, mechanical and chemical interactions, reflecting macroscopic, microscopic and chemical features of the enclaves.

METHODS

Field research of the enclaves yielded many important facts. This contributions is focused on size, shape, orientation and spatial distribution of enclaves with regard to the mineral composition of the host rock. Orientation of the enclaves versus orientation of the host rocks, and signs of mutual influence of the enclave and the host rock was also examinated

Optical microscopy was applied to study mineral composition of the enclaves and the host rocks, micrustructural elements and signs of mutual influence. SEM was applied to reveal microchemistry of feldspars and amphiboles and for identification of some accesory, opaque and secondary phases.

ACME Analytical Laboratoires Ltd., Vancouver, Canada, performed the whole-rock chemical analysis of the main and trace elements by ICP-ES and ICP/MS methods.

[1] *Institute of Geological Sciences, Masaryk University, Kotlářská 2, 611 37 Brno, Czech Republic; mirka@sci.muni.cz*

RESULTS

The enclaves are unevenly scattered in the host rocks. The most frequent swarms they form in biotite-hornblende bearing tonalites east to south-east of Blansko. Prevailing shapes are lens to ovoid usually more or less longitudally extended (see Fig. 1). Their arrangement is mutually parallel as well as parallel to mineral alignment (hornblende) of the host rocks. The size of the enclaves is in range of 5 to 30 cm. They are fine-grained and always darker then the associated host rock. Dark "chilled" fine-grained margins of the enclaves were discovered sporadically (see Fig. 2). Contacts are sharp in microscope, reaction-rim less. Enclave´s microstructure is subhedral, mostly unevenly grained, locally with fluidal fabric features. The enclaves contain the same minerals as the host rocks but they differ in amount and mutual rations of them. They display the dioritic composition. Plagioclases are often of two types: (1) the lathy type is in the matrix; (2) plagioclase megacrysts, up to 10 mm large, locally containing rounded cores with mafic minerals (hornblende, biotite) inclusions at the rims. They were observed to be penetrating the contact of the enclave and the host rock, in some cases, thus they seem to be xenocrysts. The compositon of the plagioclases is similar to that of the host rocks (An_{14}-An_{33}). Green, well preserved hornblende individuals are components of the matrix. Rarely, they constitute up to 20 mm large megacrysts, which was observed in the enclaves of hornblende-rich host rock. There is a deficiency of hornblende or it is completely missing in the enclaves of hornblende-less host rocks. Compositon of hornblende is the same in enclaves as in the host rocks and it corresponds to magnesiohornblende. Biotite is subhedral and mostly strongly replaced by chlorite. In contrary to the host rocks, alkali feldspars and quartz belong to minor constituents. Apatite, titanite and zircon are characteristic accessory minerals. Apatite crystals in the enclaves are typically thin-columned to acicular, while they are thick columned in the host rocks. Chemically the enclaves correspond to basic rocks (SiO_2

Fig. 1. The swarm of lens-shaped enclaves, Žižlavice, photo P. Gadas.

Fig. 2. The dark „chilled" fine-grained margin of the enclave, Arnoštov, photo P. Gadas.

48-53 %). They display calc-alkaline meta-aluminous character and are enriched by FeO_{tot}, MgO, CaO, TiO_2, P_2O_5 and REE.

CONCLUSIONS

The presence of some macroscopic signs (dark "chilled" fine-grained margins, parallel arrangement of minerals to the contacts) is the evidence of comagmatic evolution of the enclaves and the host rocks. Acicular crystals of apatite are indicators of rapid crystallization of the enclaves liquid (Willie et al. 1962). Plagioclase xenocrysts support a concept of mutual mechanical exchanges. Close geochemical trends of the enclaves and the host rocks are most likely caused by intensive chemical interactions.

ACKNOWLEDGEMENTS: The contribution has been elaborated in terms of The Scientific Research Programme MSM 0021622418 - Dynamic Geovisualisation in Crisis Management.

REFERENCES

BARBARIN B., DIDIER J., 1991: Review of the main hypotheses proposed for the genesis and evolution of mafic microgranular enclaves. In: Didier J., Barbarin B. (Eds.): Enclaves & Granite Petrology, 367-374.

DALLMEYER D.R., FRITZ H., NEUBAUER F., URBAN M., 1994: Ar/Ar mineral age controls on the tectonic evolution of the southeastern Bohemian Massif. Pre-Alpine Crust in Austria, Excursion guide "Geology of the Moravian Zone", 14-22.

DUDEK A., 1980: The crystalline basement block of the Outer Carpathians in Moravia Bruno-vistulikum. Rozpr. ČSAV Ř. Mat. Přír. Věd, 90: 3-85.

FINGER F., FRASL G., DUDEK A., JELÍNEK E., THÖNI M., 1995: Cadomian plutonism in the Moravo-Silesian basement. In: Dallmeyer R.D., Franke W., Weber K. (Eds.): Pre-Permian geology of Central and Eastern Europe, 495-507.

VERNON R.H., 1983: Restite, xenoliths and microgranitoid enclaves in granites. J. Proc. Roy. Soc. New South Wales (Australia), 116: 77-103.

WYLLIE P.J., COX K.G., BIGGAR G.M., 1962: The habit of apatite in synthetic systems and igneous rocks. J. Petrol., 3: 238-243.

MINERALOGIA POLONICA - SPECIAL PAPERS
Volume 28 - 2006

Bożena GOŁĘBIOWSKA[1], Adam PIECZKA[1], Jan PARAFINIUK[2]

Cu(Ag)-Pb-Bi(Sb) SULPHOSALTS FROM RĘDZINY (WESTERN SUDETES, POLAND)

INTRODUCTION

Cu(Ag)-Pb-Bi(Sb) sulphosalts are one of more common group of minerals forming ore mineralization dispersed within contact zones of amfibolites, mylonites and mica schists with a dolostone lens emplaced within them and being exploited at a large quarry at Rędziny (middle part of the Rudawy Janowickie Range; eastern metamorphic cover of the Karkonosze granite intrusion). Beside the sulphosalts, the mineralization is composed of arsenopyrite, cassiterite, base-metal sulphides, stannite-group minerals, Bi-sulphotellurides, Bi-sulphoselenides (Pieczka et al. 2004), and also an extensive assemblage of hypergenic minerals (Gołębiowska 2003).

METHODS

Optical observations in the reflected light were carried out using an OLYMPUS BX-51 microscope. Chemical compositions of the minerals were analysed at the Inter-Institute Analytical Complex for Minerals and Synthetic Substances of the Warsaw University using a CAMECA SX100 electron microprobe operating in the WDS mode under the following conditions: excitation voltage 15 kV, beam current 20 nA, peak count-time 20 s, background time 10 s.

RESULTS AND DISCUSSION

The most important occurrence of the sulphosalts was encountered in fragments of quartz-chlorite-arsenopyrite veins. They coexist there with Fe-enriched sphalerite, ferrokesterite, chalcopyrite, galena and traces of cassiterite. The sulphosalts form heterogeneous aggregates and veins up to some milimeters in size, mostly filling small cavities among the arsenopyrite crystals. Their small grains sometimes intergrowth with the sphalerite containing bleb inclusions of ferrokesterite and chalcopyrite. This latter assemblage crystalized at 320-280 °C (Pieczka et al. 2004), then an initial crystallization of the earliest Cu(Ag)-PbBi(Sb) sulphosalts took place at slightly higher temperature, probably around 370-350 °C. In more outer parts of the vein, the sulphosalts were found within another association with chalcopyrite, native Bi, ikunolite, traces of bismuthinite and Fe-depleted sphalerite. Small grains and inclusions reaching mostly 20-50 μm in size are commonly scattered within a schist belt cross-cutting the dolostone lens, where they coexist with arsenopyrite, pyrite, chalcopyrite, cubanite, bismuthinite, traces of stannite, electrum, native Bi, stannoidite, mawsonite, bornite, and as inclusions

[1] *Department of Mineralogy, Petrography and Geochemistry, AGH University of Science and Technology, al. Mickiewicza 30, 30-059 Kraków, Poland; goleb@uci.agh.edu.pl*
[2] *Institute of Geochemistry, Mineralogy and Petrology, University of Warsaw, Żwirki i Wigury 93, 02-089 Warszawa, Poland*

within grains of Bi-sulphotellurides (josèite-A and josèite-B). Relatively low temperature of crystallization of the sulphosalts can be estimated at about 170 °C for Bi-free tennantite associated with chalcopyrite and Fe-free sphalerite.

Positions of the Rędziny sulphosalts in the Cu(Ag)-Pb(Fe)-(Bi+Sb) diagram, indicate presence of phases belonging to the kobellite, pavonite and lilianite homologous series, the aikinite-bismuthinite series as well as so-called "false ferbertalite" (Ilinca 2006), berryite, wittichenite, matildite, freibergite and various members of the tetrahedrite-tennantite group sometimes enriched in Zn, Ag or Bi.

The kobellite homologous series

The order number of homologue N close to 4 calculated according to Zakrzewski and Makovicky (1986) indicates members of the giessenite-izoklakeite series. Grains of the sulphosalts occur as elongated laths up to 700 μm large, mainly in association with Ag-bearing galena, "false ferbertalite", gustavite, berryite, wittichenite, small exsolutions of Ag-bearing, Bi-enriched tetrahedrite and bournonite forming a core of aggregates, very often overgrown by a rim composed of members of the aikinite-bismuthinite series. The calculated compositions represent a Pb-deficient member (an effect of the 2Pb=Ag+(Bi,Sb) substitution) with Cu exceeding 2 *apfu*, and show the Sb/(Sb+Bi) ratio ranging from 0.149 to 0.282. The crystals with low values of the ratio correspond to giessenite, those with the highest values possible to izoklakeite, especially if the both varietes participate in formation of the same aggregate.

The lilianite homologous series

Members of the series have been found as elongated crystals up to 300 μm in size within the association described above, and also as small inclusions within the W part of the schist belt cross-cutting the dolostone lens. The N value calculated from the equation of Makovicky and Karup-Møller (1977) varies from 3.73 to 4.18. The range of content of the Ag-Bi end-member (82.95 to 99.88 mol. %) and the N value indicate gustavite, $AgPbBi_3S_6$, as a dominant phase.

The pavonie homologous series

Minerals of the series have been found in traces within the same aggregates, and also occur as small dispersed grains within chalcopyrite from the schist belt. Their positions in the Cu(Ag)–Pb(Fe)–(Bi+Sb) diagram indicate pavonite, $(Ag,Cu)(Bi,Pb)_3S_5$, and benjaminite, $(AgCu)_3(Bi,Pb)_7S_5$, as the most abundant phases.

The aikinite-bismuthinite series

Minerals of the series forming outer rims around aggregates of giessenite and other coexisting sulphosalts usually represent aikinite and friedrichite. Those occurring further away from the aggregates grade to krupkaite. Large grains of aikinite reaching even 1 mm across encountered within the association with Bi-sulphides similarly correspond to aikinite and friedrichite, whereas compositions of small grains from their outer mosaic rims grade up to gladite.

"False felbertalite"

It occurs as elongated laths up to 500 μm long or irregular grains in intergrowths with giessenite and Ag-bearing galena. Position of the phase in the

Cu(Ag)–Pb–Bi(Sb) diagram corresponds to felbertallite but, in relation to other ferbetalite samples known worldwide, it is atypicaly enriched in Sb and Ag. In contrast, these compositions normalized to *ΣMe-Cu=16 apfu* according to the cosalite structure show an excees of Cu above 2 atoms per unit cell and a small deficiency of Bi. Thus, the phase fit neither felbertalite nor cossalite, and it can be related to still not recognized "false felbertalite" (Ilinca 2006).

Berryite - $(Ag,Cu)_5Pb_3Bi_7S_{16}$

Berryite occurs as tabular, elongated crystals up to 100 μm long only in the accumulations with giessenite and gustavite. The calculated composition is close to the ideal formula, with the Cu/Ag ratio varying from 1.39 to 1.52, similarly as at berryite from other occurrences.

Wittichenite - $(Cu,Ag)_3BiS_3$

Witichenit occurs as thin elongated laths, 10-50 μm in size, associated with "false felbertallite" and giessenite, various members of the aikinite-bismuthinite sieries and Bi-sulphides, sulphselenides, and also within the mineralization from the W part of the schist belt. Usually it does not contain Ag, but in some crystals coexisting with matildite and galenobismuthite the Ag amounts reach 3.5 wt. %.

Galenobismuthite - $Pb_2Bi_2S_5$ and matildite - $AgBiS_2$

The phases were found within the schist belt only in the form of very small inclusions, coexisting sometimes with tin-bearing sulphides (stannite, stannoidite, mawsonite). Their compositions are close to the ideal formulas typical of the minerals.

ACKNOWLEDGEMENTS: These studies were supported by the AGH - University of Science and Technology grant no. 11.11.140.158 and the Ministry of Education and Science grant no. 5 T12B 043 24.

REFERENCES

GOŁĘBIOWSKA B., 2003: Okruszcowanie w złożu dolomitu Rędziny ze szczególnym uwzględnieniem minerałów strefy hipergenicznej. Ph.D. thesis, AGH University of Science and Technology, unpublished, 1-249. (in Polish).

ILINCA GH., 2006: Rare sulphosalt minerals in Romania. Acta Miner.-Petrogr., Abstr. 5: 42-46.

MAKOVICKY E., KARUP-MØLLER S., 1977: Chemistry and crystallography of the lilianite homologous series. Part I: General properties and definitions. N. Jb. Miner. Abh. 130, 3: 264-287.

PIECZKA A., GOŁĘBIOWSKA B., PARAFINIUK J., 2004: Sphalerite-chalcopyrite-stannite assemblage from a mineralization zone in Rędziny and its significance in ore-genesis explanation. Pol. Tow. Mineral. Prace Spec. 24: 315-318.

ZAKRZEWSKI M.A., MAKOVICKY E., 1986: Izoklakeite from Vena, Sweden, and the kobellite homologous series. Can. Miner. 24: 7-18.

MINERALOGIA POLONICA - SPECIAL PAPERS
Volume 28 - 2006

Bożena GOŁĘBIOWSKA[1], *Jacek MATYSZKIEWICZ*[1], *Remigiusz MOLENDA*[1], *Andrzej GÓRNY*[1]

HYDROTHERMAL MINERALIZATION IN MIDDLE JURASSIC SANDY LIMESTONES FROM ZALAS (NEAR CRACOW, S POLAND)

INTRODUCTION

The Zalas area is located about 5 kilometers south from Krzeszowice, in the southern, marginal part of the Silesian-Kraków Monocline. The monocline, including Triassic, Jurassic and Cretaceous strata, was formed during the Laramide orogeny. In the Zalas quarry the Permian volcanics have been exploited for decades. The intrusion is a ryodacitic and andesitic laccolith, formed about 280-260 Ma ago, during the Early Permian sinistral, transtensional tectonic regime dominating the Central Europe in that period (Nawrocki et al. 2005). In the Silesian-Kraków region the transtension propagated along the broad Kraków-Lubliniec deep-fracture zone, which separated the Małopolska and the Upper Silesian blocks. The zone originated in the Early Paleozoic and was active until the Cenozoic (Żaba 1999).

The succession exposed in the Zalas quarry includes Permian, Middle and Upper Jurassic rocks. In 2005 the mining operations exposed a fault, which cuts Middle Jurassic sandy limestones and is accompanied by hydrothermal mineralization. The extension of this fault into the overlying Upper Jurassic strata could not be proven.

The reasons of the appearance of carbonate buildups as early as in the Jasna Góra Beds, in the lowermost part of Oxfordian succession of the Kraków-Wieluń Upland are not fully understood. Trammer (1985) interpreted this fact in terms of synsedimentary tectonic movements, which led to the formation of heights or breaks of the sea-bottom slope inhabited by benthic fauna. However, the latest studies (Matyszkiewicz et al. 2006) point out that the development of Upper Jurassic carbonate buildups took place mainly over the Paleozoic intrusions.

The appearance of carbonate buildups with rigid framework in the lowermost part of Upper Jurassic succession in the Zalas area might have also been connected with the influence of increased temperatures from hydrothermal solutions on benthic biocenoses inhabitating the sea bottom close to the tectonic zones. There is, however, an alternative hypothesis that the formation of fault zone in Zalas and its hydrothermal mineralization took place during the Tertiary tectonic movements caused by extensional stress field related to overthrusting Carpathian flysch nappes.

METHODS

Chemical compositions of the minerals were analysed at the Inter-Institute

[1] *Faculty of Geology, Geophysics and Environmental Protection, AGH University of Science and Technology, al. Mickiewicza 30, 30-059 Kraków, Poland; goleb@uci.agh.edu.pl*

Analytical Complex for Minerals and Synthetic Substances of the Warsaw University using a CAMECA SX100 electron microprobe operating in the WDS mode under the following conditions: excitation voltage 15 kV, beam current 20 nA, peak count-time 20 s, background time 10 s.

RESULTS

Hydrothermal mineralization occurs within the fault zone, in the brecciated Middle Jurassic sandy limestones. The minerals are present in caverns, and form irregular veins intersecting the rocks or surrounding the breccia clasts. The size of aggregates in the caverns reaches 1-2 cm, whereas the thickness of veins is up to 0.5 cm. The caverns are filled, first of all, with brownish and black Fe and Mn compounds and green accumulations of malachite. Within these aggregates can be found primary copper minerals, mainly chalcopyrite (size of grains to 0.5 mm). In the reflected light and BSE images there can be recognized 1-1.5 cm large pseudomorphs after sulphides, filled with carbonates, sulphates and various hydroxyoxides.

Fine relics of the primary minerals (chalcopyrite and pyrite) and of secondary sulphides (bornite, covellite and chalcocite) are enclosed in the hypergenic „oxide" minerals. The secondary sulphides often overgrow the grains of chalcopyrite or form small veins, that penetrate the primary sulphides, but pseudomorphs composed of covellite and chalcosite after chalcopyrite are also widespread. The chemical composition of the chalcopyrite approximates its theoretical formula, only traces (<0.01 wt. %) of Ag, Bi, Pb and Cd have been found. Chalcosite replaces the primary chalcopyrite and often forms intergrowths with covellite, overgrown with copper sulphates and carbonates. The chalcocite reveals elevated Fe contents (to 1.7 wt. %) and admixtures (< 0.1 wt. %) of Ag and Te. The relics of pyrite do not exceed 100 μm and are enclosed in the secondary Fe, Mn and Cu minerals. This pyrite contains up to 1 wt% Cu and below 0.1 wt% Ag, Te and Mn.

Barite was observed in BSE images most often in a mineralized carbonate rock as irregular grains with sizes not exceeding 200 μm. In its chemical composition the admixtures of: Sr (<1.7 wt. %), Fe (< 1.5 wt. %), Ca (< 0.9 wt. %) as well as Al and Pb (< 0.1 wt. %) have been noted.

Malachite is the most common hypergenic mineral, developed as 1-2-cm large accumulations of massive or acicular grains or coatings on breccia clasts. It also fills small veins with hydrothermal calcite or quartz, often overgrowing their grains. The malachite contains up to 1.5 wt. % Fe and traces of Pb, Ba, Sr, Ca, P and S. Copper sulphates co-occur with malachite and are represented mainly by brochantite and antlerite. Most often they overgrow small relics of chalcocite, sometimes of chalcopyrite. In BSE images, the sulphates form massive accumulations, within which can be sometimes distinguished "ghost" outlines of their idiomorphic, monoclinic or orthorhombic crystals.

Within the malachite accumulations, close to the pyrite relics, there has been identified Ag iodide, most probably iodargyrite (AgI). A small size of its grains (below 5 μm) prevents their detailed assaying.

Iron compounds belong most probably to two generations. The first one has hydrothermal origin and fills small veins with chalcopyrite relics, the other one has hypergenic origin, commonly present in voids and fractures, also developed as coatings on rock fragments and as pseudomorphs after pyrite. The idiomorphic crystals of hydrothermal goethite reach sizes of 100 μm in contrast to very fine grains of hypergenic oxides and hydroxyoxides. This second type of goethite is often amorphous and shows significant concentrations, among others, of Cu, Mn, Co and Si. The goethite is associated with manganese compounds; they are represented, most probably, by asbolanes containing high amounts of Co (maximum to 13 wt. %) and admixtures of Cu, Fe, Ca, Pb, Bi and Al.

Analyses in microareas have indicated the presence of disseminated, fine grains (to 20 μm) of Pb (galena, sometimes overgrown by cerussite) and Bi minerals (native Bi and bismuthite).

The preliminary investigations of the mineral assemblage from Zalas indicate its hydrothermal origin and later advanced weathering. The first information on the Fe and Mn mineralization in Zalas was published by Brochwicz et al. (1984), but without many details.

A common coexistence of chalcopyrite and pyrite suggests an approximate crystallization temperature of these minerals slightly above 300 °C, whereas the formation of native Bi must have taken place at 273 °C. The hydrothermal Fe and Mn compounds crystallized at much lower temperatures, probably below 150 °C. The silver iodides must be of the hypergenic origin.

ACKNOWLEDGEMENTS: This work was supported by the Faculty of Geology, Geophysics and Environmental Protection, AGH-University of Science and Technology.

REFERENCES

BROCHWICZ-LEWIŃSKI W., GĄSIEWICZ A., STRZELECKI R., SUFCZYŃSKI S., SZATKOWSKI K., TARKOWSKI R., ŻBIK M., 1984: Anomalia geochemiczna na pograniczu jury środkowej i górnej w południowej Polsce. Przegl. Geol., 12: 547-650.

MATYSZKIEWICZ J., KRAJEWSKI M., KĘDZIERSKI J., 2006: Origin and evolution of an Upper Jurassic complex of carbonate buildups from Zegarowe Rocks (Kraków-Wieluń Upland, Poland). Facies, 52: 249-263.

NAWROCKI, J., POLECHOŃSKA, O., LEWANDOWSKA, A., WERNER, T., 2005: On the palaeomagnetic age of the Zalas laccolith (southern Poland). Acta Geol. Polon., 55: 229-236.

TRAMMER J,. 1985: Sponge bioherms in the Jasna Góra Beds (Oxfordian of the Polish Jura Chain). Przegl. Geol., 33: 78-81. (in Polish with English summary).

ŻABA J., 1999: The structural evolution of Lower Palaeozoic succession in the Upper Silesia Block and Małopolska Block border zone, southern Poland. Prace Państw. Inst. Geol., 166: 1-162. (in Polish with English summary).

MINERALOGIA POLONICA - SPECIAL PAPERS
Volume 28 - 2006

Miroslava GREGEROVÁ[1], Dalibor VŠIANSKÝ[1], Petr SULOVSKÝ[1],

THE MINERALS CAUSING DEGRADATION OF CONCRETE AND THEIR FORMATION PROCESSES

INTRODUCTION

The degradation of concrete has become a serious problem worldwide. One of its most significant factors is the formation of C-S-H and C-A-H products, carbonates, gypsum, ettringite, and thaumasite. The authors especially focused on sulfatation. Considering the number of concrete constructions (not just) in Central Europe and their age, the research of concrete degradation has increasing importance.

METHODS

The research consists of three parts. The first one deals with the samples of degraded concrete, which were extracted from various constructions, especially from highways, bridges and dams. These samples were examined by optical microscopy, chemical analyses and XRD.

Another part is represented by laboratory absorption experiments. These were evaluated using scanning electron microscopy and methods of chemical analyses.

And last but not least, we have been attempting to use the geochemical software Phreeqc for Windows for modelling the formation processes of degradation minerals recently.

RESULTS

The research by optical microscopy unambiguously showed that C-A-H products are of much bigger importance than it has been generally assumed (Fig. 1). The formation successions of degradation minerals were also suggested.

The first set of absorption experiments with sodium sulfate solution we have done so far was dealing with the problems of the transportation and concentration changes of the solution in the porous system of concrete binder (Fig. 2). The results of chemical analyses corresponded with the ones obtained using the Phreeqc for Windows software.

The same software was applied for the construction of the theoretical curves of ettringite chemical ballance. The charts show that the most significant factor affecting formation of this mineral is the pH of porous solution.

[1] *Institute of Geological Sciences, Kotlářská 2, 611 37 Brno, Masaryk University, Czech Republic; mirka@sci.muni.cz*

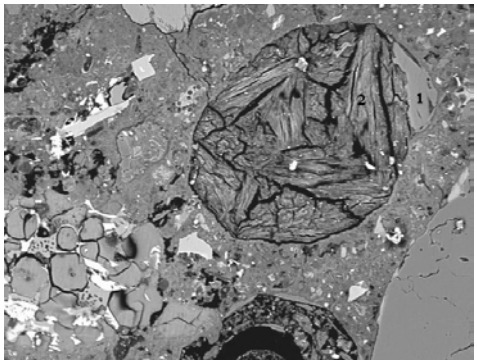

Fig. 1. Ettringite (2) and calcium-aluminium hydrate (1) filling pores of the Jevišovice dam concrete. Photo P. Sulovský.

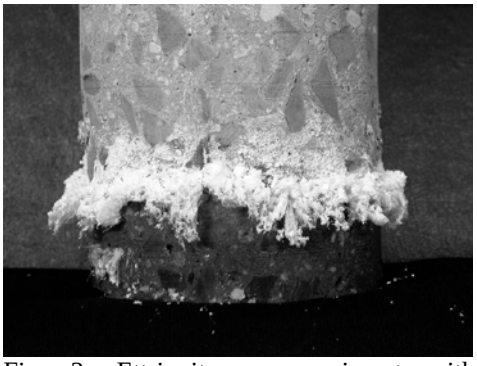

Fig. 2. Ettringite – experiment with absorption ability of 3.3% sodium sulphate solution (14 days after start of the experiment). Photo D. Všianský.

CONCLUSIONS

Although building industry is one of the main parts of economy and lots of resourses are being put into it, the interest in the material degradation has been surprisingly low so far. The presented research aims to contribute to clearing up the ways of formation of the minerals causing the degradation of concrete exposed to various conditions.

The authors found out significant differences among the sulfatation processes in highway concrete, dam constructions and in laboratory conditions.

ACKNOWLEDGEMENTS: The contribution has been elaborated within The Scientific Research Programme MSM 0021622418 – Dynamic Geovisualisation in Crisis Management.

REFERENCES

CZEREWKO M.A. et al., 2003: Sulfur species in geological materials—sources and quantification. Cement and Concrete Comp., 25: 657–671.

DENG MIN, TANG MINGSHU, 1994: Formation and expansion of ettringite crystals. Cement and Concrete Res., 24: 119-126.

ODLER I., COLÁN-SUBAUSTE J., 1996: Investigations on cement expansion associated with ettringite formation. Cement and Concrete Res., 29: 731–735.

SKALNY J., et al., 2002: Sulfate attack on concrete. Spon Press, London and New York.

SHAYAN A., IVANUSEC I., 1996: An experimental clarification of the association of delayed ettringite formation with alkali-aggregate reaction. Cement and Concrete Comp., 18: 161-170.

MINERALOGIA POLONICA - SPECIAL PAPERS
Volume 28 - 2006

Miroslava GREGEROVÁ[1], Martin HLOŽEK[2]

APPLICATION OF OPTICAL METHODS FOR THE RESEARCH OF NEOLITIC CERAMICS

INTRODUCTION

The contribution summarizes the possible ways of the application of optical methods for the identification of the basical structures and substance character of ceramic artefacts including the identification of the raw material provenience. The method also enables the assesment of the conditions and aproximate temperatures of firing. The main aim of the research is to pick the differences among the ceramics of the individual stages of the Linear Pottery culture, imported ceramic artefacts and local raw material base.

The relations between microstructure and colour of burned out ceramics were examined by Stepkowska, Jefferis (1992). Contributions aimed at the identification of petrographic types were published e.g. by Mallory-Greenough et al. (2002); Gregerová et al. (2003); Gregerová, Hložek (2005); Přichystal (2005). Papers documenting the application of optical microscopy in ceramography were published among others by Isaacson, Aleto (1989); Donahue et al. (1990), Gregerová et al. (2003) and Gregerová (1996).

Middleton et al. (1985) were concerned about the problems of ceramics structures. The suggestion for the classification of ceramic microstructures was given by Gregerová (1996).

METHODS

The basical metod is optical polarization microscopy using reflected and transmitted polarized light. In addition, the Olympus BX51 polarizing microscope allows a parallel observation using both of the polarization types.

Before optical investigation, archeological descriptive analysis and macroscopic description of artefacts is always done. The preparation of a sample for micropertrographic analyses proceeds in the following way: a thin slice is cut out from a ceramic body. The slice is glued to a slide and ground to the thickness of 0.05-0.03 mm. It can be covered with a cover slip or the surface of the thin slice can be polished and used e.g. for reflection microscopy or electron microscopy. 27 samples of complete or reconstructed vessels were analyzed and another 29 samples of the ceramics incidentally present in the soil were collected. 55 thin sections of the settlement ceramics of the Ia, Ib and IIa Linear Pottery stages were compared.

[1] *Institute of Geological Sciences, Kotlářská 2, 61137 Brno, Masaryk University, Czech Republic; mirka@sci.muni.cz*

[2] *Institute of Archaeology and Museology, Arna Nováka 1, 602 00 Brno, Masaryk University, Czech Republic*

RESULTS

We focused on the searching of conformities and differences among settlement and funeral findings during the research of technology of the Vedrovice Linear Pottery.

It was proved that typical raw materials of funeral and settlement ceramics from the „Široká u lesa“ site in Vedrovice are represented by loess, loess soils, less abundant are eluvial soils, clays and clay soils. The micropertographic analyses of non-plastics showed the presence of mineral and rock fragments. 98 % of the raw materials were of local provenience, which is also documented by typical non-plastics association: sericite shales, mica shists, gneisses, aplites, cataclazites, quarzites and metaquartzites.

From the viewpoint of the dating of substages of the “Široká u lesa“ site ceramics, there are no marked differences among them. We did not notice preference of any particular raw material in any of the investigated substages.

From the viewpoint of the examination of raw material base, there is a noticeable wide range of used raw materials and a use of common raw materials among the individual substages. This is the result of the comparative study among the individual substages of the settlement Linear Pottery from Vedrovice Ia, Ib, IIa. The clay was exploited in a close distance of settlement objects. A distinct feature of the Ia LnK substages of ceramics set (from the “Za dvorem“ site) is a considerable prevalence of binder over non-plastics. We assume that this ceramics does not contain on purpose added non-plastics. Another observable difference is in the organic compounds contants in body, which is in comparison to the previous stages high here. The raw material base is represented by loess soil and eluvia of ganitoid rocks. The firing temperatures of the substages Ia LnK ceramics set ranged about 500 °C – 600 °C. The firing was reducing.

In comparison to the previous Ia stage, the settlement ceramics of the Ib LnK stages (from the “Široká u lesa“ site) has only low contents of organic compounds and higher contents of non-plastics. Both of the examined settlement substages have common non-plastics and they correspondent to the identically dated burial ground ceramics. Some of the bodies have completely identical composition. Crushed ceramics sporadically occur in the non-plastics of the LnK stage from the “Široká u lesa“ site. The Ib LnK stage settlement ceramics was fired approximately at 700 °C.

The IIa LnK stage ceramics (from the “Za Dvorem“ site) is very close to both of the settlement ceramics (Ia and Ib). Besides higher mentioned clasts, another rock fragments (iron sandstones, duststones) also occur in non-plastics. Crushed ceramics rarely occur there as well. Occurence of imported ceramics is sporadic. The firing temperatures have a wide range between 500 – 950 °C.

CONCLUSION

It is possible to state that the raw materials of both settlement and funeral ceramics findings from the “Široká u lesa“ site are identical. This fact supports the theory that the settlement ceramics made of local subsoil was probably put into graves. Among the ceramics put into graves as a charity, the thick-walled storing

ceramics with abundant non-plastics of granitoid rocks typical for some ceramics sets from the "Za dvorem" site unambiguously misses.

ACKNOWLEDGEMENTS: The contribution was elaborated within the Scientific Research Project MSM 0021622427.

REFERENCES

DONAHUE J., WATTERS D.R., MILLSPAUGH S., 1990: Thin section petrography of northern Lesser Antilles ceramics. Geoarcheol., 5, 3: 229-254.

GREGEROVÁ M., 1996: Petrografie technických hmot. 1. vyd. Masaryk Univ., Brno, 1-139. (in Czech)

GREGEROVÁ M., HLOŽEK M., 2005: Micropetrographic analysis. In: Škrdla P (Ed.): The Upper Paleolithic on the Middle Course of the Morava River. Dolnověstonické studie, 13/2005: 223-225.

GREGEROVÁ M., NERUDOVÁ Z., HLOŽEK M., HAVLICA, J., 2003: Analysis a burnt clay fragment from the Paleolithic site Brno-Bohunice I. Anthropologie, 41/2003: 295-301.

ISAACSON J.S., ALETO T.F., 1989: Petrographic analysis of ceramic thin sections from La Puna Island, Ecuador. Archeomaterials, 3: 61-67.

MALLORY-GREENOUGH L.M., GORTON P., GREENOUGH J.D., 2002: The source of basalt vessels in ancient Egyptian archaeological sites: a mineralogical approach. Can. Mineral., 40: 1025-1046.

MIDDLETON A.P., FREESTON I.C., LEESE M.N., 1985: Textural analysis of ceramic thin sections: evaluation of grain sampling procedures. Archaeometry, 27: 64-74.

PŘICHYSTAL A., 2005: Minerály těšínitů jako ostřivo v keramice púchovské kultury na výšinné lokalitě Okrouhlá u Staříče nedaleko Frýdku – Místku. Ve službách archeologie, 6: 203-208. (in Czech)

STEPKOWSKA E.T., JEFFERIS S.A., 1992: Influence of microstructure on firing colour of clays. Applied Clay Sci., 6: 319-342.

MINERALOGIA POLONICA - SPECIAL PAPERS
Volume 28 - 2006

Miloš GREGOR[1]

MINERALOGY OF OPALS FROM CENTRAL SLOVAKIAN NEOVOLCANIC AREA: A PRELIMINARY STUDY

INTRODUCTION

Central Slovakian Neovolcanic area is know with numerous found of amourphous or paracrystalline forms of silica. Despite of this fact no exact study was made on amorphous or paracrystalline silica occurance in volcanic rocks of mentioned area except of petrified woods from limnoquartzites from Žiar basin (Forgáč et al. 1990). Aim of this study is to characterized common opals with help of standard mineralogical analytical techniques.

For this preliminary study were choosen following localities with opal occurance: Badín, Kosorín, Lehôtka pod Brehmi, Mochovce and Nevoľné. Opal occurance is connected to volcanic rocks and epiclastic deposits of andesite volcanism (Badín, Mochovce, Nevoľné) and rhyolite volcanism (Lehôtka pod Brehmi, Kosorín). In both cases epiclastic deposits consist from volcanic breccia, conglomerates or tuffs and there is no sign after hydrothermal alteration of andesitic and rhyolitic rocks (Lexa 1998).

METHODS

For this research, twenty samples from mentioned localities were studied by standard mineralogical analytical techniques that included optical microscopy, powder x-ray diffraction analyse (PXRD), scanning electron microscopy (SEM), infrared spectroscopy (IR) and microprobe analyses (EMPA). X-ray powder diffraction analysis were carried out on X-ray machine DRON-3 (Geological institute, Faculty of Natural Science, Comenius University) with following analytical conditions: Co Kα1 source was obtained under current 30 mA a 15 kV voltage and with goniometer step 0,1°2θ/s. Surface morphology of samples was acquired with JEOL JXA 840A scanning electron microscope (Laboratories for the Electric and Optic methods, Comenius University of Bratislava) using 5 nA current with a 10 kV voltage. The IR spectra were obtained with MAGNA 750 spectrophotometer (Institute of Anorganic Chemistry, Slovak Academy of Science) with use of KBr pressed pellet and DRIFT technique. Chemical composition of opal was obtained by using electron microprobe CAMECA SX100 (Geological Institute of Dionýz Štúr) using 15 mA current and 20 kV voltage. For the analysis were used following standards: BaF_2 (F), albite (Na), NaCl (Cl), wollastonite (Si), Al_2O_3 (Al), MgO (Mg), orthoclase (K), TiO_2 (Ti), hematite (Fe), chromite (Cr), rodonite (Mn), nickel (Ni).

[1] *Geological Institute, Faculty of Natural Science, Comenius University, Mlynská dolina, 842 15 Bratislava, Slovak Republic; geolgregor@yahoo.com*

RESULTS

According to macroscopic observations all opals are light to dark green in colour and they are covered with yellowish or white layer from 1 – 3 mm thick. Opals from Nevoľné show layered texture with smooth and porous fabric. These layers are variable in thickness from 8 to 15 mm. Based upon the PXRD analysis opals from Mochovce and Kosorín belong to opal-CT (Floerke, Jones 1975), opals from Lehôtka pod Brehmi and Badín belong to opal-CT/A and finally opals from Nevoľné belong to opal-A/CT (Lynne, Campbell 2004). With help of SEM analysis characteristic lepispheres morphology belonging to opal-CT, transitional opal-A/CT and opal-CT/A was detected. Samples from Badín, Nevoľné and Mochovce are cointaning variable amounth of phylosilicates with expanding layers – smectites and phylosilicates without expanding layers – most probably kaolinite were detected in samples from Kosorín, Lehôtka pod Brehmi. Also thin yellowish to white layer consist from phyllosilicates with expanding layer. All these minerals were identified with help of PXRD and IR spectroscopy. Besides this infrared spectra of opals resembles infrared spectra of tridymite. In opals were also identified inclusion of goethite and in case of Nevoľné monazite and covellite. EMPA analyses were carried out in order to estimate chemical composition but analyses did not give proper results (e.g. total sum of analysed oxides were below 88 percent).

DISCUSSION AND CONCLUSIONS

According to study of Lynne and Campbell (2004) the layered structure is due to two different initial depositional processes, polymeric or monomeric respectively.Opal-A/CT and opal-CT/A (Lynne, Campbell 2004) are metastable members of transfer from opal-A $\Rightarrow$ opal-CT $\Rightarrow$ opal-C $\Rightarrow$ quartz. The occurence of these types of opals is due to presence of phylosilicates with expanding layers, that are retarding the metastable opals from opal-CT formation (Hinman 1998).

Based upon these resutls we are not able to say if opals from studied localities are product of weathering or low hydrothermal activity.

Formation of opals due to the weathering of volcanic rocks can be supported by fact that surrounding rocks are not affected by hydrothermal activity (Lexa 1998) and opals are forming crusts with various thickness or nests in epiclastic deposits or occasionally they are filling cracks and fissures in underlaying andezites/rhyolites. The source of silica necessary for opal formation could come form upperlaying epiclastic deposits rich in volcanic glass.

Till now there is no straight evidence for opal formation from low hydrothermal fluids but also we cannot exclude this possibility as minerals like smectites, covellite and goethite were described in close relationship with analysed opals. All of these minerals can be products of low hydrothermal activity as either products of weathering (Šucha 2001).

REFERENCES

FORGÁČ J., ČURLÍK J., HARMAN M., 1990: Recrystallization of SiO_2 in petrified woods. Mineralia slovaca, 22: 273-280. (in Slovak)

HINMAN W.N., 1998: Sequences of silica phase transformations: effects of Na, Mg, K, Al and Fe ions. Marine Geology, 147: 13-24.

LEXA J., 1998: Additional text to geological map of Kremnické vrch Mts. Geological Institute of Dionýz Štúr, 1-308. (in Slovak)

JONES J.B., SEGNIT E.R., 1971: The nature of opal I. Nomenclature and constituent phases. J. of the Geol. Soc. of Australia, 18, 1: 57-68.

LYNNE Y.B., CAMPBELL A.K., 2004: Morphologic and mineralogical trasnsitions from opal-A to opal-CT in low-temperature siliceous sinter diagenesis, Taupo Volcanic Zone, New Zealand. J. Sed. Res., 74, 4: 561-579.

ŠUCHA V., 2001: Clay minerals in geological processes. Acta Geologica Universitatis Comenianae, Monographic Series, 1-159. (in Slovak)

MINERALOGIA POLONICA - SPECIAL PAPERS
Volume 28 - 2006

Stanislav HOUZAR[1], Milan NOVÁK[2]

FLUORINE-RICH CLINTONITE IN CHONDRODITE MARBLES FROM THE MOLDANUBIAN ZONE, CZECH REPUBLIC

INTRODUCTION

Clintonite $Ca(Mg,Al)_3(SiAl_3)O_{10}(OH)_2$ is a rare brittle mica occurring chiefly in contact metamorphosed marbles and skarns. It exhibits a wide stability field in PT diagrams, restricted to low X_{CO2}. Its scarcity in nature is controlled by specific chemical composition of rocks characterized by very high Al/Si ratio and low activity of K and Na (Olesch, Seifert 1976, Bucher-Nurminen 1976, Rice 1979, Mottana et al. 2002). New occurrences of clintonite (Clt) were found in marbles of the Moldanubian Zone (localities: Číhalín, Sokolí, Tasov, western Moravia).

METHODS

Chemical composition of minerals was studied using electron microprobe Cameca SX-100 (GÚDŠ, Bratislava; operator V. Kollárová). These analytical conditions were applied: accelerating voltage 15 kV, beam diameter 5-10 μm, beam current 20 nA and counting times 20 s. Following standards and Kα lines were used: wollastonite (Si, Ca), TiO_2 (Ti), orthoclase (K), albite (Na), Al_2O_3 (Al), MgO (Mg), hematite (Fe), rhodonite (Mn), BaF_2 (F), barite (Ba), and chromite (Cr).

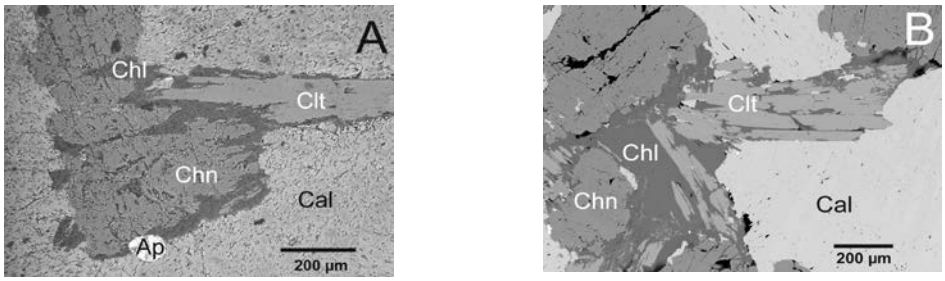

Fig. 1. BSE image of the assemblage clintonite (Clt) + chondrodite (Chn) + chlorite (Chl) + calcite (Cal) + apatite (Ap); Číhalín (A), Tasov (B).

RESULTS

Clintonite-bearing chondrodite marbles represent a rare type of metacarbonate rocks in the Moldanubian Zone (Houzar, Novák 2001). They form thin bodies (about 1 m) enclosed in migmatites occurring exclusively in envelope of melanocratic ultrapotassic granites (durbachites). They consist of dominant calcite,

[1] *Department of Mineralogy and Petrography, Moravian museum, Zelný trh 6, 659 37 Brno, Czech Republic, shouzar@mzm.cz*
[2] *Institute of Geological Sciences, Masaryk University, Kotlářská 2, 611 37 Brno, Czech Republic*

less abundant dolomite; amounts of silicates vary from about 5 to 30 vol. %. The early mineral assemblage Dol+Cal+Prg ±Phl is replaced by the assemblage Cal+Chn+Clt, and succesively by apparently retrograde chlorite. Accessory minerals include apatite, spinel, Mg-rich ilmenite, and very rare rutile and baddeleyite.

Clintonite, closely associated with calcite and chondrodite, forms colorless to pale green flakes and their sheaf-like aggregates, up to 2 mm in size, apparently replaced by chlorite (Fig. 1). It exhibits very low Al/Si (2.4-2.3), low concentrations of Ti (0.010-0.024 *apfu*) and K, Ba and Mn (below detection limit). Contents of Fe (0.041-0.128 *apfu*) and Na (0.035-0.203 *apfu*) are low as well. High concentrations of F (0.437-1.014 *apfu*) corresponding up to 25 at. % of the F-component are typical.

Table 1. Representative compositions of clintonite (Clt) and chondrodite (Chn)

	CHL 1	SOK 2	TAS 1	TAS 2	CHL 1	SOK 4	TAS 1	TAS 2
wt.%	Clt	Clt	Clt	Clt	Chn	Chn	Chn	Chn
SiO_2	19.57	20.19	21.00	20.62	34.66	34.87	34.60	34.30
TiO_2	0.17	0.06	0.09	0.09	0.66	0.30	0.34	0.41
Al_2O_3	39.51	38.36	37.02	37.97	b.d.	b.d.	b.d.	b.d.
MgO	21.81	22.82	22.44	22.57	55.50	56.98	55.51	55.40
CaO	13.23	13.09	12.83	12.86	0.57	0.02	0.03	0.06
FeO	0.72	0.48	1.07	1.07	3.01	2.22	4.53	3.98
MnO	b.d.	b.d.	b.d.	b.d.	0.09	0.04	0.14	0.14
Na_2O	0.18	0.20	0.33	0.36	b.d.	b.d.	b.d.	b.d.
K_2O	0.02	0.02	0.03	0.03	b.d.	b.d.	b.d.	b.d.
H_2O *	3.51	3.47	3.38	3.20	2.91	2.67	2.93	2.70
F	1.60	1.71	1.84	2.29	4.84	5.40	4.82	5.22
O=F	-0.67	-0.72	-0.77	-0.96	-2.04	-2.27	-2.03	-2.20
TOTAL	99.68	99.72	99.27	100.09	100.20	100.23	100.87	100.01
Number of anions	24	24	24	24	10	10	10	10
Si^{4+}	2.747	2.829	2.961	2.886	1.996	1.998	1.991	1.988
Ti^{4+}	0.018	0.006	0.010	0.010	0.029	0.013	0.015	0.018
Al^{3+}	6.535	6.336	6.152	6.263	-	-	-	-
Mg^{2+}	4.563	4.768	4.717	4.709	4.766	4.868	4.762	4.786
Ca^{2+}	1.989	1.965	1.938	1.928	0.035	0.001	0.002	0.004
Fe^{2+}	0.085	0.056	0.126	0.125	0.145	0.106	0.218	0.193
Mn^{2+}	-	-	-	-	0.004	0.002	0.007	0.007
Na^{+}	0.049	0.054	0.090	0.098	-	-	-	-
K^{+}	0.004	0.004	0.005	0.005	-	-	-	-
OH^{-}	3.290	3.242	3.179	2.986	1.118	1.021	1.123	1.043
F^{-}	0.710	0.758	0.821	1.014	0.882	0.979	0.877	0.957
Cat.sum	15.993	16.023	16.001	16.024	6.975	6.989	6.994	6.995

* calculated from stoichiometry, all Fe as FeO

Chemical composition of chondrodite varies within a single grain and X_F = 34-49 and it corresponds to *„hydroxylchondrodite*". Chondrodite is Fe-poor (except locality Tasov with Fe ≤ 0.224 *apfu*); elevated Ti was found in Chn from Číhalín (Ti ≤ 0.03 *apfu*). Chlorite shows high variability in Al (2.004-3.440 *apfu*). Fluorine rich (F ≤ 1 *apfu*) Na-Al-amphiboles (pargasite, edenite) are locally enclosed as relics in chondrodite.

DISCUSSION

Clintonite is a minor mineral in the assemblage Cal+Chn+Clt. The concentration of F ≤ 1.014 *apfu* is the highest ever recorded as well as its low Al/Si ratio (MacKinney et al. 1988). Formation of Clt coexisted with more abundant Chn is not clear, because textural relations do not show apparent replacement features. The most probable seems its origin from pargasite (Prg) according to the reaction:

$$Prg + Dol + H_2O\text{-}F \rightarrow Chn + Clt + Cal + CO_2.$$

Chlorite is a product of the retrograde reaction:

$$Chn + Clt + CO_2 \rightarrow Chl + Cal.$$

The mineral assemblage Chn+Clt+Cal in chondrodite marbles seems to be similarly as the assemblage Fo+Chu+Spl in dolomite marbles a product of regional HT/LP metamorphism: P ~ 2-4 kbar; T ~ 650 °C (Novák, Houzar 1996). Moreover, it is related to influx of H_2O ($\delta^{13}C_{calcite}$ = -0.6 - -4.2 PDB; $\delta^{18}O_{calcite}$ = 12.5 - 15.7 SMOW) and especially F from an external source.

REFERENCES

BUCHER-NURMINEN K., 1976: Occurrence and chemistry of xanthophyllite in roof pendants of the Bergell Granite, Sondrio, Northern Italy. Schweiz. Mineral. Petrogr. Mitt., 56: 413-426.

HOUZAR S., NOVÁK M., 2001: Marbles in the southeastern margin of the Bohemian Massif (Review). Vlastivěd. Sbor. Vysočiny Odd. Věd Přír., 15: 3-33 (in Czech).

MAC KINNEY J.A., MORA C.I., BAILEY S.W., 1988: Structure and crystal chemistry of clintonite. Amer. Mineral., 73: 365-375.

MOTTANA A., SASSI F.P., THOMPSON J.B., GUGGENHEIM S., 2002: Micas: crystal chemistry and metamorphic petrology. Rev. Mineral., 46: 1-499.

NOVÁK M., HOUZAR S., 1996: The HT/LP metamorphism of dolomite marbles in the eastern part of the Moldanubicum; a manifestation of heat flow related to the Třebíč durbachite Massif. J. Czech Geol. Soc., 41: 139-146.

OLESCH M., SEIFERT F., 1976: Stability and phase relations of trioctahedral calcium brittle micas (clintonite group). J. Petrol., 17: 291-314.

RICE J.M., 1979: Petrology of clintonite-bearing marbles in the Boulder aureole, Montana. Am.. Mineral., 64: 519-526.

MINERALOGIA POLONICA - SPECIAL PAPERS
Volume 28 - 2006

Dušan HOVORKA[1]

AMPHIBOLES OF THE WESTERN CARPATHIANS METAMORPHIC COMPLEX: THEIR OCCURRENCES AND TYPES

INTRODUCTION

Silicate-group minerals, which represent solid solutions of two, or even more end molecules, offer generally accepted tools for evaluation of the protolith type on one side, and the actual p-T conditions during their blasthesis, on the other one. Among such belong also amphibole-group minerals. Their sensitivity on the given protolith type and the p-T path was one of the basis to define principles of metamorphic facieses using basic rocks as the protolith (Goldschmidt 1911, Eskola 1920-1921).

The usefullness of the amphibole-group minerals in metamorphic petrology has been highly positively influenced by the: 1) introduction of an electron microprobe into petrological praxis, and 2) acceptation of the uniform nomenclature and classification of the mentioned group minerals (Leake et al. 1997).

In the Western Carpathians metamorphic complexes, which originated under the low-, medium- and even high pressure conditions and various p-T trajectories, several amphibole-group minerals are known to occur. Based on geochronological and geological evidences metamorphic rock sequences, in which amphiboles play the role of the rock-forming minerals, are known to occur in several gelogical units. They originated during the variscan as well as alpine metamorphic processes. In the paper review of the amphibole-group minerals problematic is presented.

REVIEW OF THE AMPHIBOLE-GROUP MINERALS OCCURRENCES

Variscan origin

I.1. Mineral composition of amphibolite bodies is simple: plagioclases and Ca-hornblendes of deep-green up to brown color. Amphiboles are locally replaced by brown biotite. Composition of amphiboles was not studied in detail yet.

I.2. The low grade amphibolite facies Gemeric unit Klátov nappe, is composed of metabasites and metasediments. In metabasites ferroan pargasite and ferroan edinite were identified (Hovorka et al. 1988). Radvanec (1992) in the unit identified several amphibole types, being result of local different p-T conditions.

I.3. Leptynite-amphibolite complex contains amphiboles in metabasites, as well as in „dark“ leptynite types. They correspond to Fe-pargasite and light-brown edenite; youngest generation is represented by actinolite (Méres et al. 2000).

I.4. Around serpentinites in metamorphic complexes blackwall zones were described (Hovorka 1965). Amphibole in them correspond to tremolite-actinolite series. Jelšava-Kohútik locality bears tremolites up to 20 cm in prolongation.

I.5. In metamorphosed Ol-Opx-Cpx-Hbl gabbros and troctolites to the N of Heľpa amphiboles correspond to Ti-pargasite and pargasitic hornblende (Ivan et al.1996).

[1] *Constantine the Philosopher´s University, Trieda A. Hlinku 1, 949 74 Nitra, Slovak Republic; hovorka@fns.uniba.sk*

I.6. Except of wellknown chrysotile of asbestos morphology in serpentinite at the Dobšiná locality as well as in Slovinky in the last time asbestiform actinolite and Si-edenite were identified (Hovorka and Dubíková 1995).
I.7. Boudins of retrogressed eclogites are enclosed in the LAC of several mountain ranges. Complicated history of their uplift and hydration is documented by several generation of amphiboles documented in papers by Hovorka et al. (1992), Janák et al. (1997) and Korikovsky and Hovorka (2001).
I.8. Eastward of the town Brezno in the LAC among metabasite types with dominant cummingtonite is under study. It is the most probable that it represents phase originated by recrystallization of protolithic Fe-gabbros.
I.9. In the southern veporic crystalline complex near Kokava n/Rim. positions of Fe-rich metasediments contain grunnerite (Korikovsky et al. 1989) together with actinolite, actinolitic hornblende and Mg-hornblende (Radvanec 2000).
I.10. Early Paleozoic Gemeric unit greenschists lithologies bear different amphibole-group minerals. The most common is actinolite (Korikovsky et al. 1991). Actinolitic hornblende, grunnerite, edenitic hornblende and tschermackite (Faryad 1991, 2000). In pillowed metabasalts Hovorka et al. (1988) described hastingsite, Al-taramite, barroisite, actinolite. Later on also anthophyllite, Fe-pargasite, winchite, actinolitic hornblede were identified (Radvanec 1999).
I.11. Calc-silica hornfelses (erlans) belong among rare rocks in the Western Carpathians (the Malé Karpaty Mts.: moderately aluminous pleochroic hornblendes and actinolites: Cambel et al. 1989, Tatry Mts., Nízke Tatry Mts., and Early Paleozoic of the Gemeride Unit (Kruhová near Dobšiná town): various tschermackite types: Spišiak et al. 1989).
I.12. In the last years Faryad and Peterec (1987) studied already long time ago known skarn bodies cropping out in the Early Paleozoic metamorphics of the Gemeric unit. Presence of tremolite-actinolite, tirodite, Mg-cummingtonite documents long lasting proces of the skarn mineral asssociation generation.
I.13. In the Gemeric Unit Early Paleozoic together with black shales diagenetic accumulations of Mn-rich metasediments in Čučma, Hekerová and other localities do occur. Among Mn-silicates and carbonates also Mn-tremolites (Kantor 1954), Mn-richactinolites (Faryad 1994) and Mn-rich anthophyllite (Rojkovič 2001) were reported.
I.14. Medium- till coarse-grained anchimonomineral amphibole rocks form numerous bodies in the central Western Carpathians zone crystalline. No analytical data dealing with amphiboles are at disposal. Prevailing of them, based on optical properties, seem to belong to the actinolite-tremolite group.

Alpine origin

II.1. One of the Triassic-Jurassic sedimentary-volcanic complexes of the Inner Western Carpathiuans is known as the Meliata Unit. During Alpine-age high-pressure metamorphic recrystallization from different, sedimentary as well as magmatic protoliths Faryad (1997) described Mg-hornblende from the Rudník area, crossite-rich cores with glaucophane and Fe-glaucophane rich rims in metabasites, as well as crossite-riebeckite series of amphiboles and actinolites.

II.2. Amphiboles of the Upper Carboniferous greenschist metabasites and the IInd generation of amphiboles of the Veporic Unit amphibolites are identical (Hovorka and Méres 1996). They both are products of the Alpine-age metamorphic event and are of actinolite composition.

II.3. Amphiboles in metabasites of the Gemeric Unit SW Upper Carboniferous metabasite occurrences we studied from the adjacent area to the antigorite serpentinite body at Bôrčok Hill near Kalinovo village. There were identified amphiboles of the actinolite, Mg-hornblende, Fe-hornblende and Fe-tschermackite chemical composition (Spišiak, Hovorka 2005).

CONCLUSIONS

i) Composition of the discrete amphibole, being the rock-forming constituent of various rock-lithologies, was fundamentally influenced by

a) operating p-T conditions during amphibole blasthesis,
b) leading trend (progressive or retrogressive) of metamorphic processes,
c) type of the amphibole protoliths,
d) isochemical or allochemical type of metamorphic processes

i) During the metamorphic recrystallization of some lithologies evidently allochemical processes took part. They were generally of two types:

a) allochemical processes during which only local transport of mainly alkalies is detectable: biotitization of amphiboles observed in some granite aureoles being an example,

b) allochemical processes during which input of some elements to the system is detectable. Example: processes of the blueschists origin. Tholeiitic basalts (= protolith has below 1 % of Na_2O, blueschists mostly above 3 % Na_2O).

i) Alpine recrystallization of variscan metabasite bodies nemely of the southern Veporic Unit yielded in the formation of the IInd generation of amphiboles, forming rim around the Ist amhibole generation. Composition of the IInd amphibole generation is identical with that one of the Upper Carboniferous metabasites occurring in the just the same geographic room.

i) Though amphiboles of various chemical composition belong among rock-forming minerals of various rock lithologies, in several cases (I.4, I.14) they are the only phase substantially present in the given rock body.

REFERENCES

CAMBEL B., KORIKOVSKY S.P., MIKLÓŠ J., BORONIKHIN V.A. 1989: Calc-silicate hornfelses (erlans and Ca-skarns) in the Malé Karpaty Mts. region. Geol. zborn. Geol. carpathica, 40, 3: 281-304.

ESKOLA P. 1920-1921: The mineral facies of rocks. Norsk Geol. Tidsskr. 6, Kristiania 1922, 143-494.

FARYAD S. W., PETEREC D., 1987: Manifestation of skarns mineralization in the eastern part of the Spišsko-gemerské rudohorie Mts. Geol. Zbor. Geol. Carpath., 38, 1: 111-128.

FARYAD S. W., 1991: Pre-Alpine metamorphic events in Gemericum. Miner. Slov., 23, 5-6: 395-402. (in Slovak)

FARYAD, S. W. 1994: Mineralogy of Mn-rich rocks from the greenschist facies sequences of the Gemericum, the Western Carpathians, Slovakia. Neu. Jb. Miner. Mh., 464-480.

FARYAD S. W. 1997: Lithology and metamorphism of the Meliata unit high-pressure rocks. In: Grecula P. eds.: Geological evolution of the Western Carpathians, 131-144.

FARYAD S. W. 2000: Tectonic slices with amphibolite facies assemblages: a further member of the Meliata unit. Miner. Slov., 32, 3: 173-174. (in Slovak)

GOLDSCHMIDT V. M. 1911: Die Kontakmetamorphose in Kristiangebiet. Vidensk. Skr., 11: 483.

HOVORKA D., 1965: Endokontaktné zjavy v sepentinite pri Málinci (Veporské rudohorie). Geol. Práce, Zprávy, 37: 127-134. (in Slovak)

HOVORKA D., IVAN P., JILEMNICKÁ L., SPIŠIAK J., 1988: Petrology and geochemistry of metabasalts from Rakovec (Paleozoic of Gemeric unit, Inner Western Carpathians). Geol. Carpath., 39, 4: 395-425.

HOVORKA D., MÉRES Š., CAŇO F., 1992: Petrology of the garnet-clinopyroxene metabasites from the Malá Fatra Mts. Miner. Slov., 24: 45-52. (in Slovak)

HOVORKA D., DUBÍKOVÁ K., 1995: Dva typy „azbestu“ z Dobšinej. Miner. Slov., 27: 106-112. (in Slovak)

HOVORKA D., MÉRES Š., 1996: Dve genetické typy metabazitov v juhozápadnej časti veporika Miner. Slov., 28: 273-280. (in Slovak)

IVAN P., HOVORKA D., MÉRES Š., 1996: Gabbroid rocks – a newly-found member of the leptyno-amphibolite complex of the Western Carpathians. Slovak Geol. Mag., 3-4: 199-203.

JANÁK M., HOVORKA D., HURAI V., LUPTÁK B., MÉRES Š., PITOŇÁK P., SPIŠIAK, J., 1997: High-pressure relics in the metabasites of the Western Carpathians pre-Alpine basement. In: Grecula P. ed.) Geological evolution of the Western Carpathians. 301-308.

KANTOR J., 1954: Pôvod mangánových rúd v Spišsko-gemerskom rudohorí. Geol. Práce, Spr., 1: 70-71. (in Slovak)

KORIKOVSKIJ S. P., DUPEJ J., BORONIKHIN V.V., 1989: Vysokoželezité metasedimenty z Kokavy nad Rimavicou (veporikum). Miner. Slov., 21, 3: 251-258. (in Slovak)

KORIKOVSKY S. P., BORISOVSKY S.Y., GRECULA P., 1991: Metamorfné rovnovážne stavy počiatočného stupňa biotitovej subfácie vulkanicko-sedimentárnych hornín staršieho paleozoika gemerika. Miner. Slov., 23, 1: 1-7. (in Slovak)

KORIKOVSKY S. P., HOVORKA D., 2001: Two types of garnet-clinopyroxene-plagioclase metabasites in the Malá Fatra Mountains crystalline complex, Western Carpathians: Metamorphic evolution, p-T conditions, symplectitic and kelyphytic textures. Petrology, 9, 2: 140-166.

LEAKE B., WOLLEY A.R., BIRCH W.D., GILBERT M.C., GRICE J.D., HAWTHORNE F.C., KATO A., KISCH H.J., KRIVOVICHEV V.G., LINTHOUT K., LAIRD J., MANDARINO L., MARESCH W.V., NICKEL

E.H., ROCK N.M.S., SCHUMACHER J.C., SMITH D.C., STEPHENSON N.C.N., UNGARETTI L., WHITTAKER E.J.W., YOUZHI G., 1997: Nomenclature of amphiboles. Eur. J. Min., 9: 623-651.

MÉRES Š., IVAN P., HOVORKA, D., 2000: Granaticko-pyroxenické metabazity a antigoritické serpentinity – dôkaz leptynitovo-amfibolitového komplexu v Branisku. Miner. Slov., 32, 5: 479-486. (in Slovak)

RADVANEC M. 1992: Zonálnosť nízkotlakovej polyfázovej metamorfózy v otvorenom systéme pre fluidnú fázu v rulovo-amfibolitovom komplexe gemerika. Miner. Slov., 24, 3-4: 175-196. (in Slovak)

RADVANEC N, 1999: Eklogitizované pyroxenické gabro s retrográdnou metamorfózou v pumpellyitovo-aktinolitovej fácii na vrchu Babiná a Ostrá (Gemerikum). Miner. Slov., 31, 5-6: 467-484. (in Slovak)

RADVANEC M. 2000: Metapelit, amfibolová bridlica a vznik magnetitovo-grafitovej mineralizácie vo veporiku pri Kokave nad Rimavicou. Miner. Slov., 32, 1: 1-16. (in Slovak)

ROJKOVIČ I., 2001: Early Paleozoic Manganese Ores on the Gemericum Superunit Western Carpathians, Slovakia. Geolines, 13: 34-41.

SPIŠIAK J., HOVORKA D., IVAN P., JILEMNICKÁ L., 1989: Karbonátové metasedimenty
amfibolitovej fácie klátovskej skupiny (staršie paleozoikum, gemerikum, Západné Karpaty). Geol. práce, Spr., 90: 81-94. (in Slovak)

SPIŠIAK J., HOVORKA D., 2005: Metabazity a metasedimenty z okolia ultrabázického telesa medzi Brezničkou a Kalinovom. Miner. Slov., 37, 1: 47-54. (in Slovak)

MINERALOGIA POLONICA - SPECIAL PAPERS
Volume 28 - 2006

Dušan HOVORKA[1], Ján SPIŠIAK[2]

JADEITITE LENGYEL CULTURE AXES FROM WESTERN SLOVAKIA SITES

INTRODUCTION

During the very last years also in Slovakia begun interdisciplinary/ transectorial research known as archaeometry or petroarchaeology. In connection with raw material types originated under high pressure papers by Hovorka et al. (1998) and Spišiak and Hovorka (2005) should be also mentioned. Meanwhile one axe (in the following text treated as axe No. 1) was found during field survey on surface by amateur collector near Sobotište (westernmost part of the country) and results of our laboratory studies were published in 1998 (l. c.), axes Nos. 2 and 3 were found by Golianovo, some 7 kms eastward of the Nitra town. Also in this case no archaeological field survey was performed yet and given axes fragments (together with other stone implemens and ceramic fragments) were found by amateur-collector Mr. L. Esse on agriculturaly exploited fields.

Among highly evaluated rock types used in the Neolithic and Aeneolithic as the raw material type for tools and weapons construction belong also high -pressure rocks, namely jadeitites, nephrites, eclogites ao. Their hardness on one side and elasticity, pleasant color and stability under various climatic conditions on the other one, caused their utilization by the Neolithic/ Aeneolithic craftsmen all round the world. Mentioned raw material types, namely jadeitites and nephrites (described namely by archaeologists under common denomination as „jade“) are still used namely in southeastern Asia countries as the raw material for statues of Budha and other gods or generally of sacral symbols construction. Mentioned types of rocks are used as semi-precious stones in gemmology round the world till now.

Taking into account problems connected with different use of the term „jade“ namely in archaeology on one side and gemmology on the other one in accordance with proposal by D´Amico et al. (1995), based on the mineral composition of the artefacts presented in this paper petrographic term „jadeitite“ seems to be the most adequate.

RESULTS

Realised microprobe studies of discussed 3 jadeitite Lengyel culture axes till now found on the territory of the Slovak Republic brought evidences, that during the „evolution“ (or geological history) of raw material bodies, gradual changes to clinopyroxenes with increased amount of CaO was documented in all axes studied. So in actual classification of Na-Ca clinopyroxenes (Morimoto et al. 1989) position of analysed clinopyroxenes in discriminating diagramme (Fig. 1) corresponds to

[1] *Constantine the Philosopher´s University, Trieda A. Hlinku l, 949 74 Nitra, Slovak Republic; hovorka@fns.uniba.sk*
[2] *Geological Institute Slovak Academy of Sciences, Severná 5, 974 01 Banská Bystrica, Slovak Republic*

jadeites as well as omphacites. It is the consequence of the upleaving of the source jadeitite bodies in the Earth crust, during which process their recrystallization and simultaneous change of their chemical composition took part.

All three studied jadeitite axes of Lengyel culture are constructed from massive, by naked eyes aphanitic apple green raw material. On axe No. 1 seldom occurring till 1 mm in diameter shallow negative forms (hollows) were observed. Aggregates of mentioned dimensions, formed by fine-grained zoisites and plagioclases are irregularly disseminated in the whole axe body, so we suppose that mentioned holes are consequence of zoisite-plagioclase aggregates weathering. Though we have at our disposal one more or less completely preserved axe (axe No. 1) and fragments of axes Nos. 2 and 3 only, all of them have more or less identical morphology. All three axes have not pronouncedly trapezoid shape with oblong and slightly biconvex axe bodies and partially rounded edges.

Thin section pattern of studied axes are very familiar up to identical. Highly dominant is short-columnar till isometric colorless clinopyroxene (of size below 0,1 m) of massive pattern. In all three axes studied the amount of clinopyroxene is over 95 %, so rocks belong to the category of monomineralic rocks. In accessory amount zoisite, relic plagioclases, ore minerals, rutile and light mica were identified. In axe No. 1 within its body unsharply limited zones of columnar clinopyroxenes of greater grain-size (up to 0.2 mm) are present. They represent zones of younger recrystallization in comparison to the adjacent jadeitite mass. Their presence caused preferently pseudooriented pattern of the jadeitite.

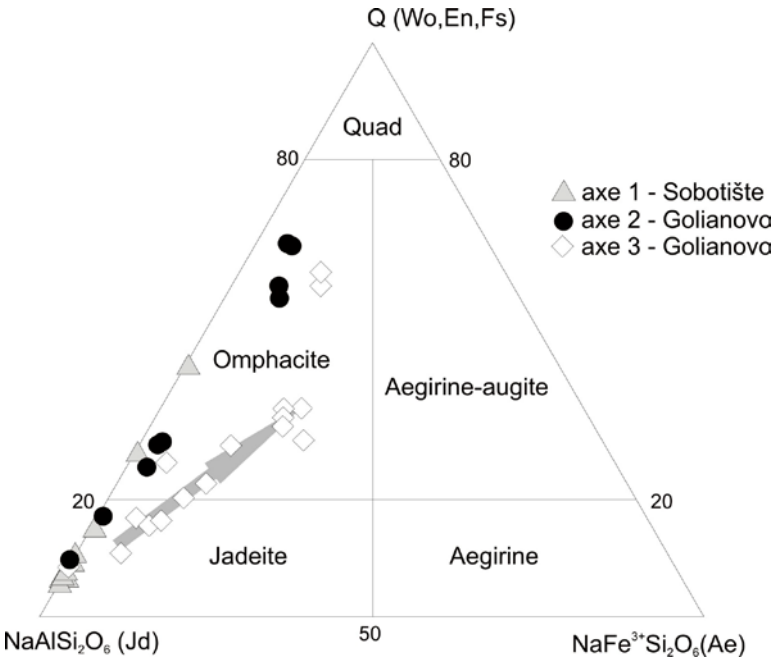

Fig. 1. Ternary diagram of analysed clinopyroxenes of jadeitite axes.

Based on results of clinopyroxene microprobe analyses of axes Nos. 1 –3 (analyses in papers by Hovorka et al. 1998, in print; Fig. 1) we should summ up that dominant rock-forming phase of axes studied belong to jadeite as well as omphacite (Fig. 1). Their distinction, because of their small size, in thin sections is impossible. Based on spatial distribution of, by microprobe identified two Na-Ca clinopyroxene types (e.g. jadeite and omphacite: Fig. 1), we rank Na-richest clinopyroxene type as older being rimmed by Ca-Na clinopyroxenes. This question was interpreted in paper by Hovorka et al. (1998). Situation is identical in all 3 studied axes (Fig. 1).

Among the most important aspects of archaeometric/petroarchaeological research belong not only problematic of identification of materials used in prae-history, but also to answer question about its provenience, on one side, and the migration paths of raw materials or already made implements from the places of their elaboration to sites of their discovery, on the other one.

As in the central European mountain ranges (the Eastern Alps, Carpathians, Dinarides, Balcans, the Bohemian Massif) no jadeitite geological bodies are known, the nearest jadeitite occurrences are cropping out in the Western Alps, wherefrom, as we considered in the past (Hovorka et al. 1998), jadeitite already made implementrs were transported via Po lowland and than following amber route. So in this case transcontinental transport of the Neolithic stone implements is considered. In the case of jadeitite made implements of just the same stratigraphical ranking documents intensive trade contacts betweeen discussed parts of the Old continents.

ACKNOWLEDGEMENTS: This study also represents a partial output from the grants APVV No. 51-012504 and VEGA No. 2/6092/26.

REFERENCES

D´AMICO C., CAMPANA R., FELICE G., GHEDINI M., 1995: Eclogites and jades as prehistoric implements in Europe. A Case of petrology applied to Cultural heritage. Eur. J. Mineral., 7, 1: 29-42.

HOVORKA D., FARKAŠ Z., SPIŠIAK J., 1998: Neolithic jadeitite axe from Sobotište (Western Slovakia). Geol. Carpath., 49, 4: 301-304.

HOVORKA D., SPIŠIAK J., in print: Two Lengyel culture jadeitite axes from Golianovo (western Slovakia).

MORIMOTO N., FABRIES J., FERGUSON A.K., GINZBURG I.V., ROSS M., SEIFERT F.A., ZUSSMAN J., AOKI K., GOTTARDI G., 1988: Nomenclature of pyroxenes. Am. Min., 73, 9-10: 1123-1131.

SPIŠIAK J., HOVORKA D., 2005: Jadeite and Eclogite: Peculiar Raw Materials of Neolithic Stone Implements in Slovakia and Their Possible Sources. Geoarchaeology: An International Journal, 20, 3: 229-242.

MINERALOGIA POLONICA - SPECIAL PAPERS
Volume 28 - 2006

Tomáš HRSTKA[1], Jiří ZACHARIÁŠ[1]

X-RAY NANOTOMOGRAPHY IN FLUID INCLUSIONS STUDY

INTRODUCTION

In this preliminary study we have tested for the first time the application of the X-RAY NanoTomography as a tool for 3D visualization and volume reconstruction of aqueous and aqueous carbonic fluid inclusions. This method was tested in order to potentially provide exact volumes and fill ratios for aqueous and complex aqueous-carbonic gas bearing non-fluorescent fluid inclusions. Such data are of great importance for the PVTX thermodynamic modeling in fluid inclusion research (Tricart et al. 2000; Grimmer et al. 2003; Bakker, Diamond 2006). As a part of this project also the potential for reconstruction of fluid inclusions trail geometry in 3D was tested.

METHODS

X-RAY NanoTomography is a method, which use the combination of X-ray transmission technique with tomographical reconstruction by using the focused X-ray beam pointed on the sample, which rotates. The data are simultaneously recorded by CCD detector and transferred to the PC, which use the Cone-beam volumetric reconstruction algorithms (Feldkamp algorithm) for creation of the 3D image of the sample from the individual recorded 2D (radiography) sections (Skyscan 1977). The great advantage of the NanoTomography is that it does not need any preparation, coating or vacuum treatment for the studied sample. The final images are a mixed combination of density and compositional information from the specimen (Skyscan 1977; Baruchel et al. 2000). The maximal diameter of the sample is 10 mm for SkyScan-2011 and about 50 mm for SkyScan 1172 where the resolution is about 150-250 nm and 5 μm respectively (Skyscan 1977). All the measurements in this study were performed on NanoTomograph SkyScan-2011 in the SkyScan laboratory in Belgium.

RESULTS

For our measurements the classical double polished thin sections prepared from the main quartz vein from the Libčice Gold deposit were used. Two Small broken chips containing numerous H_2O-CO_2-CH_4 and H_2O only inclusions were analyzed in order to obtain the accurate 3D volume reconstructions of individual fluid inclusions and the 3D space orientation and relationships of individual fluid inclusion secondary trails. The Imaris 4.0© software was used for data reduction, recalculation and 3D visualization. Some illustrative results, reconstruction images are shown on Fig.1 a, b. By this procedure we were able to visualize the individual fluid inclusions inside the quartz matrix and calculate their volume. In the

[1] *Charles University in Prague, Faculty of Science, Institute of Geochemistry, Mineralogy and Mineral Resources; Albertov 6, 128 43 Praha 2, Czech Republic; hrstka@natur.cuni.cz*

inclusions containing two or more different phases only the difference between the host mineral and void space can be seen and no phase boundaries (H_2O liquid /H_2O vapor) were recognized. The additional tests are necessary to establish the precision of the calculation of inclusion volume and test the potential of this method for use in all other fluid inclusion host minerals.

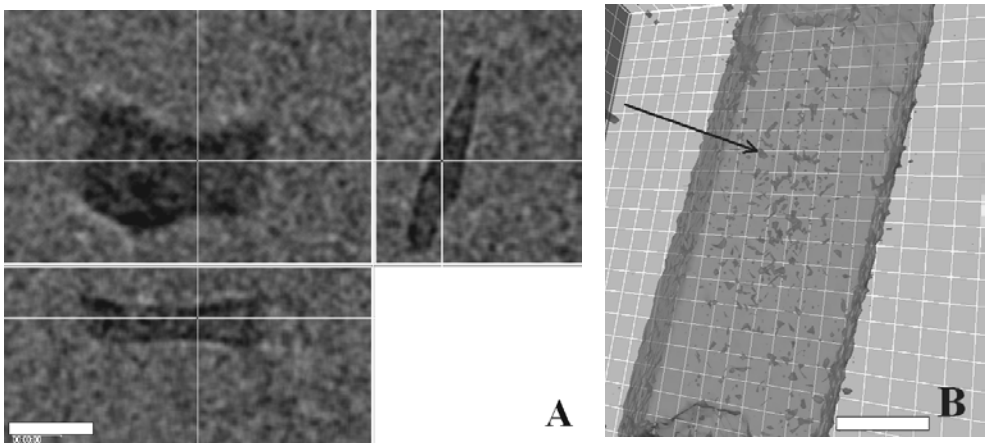

Fig.1. H_2O-CO_2 Fluid inclusions from the Libčice gold deposit visualized by nanoCT. A: xyz sections through H_2O-CO_2 inclusion in quartz (scale 10 μm). B: 3D reconstruction of the part of thin section with numerous trapped fluid inclusions arrowed (scale 150 μm).

CONCLUSIONS

We have demonstrated that the X-RAY NanoTomography is a suitable technique for 3D reconstruction and visualization of individual fluid inclusions in quartz and potentially all other inclusion host minerals including the opaque phases. There are some restrictions of its applicability so far related to its current resolution and problems related to limited use for visualization of materials with low-density difference. Nonetheless, we can see the clear potential of this methodology and its applications for study of different geological samples non-destructively in 3D and on um scale (van Geet et al. 2000).

ACKNOWLEDGEMENTS: We are grateful to the SkyScan Company for supporting the instrumentation and all necessary technical support. This project was a part of the project GACR 205/06/382.

REFERENCES

BAKKER R.J., DIAMOND L.W., 2006: Estimation of volume fractions of liquid and vapor phases in fluid inclusions, and definition of inclusion shapes. Am. Mineral., 91: 635-657.

BARUCHEL J., BUFFIÈRE J-Y., MAIRE E., MERLE P., PEIX G., 2000: X-ray tomography in material science, general principles. Hermes Science Publications, Paris, 15-21.

GRIMMER J.O.W., PIRONON J., TEINTURIER S., MUTTERER J., 2003: Recognition and differentiation of gas condensates and other oil types using microthermometry of petroleum inclusions (in Proceedings of Geofluids IV); J. Geochem. Explor., 78-79: 367-371.

SKYSCAN 1977: Skyscan 1072 Desktop microscope-microtomograph: instruction manual. Skyscan, Aartselaar, 1-43.

TRICART J.P., VAN GEET M., SASOV A., 2000: Using Micro-CT for 3D characterization of geological materials. Microscopy and analysis, 65: 1-31 .

VAN GEET M., SWENNEN R., WEVERS M., 2000: Quantitative analysis of reservoir rocks by microfocus X-ray computerised tomography. Sed. Geol., 132: 25-36.

MINERALOGIA POLONICA - SPECIAL PAPERS
Volume 28 - 2006

Jiří HYBLER[1], Slavomil ĎUROVIČ[2], Toshihiro KOGURE[3]

POLYTYPISM IN CRONSTEDTITE

Cronstedtite, a trioctahedral 1:1 phyllosilicate with the chemical composition generally expressed as $(Fe^{2+}_{3-x}\ Fe^{3+}_{x})^{VI}\ (Si_{2-x}Fe^{3+}_{x})^{IV}O_5(OH)_4$ (where x is in the range of about 0.5 ~ 0.8). It occurs in low- and medium-temperature hydrothermal deposits and also in some kinds of meteorites.

Its structure is composed of the octahedral (*Oc*) and tetrahedral (*Tet*) sheets forming the 1:1 layer by sharing apical oxygen atoms. The layers are kept together by hydrogen bonds (Fig. 1).

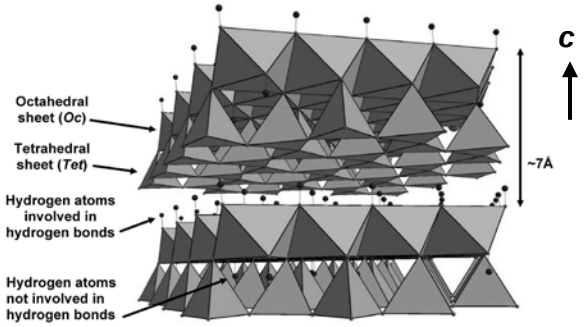

Fig. 1. Crystal structure of cronstedtite, side view.

Cronstedtite is a suitable mineral to investigate polytypism because a variety of polytypes has been reported. These polytypes are divided into four groups or OD subfamilies termed A, B, C, and D, which are distinguished by the shift and rotation between adjacent layers; $\pm a_i/3$ shifts for group A, $\pm a_i/3$ shifts combined with 180° rotation for group B, $\pm b/3$ or no shift for group C, $\pm b/3$ or no shift combined with 180° rotation for group D, where a_i and b correspond to the edges of hexagonal and orthohexagonal cell, respectively. (Bailey 1969; Dornberger-Schiff, Ďurovič 1975a, b)

Recently, the crystal structures of several polytypes of cronstedtite were refined: 3*T* (Smrčok et al. 1994), 1*T* (Hybler et al. 2000) and $2H_2$ (Hybler et al. 2001). These polytypes represent OD-subfamilies (Dornberger-Schiff, Ďurovič 1975a, b), or Bailey's (1969) groups A, C and D, respectively. No polytype of the group B has been found to date.

Polytypism of cronstedtite can be studied by following methods:

(1) Single crystal X-ray diffraction

[1] *Institute of Physics, Academy of Sciences of the Czech Republic,Na Slovance 2, 182 21 Praha 8, Czech Republic; hybler@fzu.cz*

[2] *Institute of Inorganic Chemistry, Slovak Academy of Sciences, 842 36 Bratislava, Slovak Republic*

[3] *Department of Earth and Planetary Science, Graduate School of Science, University of Tokyo, 7-3-1 Hongo, Bunkyo-ku, Tokyo, 113-0033, Japan*

(2) High-resolution electron diffraction (HRTEM)
(3) Selected area electron diffraction (SAED)
(4) Electron back-scattering pattern (EBSP)

Some other methods can be utilized as auxiliary:

(5) Electron microanalysis (EMA) including back-scattered electron (BSE) images and chemical mapping
(6) Scanning electron microscopy (SEM)
(7) Visual check of crystals

Ad (1) Subfamilies and polytypes can be identified according to the distribution of diffraction spots along the 11*l* and 10*l* reciprocal lattice rows respectively of precession photographs (Fig. 2) or, more recently in unwarped images of the reciprocal lattice converted from CCD frames.

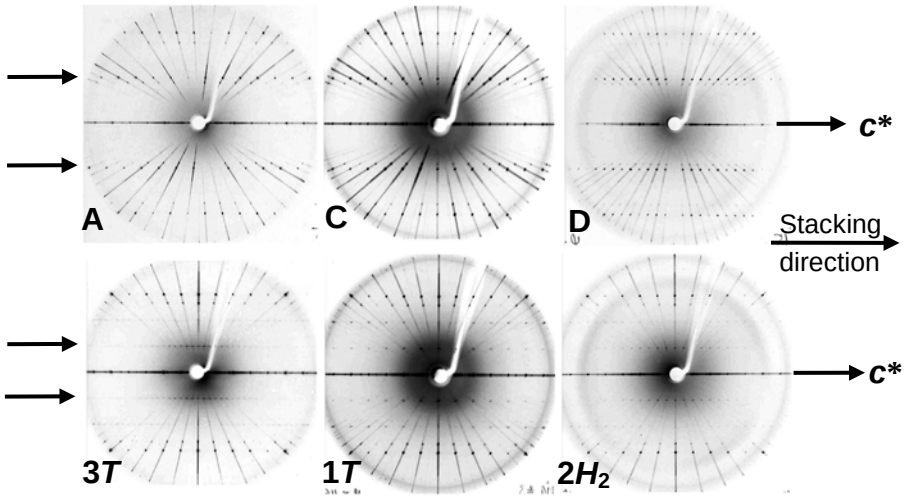

Fig. 2. The *hhl* (above) and *h*0*l* (below) precession photographs of subfamilies A, C, D and of their typical polytypes. The 11*l* and 10*l* reciprocal lattice rows are indicated by arrows.

Ad (2) Cronstedtite is very suitable for HRTEM studies because of its resistance under the electron beam due to its high iron content (Kogure *et al*., 2001, 2002). This method allows determining subfamilies and polytypes in smaller scale as well as to visualize the stacking faults and out-of-step domains (Fig. 3a, b).

Ad (3) The SAED produces similar diffraction pattern and gives the same information as X-ray diffraction but from substantially smaller volume. (Fig. 3c,d).

Ad (4) The arrangement of Kikuchi lines on EBSP pattern allows to determine the subfamily in a very small area.

Ad (5) Electron microanalysis revealed changing composition in dependence on the subfamily: from relatively Fe poor C to intermediate A and Fe rich D.

Ad (6), (7) the subfamily is very often reflected in the morphology of the crystal, it can be observed by SEM or even by naked eye. Triangular pyramids are typical for A and C, conical crystals for C, triangular acicular crystals for A, rounded acicular or columnar crystals for D subfamily.

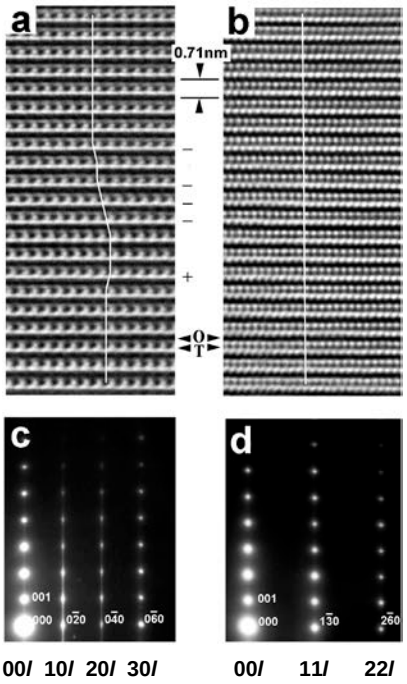

Fig. 3. The HRTEM and SAED images of cronstedtite-1*T* (subfamily C). a) projection perpendicular to *h*0*l* plane, the white line connects equivalent positions in each layer; it is straight in ordered sequences but it shows lateral stagger where stacking fault appears. b) projection perpendicular to *hhl* plane. O, T indicate positions of *Oc*, *Tet* sheets, repectively. c) SAED image of *h*0*l* reciprocal lattice plane, d) SAED image of *hhl* reciprocal lattice plane (*cf.* X-ray diffraction pattern in Fig. 2). (Indices on SAED images are related to the orthohexagonal cell, the hexagonal indices used throughout this paper are below the images).

REFERENCES

BAILEY S.W., 1969: Polytypism of trioctahedral 1:1 layer silicates. Clays and Clay Minerals, 17**:** 355-371.

DORNBERGER-SCHIFF K., ĎUROVIČ S., 1975a: OD interpretation of kaolinite-type structures - I: Symmetry of kaolinite packets and their stacking possibilities, Clays and Clay Minerals, 23: 219-229.

DORNBERGER-SCHIFF K., ĎUROVIČ S., 1975b: OD interpretation of kaolinite-type structures - II: The regular polytypes (MDO polytypes) and their derivation. Clays and Clay Minerals, 23: 231-246.

HYBLER J., PETŘÍČEK V., ĎUROVIČ S., SMRČOK Ľ., 2000: Refinement of the crystal structure of the cronstedtite-1T. Clays and Clay Minerals, 48: 331-338.

HYBLER J., PETŘÍČEK V., FÁBRY J., ĎUROVIČ S., 2001: Refinement of the crystal structure of cronstedtite-$2H_2$. Clays and Clay Minerals. 50: 601-613.

KOGURE T., HYBLER J., ĎUROVIČ S., 2001: A HRTEM study of cronstedtite: Determination of polytypes and layer polarity in trioctahedral 1:1 layer silicates. Clays and Clay Minerals, 49: 310-317.

KOGURE T., HYBLER J., YOSHIDA H., 2002: Coexistence of two polytypic groups in cronstedtite from Lostwithiel, England. Clays and Clay Minerals**,** 50: 504-513.

SMRČOK Ľ., ĎUROVIČ S., PETŘÍČEK V., WEISS Z., 1994: Refinement of the crystal structure of cronstedtite-3T. Clays and Clay Minerals, 42: 544-551.

MINERALOGIA POLONICA - SPECIAL PAPERS
Volume 28 - 2006

Peter KODĚRA[1], Jaroslav LEXA[1], Viera KOLLÁROVÁ[1], Anthony E. FALLICK[2]

SOURCE AND EVOLUTION OF FLUIDS OF MAGMATIC-HYDROTHERMAL SYSTEMS OF THE JAVORIE STRATOVOLCANO

INTRODUCTION

Central zone of the Javorie stratovolcano hosts five hydrothermal centers: Podlysec, Banisko-Červený vrch, Skalka, Podpolom and Stožok, all closely genetically and spatially related to stocks of diorite, quartz-diorite and monzodiorite porphyry (Štohl et al. 1981). Upper portions of individual intrusions grade into extensive zones of advanced argillic alteration, including metasomatic quartzites, pyrophyllite, alunite, diaspore, topaz and zunyite (Žáková 1988). Deeper parts of stocks host porphyry-type alteration and rudimentary Cu- mineralization.

PETROLOGICAL ASPECTS

Petrological study was performed mostly on samples from hydrothermal centres Banisko and Podpolom, documenting a complex evolution of fluids from their exsolution from magma down to low-temperature hydrothermal alteration. Two-feldspar geothermometry (Haselton et al. 1983) was used to determine the temperature of eutectic crystallization at ~750 °C, which corresponds roughly to the experimentally determined crystallization temperature of water-saturated melt at 1 kbar. Thus, the residual melt was able to exsolve fluids almost from the start of the eutectic crystallisation. Granophyric and myrmekite structures of the groundmass further suggest rapid crystallisation of a fluid-rich melt. The residual melt, rich in fluid was eventually segregated into clusters and nests, where coarse-grained feldspar, quartz and biotite have crystallised.

Actinolitization and biotitization of pyroxenes and recrystallization of K-feldspar form high-temperature subsolidus alteration. Secondary biotite is enriched in Mg and replaces pyroxene in the form of flakes or occurs as veinlets or in groundmass. During subsolidus regime and K-metasomatism the primary K-feldspar was replaced by low-temperature K-feldspar, rich in Or component. This type of alteration indicates interaction with fluid of higher salinity, which was found trapped in secondary fluid inclusions in magmatic quartz (halite-bearing inclusions). Based on the results of two-feldspar and ilmenite-magnetite geothermometry these high-temperature subsolidus processes occurred during decreasing temperature from 600 to 350 °C, while the rock has predominantly preserved products of alteration in the interval 500 – 400 °C.

Main low-temperature alteration includes chloritization of pyroxene and biotite, already affected by actinolitization during the earlier stage, and replacement of plagioclase by sericite, which occurs just below the zone of advanced

[1] *Geological Survey of the Slovak Republic, Mlynská dolina 1, Bratislava, 817 04, Slovak Republic; kodera@gssr.sk*
[2] *SUERC, Rankine Avenue, East Kilbride, G75 0QF, UK*

argillitization. Pyrite also frequently accompanies low-temperature alteration. Epidote, anhydrite, pyrite mineral association occurs in veinlets and also replaces pyroxene. Secondary albite and K-feldspar replace plagioclase in the form of network of tiny veinlets or they occur along with pyrite as hydrothermal veinlets in groundmass. The youngest K-feldspar is enriched in Ba up to 4.5 wt. %. The observed alteration patterns indicate interaction with fluids of lower salinity with the pH range 5.5–7.0 that are probably represented by halite-absent secondary fluid inclusions in magmatic quartz. Two-feldspar geothermometry on pairs of „hydrothermal" feldspars (occurring in veinlets with epidote, chlorite and pyrite) showed temperatures from 400 to 150 °C, with a strong mode in the interval 300 – 200 °C. Temperatures in this range were often obtained also from eutectic and high-temperature subsolidus feldspars due to the late-stage re-equilibration.

STABLE ISOTOPES

In order to determine source of fluids for alterations associated with hydrothermal centres, stable isotopes of mineral separates have been studied (O, H, S). Magmatic biotite from Banisko showed $\delta^{18}O_{fluid}$ values typical for magmatic water (6.4 and 6.9 ‰). Secondary biotite from Banisko also showed $\delta^{18}O_{fluid}$ (4.3 ‰) and δD_{fluid} (-40 ‰) values falling in the field of magmatic water.

Isotope analyses of pyrophyllite and alunite from various hydrothermal centres (Banisko, Stožok, Skalka, Podpolom) suggested magmatic-hydrothermal origin of their source fluid, while the acid environment clearly resulted from disproportionation of magmatic SO_4. This is indicated by markedly positive $\delta^{34}S$ values of alunites (10.8 to 20.7 ‰) compared to associated pyrite (-7.5 to 0.6 ‰) (Štohl et al. 1985; Repčok 1997). Furthermore, alunite-pyrite isotopic geothermometer (Rye et al. 1992) gives temperature range 200-400 °C, which is significantly higher than expected for any other alternative mechanism of origin of advanced argillic alteration (by oxidation of H_2S in ground water at ~100-120 °C, or by supergene alteration).

Internal oxygen isotope geothermometer of alunite (Stoffregen et al. 1994) showed isotopic disequilibrium, caused by re-equilibration of oxygen from the OH group with meteoric waters at lower temperatures ($\delta^{18}O_{fluid}$ -12.3 and -9.9 ‰), while oxygen from the SO_4 group has preserved its original isotopic composition, resulting from condensation of magmatic gases in meteoric water ($\delta^{18}O_{fluid}$ -2.3 and 1.9 ‰). This disequilibrium corresponds to predisposition of OH group of alunite to re-equilibrate at lower temperatures, while SO_4 remains unaffected (Stoffregen et al. 1994). Similarly, low δD values of fluids in equilibrium with alunite (-87 and -84 ‰) and most pyrophyllites (-81 to -52 ‰) are probably the result of re-equilibration during cooling with fluids of meteoric origin. Isotope analyses of gypsum from deep parts of the systems confirmed the assumed hydrogen isotopic composition of meteoric fluids during hydrothermal activity at Javorie (δD_{fluid} -88 and -75‰). However, the oxygen isotope composition of gypsum was affected by re-equilibration ($\delta^{18}O_{fluid}$ -2.5 and 0.7 ‰) resulting from wall-rock interaction (O-shift).

CONCLUSIONS

The overall stable isotope data suggest that apart from the early magmatic fluid causing advanced argillic alteration with alunite, related to the emplacement of porphyry intrusions, there was no later penetration of fluids with magmatic component, just heated meteoric waters. Therefore, a significant hydrothermal source of later stage magmatic fluids is missing, while such a fluid is usually responsible for deposition of ore mineralization in high-sulfidation systems (Arribas 1995). Therefore, the hydrothermal systems of Javorie probably will not host significant epithermal ore mineralization of the high-sulphidation type.

ACKNOWLEDGEMENTS: This study has been carried out as a a part of the project 0503 “Source of ore-bearing fluids in the metallogeny of Western Carpathians” financed by the Ministry of Environment of the Slovak Republic. SUERC is funded by a consortium of Scottish Universities and NERC.

REFERENCES

ARRIBAS A.J.R., 1995: Characteristics of high-sulfidation epithermal deposits, and their relation to magmatic fluid. In: Thompson J.F.H. (Ed.): Magmas, fluids and ore deposits. Mineral. Assoc. Canada Short Course Ser., 23: 419-454.

HASELTON H.T.JR., HOVIS G.L., HEMINGWAY B.S., ROBIE R.A., 1983: Calorimetric investigation of the excess entropy of mixing in albite-sanidine solid solutions: lack of evidence for Na, K short-range order and implications for two-feldspar thermometry. Am. Mineral., 68: 398 – 413.

REPČOK I., 1997: K/Ar datovanie vulkanitov Vtáčnika a alunitov z Javoria a Turčeka. Open file report, ŠGÚDŠ, Bratislava. (in Slovak)

RYE R.O., BETHKE P.M., WASSERMAN M.D., 1992: The stable isotope geochemistry of acid sulfate alteration. Econ. Geol., 87: 225-262.

STOFFREGEN R.E, RYE R.O., WASSERMAN M.D., 1994: Experimental studies of alunite: I. ^{18}O-^{16}O and D-H fractionation factors between alunite and water at 250-450°C. Geochim. Cosmochim. Acta, 58: 903-916.

ŠTOHL J., KONEČNÝ V., MIHALIKOVÁ A., ŽÁKOVÁ E., MARKOVÁ M., ROJKOVIČOVÁ Ľ., 1981: Metalogenetický výskum Javoria. Manuscript, ŠGÚDŠ, Bratislava. (in Slovak)

ŠTOHL J., ONAČILA D., MIHALIKOVÁ A., ŽÁKOVÁ E., MARKOVÁ M., HOJSTRIČOVÁ V., MARSINA K., STANKOVIČ J., DUBLAN L., 1985: Zhodnotenie prognóz Cu (Pb-Zn) zrudnení v oblasti Javoria (Stožok-Klokoč) a Poľany. Prognózne zásoby 25-30 mil. ton D_2-D_3. Open file report, ŠGÚDŠ Bratislava, 1-236. (in Slovak)

ŽÁKOVÁ E., 1988: Premeny vulkanických hornín v oblasti Podpolom v Javorí. Záp. Karpaty Sér. Mineral. Petrogr. Geoch. Metal., 11: 23-79. (in Slovak)

MINERALOGIA POLONICA - SPECIAL PAPERS
Volume 28 - 2006

Milan KOHÚT[1], Patrik KONEČNÝ[1], Pavol SIMAN[2]

THE FIRST FINDING OF THE IRON LAHN-DILL MINERALIZATION IN THE TATRIC UNIT OF THE WESTERN CARPATHIANS

INTRODUCTION

The highest concentrations of iron are associated with the occurrence of Precambrian sedimentary formations – so called Banded Iron Formations (BIF) form the largest world source of hematite and magnetite ores. Volcano-sedimentary deposits of the Lahn-Dill type, Devonian in age, render great importance in the mining history as well as. The Lahn-Dill type of iron ore mineralization derives its name from the Lahn-Dill iron ore district in the southern Rhenish Massif in the Central Germany. The Devonian was a period of relative silence in the Earth history between vanishing Caledonian movement in the Lower Devonian and beginning of Hercynian orogenesis in the Upper Devonian. Thick terrigeneous accumulations of so-called Old red sandstone, huge marine carbonatic and flysch sediments, as well as extensive products of submarine basic and/or bimodal volcanism represent the rocks record of this period. Sedimentary record has general feature of changing facies from terrigeneous clastic material at the north (Old red continent evolution) through a mixture of psammitic-pelitic depositions and/or neritic-pelagic interchange (Rheno-Hercynian evolution) to calcareous sedimentation with pelitic intercalation (Bohemian – Barrandian's evolution) at the southern margin of the European realm. The iron Lahn-Dill mineralization is distinctive just for Rheno-Hercynian evolution. Devonian in the Western Carpathians basement (WCB) has not large area extension in general. There are known only the Gelnica and Rakovec Groups in the Gemeric unit that consist of metagreywackes, phyllites, lydites, carbonates and basic volcanics, the Harmonia Group in the Malé Karpaty Mts. (Tatric unit) with similar metamorphosed rocks association, and the Predná hola volcano-sedimentary complex (Veporic Unit). Devonian limestones were sporadically described from deep boreholes at the southern Slovakia. Noteworthy, that Lahn-Dill ore mineralization was described only from the Gemeric unit till now.

RESULTS

Recently in the frame of construction new geological map of the Považský Inovec Mts., there was documented an unusual volcano-sedimentary complex for the Tatric unit of the WCB. This complex was displayed in the official General map of Slovakian territory as amphibolites (Kamenický in Buday et al. 1962). However, our field and petrological study proved that the dominant part of this complex consists of dark grey fine-grained laminar to weakly banded pelitic-

[1] *State Geological Institute of Dionýz Štúr, Mlynská dolina 1, 817 04 Bratislava, Slovak Republic; milan@gssr.sk*
[2] *Geological Institute of Slovak Academy of Sciences, Dúbravská cesta 9, 842 26 Bratislava, Slovak Republic*

psammitic metamorphosed rocks – metagreywackes and phyllites. There were identified locally metamorphosed sills of submarine basic volcanics – amphibolites and/or theirs pyroclastic analogues, layers of black schists respectively graphitic metaquartzites and lydites, as well as calk-silicate hornfels – erlans, and whole complex was called as Hlavinka volcano-sedimentary metamorphic complex (Kohút et al., 2005). The most common rocks of this complex – metagreywackes and phyllites are composed by quartz, plagioclase, K-feldspar, biotite and organic matter (graphite), in accessory content are present garnet, zircon and monazite. Metamorphic overprint of original volcano-sedimentary sequence reach to upper part of greenschist facies, respectively lower part of amphibolite facies with T = 500 – 550 °C and P = 300 – 350 MPa. Due to apparent dominance of amphibolites there was omitted stratigraphic determination indicated the Devonian age of palynomorphs, tracheids and phyto detritus separated from black schists. However, crucial for the Devonian classification was recent discovery of the purple-red iron-bearing metaquartzites – a typical analogue of the Lahn-Dill volcano-sedimentary iron ores within the Hlavinka Group. Geochemistry confirmed greywacke protolith character of prominent metamorphic rocks (metagreywackes and phyllites), whereas these rocks were sedimented at a continental slope in the back-arc basin. These greywacke were derivate from an acid and/or intermediate magmatic rocks source that originated in an active continental arc. Rather unusual MORB geochemical character of metabasic rocks – amphibolites was shown as standard for Rheno-Hercynian evolution of the Devonian (Floyd 1995). Relative lack of modern stratigraphic data from Hlavinka Group partially supplied dating of uraninite and monazite with the electron microprobe (CAMECA SX-100) in an attempt to broadly constrain formation ages of greywackes and iron-bearing metaquartzites. The uraninite origin 394 ± 2 Ma was the most probably synchronous to formation of submarine-exhalation iron ores, whereas monazite data 336 ± 18 Ma from identical samples indicate rather final Meso-Hercynian metamorphic overprint of volcano-sedimentary pile. Petrography and EMP study proved that magnetite is main carrier of mineralization in iron-bearing metaquartzites, and forms mainly idiomorphic phenocrysts or polycrystalline aggregates. Magnetite is very pure and contains very little of trace elements e.g. up to 1.58 wt. % TiO_2, 0.60 wt. % Al_2O_3, 0.07 wt. % Cr_2O_3, MnO and MgO, 0.29 wt. % CaO, and 0.10 wt. % ZnO. Magnetite is often transformed to martite and/or whole iron-bearing metaquartzites were subsequently in supergene stage weathered/limonitized – penetrated by goethite.

DISCUSSION AND CONCLUSIONS

Sedimentological or litho-facial evolution of Hlavinka Group – dominance of clastic terrigeneous psammitic-pelitic material (greywackes and schist), small contribution of organic matter (black schists) with minimal limestone intercalations and typical basic volcanism causing Lahn-Dill iron ores (iron metaquartzites) clearly affined with Rheno-Hercynian evolution of the European Variscan mobile zone. One can observe an analogous evolution today from the Lizard complex in Cornwall, through the Ardennes, the Rhenish Massif, the Harz Mts., to the

easternmost part of Bohemian Massif – Moravo-Silesian zone (Jeseník Mts., and Drahany Upland). The Devonian rock sequences in the Alps are well preserved in the Austro-Alpine realm, mainly in the Graywacke Zone and Graz Paleozoic which form a part of the Ordovician – Carboniferous extensive volcano-sedimentary complexes, showing an affinity to Bohemian evolution, indeed faunal indications display strong Rheno-Hercynian similarity (Schönlaub, 1993). Since Kossmat (1927) it is known that an elemental part of the Devonian basin remnants form Rhenohercynian zone of the European Variscides. The Rheno-Hercynian ocean was opened as a Devonian oceanic domain within the southern Laurussia margin, due to Gondwana-directed slab pull, and was situated between the southern margin of Laurussia (Avalonia) and Hanseatic terrane (Stampfli, Borel 2002; von Raumer et al. 2003). Due to Middle Devonian collision became weak Hanseatic block part of Hunic superterrane which collided during main Meso-Hercynian period (Visean) with Laurussia what caused widespread granitization in whole Central European realm. It is generally accepted that Hercynian basement of the Western Carpathians formed part of Hunic superterrane, however our study proved that before the docking of the Hunic terrane against Laurussia, part of the Carpathians pre-Hercynian basement recorded history of Rheno-Hercynian ocean and/or Hanseatic terrane, showing that affinity to Avalonia origin.

ACKNOWLEDGEMENTS*:* This is contribution to Grant APVT-20-016-104.

REFERENCES

BUDAY T., CAMBEL B., MAHEĽ M., BRESTENSKÁ E., KAMENICKÝ J., KULLMAN E., MATĚJKA A., SALAY J., ZAŤKO M., 1962: General geological map of ČSSR 1: 200 000; sheet M-33-XXXVI – Bratislava and its explanation. Archive ŠGÚDŠ, Bratislava, 1-249. (in Slovak)

FLOYD P.A., 1995: Igneous Activity. In: R.D. Dallmeyer, W. Franke, K. Weber eds., Pre-Permian Geology of Central and Eastern Europe. Springer, 59-81.

KOHÚT M., SIMAN P., KONEČNÝ P., HOLICKÝ I., 2005: Not amphibolites, but Hlavinka metamorphic complex in the southern part of the Bojná block – Považský Inovec Mts., Miner. Slov., 37, 1: Geovestník, 6. **(**in Slovak)

KOSSMAT F., 1927: Gliederung des varistischen Gebirgsbaues. Abh. Sächs. Geol. Landesamt, 1: 39.

RAUMER J.F. von, STAMPFLI G.M., BOREL G.D., BUSSY F., 2003. Organization of pre-Variscan basement areas at the north-Gondwanan margin. Int. J. Earth. Sci., 91: 35-52.

SCHÖNLAUB H.P., 1993: Stratigraphy, Biography and Climatic Relationships of the Alpine Paleozoic. In: J.F. von Raumer F. Neubauer eds., Pre-Mesozoic Geology in the Alps. Springer, 65-91.

STAMPFLI G.M., BOREL G.D., 2002: A plate tectonic model for the Paleozoic and Mesozoic constrained by dynamic plate boundaries and restored synthetic oceanic isochrons. Earth Planet. Sci. Lett., 196: 17-33.

MINERALOGIA POLONICA - SPECIAL PAPERS
Volume 28 - 2006

Ján KROMEL[1], *Marián PUTIŠ*[1]

INTRODUCTION TO SYMPLECTITE MODELING – PHYSICAL-CHEMISTRY AND NUMERICAL APPROACH

INTRODUCTION

Almost all rocks and minerals in normal conditions on the earth surface or near it have a complex history, which reflects pressure and temperature conditions of their creation and evolution. When rock, which is formed of minerals stable at high conditions is exhumed, these particular minerals tends to break down to more stable minerals at given conditions and this often produce typical microstructures (Putnis 1992), in our glance symplectites (e.g. eclogites are formed mainly of garnet and omphacite, which is Na-rich pyroxene stable only at high pressure, after exhumation it tends to break down to a less Na-rich pyroxene and plagioclase).

The symplectites are fine-grained intergrowths of two or more phases (Goergen 2004) and are similar phenomenon as exsolution, but in contrast to exsolutions, symplectites are formed in an open system, which may involve fluids and/or small amounts of residual magma (Kuhl, Schmid 2006) and occurs as in terrestrial high-grade metamorphic terranes (Goergen, Whitney 2004) as in meteorites, e.g., martial basaltic meteorites consist of two (fayalitic olivine and an SiO2 polymorphs) and three phases (hedenbergitic pyroxene, fayalitic olivine and an SiO_2 polymorph) (Aramovich 2002). Symplectites may be classified by many criteria e.g., chemical composition of the phases, structure. Because of their complexity and variations, complex classification probably couldn't be done.

We can use a lot of methods to model many aspects of symplectites: classical method - thermodynamic modeling to model p, T, X conditions of creation and evolution, experimental method - either using inorganic, or organic compounds to simulate behaviour of mixing process, thin films experiments (Milke et al. 2003), chemical method - reactions to find out, what is really going on, numerical method - computational models either to combine all of already mentioned methods or make completely everything from the beginning (Kuhl, Schmid 2006). Today's models are trying to reproduce either geometry or formation as the separate problems, or formation and created geometry as the whole process. Many models are intersecting each other and using different mathematical and physical-chemistry approaches.

Many attends to make realistic model of symplectite formation were done and are still in progress, e.g. exsolution, oxidation (Goergen, Whitney 2004). From these entire approaches one can separate two main driven processes: concentration gradient and chemical potential gradient.

The first approach is based on Fick's Laws. Fick's First Law states that the flux (J) of a component of concentration (C) across a membrane of unit area, in a

[1] *Department of Mineralogy and Petrology, Faculty of Natural Sciences, Comenius University, Mlynská dolina, 842 15 Bratislava, Slovak Republic; kromel@fns.uniba.sk*

predefined plane, is proportional to the concentration differential across that plane (Steward 1995):

$$J = -D\nabla C$$

Fick's First Law is used in steady state diffusion, i.e., when the concentration within the diffusion volume does not change with respect to time ($J_{in}=J_{out}$) (Atkins 2001). Fick's Second Law states that the rate of change of concentration in a volume element of a membrane, within the diffusional field, is proportional to the rate of change of concentration gradient at that point in the field (Steward 1995):

$$\nabla.(D\nabla C) = \frac{\partial C}{\partial t}$$ where t = time

Fick's Second Law is used in non-steady or continually changing state diffusion, i.e., when the concentration within the diffusion volume changes with respect to time (Atkins 2001).

Main problem with Fickian diffusion equation is that it tends to generate uniform concentration profiles (Kuhl, Schmid 2006).

Chemical potential gradient on the other side tends to solve problems connected with Fickian diffusion equation and appears to be more accurate model compared to the nature. Flory-Huggins thermodynamic of mixing defines phase separation driven by gradients in the chemical potential as oppose to Fick's Laws concentration gradients. Adaptation of Landau-Ginzburg functional to add gradient energy leads to the Cahn-Hilliard fourth order diffusion equation (Kuhl, Schmid 2006). The Cahn-Hilliard theory is basically extension of free energy to non-uniform systems witch have concentration gradient within them (Shimizu, Takei 2005).

METHODS

Our approach was to test and lately combine as much as possible methods and factors to get closer realistic view of symplectites creation and evolution. The first modeling was done by using thermobarometry to get P, T conditions of symplectite evolution. We used THERIAK-DOMINO software by de Capitani (de Capitani, Brown 1987) and Holland and Powell internally consistent thermodynamic data set (Holland, Powell 1998). Then we took different way to strictly model evolution by using concentration gradient and chemical potential gradient. We looked on evolution of microstructure complexity of phase separation as on the factors which are responsible for geometry. We used Gnuplot and Octave in combination with some C++ and Python programming.

RESULTS

Preliminary results were accomplished by using geothermobarometry on symplectites using eklogite samples from Sieggraben Structural Complex in the Eastern Alps. The calculated p, T conditions were equal to proposed and to

calculated, by using different mineral pairs, around 600 °C and 1.6 GPa. The numerical modeling was a little bit tricky, because all sorts of implementations of selected routines, but leaded into satisfactory results.

CONCLUSIONS

From our point of view the final conclusion couldn't be done. Much work has already been done by people from all around the world, but there is still a lot of work to do. Many attends to combine different methods produce many different results and that raises questions about right interpretation. As we see it, even interpretations of the same result and used method could be sometimes right only from the one point of view. From all this we can say, that with interdisciplinary combinations of methods in the future we can expect some interesting results and we are heading to "natural model".

REFERENCES

ARAMOVICH C.J., HERD C.D.K., PAPIKE J.J., 2002: Symplectites derived from metastable phases in martial basaltic meteorites. Am. Mineral, 87: 1351-1359.

ATKINS P., DE PAULA J., 2001: Atkin's physical chemistry, 7th Ed. Oxford University Press, 1180.

DE CAPITANI C., BROWN T.H., 1987: The computation of chemical equilibrium in complex systems containing non-ideal solutions. Geochim. Cosmochim. Acta 51: 2639-2652.

GOERGEN E.T., 2004: Modeling symplectites. Denver Annual Meeting.

GOERGEN E.T., WHITNEY D.L., 2004: Patterns and processes of symplectite formation. Geophysical Research Abstracts, 6.

HOLLAND T.JB., POWELL R., 1998: An internally consistent thermodynamic data set for phases of petrological interest. Journal pf Metamorphic Geology, 16:309-343.

KUHL E., SCHMID D.W., 2006: Computational modeling of mineral unmixing and growth - An application of the Cahn-Hilliard equation. Computational Mechanics, accepted for publication.

MILKE R., DOHMEN R., WIEDENBECK M., WIRTH R., BECKER H.-W, ABART R., 2003: Grain boundary diffusion studied on nano scale by rim growth experiments with isotopically doped thin films. EGS-AGU-EUG Joint Assembly, Nice.

PUTNIS A., 1992: Introduction to mineral sciences. Cambridge University Press, London, 479.

SHIMIZU I., TAKEI Y., 2005: Temperature and compositional defence of solid-liquid interfacial energy: application of the Cahn-Hilliard theory. Physica B: Condensed Matter, Vol. 362, 1-4: 169-179.

STEWARD P.A, 1998: Fick's Laws of diffusion. http://www.initium.demon.co.uk/fick.htm.

MINERALOGIA POLONICA - SPECIAL PAPERS
Volume 28 - 2006

Łukasz KRUSZEWSKI[1]

OLDHAMITE-PERICLASE-PORTLANDITE-FLUORITE ASSEMBLAGE AND COEXISTING MINERALS OF BURNT DUMP IN SIEMIANOWICE ŚLĄSKIE – DĄBRÓWKA WIELKA AREA (UPPER SILESIA, POLAND) – PRELIMINARY REPORT

INTRODUCTION

Fluorite and periclase are relatively common minerals in geological environments, though periclase formation is restricted rather to contact metamorphic areas (Ferry, Rumble 1997). Other simple Ca and Mg compounds like CaS, MgS, CaO and $CaCl_2$ are quite rare in nature, mostly due to their chemical instability. CaO is highly hygroscopic, whereas sulfides and $CaCl_2$ undergo hydrolysis and solvatation (respectively) in water solutions. Portlandite, $Ca(OH)_2$, which changes into calcite in humid atmosphere, is also regarded as rare mineral, excluding its possible role as a source of Ca and H_2O in upper mantle (Pavese et al. 1997). Oldhamite CaS is a constituent of some meteorites (Farrell et al. 2002). Actually the only terrestrial conditions, in which oldhamite and other mentioned minerals may form and coexist, brings about coal- and bitumen-fire sites, like burning dumps. Such minerals are formed there during so-called burn-phase. Among three phases of mineral formation (Srebrodolskiy 1989) this one is characterized by the highest temperatures (even over 1000 °C).

METHODS

Minerals of researched assemblage were detected by PXRD method performed on DRON 2.0 (Faculty of Geology, Warsaw University) and Bruker D5005 (Department of Soil Environmental Sciences, Warsaw Agriculture University) diffractometers. Semi-quantitative EDS analyses, SEM and BSE photos were performed on JEOL JSM-6380LA scanning electron microscope (Faculty of Geology, Warsaw University) to confirm XRD results.

RESULTS AND DISCUSSION

Described assemblage was found on an already recultivated coal waste-dump located between Siemianowice Śląskie and Dąbrówka Wielka (Upper Silesia, Poland) (E 19°00' N 50°20'). Minerals occur in a small (about 4 x 3 x 2.5 cm), porous, concretion-like segregation with two macroscopically distinct accumulations (zones) (Fig. 1). Green, botryoidal and porous ones (no. 1 on Fig. 1) occupy about 60 % of the concretion volume, forming a zone up to 1.5 cm thick. According to XRD results, green accumulations consist mainly of oldhamite, periclase (Fig. 2) and calcite in company of fluorite, cuspidine $Ca_4(Si_2O_7)(F,OH)_2$ and thaumasite $Ca_3(SO_4)(CO_3)[Si(OH)_6]\cdot 12H_2O$. EDS analyses show presence of Fe in periclase. Fe together with Zn is also present as sulfide-phases in black areas

[1] *Institute of Geochemistry, Mineralogy And Petrology, Faculty of Geology, Warsaw University, Al. Żwirki i Wigury Street 93, 02-089 Warsaw, Poland; lkruszewski@uw.edu.pl*

(no. 2 on Fig. 1) occurring among green accumulations. Concentrations of second type are white, powdery (somewhat granular), and partially fill up the core (no 3 on Fig. 1) or cover the green zone (no 4 on Fig. 1). Their XRD shows portlandite, periclase and calcite as main constituents. Fluorite, spurrite (or paraspurrite) $Ca_5(SiO_4)_2(CO_3)$ and possibly vaterite γ-$CaCO_3$ occur in lesser amounts.

High-temperature decomposition of dolomite is the most probable source of

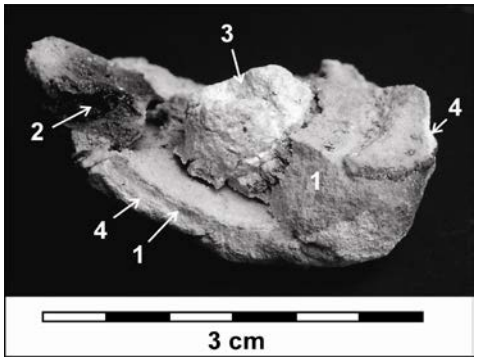

Fig. 1. Fragment of concretion-like segregation of described minerals. Zones: 1 – green, 2 – black, 3 – white (inner), 4 – white (outer).

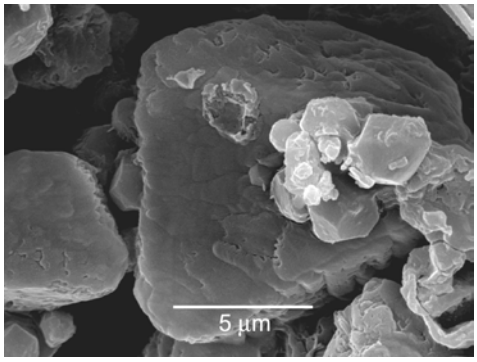

Fig. 2. SEM image of small periclase crystals growing on oldhamite.

periclase. Dolomite transforms to periclase (and calcite) at 700-750 ^oC, while calcite, if pure, changes into lime (CaO) at 950^o C (Reifenstein et al. 1999). According to Sokol et al. (2002), lime (in opposition to periclase) is exposed to affection of most hot coal-derived gases (like H_2F_2, H_2S and HCl), that occur in the environment of burning dumps. Interaction of gases with lime results in originating of specific assemblage. Sokol et al. (2002) report such an assemblage, forming at 1000-1200 ^oC, and mention oldhamite as its common constituent. They affirm, that oldhamite forms in reducing conditions. In course of such reasoning, oldhamite and fluorite of assemblage described from Upper Silesia formed thanks to effect of gaseous phase, in high H_2S and H_2F_2 fugacity conditions. Cl, though present in researched material (after EDS analyses), appears in lesser amounts, hence fugacity of HCl in gaseous phase can be find relatively low. The same is for H_2O, due to oldhamite instability by high $f(H_2O)$. Gaseous phase participating in oldhamite and fluorite formation was H_2S and H_2F_2 rich, as well as HCl and H_2O poor.

Portlandite and vaterite are reported from combustion-metamorphosed bituminous carbonate-rocks (analogous to sanidinite facies) in Hatrurim Basin (Israel) representing so-called retrograde assemblage, which is connected with late-stage recarbonization and hydratation. Formation of this assemblage takes place at temperatures lower than for previous, prograde assemblage (formed between 500 and 1000 ^oC), consisting mailny of different Ca silicates, including spurrite (Gur et al. 1995). It is now supposed, that portlandite and thaumasite of described Silesian assemblage are later than oldhamite, fluorite and periclase, and formed in presence

of H_2O and by relatively low temperatures. Portlandite could be derived from oldhamite hydrolysis. Spurrite and cuspidine are though to be high-temperature products, formed in relatively high Eh conditions (Sokol et al. 2002). In green accumulations contents of cuspidine and fluorite is distinctly dependent, however their exact genetic relation (both Ca- and F-bearing) was not confirmed yet.

CONCLUSIONS

Relation of coal-combustion sites to typical magmatic and metamorphic envionments was stressed by many authors (*e.g.* Wielogórski et al. 1975, Srebrodolskiy 1989, Sokol et al. 2002). Minerals of burn-phase are known from many natural, geological environments. Occurrence of primary spurrite and periclase in carbonatite lavas (Woolley, Church 2005) is just an example.

ACKNOWLEDGEMENTS: Author would like to thank D.Sc. Jan Parafiniuk (Institute of Geochemistry, Mineralogy and Petrology, Warsaw University) for valuable suggestions, D.Sc. Zbigniew Zagórski (Department of Soil Environmental Sciences, Warsaw Agriculture University) for making Bruker diffractomer accessible and M.Sc. Maciej Krajcarz for technical help.

REFERENCES

FARRELL S. P., FLEET M. E., STEKHIN I. E., KRAVTSOVA A., SOLDATOV A. V., LIU X., 2002: Evolution of local electronic structure in alabandite and niningerite solid solutions [(Mn,Fe)S, (Mg,Mn)S, (Mg,Fe)S] using sulfur *K*- and *L*-edge XANES spectroscopy. Am. Mineral., 87: 1321-1332.

FERRY J. M., RUMBLE III D., 1997: Formation and destruction of periclase by fluid flow in two contact aureoles. Contrib. Mineral. Petrol., 128: 313-334.

GUR D., STEINITZ G., KOLODNY Y., STARINSKY A., MCWILLIAMS M., 1995: $^{40}Ar/^{39}Ar$ dating of combustion metamorphism ("Mottled Zone", Israel). Chem. Geol. (Isotope Geoscience Section), 122: 171-184.

PAVESE A., CATTI M., FERRARIS G., HULL S., 1997: P-V equation of state of portlandite, $Ca(OH)_2$, from powder neutron diffraction data. Phys. Chem. Mineral., 24: 85-89.

REIFENSTEIN A. P., KAHRAMAN H., COIN C. D. A., CALOS N. J., MILLER G., UWINS P., 1999: Behaviour of selected minerals in an improved ash fusion test: quartz, potassium feldspar, sodium feldspar, kaolinite, illite, calcite, dolomite, siderite, pyrite and apatite. Fuel, 78: 1449-1461.

SOKOL E. V., NIGMATULINA E. N., VOLKOVA N. I., 2002: Fluorine mineralisation from burning coal spoil-heaps in the Russian Urals. Miner. Petrol., 13: 791-800.

SREBRODOLSKIY B. I., 1989: Tajny Sezonnykh Mineralov. Nauka, Moskva, 59-119 [in Russian].

WIELOGÓRSKI Z., ZAWIDZKI P., KOISAR B., 1975: Processes of mineral formation in fire zones of "Słupiec" coal mine dump. Przeg. Górn., 9: 443-448 [in Polish].

WOOLLEY A. R., CHURCH A. A., 2005: Extrusive carbonatites: A brief review. Lithos, 85: 1-14.

MINERALOGIA POLONICA - SPECIAL PAPERS
Volume 28 - 2006

Michal KUBIŠ[1,2], Igor BROSKA[2]

PETROGRAPHY, MINERALOGY AND GEOCHEMISTRY OF BETLIAR GRANITE BODY (GEMERIC UNIT, WESTERN CARPATHIANS, SLOVAKIA)

INTRODUCTION

Mineralogically and gechemically the most remarkable granites crop out in the Gemeric unit as small bodies in low-grade metasediments and metavolcanics. The cliffs (500 to 500 m) in the area of Betliar village represents mainly the porphyry granite (granite porphyry) and less the fine-grained (leuco)granite in northern part of granite body.

PETROGRAPHY AND MINERALOGY

The Betliar porphyry granite is composed of quartz, plagioclase, K-feldspar, rarely muscovite, biotite and accessory minerals. K-feldspars form mainly phenocrysts (2 to 4 cm in size), locally subhedral to anhedral crystals, the groudmass is fine-grained (0.01 to 0.1 cm). Plagioclase is subhedral, intensive sericitized, muscovite forms mainly the irregular grains, but locally also flakes of white mica occurs as a secondary products in plagioclases. Biotite form usually subhedral plates with a size of 0.3 to 1 mm, frequently clustered in aggregates. Quartz is partly undulose and magmatic corroded. Accessory minerals are represented mainly by schorl to dravite, fluorapatite, zircon, monazite-(Ce), xenotime-(Y), rutile and fluorite.

The fine-grained granite (0.1 to 1.5 mm) consists of subhedral columns of K-feldspar, albite and white mica. Quartz forms mostly anhedral crystals up to 1 mm. The most common accessory minerals are schorl, fluorapatite, zircon, fluorite, rare Nb-Ta oxides, topaz, ferberite and cheralite-(Ce).

COMPOSITION OF THE ROCK-FORMING MINERALS

All two rock types contain nearly pure end-members of alkali feldspar: albite with An_{05} and K-feldspar (Kfs) with a maximum of 0.1 % Ab and <0.1 % An. P_2O_5 content in Kfs in the porphyric granite is between 0.1 and 0.3 wt. %, whereas its content in albites varies between 0.02 and 0.2 wt. %. On the other hand, the P_2O_5 content in albite in the fine-grained granite is very low (up to 0.1 wt. %).

Trioctahedral mica in porphyric granite is generally annite with high at. ratio Fe/(Fe+Mg) = 0.79-0.81. Crystals of annite contains small inclusions of radioactive minerals with pleochroic haloes (uraninite, thorianite). A flourine content is relatively low (0.01-0.28 *apfu*).

Dioctahedral mica in both granite types corresponds to ferro-aluminoceladonite and aluminoceladonite. The white mica contains relatively high concentrations of

[1] *GEOFOS, Ltd., Veľký diel 3323, 010 08 Žilina, Slovak Republic; geolkubo@savba.sk*
[2] *Geological Institute, Slovak Academy of Sciences, Dúbravská cesta 9, 840 05 Bratislava, Slovak Republic*

Fe, but it is heterogeneously distributed (1.7-6.0 wt. % FeO_{tot}), what is not simply a reflection of Alpine metamorphic overprinting of these granites.

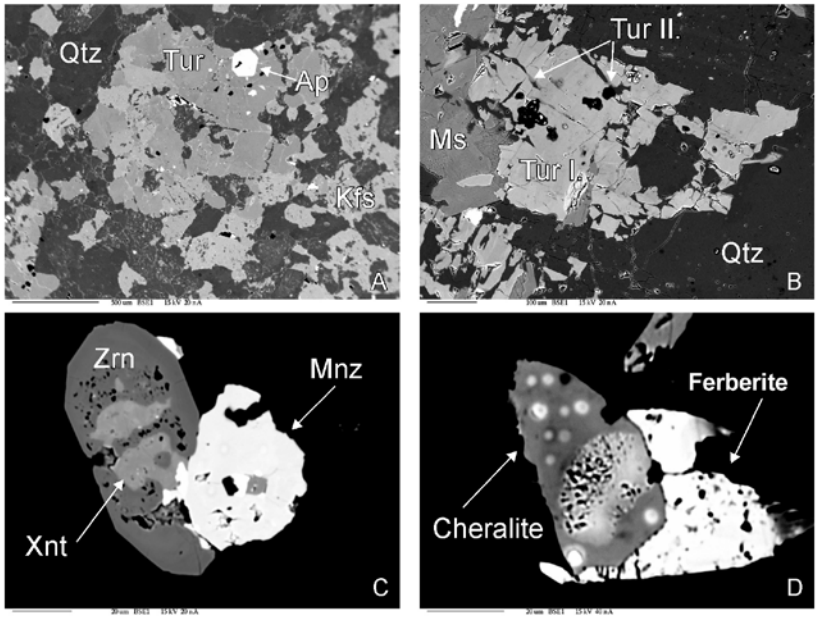

Fig. 1. BSE images: A – schorl-fluorapatite assemblage from porphyric granite; B – two generations of schorl from fine-grained granite; C – monazite-xenotime-zircon assemblage from porphyric granite; D – cheralite-ferberite paragenesis from fine-grained granite.

ACCESSORY TOURMALINES

Tourmalines are widespread accessory minerals in all granite types, which form two genetic types. First type is represent by a primary magmatic schorl with high at. ratio Fe/(Fe+Mg) = 0.7-1.0 and lower X-site vacancy ($^{X}\square$ = 0.1-0.45 *apfu*). Second type is represent by a late-magmatic or metamorphic schorl with lower Fe/(Fe+Mg) = 0.59-0.65. The first type is scattered in the rock, second type forms mobilised veins and flakes in the rock (Fig. 1A-B).

ACCESSORY PHOSPHATE MINERALS

Fluorapatite is present in two types (generations). First type (primary) is represented by large crystals (~150 μm), which is enriched in Fe and Mn (0.2-0.9 wt. % FeO; 3.0-4.2 wt. % MnO), the secondary one is distributed within alkali feldspars as a product of leaching of berlinite molecule. They form very small crystals (~3 μm) with the low content of Mn and Fe and usually within plagioclases.

Monazite-(Ce) with 3.3-9.5 wt. % ThO_2 and 0.1-0.25 wt. % UO_2 is a main LREE phase in porphyric granite. Locally is enriched by cheralite molecule (~10 vol. %). Cheralite-(Ce) contains 26.7-32.7 wt. % ThO_2 and 0.9-4.1 wt. % UO_2, it also occurs in fine-grained granite in association with ferberite (Fig. 1D).

Xenotime-zircon paragenesis is typical for the porphyric granite. The zonality observed in the xenotime-(Y) is mainly due to the variations in concentrations of U (Fig. 1C).

GEOCHEMISTRY AND AGE

Both granite types from Betliar are peraluminous (A/CNK 1.2-1.4) and poor in Ca, Fe, Mg, Sr and Ba. The porphyry granite with 72.8 wt. % SiO_2, K/Na ~ 1.1, 0.15 wt. % P_2O_5, Rb (~340 ppm), Nb (~12 ppm) is enriched in B (~375 ppm).The rock shows pronounced negative Eu anomaly (Eu/Eu* = 0.31) and low Ce_N/Yb_N (2.2).

The fine-grained granite is more enriched in P (~0.5 wt. % P_2O_5), Rb (~700 ppm), Nb (~47 ppm) and Ta (~14 ppm). The REE contents are generally very low. The chondrite-normalized patterns are relatively flat (Ce_N/Yb_N = 1.2) having negative Eu anomalies (Eu/Eu* = 0.3).

EMPA monazite dating revealed 247 ± 5 Ma, for porphyry granite, the single-grain zircon dating controlled by cathodoluminiscence gives a concordant age with the minimum age of 246 ± 5 Ma (Poller et al. 2001). LA ICP zircon dating indicates an Upper Permian age (258±19 Ma) for the fine-grained granites. A Permian/Triassic age (251 ± 4 Ma) was also obtained from electron-microprobe dating of monazite from fine-grained granite.

CONCLUSIONS

The Betliar granite porphyry was intruded into subvolcanic level because of high amount of volatiles, together with low melt viscosity and tectonic predisposition. This intrusion was derived from middle-crustal magma where started the growth of K-feldspar megacrysts, later was followed by emplacement of co-magmatic (leuco)granite body.

ACKNOWLEDGEMENTS: The work has been financed by Project APVT-51-013604.

REFERENCES

POLLER U., UHER P., BROSKA I., PLAŠIENKA D., JANÁK M., 2002: First Permian-Early Triassic zircon age for tin-bearing granites from the Gemeric unit (Western Carpathians, Slovakia): connection to the Variscan orogen and S-type granite magmatism. Terra Nova, 14: 41-48.

MINERALOGIA POLONICA - SPECIAL PAPERS
Volume 28 - 2006

Bronislava LALINSKÁ[1], Juraj MAJZLAN[2], Martin CHOVAN[1], Peter ŠOTTNÍK[3], Stanislava MILOVSKÁ[4]

MINERALOGICAL AND GEOCHEMICAL STUDY OF MINE TAILINGS MATERIAL FROM THE ANTIMONY DEPOSIT PEZINOK – KOLÁRSKY VRCH (SLOVAKIA), VOLUME OF CONTAMINATION AND REMEDIATION PROJECT

INTRODUCTION

Weathering and dissolution processes in the environment of mine tailings mobilize elevated levels of toxic elements such as arsenic and antimony, which represent dangerous contaminants for the surrounding ecosystem. One of the potentially dangerous areas is the Sb deposit Pezinok-Kolarsky vrch in Slovakia. In this work we have investigated mineralogical and chemical changes taking part in weathering of tailing minerals. We were studying chemical composition of included minerals, oxidation rims and ochres. Considering to arsenic danger we have also studied ageing and structure of As-rich ferrihydrite. To be able to solve problem of contaminated water, we have done few pilot experiments using Fe^0 as sorbent for As and Sb.

The abandoned Sb deposit Pezinok lies in the Malé Karpaty Mts. (western Slovakia). The deposit is located in carbonaceous and actinolite shales and amphibolites and contained abundant stibnite and smaller amounts of other Sb minerals. In addition to the Sb minerals, pyrite and arsenopyrite were also common. The mineralization occurred as quartz-carbonate lenses, veinlets, nests, and impregnations in the host rocks. The ores were milled and Sb minerals were collected by flotation. The waste was then deposited in two large tailing impoundments.

METHODS

The ore minerals and their weathering products were studied in reflected polarized light microscope and consequently analyzed by electron microprobe CAMECA SX100 (State Geological Institute of Dionýz Štúr, Bratislava), under following conditions: accelerating voltage 15 kV, current 20 nA, diameter beam 2 to 5 μm. Concentrations of Fe, As, Sb, Ca, Mg, $(SO)_4^{2-}$ and Zn in ochres were determinated in solution after leaching in 5M HCl by AAS method (ŠGÚDŠ, Spišská Nová Ves). X-ray diffraction (XRD) spectra were made by Philips PW 1710 diffractometer (SAV, Bratislava). The XAS spectra of the samples were

[1] *Department of Mineralogy and Petrology, Faculty of Natural Sciences, Comenius University, Mlynská dolina, 842 15 Bratislava, Slovak Republic, lalinska@fns.uniba.sk*
[2] *Institute of Mineralogy and Geochemistry, Albert-Ludwig University, Albertstraße 23b, 791 04 Freiburg, Germany*
[3] *Department of Geology of Mineral Deposits, Faculty of Natural Sciences, Comenius University, Mlynská dolina, 842 15 Bratislava, Slovak Republic*
[4] *Geological Institute of Slovak Academy of Sciences, Severná 5, 974 01 Banská Bystrica, Slovak Republic*

collected at the beamline X11B of the National Synchrotron Light Source (NSLS, Upton, NY, USA) and also at ANKA synchrotron (Angströmquelle Karlsruhe, Germany).

RESULTS AND DISCUSSION

The most abundant minerals of tailings are quartz, carbonates, chlorites, feldspars, clays (smectite and illite). Pyrite is most dominant ore mineral, arsenopyrite occurs also frequently, less common is berthierite. Stibnite and gudmundite are rare.

Ore minerals are being replaced by rims in oxidation zone (Fig. 1, 2), content of As in the rims of arsenopyrite varies from 7,26 wt.% to 9.59 wt. %, Sb up to 4.02 wt. %, exceeding Sb content in primary arsenopyrite (highest content – 0, 05 wt. %). The enrichment of the weathering rims is evident also in case of pyrite, which contain up to 1.67 wt. % As and up to 3.85 wt. % Sb. The same situation is characteristic for the rims on berthierite grains, where content of As varies from 2.58 wt. % to 4.31 wt. %, Sb from 8.13 wt. % to 11.87 wt. %. There is nearly no stibnite in the oxidation zone of tailings, so we assume that the most of stibnite grains have already been oxidized.

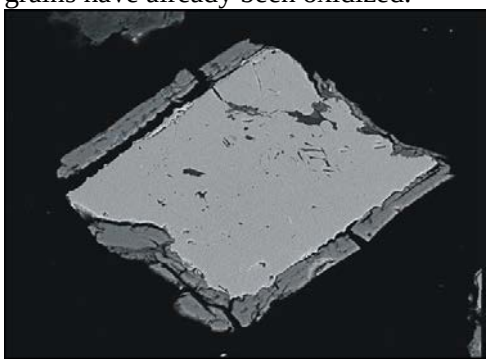

Fig. 1. The oxidation rim on arsenopyrite grain.

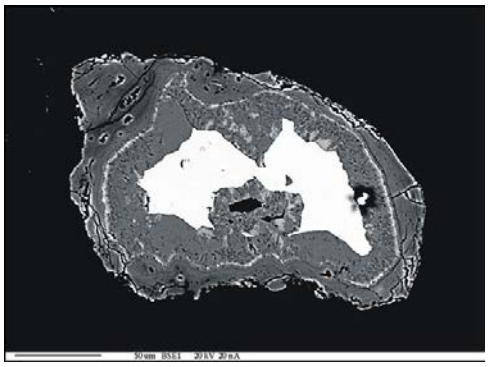

Fig. 2. The oxidation rim on pyrite grain.

The final products of sulfide weathering are Fe - ochres. Content of $(SO)_4^{2-}$ in ochres was relatively low, in the most of the samples did not reach the detection limit. Four samples showed values in interval of 7.43-258.25 mg/kg. Concentration of arsenic was high (0.81 – 51.39 g/kg), as well as of antimony (0.33 – 53.97 g/kg). Fe content varied from 154.95 g/kg to 763.16 g/kg. According to neutral pH of water, ferrihydrite is the most abundant mineral of Fe – ochres. Because of the lack of long-range order, techniques other than X-ray diffraction (XRD) had to be used to describe this mineral.

Using X-ray absorption near-edge structure (XANES) spectroscopy, we have determined that all probed elements (Fe, As, S) are present in their highest oxidation states. Thus, the material escaping from the impoundments is already fully oxidized, and no further changes in its oxidation state should be expected.

Extended X-ray absorption fine-structure (EXAFS) spectroscopy gave valuable evidence about the structure of As-ferrihydrite. EXAFS spectra at the Fe K edge have shown that the particles in the studied material are extremely depolymerized. The octahedra $Fe(O,OH,OH_2)_6$ are connected almost exclusively by edges, forming short polyhedral chains. EXAFS spectra at the As K edge indicate that the AsO_4 tetrahedra are attached to the iron oxide particles in a binuclear-bidentate fashion. Our results agree well with previous conclusions of Waychunas et al. (1993), obtained on a chemically similar synthetic material.

The environmental problem associated with sulfide decomposition is water contamination. To solve this problem we have to find out the proper reactive medium for the geochemical barrier. Recently we have done 2 pilot experiments using Fe for As and Sb removal from contaminated water. The water was collected from the drills in both tailings. We have used laboratory Fe chip (content of Fe 99.98 %, Lambda), Fe – powder (Slavus) and also some steel manufacturing by-products. All procedures were successful in As and Sb removal. The best results were reached by using of laboratory iron chip (Fig. 3-4).

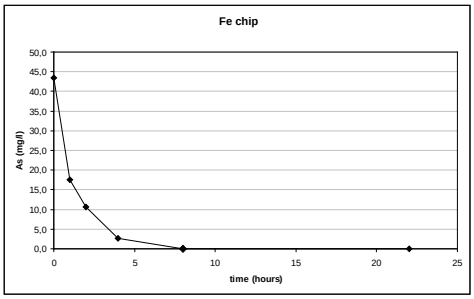

Fig. 3. Kinetic of As removal by Fe chip. (Lambda)

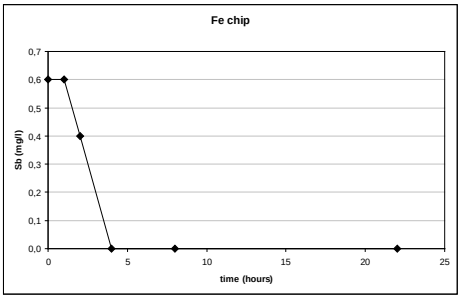

Fig. 4. Kinetic of Sb removal by Fe chip. (Lambda)

CONCLUSIONS

The enrichment of the oxidation rims indicates that the pore waters are able to transport the elements even at circumneutral pH. XAS data shows that AsO_4 tetrahedra is attached to the iron oxides in binuclear-bidentate fashion. According to the fact, that Fe oxides are the most successful natural sorbent of toxic elements in this area, we have decided to choose Fe^0 as appropriate filling material for reactive permeable barrier. Preliminary experiments show feasibility of this reactive medium.

REFERENCES

WAYCHUNAS G.A., REA B.A., FULLER C.C., DAVIS J.A., 1993: Geochimica et Cosmochimica Acta, 57: 2251–2269.

MINERALOGIA POLONICA - SPECIAL PAPERS
Volume 28 - 2006

František LAUFEK[1,2], Milan DRÁBEK[1], Roman SKÁLA[3], Jakub HALODA[1], Zdeněk TÁBORSKÝ[1], Ivana CÍSAŘOVÁ[2]

VAVŘÍNITE, Ni_2SbTe_2, A NEW MINERAL SPECIES FROM KUNRATICE NEAR ŠLUKNOV Cu-Ni-SULFIDE DEPOSIT, CZECH REPUBLIC

INTRODUCTION

A tellurium-bearing mineralization consisting of fine-grained pyrrhotite, pentlandite and chalcopyrite associated with an unknown Ni_2SbTe_2 phase was identified at the Cu-Ni-sulfide deposit Kunratice near Šluknov (Figure 1), Czech Republic (50º 58' 35" N, 14º 26' 34" E) by Vavřín, Frýda (1998). The new Ni-Sb telluride is named after mineralogist Dr. Ivan Vavřín (b.1937), Czech Geological Survey, for his role in long-term investigations of tellurium minerals and significant contribution to research of Cu-Ni-sulfide deposits. The mineral and mineral name has been approved by the Commission on New Minerals and Mineral Names of the IMA (IMA 2005-045).

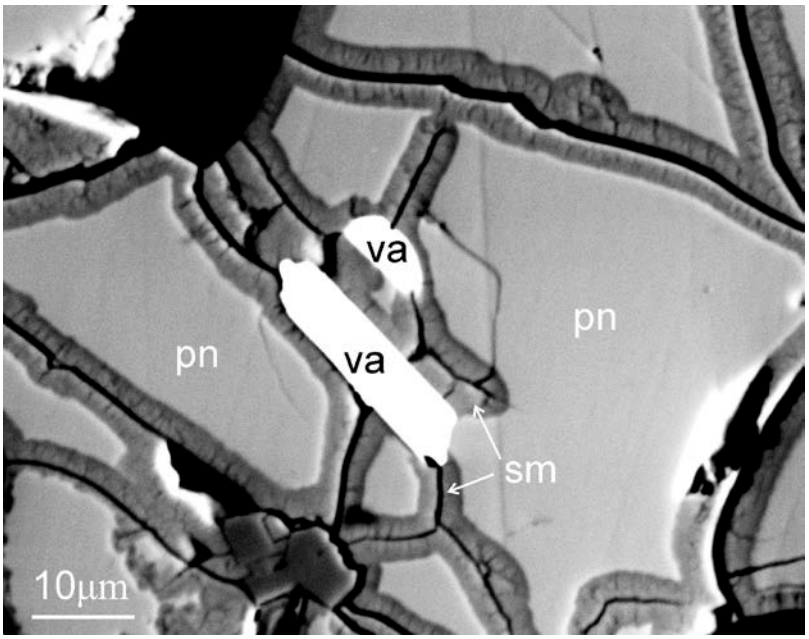

Fig. 1. BSE image of vavřínite and associated minerals. The abbreviations are: va (vavřínite), pn (pentlandite), sm (smythite).

[1] *Czech Geological Survey, Geologická 6, 152 00 Praha 5, Czech Republic; laufek@cgu.cz*
[2] *Faculty of Science, Charles University, Hlavova 8, 128 43 Praha 2, Czech Republic*
[3] *Institute of Geology, Academy of Sciences of the Czech Republic, Rozvojová 135, 165 02 Praha 6, Czech Republic*

METHODS

Vavřínite could not be isolated – due to very small size of its grain – in an amount required for its thorough characterization. Therefore, an analogue was synthesized. This synthetic Ni_2SbTe_2 phase was used to refine the crystal structure, to collect powder data, to refine cell parameters, to measure reflectance and to determine other selected physical properties. The synthetic analogue of vavřínite was prepared using silica glass tube method. The stoichiometric amounts of nickel, antimony and tellurium were loaded into a silica glass tube and sealed under vacuum. The sample was heated in a programmable furnace at 400 °C for three weeks and then slowly cooled to room temperature at the rate of 15°C/h. The resulting product is composed exclusively of recrystallized Ni_2SbTe_2.

Data for crystal structure study were acquired using a 4-circle single-crystal diffractometer Nonius KappaCCD at the Centre of Molecular Structures at the Faculty of Science, Charles University, Prague. After correcting the data for absorption, the crystal structure refinement was carried out by SHELX97 (Sheldrick 1997) program using initial structure model by Reynolds et al. (2004).

To ensure unequivocal identity of natural material and synthetic analogue, an electron backscattered diffraction technique (EBSD) was applied. We used CamScan CS 3200 scanning electron microscope (SEM) combined with an EBSD system manufactured by HKL Technology.

RESULTS

The crystal structure for synthetic phase was refined using initial structural model provided by Reynolds *et al.* (2004) to R_1 index of 0.0581 for 101 observed unique reflections [$I>2\sigma(I)$], corrected for absorption with an empirical correction. The structure is hexagonal with space group $P6_3/mmc$, cell parameters a 3.9090(2), c 15.6820(9) Å, V 207.52(2) $Å^3$, Z = 2 for synthetic Ni_2SbTe_2. Atomic parameters are given in Table 1, structure is presented in Figure 2.

Table 1. Atomic positions and equivalent displacement parameters for synthetic vavřínite.

Atom	*x*	*y*	*z*	*Ueq*
Ni	0	0	0.1657(1)	12.5(10)
Sb	1/3	2/3	1/4	8.2(9)
Te	1/3	2/3	0.58704(6)	8.6(9)

The crystal structure of vavřínite can be described as "hybrid" of breithauptite (NiSb) and melonite ($NiTe_2$) with an elongated *c*-axis. The resulting vavřínite five-layered structure consists of stacking sequence CABAC (A – Ni, B – Sb, C – Te). The weak interlayer Te bonding results in a perfect cleavage along {0001} and plate-like morphology of crystals.

The structure identity of vavřínite and synthetic material was confirmed by results of the electron backscattered diffraction (EBSD) study. The EBSD patterns (also known as Kikuchi bands) obtained from a natural material (3 measurements

from a lath-shaped grain and 2 measurements from an adjacent small grain) easily matched the patterns generated from structure data of synthetic Ni_2SbTe_2 yielded by our single crystal structure refinement.

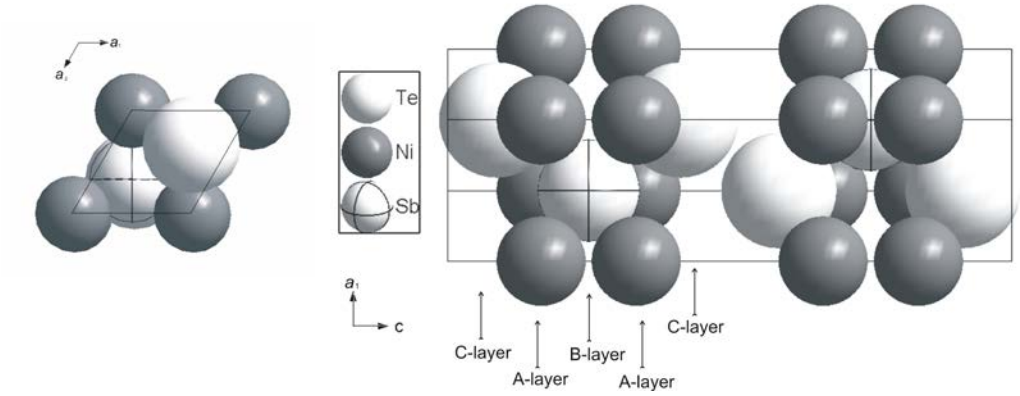

Fig. 2. Crystal structure of synthetic vavřínite. Projection onto a_1-a_2 and a_1-c planes.

CONCLUSIONS

On the Cu-Ni-sulphide deposit Kunratice near Šluknov we described new mineral vavřínite (IMA 2005-045). Vavřínite with crystallochemical formula Ni_2SbTe_2 is hexagonal with space group $P6_3/mmc$ and occurs in the mineral assemblages with pyrrhotite, pentlandite and chalcopyrite.

ACKNOWLEDGEMENTS: This work was supported by a Grant Agency of Charles University (project No. 43-203391).

REFERENCES

REYNOLDS T.K., KELLEY R.F., DISALVO F.J., 2004: Electronic transport and magnetic properties of a new nickel antimonide telluride, $SbNi_2Te_2$. J. Alloy Comp. 366: 136 -144.

SHELDRICK G.M., 1997: SHELX97. Programs for Crystal Structure Analysis. Release 97-2. Institut für Anorganische Chemie, Universität Göttingen, Germany.

VAVŘÍN I., FRÝDA J., 1998: Pt-Pd-As-Te mineralization from the Kunratice and Rožany cooper-nickel deposits of Šluknov area. Věst. Čes. geol. Úst. (Bull. Czech. geol. Surv.), 73: 177-180. (in Czech.)

MINERALOGIA POLONICA - SPECIAL PAPERS
Volume 28 - 2006

Jaromír LEICHMAN[1] , Kamil MAREK[1] , Josef ZEMAN [1], Petr KLAPETEK [2]

CARBONATIZATION OF AGATE NODULES FROM PERMIAN ANDESITES, KRKONOŠE PIEDMONT BASIN

INTRODUCTION

Agates from Permian andesites are usually formed by concentric bends of chalcedony. Quartz, calcite, chlorites and Fe-oxides were identified within the nodules too. However CL study reveals that some agates are partly carbonatized. Carbonatization occurs in several textural forms, depending on primary chalcedony habit. We focus our attention on the case, where carbonate replaces the banded thin chalcedony layers.

METHODS

We used optical microscopy, cathodoluminescence microscopy (CL) to study a relatively coarse-structures. Electron microprobe (EMP) was used to study fine structures, to get precise analyze of individual mineral phases, and to obtain element distribution maps. The very fine structures were observed using Atomic force microscopy (AFM).

RESULTS

The individual chalcedony bands could be replaced by calcite in two different styles. The contact between chalcedony and calcite is in XPL, PPL, CL and BSE fuzzy in the first case. No Becke line could be observed between chalcedony and calcite.

Calcite penetrates along the superficies between two chalcedony layers. However, both frontal as well as lateral contacts with surrounding chalcedony are diffuse. Element distribution maps documents this feature best.

Fig. 1 display a part of agate nodules with alternating of aproximately 10 μm thick bands of chalcedony and 40 μm thick bands with elevated concentration of $CaCO_3$. The contact between these two bands is gradual; however a certain amount of Si remains in the Ca-rich strip, which appears to be formed by calcite in XPL and CL photographs.

Figs. 2-4 document the second style of chalcedony replacement. The contact between calcite and chalcedony is sharp in CL and BSE; the distinct Becke line could be seen in PPL. However the careful inspection of CL and mainly BSE images detect slight differences, which indicate that the calcite is not homogenous.

Spot EMP analyses find out admixture of SiO_2 in the calcite. This feature was confirmed by the study of element distribution. Calcium is distributed unevenly; the lower Ca concentrations are balanced by higher Si content. The pure calcite

[1] *Department of Geological Sciences, Masaryk University, Kotlářská 2, 611 37 Brno, Czech Republic; leichman@sci.muni.cz*
[2] *Czech Metrology Institute, Okružní 31, 638 00 Brno, Czech Republic*

was found in the small vein only, which is located in the central part of the calcite domain.

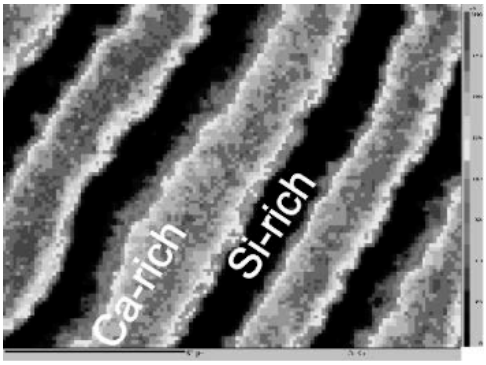

Fig. 1. Ca distribution map. Ca-rich strip alternates with Si-rich strips.

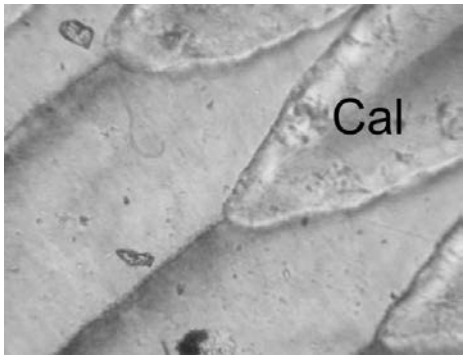

Fig. 2. Contact between calcite and chalcedony in PPL.

Spot EMP analyses find out admixture of SiO_2 in the calcite. This feature was confirmed by the study of element distribution. Calcium is distributed unevenly; the lower Ca concentrations are balanced by higher Si content. The pure calcite was found in the small vein only, which is located in the central part of the calcite domain.

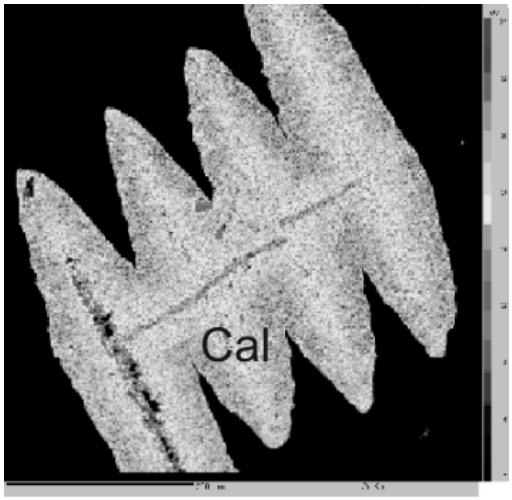

Fig. 3. Ca distribution within the calcite replacing chalcedony.

Exactly from this vein the carbonatization progress into the chalcedony and carbonate starts to replace chalcedony along the superficies between two chalcedony layers again. We study this part of agate, which is seemingly homogenous in PPL and CL, but chemical analyses evidence admixture of Si.

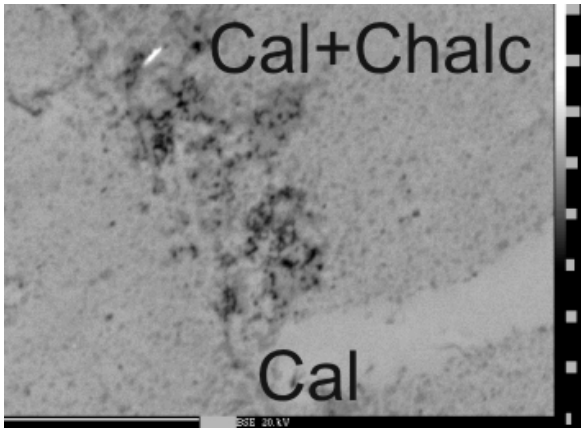

Fig. 4. Chalcedony globulites (Chalc) survive within the calcite matrix (Cal).

A very high magnification (~4000), achieved in BSE and AFM, detect the globulite structure of chalcedony (Moxon 2002).

The size of individual globulites is around 1 to 2 μm. The SiO_2 globulites "survive" even in the strongly carbonatized parts of chalcedony. The central calcite vein is free of globulites. Domains which exhibit higher Ca concentration on Fig. 4 are relatively depleted on SiO_2 globulites, and vice versa.

CONCLUSIONS

Chalcedony from agate nodules is commonly replaced by calcite. This feature indicates essential change in the fluid composition. Carbonates penetrate into the interior of the nodule along cracks or along discontinuous zones between individual chalcedony growth centres. Two styles of chalcedony replacement were distinguished.

Calcite "impregnates" the porous segment of the individual chalcedony layer. The domain composed of pure chalcedony alternates with chalcedony domain impregnated by calcite. The contacts between both parallel domains are diffuse in this case. Fe content correlates positively with Ca, and Al with Si.

Calcite could penetrates and replaces chalcedony along plane between two adjoining chalcedony layers. Calcite replaces symmetrically both, lower and upper layers. The boundary between calcite and chalcedony is irregular, but rather sharp. However some chalcedony globulites could survive within the calcite.

Both replacement mechanisms could cause the almost complete substitution of chalcedony by calcite. Reverse process – chalcedony or opal after calcite - is feature common during diagenesis of sedimentary carbonates. The calcite after silica is more seldom in the nature, however both processes indicate important role of SiO_2 and carbonate-rich fluids in the evolution of upper crust.

REFERENCES

MOXON T., 2002: Agate: a study of ageing. Eur. J. Mineral., 14: 1109-1118.

MINERALOGIA POLONICA - SPECIAL PAPERS
Volume 28 - 2006

Jiří LITOCHLEB[1], Jiří SEJKORA[1], Vladimír ŠREIN[2]

THE Au-Ag-Sb-Bi-Te MINERALIZATION FROM THE DEPOSIT BYTÍZ (MINE 19), THE PŘÍBRAM URANIUM-POLYMETALLIC ORE DISTRICT, CZECH REPUBLIC

INTRODUCTION

The gold-bearing hydrothermal ore mineralization represents the oldest and relatively widespread type at the Příbram uranium-polymetallic district. The wavy quartz to quartz-sulphide veins with thickness in the range cm-dm form coulisse-like arranged system of directions NW-SE to E-W in rock of the Barrandien Neoproterozoic and in granitoids of the Central Bohemian pluton. In the central part of this ore district, gold-bearing mineralization was verified by mining works up to the depth of about 1400 m. Some ore veins are locally characterized by high metal content (about 100 ppm Au) and varied mineral associations with representations of Bi, Te, Ag, Sb, Pb, Cu, Fe, As, S (Litochleb, Šrein 1989; Litochleb et al. 2000).

Our research was concentrated on the quartz-sulphide vein of the U and Pb-Zn deposit Bytíz (the vein cluster Bt17B-Bt22). This vein was found during mining of polymetallic ores above the 20th level (at depth 900-950 m) of the mine 19 (Bytíz). The vein had wavy character with thickness 3-25 cm, NW direction and was located in close proximity of a younger polymetallic vein Bt23C; according to chip sampling in the length 18 m**,** it may be characterized by very variable contents of Au from 0.43 to 111 ppm Au. The vein-fillings are represented by grey-white to grey massive quartz with abundant arsenopyrite predominated pyrite with younger tiny veins of dolomite-ankerite and at some places with fine-grained gold (0.X mm) and grey aggregates of associated minerals with the size about 1 mm.

METHODS

The polished sections for microscopic study and electron microanalyses (CAMECA SX100, D. Štúr State Geol. Inst., Bratislava) were prepared from the rich mineralized quartz-sulphide gangue with the following contents - Au: 183-232, Ag: up to 41.9, Pb: 70.5-643, Zn: 297-719, Sb: 37.2-270, Cu: up to 93.4, Bi and Hg below 10 (all contents in ppm, AAS).

RESULTS

The oldest arsenopyrite is strongly cataclastic broken, and is penetrated and closed up by younger quartz. The filling of thin net-arranged fissures is formed by minerals of the series Au-Ag or by dolomite-ankerite with Au, Ag, Sb, Bi and Te

[1] *Department of Mineralogy and Petrology, National Museum, Václavské nám. 68, 115 79 Praha 1, Czech Republic; jiri.litochleb@nm.cz*

[2] *Institute of Rock Structures and Mechanics, Academy of Science of Czech Republic, V Holešovičkách 41, 182 09 Praha 8, Czech Republic*

minerals. These ore minerals also form tiny irregular aggregates between individual fragments of arsenopyrite crystals. Fine-grained mineral phases of the series Au-Ag occur in quartz close to arsenopyrite aggregates or form tiny thin veins directly in arsenopyrite. Individual different (by colour, chemistry etc.) types of Au-Ag phases form separate grains or intergrow as aggregates (in that case Ag-rich members are evidently younger). Chemical composition of Au-Ag phases is strongly variable (Fig. 1) - Au 0.31-0.93, Ag 0.07-0.67, Hg up to 0.03 and Sb up to 0.02 *apfu*. Phases of the Au-Ag series are accompanied by galena, sphalerite, chalcopyrite, native bismuth (grain up to 10 μm in gold), Bi-Te minerals - tsumoite, tetradymite and tellurobismutite (aggregates up to 200 μm), Bi-rich varieties of boulangerite and jamesonite and distinctly younger phases Au-Sb, Au-Ag-Sb, Ag-Sb and (Au,Ag)-Sb-O.

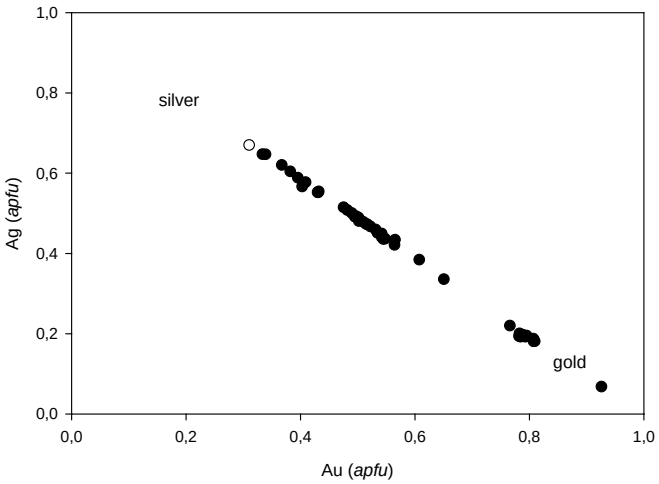

Fig. 1. Graph Au vs. Ag (*apfu*) for members of the series gold-silver from studied mineralization, Bytíz near Příbram.

Tellurides are constituent of filling of tiny carbonate (zoned dolomite-ankerite phases) veins in quartz. Tsumoite is the prevailing telluride (Fig. 2)**.** It intensively replaces Sb-rich tetradymite (up to 0.25 *apfu* Sb) and tellurobismutite. Tsumoite forms two types: (1) is close to ideal BiTe and (2) is slightly nonstoichiometric with $Bi_{0.88}Te_{1.11}$ - $Bi_{1.17}Te_{0.83}$ composition. It usually contains some Sb (up to 0.05 *apfu*) and Pb (up to 0.06 *apfu*). Younger ore minerals are represented by Ag-rich members of the Au-Ag series and by aurostibite (grains 10-20 μm in size). Aurostibite closes up older Ag-poor gold and is overgrown by younger Ag-rich gold to Au-rich silver. It is associated with Ag-Au-Sb and unnamed $(Au,Ag)SbO_3$ phases (some of them with Ag contents up to 0.69 *apfu*) overgrowing and replacing aurostibite. A part of aurostibite grains is in BSE images zoned and contents up to 0.05 *apfu* Bi in their margins. Together with Ag-rich members of the Au-Ag series and aurostibite**,** there were observed in close intergrowths also Ag-Sb phases -

dyscrasite (grains up to 30 μm) and other phases wit variable ratio Ag/Sb, hessite (grains up to 15 μm) with rims formed by Ag-Bi-S phase (similar to matildite) and Ag-Au-Sb phase with contents 17.02-27.02 wt. % Sb and a variable ratio Au/Ag.

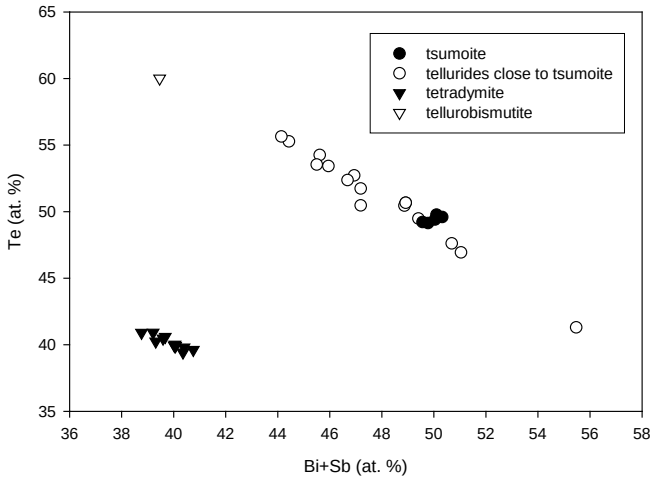

Fig. 2. Graph (Bi+Sb) vs. Te (at. %) for Bi-tellurides from studied mineralization, Bytíz near Příbram.

From the genetic point of view, the observed mineral association of this vein had to origin in several distinct stages. The first stage is characterized by the origin of arsenopyrite mineralization and crystallization of gold-bearing mineralization with Ag-poor gold and Bi-Te minerals after its cataclasy. There was observed an intensive replacement of Au mineralization by hydrothermal solutions containing polymetallic elements (as Ag and Sb) connected with the origin of low-temperature phases Au-Ag, Au-Ag-Sb, Au-Sb, Ag-Te, Ag-Bi-S and later also younger unnamed $(Au,Ag)SbO_3$ replacing aurostibite. The preservation degree of individual phases of successive conversions within the framework of one gold-bearing vein structure is entirely unique.

ACKNOWLEDGEMENTS: We thank D. Ozdín (Comenius Univ., Bratislava) for his kind cooperation. This work was supported by the grants MK00002327201 and 205/06/0702.

REFERENCES

LITOCHLEB J., ČERNÝ P., ŠREIN V., LANTORA M., SEJKORA J., 2000: Mineralogy of the gold-bearing mineralization in the underground gas reservoir at Háje near Příbram (central Bohemia). Bull. Mineral. Petrol. Odd. NM, 8: 195-201 (in Czech).

LITOCHLEB J., ŠREIN V., 1989: The chemical composition of bismuth and tellurium minerals from the gold-bearing veins of the Příbram uranium deposit. Acta Univ. Carol. Geol., 4: 511-519. (in Czech).

MINERALOGIA POLONICA - SPECIAL PAPERS
Volume 28 - 2006

Jarmila LUPTÁKOVÁ[1], Martin CHOVAN[2]

CHARACTER OF HYDROTHERMAL FLUIDS IN PB-ZN VEIN MINERALIZATION IN THE TATRIC UNIT OF THE WESTERN CARPATHIANS

INTRODUCTION

Pb-Zn mineralization is developed as one stage of hydrothermal vein mineralization at many deposits or occurences in the Tatric Unit. According to Chovan et al. (1996), hydrothermal mineralizations hosted by Hercynian crystaline basement can be divided into following types: molybdenum, tungsten, arsenopyrite-pyrite (± gold), gold, antimony, base metal (Pb-Zn), siderite, barite, and hematite. Pb-Zn mineralization stage comprises of galena, quartz, sphalerite, and pyrite as main minerals, with minor but characteristic Pb-Sb sulphosalt boulangerite, bournonite, Ag-bearing minerals Ag-tetrahedrite, freibergite and others. In this paper, we compare the composition of ore forming fluids from three occurences of Pb-Zn mineralization in the Tatric Unit: Jasenie-Soviansko, Dve Vody (both in Nízke Tatry Mts.), and Pod Babou (Malé Karpaty Mts.).

METHODS

Transparent minerals (quartz, sphalerite, and calcite) of Pb-Zn mineralization stage were observed under transmitted polarized light and suitable samples were used for microthermometric study. Phase transitions in fluid inclusions were measured in the Linkam THMSG 600 heating/freezing equipment mounted on an Olympus microscope.

RESULTS

Jasenie-Soviansko: Quartz contains primary and pseudosecondary two- and three-phase inclusions, with aqeous phase, vapor bubble and halite crystal. Volume ratios of phases are constant. Eutectic temperature varies between -57 and -49 °C, which suggest the presence of NaCl-$CaCl_2$-H_2O system. Ice melts in the temperature range of -34.6 and -23.3 °C. Hydrohalite is metastable and decomposes at temperatures above 0°C. In pseudosecondary two-phase inclusions small amount of CO_2 was recorded by presence of CO_2-clathrate which melts at temperatures ranging from -2.1 to 2.5 °C. Three-phase inclusions homogenize by halite dissolution (145-308 °C) or dissapearance of bubble (142-322 °C). This allowed us to estimate minimal fluid trapping PT conditions, considering 40 % NaCl liquidus (Bodnar 1994). Minimal temperature is 300 °C and minimal pressure is 220 MPa. Densities of two-phase and three-phase inclusions are near to 0.95 and 1.1 g/cm^3, respectively. Salinity varies between 15.96 and 38.84 wt. % NaCl eq.

[1] *Geological Institute, Slovak Academy of Sciences, Severná 5, 974 01 Banská Bystrica, Slovak Republic; luptak@savbb.sk*
[2] *Department of Mineralogy and Petrology, Faculty of Natural Sciences, Comenius University, Mlynská dolina, 84215 Bratislava, Slovak Republic*

Primary inclusions concentrate near upper salinity limit, while pseudosecondary near lower one. Estimated $CaCl_2/(CaCl_2+NaCl)$ weight ratio varies between 0.08-0.35.

Younger sphalerite contains two- and rarely three-phase inclusions. Eutectic temperature varies from -49 to -34 °C, which indicates solutions with Na^+, Fe^{2+}, Ca^{2+}, and Mg^{2+} content. Ice melts in temperature range of -22.0 to -26.7 °C, CO_2-clathrate between -18.7 and -16.0 °C and hydrohalite from -24.5 to 26.8°C. In three-phase inclusions halite melts at temperatures between 120.0 and 191.6 °C. Inclusions homogenize to liquid between 119 and 289 °C. Salinity and density vary from 21.87 to 31.46 wt. % NaCl eq. and from 0.97 to 1.1 g/cm^3, respectively. Few measured inclusions hosted by calcite and quartz associated with sphalerite yielded comparable parameters.

Dve Vody: Quartz contains two-phase inclusions that are primary and pseudosecondary in origin. Eutectic temperatures vary in large interval ranging from –48 to –20°C which indicates that fluid composition is more complex. Except for $NaCl-H_2O$ it contains also divalent cations, probably Ca^{2+}; Mg^{2+}. Ice melting temperature varies within two intervals -24.1 to -20.6 and -17.3 to -3.9 °C which equals to salinities 22.76-25.02 and 6.23-20.43 wt. % NaCl eq. Most inclusions with higher salinity were identified as pseudosecondary. All inclusions homogenize to liquid phase between 144 and 286 °C. Fluid density varies between 0.92 and 1.06 g/cm^3.

Pod Babou: Quartz contains two-phase inclusions with vapor bubble volume below 10 % of total volume. Eutectic temperatures are equal to or below eutectic point of $NaCl-H_2O$ which indicates presence of other cations (K^+, Fe^{2+}). Ice melting temperatures between -11.0 and -1.2 °C correspond to salinities from 1.98 to 14.18 wt. % NaCl eq. CO_2-clathrate occured in few inclusions indicating presence of small CO_2 content. Inclusions homogenize to liquid in the temperature range of (110) 152 – 260 °C. Fluid density ranges from 0.83 to 1.01 g/cm^3.

CONCLUSIONS

Pb-Zn mineralization in the Tatric Unit originated from fluids of complex composition. Observed data indicate $NaCl-H_2O\pm CaCl_2-MgCl_2-FeCl_x-KCl$ system, sometimes with small content of CO_2. Fields of salinity *vs.* homogenisation temperature for individual occurences are shown in the Fig. 1. Fluids with the highest salinity and density were identified at Jasenie-Soviansko deposit. Formation p, T conditions have been estimated at 300 °C and 220 MPa. Fluids from other deposits were lower both in temperature and salinity.

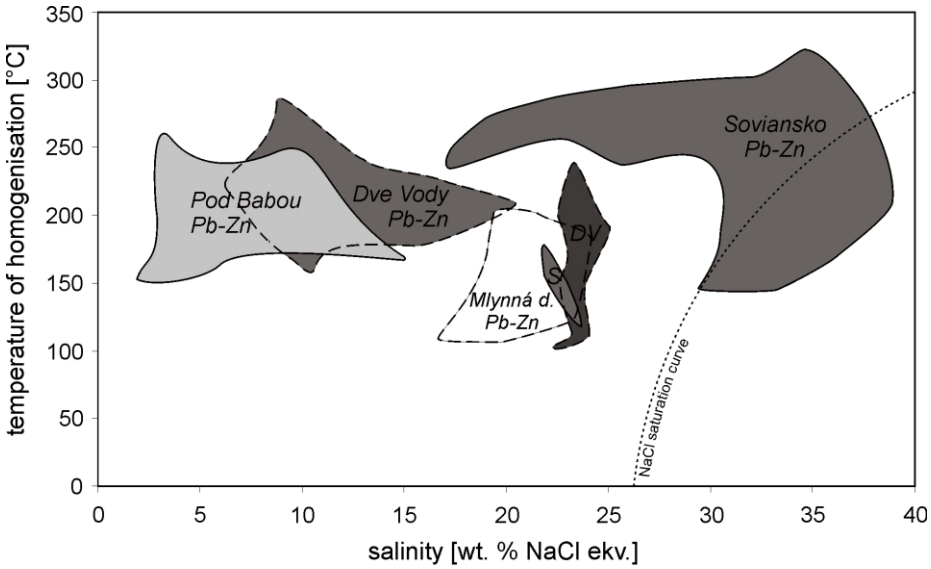

Fig. 1 Plot of salinity vs. temperature of homogenisation for fluid inclusions from Pb-Zn mineralisation in the Tatric Unit. Data for Mlynná dolina valley are from Majzlan et al. (2002). Abbreviations: S - Jasenie-Soviansko deposit, DV - Dve Vody deposit.

REFERENCES

BODNAR R. J., 1994: Synthetic fluid inclusions: XII. The system H_2O-NaCl. Experimental determination of the halite liquidus and izochores for a 40 wt. % NaCl solution. Geochim. Cosmochim. Acta 58: 1053-1063.

CHOVAN M., SLAVKAY M., MICHÁLEK J., 1996: Ore mineralizations of the Ďumbierske Tatry Mts. (Western Carpathians, Slovakia). Geol. Carpath., 47: 371-382.

MAJZLAN J., HURAI V., CHOVAN M., 2002: Fluid inclusion study on hydrothermal As-Au-Sb-Cu-Pb veins in the Mlynná dolina valley (Western Carpathians, Slovakia). Geol. Carpath., 52: 277-286.

MINERALOGIA POLONICA - SPECIAL PAPERS
Volume 28 - 2006

Jarosław MAJKA[1]

MONAZITE DATING RESULTS FROM THE S PART OF WEDEL JARLSBERG LAND, SVALBARD

INTRODUCTION

Stratified volcano-sedimentary polymetamorphic complex is distinguished in the S part of Wedel Jarlsberg Land (Svalbard Archipelago) as an exotic terrane. This complex comprises metasedimentary sequence known as the Isbjørnhamma Group, and bimodal metavolcanic rocks of the Eimfjellet Group (Birkenmajer 1958; Czerny et al. 1993). The Isbjørnhamna Group rocks are composed of garnet bearing mica schists and paragneisses, calcite mica schists and marbles. These rocks were affected by metamorphism twice: firstly, under amphibolite facies conditions; secondly, under greenschist facies conditions (Smulikowski 1960; Majka et al. 2004).

The earliest dating of Isbjørnhamna Group by Gayer et al. (1966), with use of K/Ar method, indicates the age ca. 600 Ma. Another age determinations of these rocks (Rb/Sr method, Gavrilenko et al. 1993; Balashov et al. 1996) revealed Grenvillian age ca. 936 Ma. Similar ages were reported by Balashov et al. (1995) from zircons separated from rhyolitic metacoglomerates belonging to the upper laying Eimfellet Group. Ar/Ar age determinations made by Manecki et al. (1998) revealed even younger dates of 616 Ma (hornblende from Eimfjellet Group) and 585-575 Ma (micas from Isbjørnhamna Group). Additionally, Manecki et al. (1998) reported Caledonian Ar/Ar ages obtained on micas (ca. 459-432 Ma), resulting from latter diaphtoritic greenschist facies event. Use of monazite dating was necessary due to discrepancy in existing data. This study presents the first monazite dating results from metamorphosed rocks from southern Svalbard.

SAMPLES SELECTION AND METHODS

Four rocks from the Isbjørnhamna Group were selected for the study: three samples of fine- to medium-grained mica schists and one sample of paragneiss. The rocks are slightly affected by Caledonian metamorphic event with relatively weak diaphtoritic changes (e.g., partial chloritization of garnet and biotite). Monazite grains were selected for in situ EMP on the basis of overall size and microtextural context. Large matrix monazite grains as well as monazites occurring as inclusions in garnet porphyroblasts were preferentially selected. The existence of patchy domains was revealed with back-scattered electron (BSE) imaging. Subhedral to anhedral monazite grains in matrix, up to 70 μm long, are occasionally surrounded by the aggregates of apatite or apatite-allanite coronas (Majka, Budzyń 2006).

In situ analyses were made in polished thin sections using the electron microprobe EMP, Cameca SX-100, at the Electron Microanalysis Department of

[1] *AGH - University of Science and Technology, Department of Mineralogy Petrography and Geochemistry, al. Mickiewicza 30, 30-059 Kraków, Poland; jmajka@poczta.fm*

the Geological Survey of Slovak Republic in Bratislava. Details of analytical methodology and recalculations are as described by Konečný et al. (2004). The age calculation is based on the formulation of Montel et al. (1996).

RESULTS AND DISCUSSION

Chemical U-Th-total Pb dating performed on all monazite grains provided uniform Neoproterozoic ages (643±9 Ma), corresponding to Cadomian/Baikalian orogeny. The linear distribution of analytical results on the isochrone indicates that all dated monazites from four analyzed samples belong to the same population. All domains revealed with BSE imaging within monazite grains yielded similar age within the error. Also, monazite included in garnet revealed the same age as monazite grains in the matrix. Monazites exhibiting secondary alterations apparent as allanite-apatite coronas are also of the same age.

Based on the fact that monazites enclosed in garnets yield the same age, it is unquestionable that metamorphic event under amphibolite facies conditions took places around 643 Ma. These results are consistent with most recent Ar/Ar dates of hornblende and micas from these rocks (Manecki et al. 1998).

Grenvillian ages described by Gavrilenko et al. (1993) and Balashov et al. (1995, 1996) could signify the oldest metamorphic event, which took place in the S part of the Wedel Jarlsberg Land. However no structural or mineral relics of this event are preserved in the studied rocks; it could probably signify metamorphism under lower then amphibolite facies conditions. On the other hand, ages of zircon grains separated from metarhyolites are determined from lower intercept of discordia. This discordia was constructed on the basis of metamorphic and detrital zircons separated from different samples, what makes the dating questionable. Also, Rb/Sr dates of Isbjørnhamna Group rocks are based on small, pre-selected and rather unrepresentative population of samples.

CONCLUSIONS

The detailed U-Th-total Pb monazite dating presented here lead to the following interpretation of metamorphic history of the exotic terrane the S part of Wedel Jarlsberg Land around Honsund:

(1) K/Ar (Gayer et al. 1966), Ar/Ar (Manecki et al. 1998) and monazite U-Th-total Pb ages reported herein consistently indicate that the strongest metamorphic event under amphibolite facies conditions took place during Neoproterozoic and correspond to Cadomian/Baikalian orogeny.

(2) Grenvillian metamorphic event could take place, however under lower then amphibolite facies conditions: pre-Neoproterozoic structures in the Isbjørnhamna and the Eimfjellet Group rocks are not apparent.

(3) Later diaphtoritic changes are Caledonian in age (Manecki et al. 1998).

ACKNOWLEDGEMENTS: These investigations were sponsored by MN research grant no. 2 P04D 039 30.

REFERENCES

BALASHOV JU.A., TEBENKOV A.M., OHTA Y., LARIONOV A.N., SIROSTKIN A.N., GANNIBAL L.F., RYUNGENEN G.I., 1995: Grenvillian U-Pb zircon ages of quartz porphyry and rhyolite clasts in a metaconglomerate at Vimsodden, southern Spitsbergen. Polar Res., 14: 291-302.

BALASHOV JU.A., TEBENKOV A.M., PEUCAT J.J., OHTA Y., LARIONOV A.N., SIROSTKIN A.N., 1996: Rb-Sr whole rock and U-Pb zircon datings of the granitic-gabbroic rocks from the Skålfjellet Subgroup, southwest Spitsbergen. Polar Res., 15: 167-181.

BIRKENMAJER K., 1958: Preliminary report on the stratigraphy of the Hecla Hoek Formation in Wedel Jarlsberg Land, Vestspitsbergen. Bull. Acad. Pol. Sci. Ser. Sci. Chim. Geol. Geogr., 6: 143-150.

CZERNY J., KIERES A., MANECKI M., RAJCHEL J., (MANECKI A. Ed.), 1993: Geological map of the SW part of Wedel Jarlsberg Land, Spitsbergen 1:25000. Institute of Geology and Mineral Deposits, Cracow, 1-61.

GAVRILENKO B. V., BALASHOV JU.A., TEBENKOV A.M., LARIONOV A.N., 1993: U-Pb early Proterozoic age of “relict” zircon from high potassium quartzose porphyries of Wedel Jarlsberg Land, SW Spitsbergen. Geokhimiya, 1: 154-158.

GAYER R.A., GEE D.G., HARLAND W.B., MILLER J.A., SPALL H.R., WALLIS R.H., WINSNES T.S., 1966: Radiometric age determinations on rocks from Spitsbergen. Norsk Polarinstitutt Skrifter, 137: 1-39.

KONEČNÝ P., SIMAN P., HOLICKÝ I., JANÁK M., KOLLÁROVÁ V., 2004: Metodika datovania monazitu pomocou elektrónového mikroanalyzátora. Mineralia Slov., 36: 225-235.

MAJKA J., BUDZYN B., 2006: Monazite breakdown in metapelites from Wedel Jarlsberg Land, Svalbard. Miner. Polon., 37/1 (in print).

MAJKA J., CZERNY J., MANECKI M., 2004: Petrographical characteristics of the Isbjørnhamna Group Rocks (Wedel Jarlsberg Land, Spitsbergen). Pol. Tow. Mineral. Prace Spec., 24: 279-282.

MANECKI M., HOLM D. K., CZERNY J., LUX D, 1997: Thermochronological evidence for late Proterozoic (Vendian) cooling in southwest Wedel Jarlsberg Land, Spitsbergen. Geol. Mag., 135:, 63-69.

MONTEL J.M., FORET S., VESCHAMBRE M., NICOLLET C., PROVOST A., 1996: Electron microprobe dating of monazite. Chem. Geol., 131: 37-53.

SMULIKOWSKI K., 1960: Preliminary Report on the Petrology of the Isbjørnhamna Formation (Hornsund Area, Vestspitsbergen). Bull. Acad. Pol. Sci. Ser. Sci. Chim. Geol. Geogr., 8: 159-163.

MINERALOGIA POLONICA - SPECIAL PAPERS
Volume 28 - 2006

Juraj MAJZLAN[1], *Rodney GRAPES*[2]

MINERALS FROM THE EXOCONTACT OF A PEGMATITE AND SERPENTINITES IN HEŘMANOV, CZECH REPUBLIC

INTRODUCTION

Unusual concentrically-zoned nodules at the contact of a pegmatite intruding serpentinite near the village of Heřmanov have been known for more than 200 years (André 1804) and are popular among mineral collectors. Brezina (1874) analyzed the external portion of the nodules and concluded that the principal mineral is anthophyllite. This identification has become a 'general wisdom' over the decades and has not been questioned.

ANALYTICAL METHODS

Minerals of the nodules were observed and analyzed by transmitted light microscopy, electron microprobe (EMP) (Cameca SX100), and X-ray diffraction (XRD) (Bruker AXS D8 Advance). Mineral formulae together with lattice parameters calculated from XRD patterns by Rietveld refinement using GSAS (Larson and von Dreele 1994) are presented in Table 1.

RESULTS

The nodules consist predominantly of an Mg-rich assemblage of phlogopite, talc, and amphibole. The central portion of the nodules consists of phlogopite (XMg$_{0.95}$) surrounded by a thin zone of mostly talc (XMg$_{0.97}$), with an outermost zone composed of radiating bundles of acicular amphibole. In different samples, we have identified the amphibole to be either tremolite (XMg$_{0.96}$) or anthophyllite (EDS and XRD identification). Tremolite contains very fine exsolution lamellae of anthophyllite. Accessory minerals are chromite (XMg$_{0.19}$), graphite, ilmenite, apatite, and vermiculite, which is most likely a weathering product.

CONCLUSIONS

Our work indicates that the Heřmanov nodules contain both tremolite and anthophyllite, despite the long-held belief (cf. Brezina 1874) that the amphibole is exclusively anthophyllite. Anthophyllite exsolution lamellae in tremolite may be used as a semi-quantitative indicator of the temperature of nodule formation. The presence of ilmenite, chromite and graphite indicates a reducing environment. The mechanism that controlled the size, shape and zonation of the nodules remains unknown. The mineral paragenesis of the nodules invites comparison with the zoned reaction sequence from unaltered cores of olivine through talc-anthophyllite to phlogopite in dunite by metasomatic reaction between dunite and intrusion of

[1] *Institute of Mineralogy and Geochemistry, Albert-Ludwig-University of Freiburg, Albertstrasse 23b, 79104 Freiburg, Germany; juraj.majzlan@minpet.uni-freiburg.de*
[2] *Department of Earth Sciences, Zhongshan University, Guangzhou 510275, China*

pegmatites, North Carolina (Kulp, Brobst 1954). However, in contrast to the Heřmanov nodules, the outmost zone developed nearest the pegmatite consists of phlogopite.

Table 1. Lattice parameters and formulae of Heřmanov nodule minerals.

Mineral	Space group	Lattice parameters Crystal chemical formula
tremolite	*C*2/*m*	a = 9.839(2), b = 18.052(3), c = 5.2777(6), β = 104.57(1) $(Ca_{1.57}Na_{0.40}K_{0.06})(Mg_{4.77}Fe^{2+}_{0.22}Mn_{0.01}Cr^{3+}_{0.01})$ $(Si_{7.82}Fe^{3+}_{0.12}Al_{0.06}Ti_{0.01})O_{22}[(OH)_{1.80}F_{0.20}]$
anthophyllite	*Pnma*	a = 18.5401(4), b = 18.0003(3), c = 5.2776(1)
talc	*P*-1	a = 5.2875(7), b = 9.1747(12), c = 9.4595(12), α = 90.472(9), β = 98.683(10), γ = 90.039(9) $(Mg_{2.92}Fe_{0.08})(Si_{3.98}Al_{0.01})O_{10}(OH)_2$
phlogopite	*C*2/*m*	a = 5.274(2), b = 9.178(2), c = 10.278(1), β = 100.75(3) $(K_{0.82}Na_{0.03})(Mg_{2.77}Fe_{0.16}Ti_{0.07}Cr_{0.04})(Si_{3.07}Al_{0.94})O_{10}[(OH)_{1.76}F_{0.24}]$

REFERENCES

ANDRÉ C.C., 1804: Anleitung zum Studium der Mineralogie. Camesimanische Buchhandlung Wien.

BREZINA A., 1874: Anthophyllit von Hermannschlag. Mineral. Mitt., 247.

KULP J.L., BROBST D.A., 1954: Notes on the dunite and the geochemistry of vermiculite at the Days Brook dunite deposit, Jancey County, North Carolina. Econ. Geol., 49: 211.

LARSON A.C., VON DREELE R.B., 1994: GSAS. General Structure Analysis System. LANSCE, MS-H805, Los Alamos, New Mexico.

MINERALOGIA POLONICA - SPECIAL PAPERS
Volume 28 - 2006

Emil MAKOVICKY[1]

SULFOSALTS – CRYSTALLOGRAPHY AND MINERALOGY

GENERAL CONSIDERATIONS

Sulfosalts (and selenosalts) are complex sulfides (and selenides) of As^{3+}, Sb^{3+}, Bi^{3+} and, rarely also Te^{4+} with Pb and/or Ag, Cu, Fe, Tl, and other metals. Their crystal structures are determined by the requirements of the trivalent metalloids, which in nearly all cases display a non-bonded pair of *s* electrons, situated at one side of the cation. Because of their steric requirements, these 'lone electron pairs' (LPE) often congregate, forming inflated common spaces, so called 'lone electron pair micelles'.

In their chemical and structural complexity, sulfosalts are comparable to silicates. For example, neyite is $Ag_2Cu_6Pb_{25}Bi_{26}S_{68}$, *a* 37.53, *b* 4.07, *c* 43.70 Å, β 108.80°, Z=2, with 26 distinct large-cation sites, an Ag site and 3 Cu sites. Therefore, a polyhedral description is of little relevance and must be replaced by a modular one, studying rods, blocks or layers formed by aggregation of a number of coordination polyhedra. Because of the steric requirements of the large or of the predominant cations, these aggregates are usually slightly distorted derivatives of simple, *archetypal* structures, such as PbS, SnS, ZnS, etc. These archetype-like blocks can assume different sizes, shapes and arrangements. Because of the coordination properties of Pb and of the LEP cations, the relationship between adjacent blocks is not limited to reflection or glide-reflection but often these blocks match via non-commensurate interfaces, with different structure (sub) periodicities on the two block surfaces involved.

About a half of all sulfosalts are sulfosalts of Pb alone or in combination with other cations. In a number of cases, these cations are minor but inevitable, like, e.g., in kobellite $(Cu,Fe)_2Pb_{12}(Bi,Sb)_{14}S_{35}$. Two substitution schemes are of general importance for sulfosalts, 2Pb = Ag+Bi (or Sb) and Bi = Pb+interstitial Cu. The multiple element substitutions in tetrahedrite-tennantite, especially the Cu-Fe substitutions with the changing role of Fe^{2+} and Fe^{3+}, make a fascinating story by themselves.

HOMOLOGOUS SERIES

The block-like architecture of many (mainly) Pb sulfosalts facilitates formation of accretional homologous series. Individual members of this series differ in the size, but not in the shape, of structural blocks. Presence of non-commensurate interfaces between adjacent blocks may limit the number of existing homologues because the geometric match of the blocks across the interface has to be satisfied for each viable stage of accretion. The pair kobellite – izoklakeite can serve as an example.

[1] *Geological Institute, University of Copenhagen, Oestervoldgade 10, 1350 Copenhagen, Denmark; emilm@geol.ku.dk*

The lillianite homologous series $Pb_{N-1-2x}Bi_{2+x}Ag_xS_{N+2}$ (N is the order of a given homologue, i.e., a number of coordination polyhedra along a definite direction), pavonite homologues, sartorite homologues $Pb_{4N-8}As_8S_{4N+4}$, meneghinite homologues $Cu_xPb_{2N+x-4}(Sb,Bi)_{4-x}S_{N+2}$, and cuprobismutite homologues are the classical homologous series. The bismuthinite – aikinite Bi_2S_3 – $CuPbBiS_3$, and the andorite series of Pb-Ag-Sb sulfosalts are not homologous series: they are series of homeotypes, i.e. ordered derivatives of appropriate (high-temperature) solid solutions.

Two of the classical series have been restudied recently. The homologues of pavonite consist of $(311)_{PbS}$ layers of variable thickness, interleaved by one-octahedron thick layers containing columns of paired coordination pyramids of Bi. Recent investigations yielded not only sulfide and selenide members from N=2 to N=8 but they also contributed to the decidedly heterochemical character of this series, involving sulfosalts (selenosalts) of Cu (ionic conductors), Ag, Pb, Hg, Cd, In, Mn, Li, etc. Furthermore, the fascinating difference between the exsolution pairs pavonite-cupropavonite and makovickyite-cupromakovickyite has been explained. Besides having excess copper, the cupro- varieties have a very distinct role for Pb in the structure – its coordination polyhedron replaces one of the Bi pyramids in the columns of paired Bi pyramids mentioned above.

A detailed restudy of the homologues of cuprobismutite have recently been undertaken. Although the homologous relationship between kupčíkite $Cu_{3.0}Fe_{0.7}Bi_5S_{10}$ (N=1), cuprobismutite $Cu_8AgBi_{13}S_{24}$ (N=2) and hodrushite (for example, $Cu_{7.6}Ag_{0.4}Fe_{0.4}Bi_{11.6}S_{22}$ (N=1;2) for the material from Felbertal) has been known for a number of years, only now the nature of minor cation substitutions without which these phases do not exist became clear as a result of crystal structure determinations and microprobe analyses on the same material. A new reinterpretation of paděraite $Cu_7(Cu,Ag)_{0.33}Pb_{1.33}Bi_{11.33}S_{22}$ opens possibilities for further varieties of cuprobismutite-related structures.

THE BISMUTHINITE – AIKINITE SERIES

The series of ordered derivatives of the high-temperature Bi_2S_3 – $CuPbBiS_3$ solid solution has been extended to eleven distinct mineral species (homeotypes). These superstructures of Bi_2S_3 display multiplicities of the b_{Bi2S3} parameter as follows: 1 (bismuthinite), 3, 3, 4, 5, 1, 5, 4, 3, 3, 1 (aikinite). Beside the classical way of description of these structures, by means of bismuthinite-, krupkaite- and aikinite- like ribbons, a modular description now exists, in which modules are the (in principle) Cu-free structural intervals situated between two consecutive (010) planes in which interstitial tetrahedra are occupied by copper. In the direction of decreasing thickness, gladite-like modules are replaced by krupkaite-like, and then by aikinite-like modules; intermediate phases are combinations of such modules, e.g. salzburgite is G-G-K-G-G-K in this interpretation. This series offers fascinating examples of several stages of exsolution and possible metastability.

MINERALOGIA POLONICA - SPECIAL PAPERS
Volume 28 - 2006

SULFOSALTS WITH LAYER-LIKE STRUCTURES

Among the sulfosalts with layer-like structures, cannizzarite $Pb_{46}Bi_{54}S_{127}$ with alternation of mutually non-commensurate pseudotetragonal and pseudohexagonal (octahedral) layers plays a role of parent structure for a plethora of sulfosalts in which these layers are variously sheared into stripes of variable thickness. Two types of homologous relationships have recently been defined: (1) a series comprised of junoite $CuPb_3Bi_7(S,Se)_{14}$ - felbertalite $Cu_2Pb_6Bi_8S_{19}$ – portions of the structure of neyite (N=1 to 3 in terms of the thickness of the octahedral layer), and (2) a series of structures with double-octahedral layers, makovickyite – felbertalite – proudite (structure revised), in which the width of layer stripes increases. In this case we observe an intersection of the latter homologous series with the pavonite series, exemplified by the structure of makovickyite.

Berryite $Cu_3Ag_2Pb_3Bi_7S_{16}$ has a different character: thicker pseudotetragonal layers are in a *lock-in*, commensurate relationship with pseudohexagonal planes of atoms, populated by Cu and S. Both an orthorhombic and a monoclinic polytype of berryite will be shown. A modern refinement of the crystal structure of cylindrite (a sulfosalt of tin) has been started as well, yielding a surprisingly smooth undulating structure composed of alternating layers.

ROD-BASED AND BOX-WORK STRUCTURES

The series of Pb-Sb and Pb-Sb-Bi sulfosalts with rod-based structures (layer-like: e.g., jamesonite and robinsonite), cyclic (zinkenite), and chess-board like (kobellite, izoklakeite) are among the principal sulfosalts present in many Carpathian deposits. Among them, we shall demonstrate the newly refined structure of dadsonite $Pb_{23}Sb_{25}S_{60}Cl$. It appears to embody all of the features observed in Pb-Sb sulfosalts: the two types of rod-layers present display the two known, fundamentally different arrangements of Sb-S bonds resulting in different layer symmetries, Pb-Sb substitutions in specific sites, split Sb positions, pseudoperiods, potential OD character resulting in frequent twinning, and chlorine in a specific anion site of one layer set.

A fascinating recent development have been the structures of a box-work type, known also as variously degenerate cyclic structures. They contain more than two types of rods and in some cases also a layer with complex configuration. In the majority of Pb-Sb cases, one or two types of rods form rod-layers which are cross-connected by another type of rods and the resulting ‘boxwork’ is filled by one more type of rods. The Pb-Bi cases (neyite) deviate more from the’degenerate cyclic’ character whereas the newly described Pb-As-Bi-Sn sulfosalt vurroite adheres to it more closely. The problems of layer/rod fit observed in some of these structures are solved either by insertion of cations with appropriate coordination (Ag, Hg) or by means of kermesite (Sb_2S_2O)-like adjustments involving oxygen. Amounts of oxygen in these oxy-sulfides are minimal, making it an analytical problem. Charge balance problems may be solved by replacing S by Cl, similar to dadsonite. The channels of the box-work are smallest for vurroite, hosting a coordination octahedron of Sn, and increase through the series of Pb-Sb sulfosalts to the maximum observed in a still enigmatic sulfosalt from Nízke Tatry Mts. which was

found only as a single 0.n millimeter grain when searching for good dadsonite crystals.

CHEMICAL IMPLICATIONS

General formulae of homologous series, some of which were quoted above, offer us a possibility to determine a homologue (mineral species) from a good microprobe analysis alone, without employing single-crystal methods. For example, for the meneghinite homologues (Cu-Pb-(Bi,Sb) sulfosalts which include meneghinite, jaskolskiite and the entire bismuthinite-aikinite series), the general formula of the series is $Cu_xPb_{2N+x-4}(Sb,Bi)_{4-x}S_{N+2}$. In order to simplify the calculations, we can 'back-convert' nCu+nPb into n(Bi+Sb)+vacancy. Then, $Pb_{corr}/(Sb+Bi)_{corr}=(2N-4)/4$, and the order of the homologue studied is $N= 2Pb_{corr}/(Sb+Bi)_{corr} + 2$. Thus, for aikinite $CuPbBiS_3$, $Pb_{corr}=0$ and N=2. Such formulae have been proposed and used for lillianite homologues, sartorite (Pb-As) homologues, kobellite homologues, etc. They break down when one of the elements plays a double, substitutional and interstitial role in the structure – then a number of solutions become equally probable. Such is the case of Cu-Bi pavonite homologues and those cuprobismutite homologues in which Cu-Bi substitutions take place. Results of the above formulae can be plotted into appropriate composition diagrams and the phase studied can be determined by graphical means.

EPILOGUE

In this, rather targeted presentation we have omitted a number of other sulfosalt families, e.g. Tl-As, Tl-Sb and Pb-Sn sulfosalts which, so far, have not been relevant for the central Carpathian region. The topics presented are a result of collaboration with Drs. Topa (Salzburg), Balić-Žunić (Copenhagen), Moëlo (Nantes), Pinto (Bari), Mumme (Melbourne), Petříček (Prague), the group of Prof. Chovan (Bratislava), and others, in various stages of publication. For older references see Ferraris et al. (2005). Support of Danish National Research Council (Natural Sciences) is acknowledged.

REFERENCES

FERRARIS G., MAKOVICKY E., MERLINO S., 2005: Crystallography of Modular Materials. Oxford Sci. Publ., 1-370.

MINERALOGIA POLONICA - SPECIAL PAPERS
Volume 28 - 2006

Leszek MARYNOWSKI [1], *Michał ZATOŃ* [1]

DIFFERENCES IN FATTY ACIDS COMPOSITION BETWEEN THE MIDDLE JURASSIC CLAYS AND CARBONATE CONCRETIONS FROM THE POLISH JURA

INTRODUCTION

The Polish Jura is the area where Middle Jurassic deposits occur in ca. 10-33 km wide belt in the southern part of central Poland. The exposed deposits mostly consist of clays, currently used in the production of bricks. Many years ago, massive siderite beds occurring within the clays in several places were mined as iron ore. Up to now, the study of the Middle Jurassic clays have been concentrated mainly on stratigraphy and palaeontology (e.g., Matyja, Wierzbowski 2000, Zatoń, Marynowski 2006 and references therein). Investigations of the organic matter present in some carbonate concretions and clays (Zatoń, Marynowski 2004, 2006), concerned mainly depositional environment of sedimentary organic matter. Although clays and concretions differ from each other when the amount of total organic carbon (TOC) is taken into account, the molecular study of the concretions and clays show significant similarities between them (Zatoń, Marynowski 2004). Nevertheless, a detail study of the organic matter (OM) shows some molecular differences. Here we compare the extractable OM composition originated from carbonate concretions and surrounding clays, and demonstrate what differences are found, and what is their reason.

SAMPLES AND METHODS

In total, 19 samples, consisting of clays (11 samples), carbonate concretions and massive siderite levels (8 samples) were collected from the active clay-pits situated in the Polish Jura. The total organic carbon (TOC) content was determined using an automated LECO CR-12 analyser. Determination of the carbonate percentage was based on the acid method.

Extraction and separation. The clays were Soxhlet-extracted in pre-extracted thimbles with dichloromethane. Extracts were further separated using pre-washed TLC plates coated with silica gel (Merck, 20 x 20 x 0.25 cm and 10 x 20 x 0.25 cm) (more details in Zatoń, Marynowski 2004).

Methylation. The polar fraction was treated with BF_3/methanol (5 ml; 4 h) and extracted with dichloromethane.

GC-MS. The analyses were performed with the use of a Agilent 6890 Series Gas Chromatograph interfaced to a Agilent 5973Network Mass Selective Detector with Agilent 7683 Series Injector, Agilent Technologies (more details in Zatoń, Marynowski 2004).

[1] *University of Silesia, Faculty of Earth Sciences, ul. Będzińska 60, 41-200 Sosnowiec, Poland; marynows@wnoz.us.edu.pl*

RESULTS

Taking into account the bulk geochemical data, concretions contain much lower amounts of TOC than clays (Fig. 1 see TOC versus carbonates plot) due to dilution of the organic carbon by early diagenetic carbonates and also bacterial OM

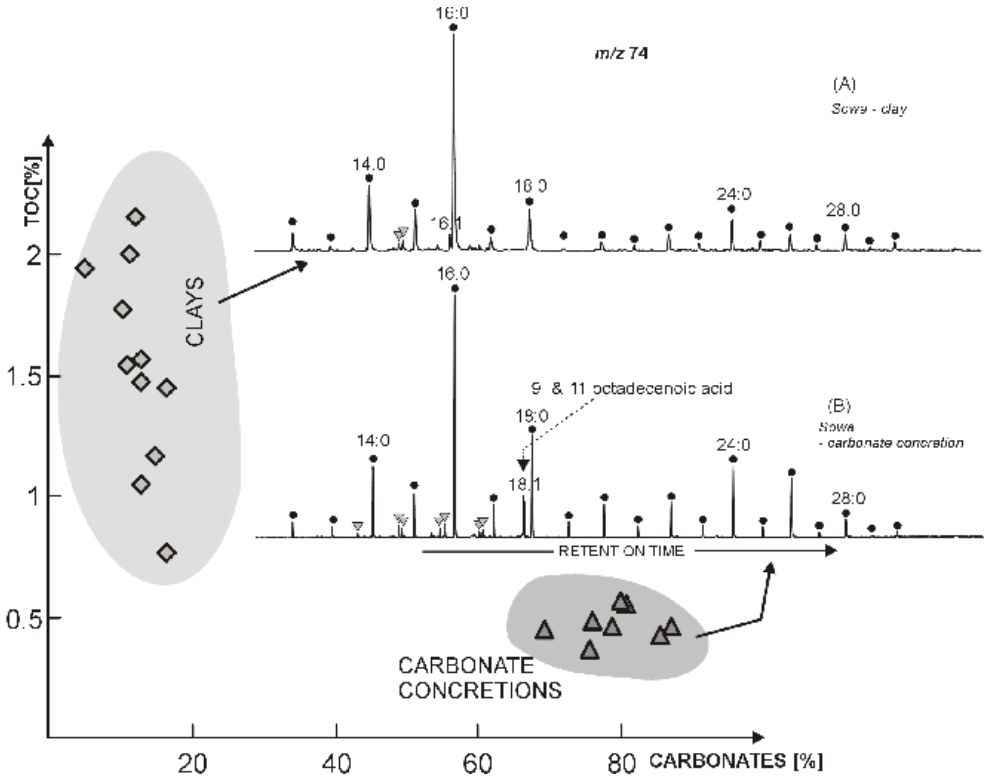

Fig. 1. Correlation diagram of total organic carbon (TOC) values vs. carbonate content values and mass chromatograms (*m/z* 74) showing distribution examples of fatty acids (as methyl esters) of the (A) clay and (B) carbonate concretion from the Polish Jura. Key: filled circles – *n*-alkanoic acids; filled triangles – iso- and anteiso-alkanoic acids.

degradation. Composition of OM trapped in carbonate concretions is similar to those of the parent clays (Zatoń & Marynowski 2004), but we observed some exceptions in the fatty acid distribution. The distribution of saturated fatty acids (peaks with dots – Fig. 1) in clays and concretions is similar with clearly marked bimodal character. Two maxima at *n*-C_{16} and *n*-C_{24} are present, and the first maximum clearly dominates (Fig. 1 – *m/z* 74). Such a composition may suggest a mixed origin for the fatty acids. Long-chain fatty acids with even over odd carbon number predominance are most probably derived from leaf epicuticular waxes of land plants, whereas the origin of short chain fatty acids may be more complex (terrestrial/marine). However, unsaturated fatty acids (UFA) are present in high relative concentrations only in concretions, whereas in clays they are present as traces only. UFA are represented by C18:1 fatty acids, occurring as isomeric

mixtures of 9-octadecenoic and 11-octadecenoic acids (Fig. 1B), and small concentrations of other low molecular weight UFA (triangles in Fig. 1, see also Kiriakoulakis et al. 2000). The presence of 10-methylhexadecanoic acid, which is derived from sulphate reducing bacteria and would indicate the formation of the concretion in the sulphate reduction zone (Kiriakoulakis et al. 2000), was not found. However, occurrence of the C18:1 fatty acids may be connected with sedimentary bacteria, which actively degraded OM, and sourced carbonates. Such processes may take place during methanogenesis and Fe/Mn reduction (see Wolff et al. 1991).

CONCLUSIONS

Although clays and concretions are characterised by similar molecular composition of many biomarkers from the extractable OM, significant differences were found in fatty acids distribution. Concretions contain unsaturated fatty acids which are represented by C18:1 fatty acids, occurring as isomeric mixtures of 9-octadecenoic and 11-octadecenoic acids and small concentrations of other low molecular weight unsaturated fatty acids. These compounds are practically absent in clays. Occurrence of the C18:1 fatty acids may be connected with sedimentary bacteria, which degraded OM, and sourced carbonates.

ACKNOWLEDGEMENTS: Research has been financed in part by University of Silesia grants: BW19/2005 and BW20/2006.

REFERENCES

KIRIAKOULAKIS K., MARSHALL J.D., WOLFF G.A., 2000: Biomarkers in a Lower Jurassic concretion from Dorset (UK). J. Geol. Soc., 157: 207-220.

MATYJA B.A., WIERZBOWSKI A., 2000: Ammonites and stratigraphy of the uppermost Bajocian and Lower Bathonian between Częstochowa and Wieluń Upland, Central Poland. Acta Geol. Polon., 50: 191-209.

WOLFF G.A., RUKIN N., MARSHALL J.D., 1992: Geochemistry of early diagenetic concretion from the Birchi Bed (L. Lias, W. Dorset, U.K.). Organic Geochem., 19: 431-444.

ZATOŃ M., MARYNOWSKI L., 2004: Konzentrat-Lagerstätte-type carbonate concretions from the uppermost Bajocian (Middle Jurassic) of the Częstochowa area, SC Poland. Geol. Quarterly, 46: 339-350.

ZATOŃ M., MARYNOWSKI L., 2006: Ammonite fauna from uppermost Bajocian (Middle Jurassic) calcitic concretions from the Polish Jura – biogeographical and taphonomical implications. Geobios, 39, (in press).

MINERALOGIA POLONICA - SPECIAL PAPERS
Volume 28 - 2006

Martina MESIARKINOVÁ[1], *Daniel OZDÍN*[1]

NEW OCCURRENCE OF SILICA WOODS IN NEOVOLCANIC ROCKS OF WESTERN SLOVAKIA

INTRODUCTION

Silicified woods occur in Western Carpathian territory, exactly in neovolcanic rock enviroment. More than 90 % neovolcanics of andezit type are situated in the middle and east of Slovakia. Less appearence of volcanic rocks were found along klippen belt. According to Kováč, Plašienka (2003) the following are classified as volcanism of Neogene age in Slovakia:

a) areal type of dacite up to rhyolite volcanism, Eggenburg age till Lower Badenian age
b) areal type of andesite volcanism, lower Badenian age till lower Pannonian age. Products this type cover biggest area of Slovakia (neovolcanics of middle Slovakia - etc. Poľana stratovolcano)
c) arch type of andesite volcanism, upper Badenian age till Sarmatian age. Products of this type occur along klippen belt (Horné Sŕnie, Piennin andesit line in Poland) and in Morava occuring also in flysch zone (Uherský Brod)
d) post-orogen alkaline basalts up to basanite volcanism, Pannonian age till Pleistocene age. These relative less appearent types of basalt volcanics are in region of Salgótarján, Fiľakovo, Zvolen and etc. (Kováč and Plašienka, 2003).

In this study we describe silicified woods in new area of western Slovakia in the Čachtické Malé Karpaty Mts.

METHODS

Silicified woods were studied microscopically using polarising microscope Jenapol Carl Zeiss, and detailed pictures were taken using camera Nikon Coolpix 4500. Samples were formed to thin sections and further analysed using powder X-ray diffractometer DRON-3 under following conditions: accelerating voltage 20 kV, current beam 40 mA, step 1°/min, cathoda Cu, filter Ni.

RESULTS

During geological research we have discovered silicified woods (Fig. 1), which we found in Čachtické Malé Karpaty Mts. in western of Slovakia. These woods occur in enviroment of neogene (Badenian-Sarmatian) sedimentary rocks. Macroscopically are central parts of this woods mostly coloured brown-black, turning light brown on the rim. Lighter rims of silicified woods are not formed from crust, but from less silicified woods. Degree of silicification is increasing to

[1] *Department of Mineralogy and Petrology, Faculty of Natural Sciences, Comenius University, Mlynská dolina, 84215 Bratislava, Slovak Republic; ozdin@fns.uniba.sk*

center of wood and can be observed by most intensive colour of wood. By means of microscopically research we studied on longitudinal (Fig. 2), cross and chamfer sections the structure of woods, mineral composition etc. According to particular results silicified woods are formed from trunks of pine (*Pinus*). Other species of trees were not identified. In polarized light silica wood consists mostly of α-quartz and particularly are cavities filled with microcrystalline variety of quartz chalcedony (fig. 2). The studied silicified woods did not contain any amorphous opal. X-ray patterns show that woods are formed only by α-quartz.

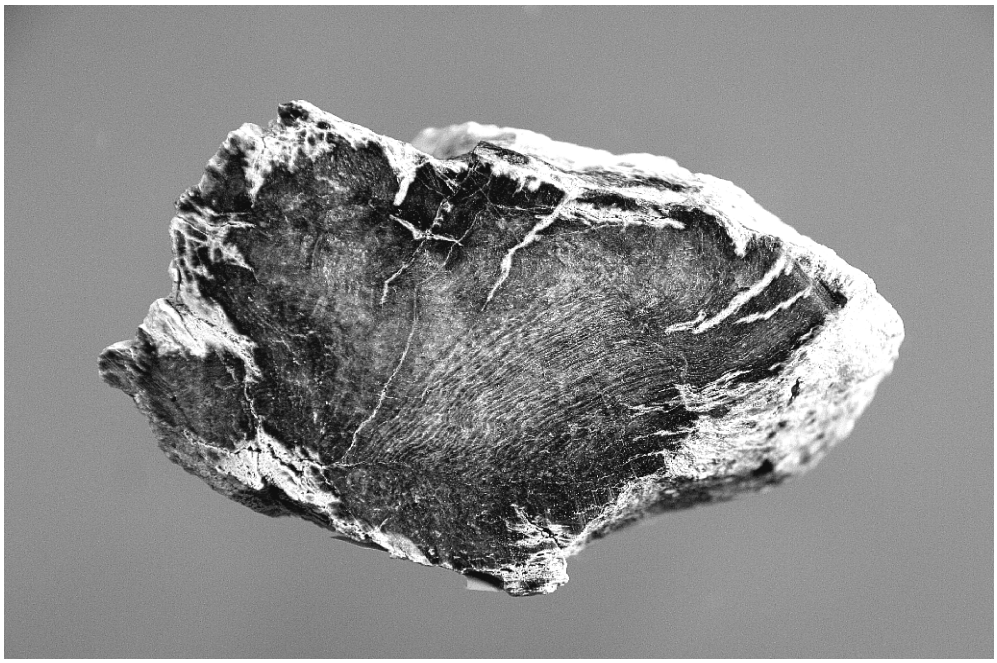

Fig. 1. Cross section of siliceous wood of pine (*Pinus*) with radius of 7 cm.

CONCLUSIONS

Due to terrain research we described new ocuurrence of silicified woods in Slovakia. This occurrence is in westernmost locality in the Western Carpathians. Silica woods are composed from α-quartz and its microscrystalline variety chalcedony. These woods did not stricken opalescence. After the preliminary study of structure silicified woods they are formed of pine (*Pinus*).

ACKNOWLEDGEMENT: We thank for dedication of specimens on the research by R. Janda from Častkovce and for consultancy and assistance when identifying the woods we thank to Doc. V. Sitár, PhD.

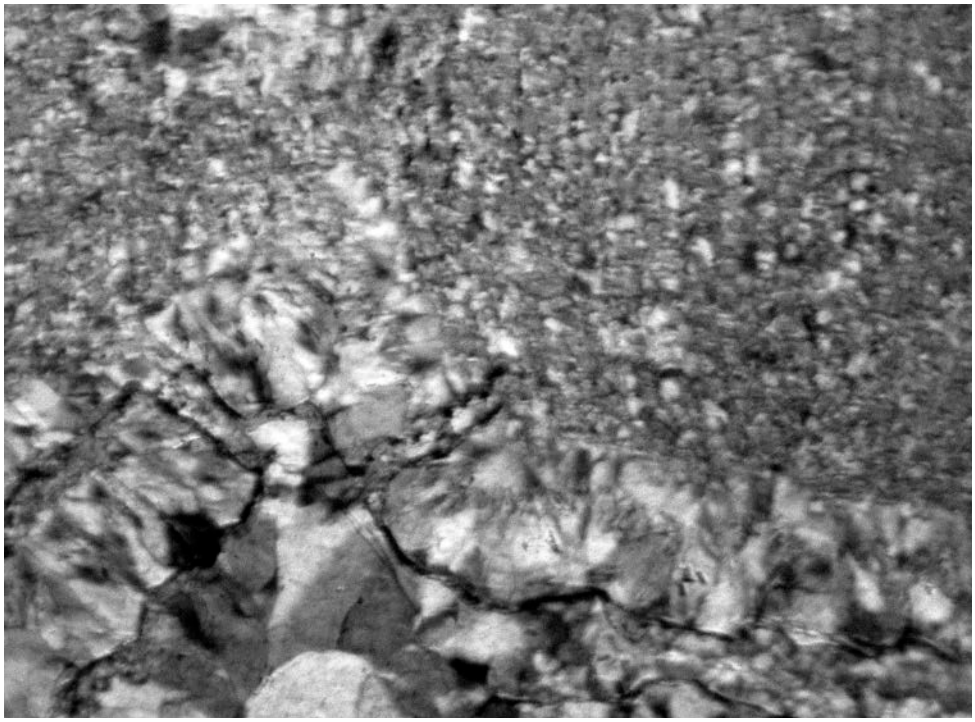

Fig. 2. Cross section of silica wood. 1 mm thick chalcedony vein filled cavity.

REFERENCES

KOVÁČ M., PLAŠIENKA D., 2003: Geological building of contact region of Alpine-Carpathian-Pannonian system and adjected slopes of Bohemian massif Comenius University, Bratislava, 1-58.

MINERALOGIA POLONICA - SPECIAL PAPERS
Volume 28 - 2006

Tomáš MIKUŠ[1], Ján SPIŠIAK[1], Milan SÝKORA[2]

CLINOPYROXENE PHENOCRYSTS OF THE CRETACEOUS ALKALI VOLCANIC ROCKS FROM THE CENTRAL WESTERN CARPATHIANS

INTRODUCTION

Clinopyroxene (Cpx) is widespread mineral in Cretaceous alkali volcanics in the Central Western Carpathians (CWC). Cpx phenocrysts were studied from Podmanín (Manín unit), Dobrá (Fatric superunit – Krížna nappe) and Štepnica (Czorstyn unit, Púchov-Jarmuta group) localities. Hyaloclastites and autometamorphosed basalts represent host rocks. Cpx chemical composition changes can be used for reconstruction of magma evolution.

METHODS

Cpx phenocrysts were handpicked from the crushed rocks and analyzed with a Cameca SX100 electron-microprobe at the ŠGÚDŠ Bratislava under the following conditions: 15 kV, 20 nA, beam diameter 2-5 μm, standards – albite, wollastonite, Al_2O_3, orthoclase, rhodonite, hematite, MgO, TiO_2, Ni, chromite. Fe^{3+} in clinopyroxenes was calculated according charge balance proposed by Ryburn et al. (1976).

RESULTS

The euhedral Cpx phenocrysts are up to 1.5 mm in size. Cpx phenocrysts from Štepnica and Dobrá correspond to diopside according classification of MORIMOTO, (1989) and are associated with Fe-Ti spinel and apatite. These Cpx phenocrysts (Štepnica and Dobrá) are usually oscillatory zoned (Fig.1). Zonation is caused by small differences in Al_2O_3 (e.g. 2.3-3.7 wt. %), TiO_2 (e.g. 1.2-1.7 wt. %), FeO and MgO content in the individual zones. Al^{VI}/Al^{IV} ratio is always less than 1 in this Cpx group.

Zoned Cpx phenocrysts rarely contain Fe-rich anhedral cores. The biggest differences are in chemical composition between cores and zoned rim in the TiO_2 and FeO content. Cores are richer in FeO (10.4 wt. %) and Na_2O (1.9 wt. %) content. Al^{VI}/Al^{IV} ratio is above 1. Zoned Cpx rim is richer in TiO_2 (2.1 wt. %) than Fe-rich cores. These cores represent an earlier Cpx phase, which could represent high-pressure phase originated probably in upper-mantle.

Several Cpx phenocrysts from the Dobrá contain lenticular Opx exsolutions (up to 10 μm in large). Cpx host have the highest Al_2O_3 content (6.7 wt. %) and the lowest FeO content (2.6 wt. %). Opx (enstatite) exsolutions contain up to 4.9 wt. % Al_2O_3 and 2 wt. % of CaO.

[1] *Geological Institute, Slovak Academy of Sciences, Severná 5, 974 01 Banská Bystrica, Slovak Republic; mikus@savbb.sk*
[2] *Faculty of Natural Sciences, Comenius University, Mlynská dolina, 842 15 Bratislava, Slovak Republic*

Tab. 1. Representative microprobe analyses of clinopyroxene.

locality	Štepnica			Dobrá	Podmanín	
type	Fe-rich cores	Ti-rich zoned cpx		Host of Opx exs	Cr-rich diopside	
analyses	11	16	25	29	3	12
SiO_2	52.80	48.58	49.85	49.29	54.55	52.40
TiO_2	0.39	1.69	1.03	1.04	0.05	0.19
Al_2O_3	2.81	3.57	2.31	6.29	0.91	5.02
Cr_2O_3	0.07	0.02	0.04	0.79	1.85	1.89
FeO	10.44	7.28	7.30	2.40	3.80	2.13
MnO	0.54	0.17	0.16	0.10	0.23	0.12
MgO	11.77	13.51	14.19	14.85	16.26	14.25
CaO	20.94	23.02	23.10	22.04	21.23	20.83
Na_2O	1.94	0.85	0.88	1.43	1.75	2.27
K_2O	0.01	0.02	0.00	0.01	0.02	0.00
Total	101.70	98.91	98.98	98.43	100.70	99.16

The last compositional group represents Cpx phenocrysts from Podmanín, which have the lowest TiO_2 (up to 0.8 wt. %) and Al_2O_3 (0.6-1.4 wt. %) content. They show the highest Cr_2O_3 (0.7-2.0 wt. %), Na_2O (up to 2 wt. %) contents and the highest Al^{VI}/Al^{IV} ratio (1.56-3.30).

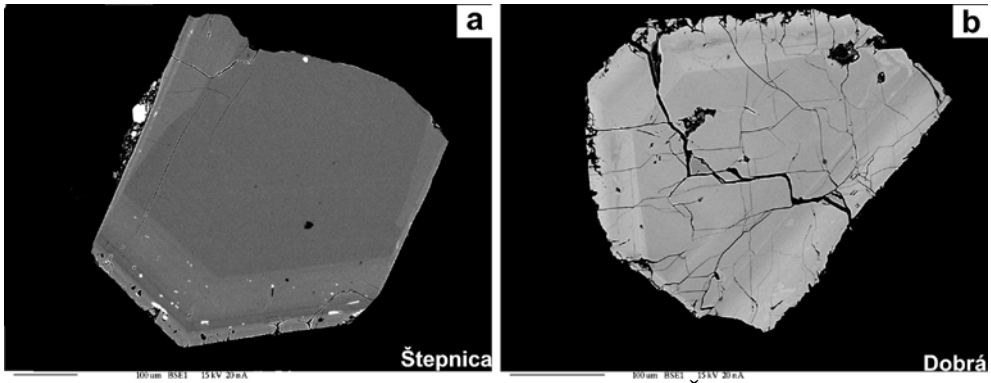

Fig.1a,b. Oscillatory zoned Cpx phenocrysts from the localities Štepnica (a) and Dobrá (b).

CONCLUSIONS

Essentially four types of Cpx phenocrysts can be distinguished according to their chemical composition: zoned Ti-rich diopsides with Fe-rich cores, Cr-rich diopside and diopsides with Opx exsolutions. Between above mentioned Cpx groups are the most important differences in compositional parameters such as Al^{VI}/Al^{IV} ratio, Na_2O and TiO_2 content. In general, high-pressure Cpx have higher Al^{VI}/Al^{IV} ratio (> 1) along with higher Fe/(Fe+Mg) ratio, higher Na_2O content and lower TiO_2 content. According to these criteria, high- and low-pressure Cpx phenocrysts can be distinguished (theoretical background is fully discussed in Dobosi, Horváth 1988). Cr-rich diopsides and Fe-rich cores belong to high-pressure Cpx phases, which crystallized probably in the upper mantle. Ti-rich zoned diopsides correspond to low-pressure Cpx, which could crystallize in the

magmatic reservoir in the Earth crust or during magma ascent. Very similar compositions of Cpx phenocrysts are known from alkali lamprophyres of the Velence and Buda Mts., Hungary (Dobosi, Horváth 1988).

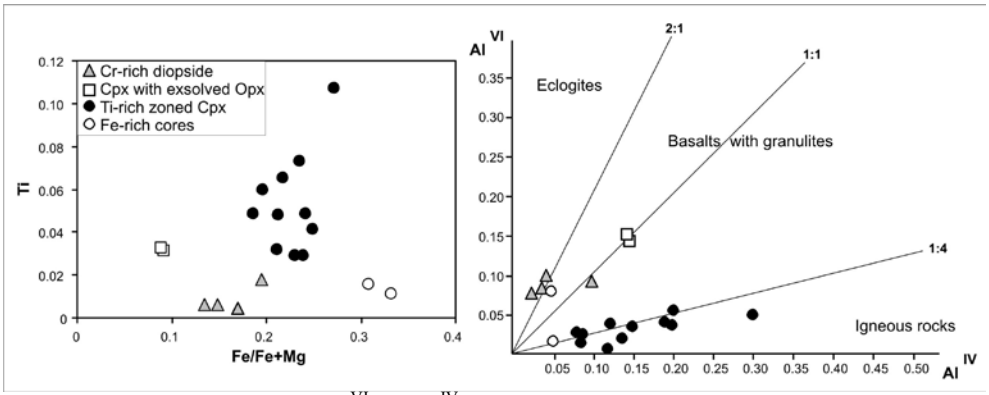

Fig.2. Ti vs. Fe/(Fe+Mg) and Al^{VI} vs. Al^{IV} in studied pyroxenes. Fields in diagram are from Aoki, Shiba (1973).

REFERENCES

AOKI K., SHIBA I., 1973: Pyroxene from lherzolites inclusions of Itinomegata, Japan. Lithos, 6: 41-51.

DOBOSI G., HORVÁTH I., 1988: High- and low pressure cognate clinopyroxenes from alkali lamprophyres of the Velence and Buda Mountains, Hungary. N. Jahrb. Miner. Abh., 158: 241-256.

MORIMOTO N., 1989: Nomenclature of pyroxenes. Subcommittee on pyroxenes. Commision on new minerals and mineral names. Can. Mineral., 27: 143-156.

RYBURN R.J., RAHEIM A., GREEN D.H., 1976: Determination of P, T paths of natural eclogites during metamorphism – record of subduction. A correction to a paper by Raheim and Green (1975). Lithos, 9: 161-164.

MINERALOGIA POLONICA - SPECIAL PAPERS
Volume 28 - 2006

Ihor M. NAUMKO[1]

FLUID INCLUSION RESEARCH IN GEMS FROM CHAMBER PEGMATITES OF THE UKRAINIAN SHIELD

INTRODUCTION

The gems such as topaz, beryl, jewellery quartz varieties are widespread within pegmatites of so called chamber type in the northwestern part of the Ukrainian Shield. The typical pegmatite bodies are characterized by nearfounded shape, great size and well-pronounced mineral and structural zonation (from margin to core): graphic, pegmatoid, block zones and chamber region that is underlain by leaching zone. Topaz and beryl are restricted there to mineral parageneses of chamber regions as well as leaching zones.

METHODS

We have investigated fluid inclusions in topaz and beryl from leaching zones with one's own hand using such research methods of knowledge about mineral forming fluids (Kalyuzhnyi 1982) as ontogeny observations, thermometric and cryometric studies, determination of volatile (by means of mass-spectrometry chemical techniques) and soluble components (based on examination of water extractions) as well as carbon isotope of CO_2 studies (by means of mass-spectrometry isotopic techniques). Depositional environment for these minerals in chamber regions was studied earlier (Voznyak 1971; Remeshilo 1971).

RESULTS

Topaz

Primary inclusions:

(1) liquid-gas ones that are "sticked" to quartz crystals with phase relations 40L (liquid) + 60G (gaseous); concentration consists 10 wt.% (equal to NaCl + KCl); $61.1CO_2 + 4.8N_2 + 4.1CH_4$ (vol. per cent); (2) complex carbon dioxide inclusions: (a) in growth pyramid {011}; 10–14L + 5–1L_1 (liquid carbon dioxide) + 85G; Th (homogenization temperature) CO_2 = 19–22 °C in G; $96.8CO_2 + 3.2\ CH_4$ (vol. %); (b) that formed during mutual pushing, growth and capturing of solid particles; 25–60L + 35–20L_1 + 40–20G.

Early-secondary inclusions:

(1) multiphase with solid mineral-daughter phases; 50L + 35G + 15B; Th = 430 °C in L; concentration higher than 40 wt. per cent (equal to NaCl); (2) syngenic gas-liquid with solid mineral-daughter phases and liquid-gas of heterogeneous origin; L + G + B (solid) with diverse L and 5–85B; Th = 380–410 °C in L and G.

[1] *Institute of Geology and Geochemistry of Combustible Minerals of National Academy of Sciences of Ukraine, Naukova St. 3a, 79053, Lviv, Ukraine; naumko@ukr.net*

Late-secondary inclusions:
(1) liquid-gas; 30L + 70G; Th = 395–400 °C in G; (2) essentially gaseous; (3) complex CO_2 inclusions; 8–10L + 12–10L_1 + 80G; Th CO_2 = 25.5–27 °C in G; Th = 260–300 °C in G; 66.4CO_2 + 33.6N_2 (vol. %).

Beryl

Primary inclusions: (1) essentially gaseous to liquid-gas elongated parallel to L_6, L up to 30 %; Th = 425 °C in G; (2) gas-liquid elongated across prism grain {1010}; 80–85L + 20–15G; Th = 275 °C in L.
Early-secondary inclusions: diverse-filled with mineral-daughter and -satellites; L+G+B with different B.
Late-secondary inclusions:
(1) essentially gaseous often with anisotropic mineral-satellites and liquid CO_2; 3–5L + 5–7L_1 + 90G; various B; (2) complex CO_2 inclusions; 10–13L_1 + 90–87G, Th CO_2 = 24–25 °C in G; 60L + 35L_1 + 5G, Th CO_2 = 19–20 °C in L.

The gems were mainly crystallized during the second acid period after inversion stage of pegmatite process within fully differentiated pegmatite bodies that were hardly affected by this period (Kalyuzhnyi et al., 1985). Temperature interval of the second period was the same, but the pH of mineral-forming fluids for topaz and beryl was very different determined by CO_2, F and alkaline relations. The existence of inclusions populations homogenized into various phases (liquid or vapour) at the same temperatures suggests heterogeneous state of mineral-forming medium. It was the natural hollowness walls related to crystal growth (chamber regions and leaching zones) where favorable conditions stored for the boiling both when the pressure sharply fell at walls breakthrough and as a result of different hollowness heating at the temperatures slightly lower than critical values. Due to heterogeneous subcritical fluid state the temperatures and pressures that are observed on the syngenic inclusions of heterogeneous origin correspond (or close) to the actual ones and suggest for general temperature decreasing (Kalyuzhnyi, Naumko 1986) during crystallization process from 600 °C (first acid period) to 180–200 °C (third acid period) and pressures from 30–40 MPa to 23–25 MPa respectively, in particularly range of 372–392 °C – 410–415 °C for conditional topaz crystals (Voznyak 1971) and of 373– 415 °C for beryl (Remeshilo 1971) in chamber regions and likely temperatures around 400 °C in leaching zones (Naumko 1986, 1999). Intensive albitization by the temperatures is contemporaneous to crystallization of topaz, beryl, phenakite, green fluorite-I and fractures in quartz filling (Naoumko, 1994). In the topaz water extractions Na^+, Cl^- and F^- predominate (calculated whole concentration of such the fluids is 58–60 wt. per cent). For the water extractions from beryl K^+ is more typical whereas fluorine acted as catalyser. Direct determined complex inclusions solutions pH values for topaz are of 4.3–5.6 (Kalyuzhnyi 1957; Voznyak 1971), for beryl of 7.2–8.5 (Kalyuzhnyi 1960). Volatile are characterized by such correlation as CO_2 : N_2 : CH_4 with CO_2 predominance in the chamber regions (topaz to 98.2, beryl to 88.5 vol. %) and CO_2 : CH_4 with increased CH_4 content in leaching zones (topaz – to 37.0, beryl – to 74.0 vol.%). Carbon of CO_2 from topaz inclusions is

enriched with light isotope ($\delta^{13}C$ = -18.7÷-19.4 ‰ PDB) as well as fluid inclusions in quartz (-19÷-15,-19.2÷-9.3,-17.3÷-12.5, -15.1÷-10.9 ‰ PDB) and carbon of carbonates (-15.7÷-9.8 ‰ (Naoumko 1994; Naumko 2002)).

CONCLUSIONS

The results shown the extra-ordinary significant role of leaching and recrystallization processes in the gem-holding parageneses (topaz, beryl) forming as heterogenization phenomenon, temperature change (Naumko 2002) and mixing abilities of fluids of different origin in mineral-forming medium (Kovalishin et al. 2000): fluids of depth (under crust) origin and fluids of granite melt.

REFERENCES

KALYUZHNYI V.A., 1957: On the results of the determination of pH of solutions of the liquid inclusions. Geochemistry, 1: 77-79 (in Russian).

KALYUZHNYI V.A., 1982: Principles of knowledge about mineral forming fluids. Kiev: Naukova dumka, 1-240 (in Russian).

KALYUZHNYI V.A., NAUMKO I.M., 1986: The topaz genesis in pegmatites of chamber type of the Ukraine. Morphology and phase equilibrium of minerals. Sofia. Proc. of Bulg. Acad of Sci.: 395-401 (in Russian).

KALYUZHNYI V.A., VOZNYAK D.K., NAUMKO I.M., 1985: The acid-alkaline periods of mineral formation and parageneses of minerals of pegmatites of miarolitic type of the Ukraine (according to data of fluid inclusion research). Geol. J., 45, 6: 55-60 (in Russian).

KOVALISHIN Z., KALYUZHNYI V., NAUMKO I., 2000: Physico-chemical state of mineral-forming fluid during crystallization of the Volhyn chamber pegmatites, Ukraine. Arch. Mineral. A Journ. of Geochemistry, Mineralogy and Petrology: *LIII*, 1-2: 133-136.

NAUMKO I. M., 1994: Granitic chamber-type pegmatites of Ukraine: new data on mineralogy, geochemistry and fluid inclusions IMA 16th General Meeting: Abst. Pisa: 296-297.

NAUMKO I., 1986: The conditions of formation of gems and rare metal mineralization in the granitic pegmatites of the Ukrainian shield (according to data of fluid inclusion research). Thesis for a Candidate's degree of Geol.-Mineral. Sciences. L′vov, 1-16 (in Russian).

NAUMKO I., 1999: Accessory beryl from leaching zones of topaz-morion pegmatites of the Volyn′. Mineral. Journ., 21, 5–6: 22–28 (in Ukrainian).

NAUMKO I., 2002: The new data on mineralogy, geochemistry and genesis of miarolitic type pegmatites of Ukraine. Mineral Coll., 51, 2: 58-68 (in Ukrainian).

REMESHILO B. G., 1971: On the liquid inclusions in accessory beryl of miarolitic pegmatites of the Ukraine. Mineral Coll., 25, 3: 262-264 (in Russian).

VOZNYAK D.K., 1971: The physico-chemical characteristics of mineral forming solution in period of formation of chambers of pegmatites of Volyn′ (on inclusions in minerals). PhD Thesis, Kiev, 1-26 (in Russian).

MINERALOGIA POLONICA - SPECIAL PAPERS
Volume 28 - 2006

Krzysztof NEJBERT[1], Elżbieta DUBIŃSKA[1], Paweł BYLINA[2]

ON THE OCCURRENCE OF Ta-Ca-Nb OXIDES IN ZOISITE-BEARING ROCKS FROM EASTERN PART OF SUDETIC OPHIOLITE (LOWER SILESIA, POLAND)

INTRODUCTION

The Jordanów-Gogołów Serpentinite Massif (JGSM) is the largest ultrabasic massif of the Sudetic Ophiolite (Fig. 1). JGSM consists of serpentinized mantle tectonites and ultramafic cumulate interpreted as highly dismembered ophiolite sequence (e.g., Majerowicz 1979; Dubińska, Gunia 1997). Dubińska and Szafranek (1990), Dubińska (1995) described numerous occurrences of leucocratic rocks (rodingites and other calc-silicate rocks) within JGSM ultrabasic rocks. The aim of this study is to present new data on the occurrence of the Ta-Ca-Nb phases in the mentioned above calc-silicate rocks.

Fig. 1. Simplified geological sketch of the studied area.
1. ultrabasic rocks (JGSM, ophiolitic sequence), 2. Ślęża gabbro (SG, ophiolitic sequence), 3. gneisses of Góry Sowie Block (GSB), 4. gneisses and schists of Niemcza Zone (NZ), 5. Strzegom-Sobótka granitic massif SG), 6. undifferentiated Variscan rocks, 7. occurrence of Nb-Ta minerals.

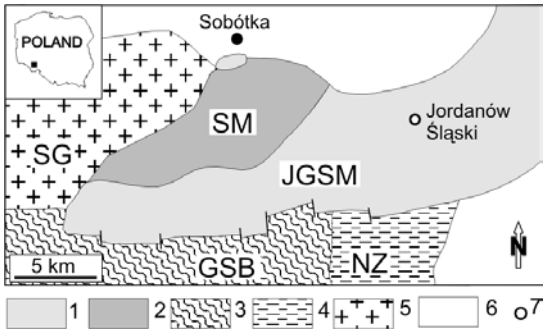

METHODS

Authors selected a few samples bearing Ta-Ca-Nb oxides from the collection comprising ca. 500 samples. The samples were investigated using conventional petrographic and XRD methods. Mineral chemical compositions were determined by electron microprobe (CAMECA SX100, Inter-Institute Analytical Complex for Minerals and Synthetic Substances, Warsaw University).

RESULTS

Ta-Ca-Nb minerals were found in so-called leucocratic zone at Jordanów Śląski quarry (Fig. 1). The leucocratic rocks form lenticular boudins within serpentinite, the boudins being typically surrounded by vermiculite-bearing schists formed at expense of trioctahedral mica (Dubińska, Wiewióra 1988); these rocks are

[1] *Institute of Geochemistry, Mineralogy and Petrology, Faculty of Geology, Warsaw University, al. Żwirki i Wigury 93, 02-089 Warsaw, Poland; knejbert@uw.edu.pl*
[2] *Institute of Geological Sciences, Polish Academy of Sciences, ul. Twarda 51/55, 00-818 Warsaw, Poland*

composed of quartz, albite, and adularia habit microcline (thin veins) as well as minor biotite (Fig, 2A). The leucocratic rock texture record several metamorphic events (see for details Dubińska, Szafranek 1990; Dubińska 1995).

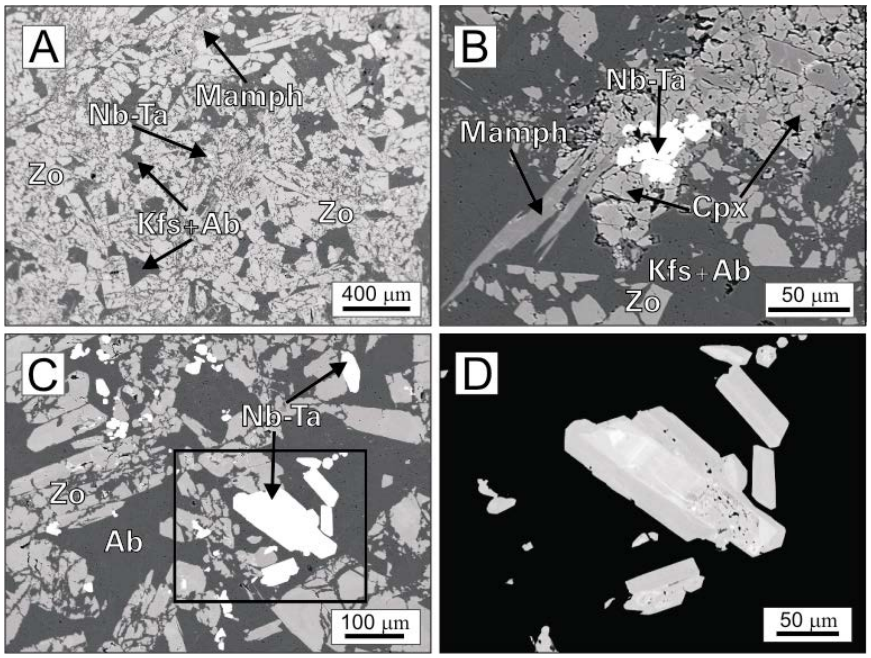

Fig. 2. BSE images of Ta-Ca-Nb oxides bearing leucocratic rocks from Jordanów Śląski. A) albite-zoisite rock, intergrown by tremolite with minor amount of Ta-Ca-Nb oxides (arrowed); B) aggregate Ta-Ca-Nb oxides in clinopyroxene xenolith, surrounded by matrix consisting of Na, K-feldspars, zoisite, overgrown by late tremolite; C) fragment of albite-zoisite rock containing Ta-Ca-Nb oxides, D) enlarged fragment (black rectangle at C) displaying inhomogeneity of Ta-Ca-Nb oxides; Ab – albite, Cpx – clinopyroxene, Kfs – potassium feldspar, Mamph – monoclinic amphibole (tremolite), Nb-Ta – Ta-Ca-Nb oxides, Zo - zoisite.

Ta-Ca-Nb oxides occur as small grains and euhedral crystals randomly distributed within the leucocratic rock (Fig. 2A and 2C). Moreover, they can be found in clinopyroxene xenoliths (Fig. 2B); the chemistry and habit of the clinopyroxene is close to diopsidic pyroxene from metarodingitic rocks from JGSM (e.g., Dubińska 1995). The chemical composition of the Ta-Ca-Nb oxides is close to fersmite (Ca, Ce)(Nb, Ta, Ti)$_2$O$_6$ (CaO: 15-17; Ta_2O_5: 1-6; Nb_2O_5: 75-82, TiO_2: 0.2-0.8, and Ce_2O_3: <0.2, all contents in weight %). The central parts of the inhomogeneous grains are Nb, Ta, Ce, and Y-rich (bright zones at BSE image, Fig. 2D), whereas outer zone is Nb-enriched as well as Ta, and Ce poorer as compared to core zone (dark zones at BSE image, Fig. 2D). Ta-Ca-Nb oxide bearing samples contain also allanite, REE-rich zircon, and Nb-Ta-rich titanite.

CONCLUSIONS

Our results are consistent with occurrence of Nb-Ta minerals in pegmatite (columbite described by Lis, Sylwestrzak 1981) and unidentified Nb-Ta oxide found in chlorite-vermiculite schists (Dubińska, Szafranek 1990), both from Jordanów Śląski quarry. The occurrence of Ta-Ca-Nb oxides in Jordanów Śląski probably records an impact of fluids genetically related to neighboring Variscan magmatism on the Sudetic ophiolite. This conclusion is supported by an appearance of Nb-Ta enriched minerals in SG massif (e.g. Janeczek 1996) as well as common findings of such minerals in granitic pegmatites (e.g. Černý 1991a, b; Ercit 2005).

ACKNOWLEDGEMENTS: This research was supported by UW IGMiP BW and ING PAS internal grants.

REFERENCES

ČERNÝ P., 1991a: Rare-element granitic pegmatites. Part I. Anatomy and internal evolution of pegmatite deposits. Ore Deposits Models, v. 2, Geosci. Canada Reprint Series, 6: 29-47.

ČERNÝ P., 1991b: Rare-element granitic pegmatites. Part II. Regional to global environments and petrogenesis. Ore Deposits Models, v. 2, Geosci. Canada Reprint Series, 6: 49-62.

DUBIŃSKA E., 1995: Rodingites of the eastern part of Jordanów-Gogołów serpentinite massif, Lower Silesia, Poland. Can. Mineral, 33: 585-608.

DUBIŃSKA E., GUNIA P., 1997: The Sudetic ophiolite: current view on its geodynamic model. Geol. Quart., 41: 1-20.

DUBIŃSKA E., SZAFRANEK D., 1990: On the origin of layer silicates from Jordanów (Lower Silesia, Poland). Arch. Min., 46: 19-36.

DUBIŃSKA E., WIEWIÓRA A., 1988: Layer silicates in the contact zone between granite and serpentinite, Jordanów, Lower Silesia, Poland. Clay Min., 23: 459-470.

ERCIT T.S., 2005: Identification and alteration trends of granitic-pegmatite-hosted (Y,REE,U,Th)-(Nb,Ta,Ti) oxide minerals: a statistical approach. Can. Mineral, 43: 1291-1303.

JANECZEK J., 1996: Nb-, Ta- and Sn-rich titanite and its alteration in pegmatites from Żółkiewka, Poland. N. Jb. Miner.Mh., 10: 459-469.

LIS J., SYLWESTRZAK H., 1981: Nowy zespół mineralny w leukokratycznej strefie Jordanowa k. Sobótki i jego znaczenie genetyczne. Przegl. Geol., 29: 67-71. (in Polish)

MAJEROWICZ A., 1979: The Mountain Group of Ślęża and recent petrological problems of the ophiolites, Selected Stratigraphical, Petrographical and Tectonic Problems of the Eastern Border of the gneisses of Sowie Góry Mts. and Kłodzko Metamorphic Structure. Materiały Konferencji Terenowej, Nowa Ruda, Wyd. Uniwersytetu Wrocławskiego, 9-34. (in Polish)

MINERALOGIA POLONICA - SPECIAL PAPERS
Volume 28 - 2006

Martin ONDREJKA[1], Pavel UHER[2], Jaroslav PRŠEK[1], Juraj LETKO[1], Daniel OZDÍN[1]

EVIDENCE FOR "CLINOANHYDRITE" SUBSTITUTION IN THE LREE*X*O_4 MONAZITE-TYPE STRUCTURE MINERALS

INTRODUCTION

An unique REE–Y–(Th)–P–As–(Si)–(Nb)–(S) accessory mineral assemblage was identified in a small body of Lower Triassic A-type rhyolite of the Silicicum Superunit near Tisovec - Rejkovo, Central Slovakia. Arsenian monazite-(Ce) to phosphatian gasparite-(Ce) and arsenian xenotime-(Y) to phosphatian chernovite-(Y) solid solutions in association with REE carbonates (bastnäsite, parisite, röntgenite?, synchysite) and rare cerianite-(Ce) form anhedral to subhedral grains and aggregates (≤0.3 mm), scattered in the groundmass or as intergrowths with zircon and Fe–Ti oxides (Ondrejka et al. 2006 in press).

METHODS

Electron–microprobe analyses were obtained at the Geological Survey of Slovak Republic, Bratislava, using a Cameca SX100 microprobe in a wavelength-dispersion mode. The analytical conditions were following: accelerating voltage 15 kV, beam current 15 or 20 nA, and beam diameter 1-4 μm. The following standards and spectral lines were used: barite (S Kα), apatite (P Kα), GaAs (As Lα), $LiNbO_3$ (Nb Lα), $LiTaO_3$ (Ta Mα), wollastonite (Si Kα, Ca Kα), ThO_2 (Th Mα), UO_2 (U Mβ), Al_2O_3 (Al Kα), YPO_4 (Y Lα), $LaPO_4$ (La Lα), $CePO_4$ (Ce Lα), $PrPO_4$ (Pr Lβ), $NdPO_4$ (Nd Lβ), $SmPO_4$ (Sm Lβ), $EuPO_4$ (Eu Lβ), $GdPO_4$ (Gd Lα), $TbPO_4$ (Tb Lα), $DyPO_4$ (Dy Lβ), $HoPO_4$ (Ho Lβ), $ErPO_4$ (Er Lβ), $TmPO_4$ (Tm Lα), $YbPO_4$ (Yb Lα), $LuPO_4$ (Lu Lβ), hematite (Fe Kα), rhodonite (Mn Kα), BaF_2 (F Kα) and NaCl (Cl Kα). Other elements such as Sr, V, and Pb were sought but not detected. The matrix effects were corrected by the conventional ZAF method.

RESULTS

Compositions show a wide AsP_{-1} anion group substitution in monazite–gasparite solid solutions; at. % As/(As+P) = 0.00 to 0.73, accompanied by minor $(SO_4)^{2-}$, $(SiO_4)^{4-}$, $(NbO_4)^{3-}$ substituting anion groups (Fig. 1).

The presence of sulfur in monazite-gasparite s.s. (up to 4.8 wt.% SO_3, ≤0.14 S apfu), together with analogous Ca enrichment, but not with analogous Th-rich compositions indicate "clinoanhydrite" substitution, $CaS(REE,Y)_{-1}(P,As)_{-1}$ (Fig.

[1] *Department of Mineralogy and Petrology, Faculty of Natural Sciences, Comenius University, Mlynská dolina G, 842 15 Bratislava, Slovak Republic; mondrejka@fns.uniba.sk*

[2] *Department of Mineral Deposits, Faculty of Natural Sciences, Comenius University, Mlynská dolina G, 842 15 Bratislava, Slovak Republic*

2), rather than the incorporation of brabantite, along the $CaTh(REE,Y)_{-2}$ exchange vector (Fig. 3).

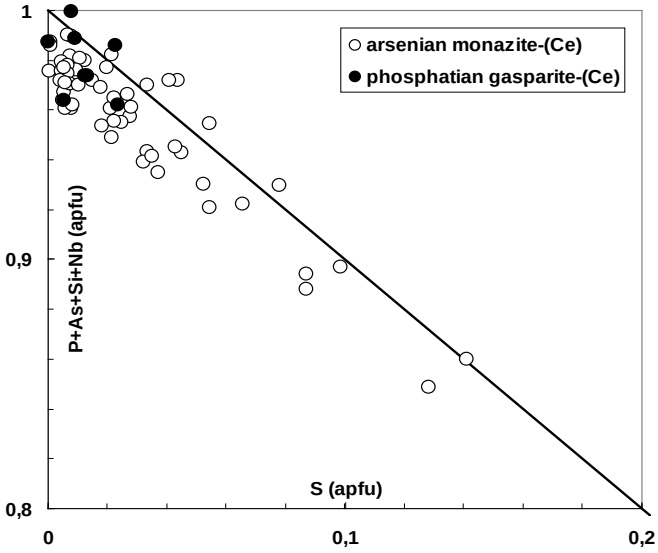

Fig. 1. Compositions of REE phosphates to arsenates from the Tisovec – Rejkovo rhyolite in S vs. P+As+Si+Nb substitution diagram. The straight line represents the ideal substitution ratio.

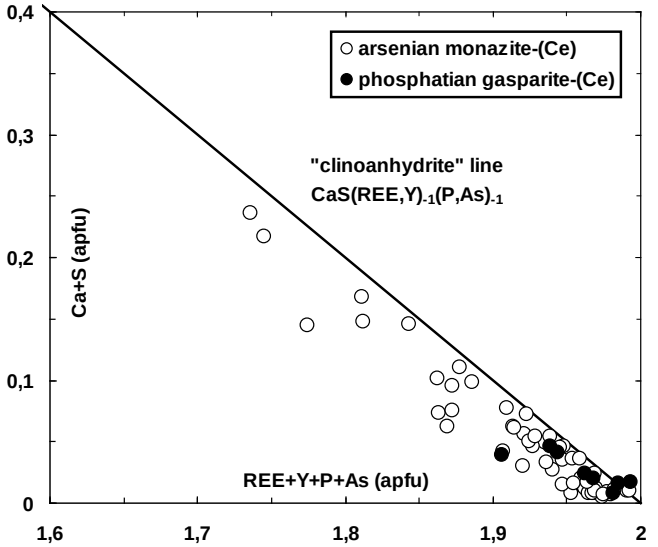

Fig. 2. Compositions of REE phosphates to arsenates from the Tisovec – Rejkovo rhyolite in Ca+S vs. REE+Y+P+As substitution diagram. The straight line represents the ideal "clinoanhydrite" $CaS(REE,Y)_{-1}(P,As)_{-1}$ substitution vector.

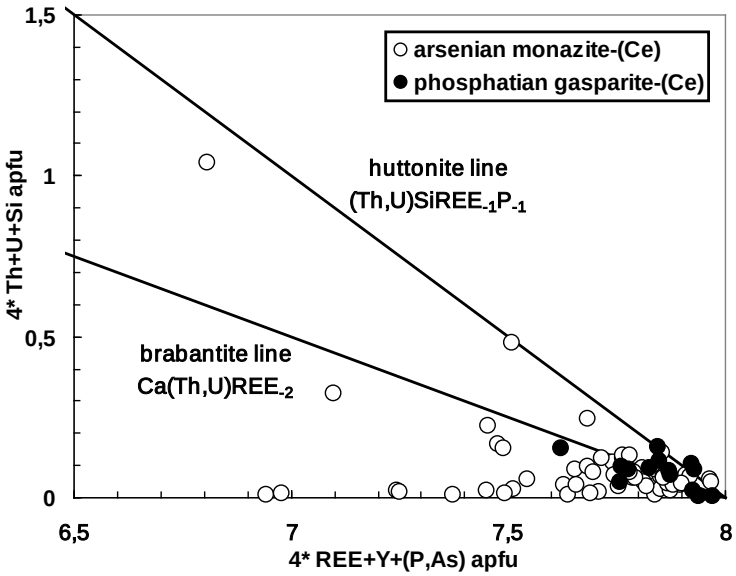

Fig. 3. Compositions of REE phosphates to arsenates from the Tisovec – Rejkovo rhyolite in Th+U+Si vs. REE+Y+(P,As) substitution diagram normalized to 4 apfu with ideal brabantite and huttonite substitution vectors (straight lines).

DISCUSSION AND CONCLUSION

The presence of the hypothetical "clinoanhydrite" $CaSO_4$ molecule in monazite-gasparite s.s. is supported by the existence of a monazite-type structure of $CaSO_4$ at high pressures and temperature (experiments up to 120 kbar and ca. 1000 °C; Crichton et al. 2005). However, the "clinoanhydrite" substitution is probably limited at the natural low-pressure conditions, analogous to the Tisovec – Rejkovo rhyolite formation (Ondrejka et al., 2006 in press).

Formation of As-rich monazite-(Ce) to gasparite-(Ce) with elevated Ca and S contents as well as associated xenotime-chernovite-(Y) and REE carbonates is connected with post-magmatic alteration of the primary magmatic monazite-(Ce) and xenotime-(Y) by As, S-rich fluids. The absence of As-bearing sulphides or arsenides (arsenopyrite, löllingite), and the presence of accessory strontian barite is probably a result of relatively high fO_2 during the post-magmatic alteration of the rhyolite.

REFERENCES

CRICHTON W.A., PARISE J.B., ANTAO S.M., GRZECHNIK A., 2005: Evidence for monazite-, barite-, and $AgMnO_4$ (distorted barite)-type structures of $CaSO_4$ at high pressure and temperature. Am. Mineral., 90: 22–27.

ONDREJKA M., UHER P., PRŠEK J., OZDÍN D., 2006: Arsenian monazite-(Ce) and xenotime-(Y), REE arsenates, carbonates from Tisovec-Rejkovo rhyolite, Western Carpathians, Slovakia: Composition and substitutions in the REEXO$_4$ system (X=P, As, Si, Nb, S). Lithos, in press.

MINERALOGIA POLONICA - SPECIAL PAPERS
Volume 28 - 2006

Monika ORVOŠOVÁ[1]

CAVE MINERALS OF THE NÍZKE TATRY MTS. (SLOVAKIA)

INTRODUCTION

The total amount of caves in the Nízke Tatry Mts. is 647 (cave database of Slovak Museum of Nature Protection and Speleology), from which 549 (85 %) belongs to the Demänovské vrchy. Karst region with authigenic cave minerals in the northern part of the Nízke Tatry Mts. is mostly built by Triassic guttenstein limestones and dolomites, thrusted on the Tatric granitoides. Therefore the total prevalence of the mineral occurrences is connected with the variable lithology, they provide the suitable conditions for generation and development of more mineral groups or various crystal forms than it is common in karst rocks.

This article shows that many other components are released into karstic solutions, which can form unusual secondary minerals on the suitable places. Minerals presented in this paper have already been described in details in several speleological papers, which are out of attention of mineralogists and they not appear in summary mineral register of Slovakia.

ARAGONITE - $CaCO_3$ Aragonite coexists with calcite in many speleothem of Starý hrad Cave, Záskočie Cave and Demänová Cave of Liberty (Cílek, Šmejkal 1986). Aragonite forms frostwork or acicular needlelike crystals (3 mm in diameter) which cover cave walls and a part of speleothems.

CALCITE - $CaCO_3$ Large calcite crystals of two crystal forms which have been reported from Silvošova Diera and Nová Stanišovská caves in Ohnište karst massif (Hochmuth, Holubek 1996, Orvošová 1999). Both represent the products of hydrothermal activity before younger vadose speleogenesis (Orvošová et al. 2004, Orvošová 2005). *Prismatic-scalenohedral calcites* have typical prismatic-scalenohedral shape created by combination of dominant hexagonal prism (10-10) and flat scalenohedron.The maximum leng of the doubly terminated and partly translucent ochre-coloured crystals is 10 cm. Detached crystals were found in allochthonous clastic fill of a sump. *Scalenohedral calcites* are partly translucent, grey or yellow, 10 –20 cm in size, and exhibit scalenohedral habit with dominant first-order (21$\underline{3}$1) scalenohedron. Crystals partly or completly fill small dissolution cavities, up to several decimeters in diameter Both are the unique finds of perfectly developed calcite crystals in Slovakia and are protected minerals because of its dimension.

CARBONATE-HYDROXYLAPATITE - $Ca_5(PO_4,CO_3)_3(OH)$ The mineral most usually forms as light-brown to dark-brown coating or crust on the cave walls and

[1] *Slovak Museum of Nature Protection and Speleology, Školská 4, 031 01 Liptovský Mikuláš, Slovak Republic; orvosova@smopaj.sk*

ceilings. These coatings usually are smooth and shiny. They were found as glaze flowstone and less small stalaktites of carbonate-hydroxylapatite which cover mostly cave walls and less sinter deposits at the Záskočie Cave (Cílek 1984), the Starý hrad Cave (Cílek, Šmejkal 1986) and the Slnečný lúč Cave (Orvošová 2005). Phosphate occurences have a small surface extent (about some square centimeters), 1 – 20 mm thick The source of phosphates is not connected with bat guano but with Triassic limestones (Cílek, Šmejkal 1986).

CERUSSITE - $PbCO_3$. This mineral has been found as tiny veinlets with hemimorphite and remnants of sulphide ore minerals in limonitized infilling at fault zone of the Zlomiská Cave. Small amounts of secondary mineral originate in oxidation of galena. Details of its occurence are described lower.

GYPSUM - $CaSO_4 \cdot 2H_2O$ is described from the Javorová Abyss (Mitter 1989), Demänovská Cave of Peace (Pavlarčík 1986), Repiská Cave (Cílek 2000) and Nová Stanišovská Cave (Orvošová 2005). Gypsum occures as crusts, fibrous speleothems and cave flowers usually colorless and white. *Granular crusts* are composed of equant, curved or tabular crystals a few mm long. They are covering the cave walls, ceilings and floor sediments; occur over many square meters of cave sparkling passages. *Fibrous gypsum* is composed of crystal fiber aggregates and forms cave cotton, masses of intergrown, fibrous of very finegrained or needle-like flexible crystals less than 0,1 mm in diameter and up to a centimeter or so in length. Gypsum cottonball, about 4 cm in diameter, occurs on the floor sediments. *Gypsum flowers* consist of an aggregate of branching and curving parallel growth prismatic or fibrous crystals packed together. White sparkling flowers are about 3 cm long.

HEMIMORFITE - $Zn_3Si_2O_7(OH)_2 \cdot H_2O$ Mineral has been found as tiny veinlets with cerussite in limonitized crust with remnants of sulphide ore minerals (pyrite, sphalerite and galena) in fault zone of the Zlomiská Cave. Hemimorphite forms fan-like aggregates of grey-white crystals, up to 3 mm long, and is a product of hypergene alteration of sphalerite-bearing sulphide-rich assemblange. Polymetallic sulphides probably together with Fe karbonates were a part of polymethallic mineralization which has regional character in the Nízke Tatry Mts.(Ozdín et al. 2001).

HEXAHYDRITE - $MgSO_4 \cdot 6H_2O$ Hexahydrite associated with starkeyite forms 80 – 95 % of sulphur flowers mass, occur as white fibrous salt crystals about 1 cm long, and are product of epsomite dehydration. Hexahydrite is not known as a karst mineral in Slovakia (Cílek 2000).

STARKEYITE - $MgSO_4 \cdot 4H_2O$ Starkeyit is the second essential mineral of sulphur flowers which intergrows hexahydrite. Gradual dehydration forms starkeyite and hexahydrite pseudomorphs after epsomite. Starkeyite is first karst occurences in the world (Cílek 2000).

SYNGENITE - $K_2Ca(SO)_4 \cdot 2H_2O$ White sulpho-salt is associated with other secondary sulphide minerals (gypsum, hexahydrite, starkeyite). Syngenite sulphur flowers also called „earthy aggregates“ crystallize on hexahydrite crystals, and cover the dolomite

breccia of the shelter Repiská Cave (Cílek 2000). It occurs as elongated star crystal agregates whose size is about 20 microns and presents 5 – 10 % of unit sulphur mass. Syngenite has not been described yet in Slovakia.

CONCLUSION

Research of cave minerals gives a new view at weathering proceses in which appear characteristic types of paragenesis connecting with releasing other components into karst solutions common in limestones.

ACKNOWLEDGEMENTS: The financial support, obtained from Slovak Grant Agency for Science (VEGA No. 1/3057/06), is gratefully, acknowledged.

REFERENCES

CÍLEK V., 1984: Some minerals from Czechoslovak caves. Československý kras, 35: 85. (in Czech).

CÍLEK V., ŠMEJKAL V., 1986: Aragonite origin of caves, the study of stable isotopes. Československý kras, 37: 7-13. (in Slovak).

CÍLEK V., 2000: „Arid“ magnesium sulphates from the Repiská in the Demänová valley. Aragonit, 5: 6-8. (in Slovak).

MITTER P., 1989: Gypsum in the Javorova Abyss. Spravodajca SSS, 20, 2: 46. (in Slovak).

PAVLARČÍK S., 1986: Gypsum in the Demänovska Cave of Piece. Slovenský kras, 24: 193-195. (in Slovak).

ORVOŠOVÁ M., 1999: Allochthonous sediments of the caves in the Nízke Tatry Mts. Open File Report SMOPaJ, Liptovský Mikuláš, 1-32. (in Slovak).

ORVOŠOVÁ M., HURAI V., KLAUS S., WIEGEROVÁ V., 2004: Fluid inclusion and stable isotopic evidence for early hydrothermal karstification in vadose caves of the Nízke Tatry Mts. Geol. Carpath. 55, 5: 421-429.

ORVOŠOVÁ M., 2005: Interesting cave minerals in Demänovske vrchy Mts., Liptovský Mikuláš, Sinter, 12: 12-15. (in Slovak)

OZDIN D., UHER P., SLIVA Ľ., ORVOŠOVÁ M., FEJDI P., ŠAMAJOVÁ E., 2001: Hemimorfite $Zn_3Si_2O_7(OH)_2 \cdot H_2O$ from the Zlomiská Cave in Nízke Tatry Mts. Miner. Slov., 33: 61-64. (in Slovak).

VOTOUPAL S., HOLUBEK P., 1996: A new speleological locality at the Ohnište – the Silvošova Diera cave., Spravodaj SSS1, 39-41. (in Slovak).

MINERALOGIA POLONICA - SPECIAL PAPERS
Volume 28 - 2006

Elemér PÁL-MOLNÁR[1], Tibor JÁNOSI[1], Krisztián FORRAI[2]

A NEW MINERALOGICAL ARCHIVATION METHOD

INTRODUCTION

The main goal of the new mineralogical archivation method is to compile the digital archive of the Koch Sándor Mineral Collection, which is located at the Department of Mineralogy, Geochemistry and Petrology, University of Szeged. The archive would be managed by an up-to-date software, handling 2D and 3D photographs and databases on the characteristics of minerals. As an early outcome of the project we have already set up a software, which goes well beyond the execution of ordinary database commands, and ensures the technical background for various educational, demonstrational and promotional projects (Pál-Molnár**,** Kóbor 2000; Pál-Molnár**,** Jánosi 2005, 2006).

METHODS

Preliminary work has started with the planning of the general setup of the system. As a first step a Systematic Mineralogy Database was constructed on the basis of the mineral-database of the IMA (International Mineralogical Association). According to IMA standards, our database (mindat.org, webmineral.com) contains the name, taxonomy, formula, elementary composition, physical characteristics, and photographs of the minerals. Further sub-databases were also added to the software in order to enhance the primary, systematic framework. These are: the digital Koch Sándor Mineral Database, the archive of Hungarian mineralogical publications, and the most important places of occurrences within the Carpathian Basin, supplemented with maps. The basis of the software, i.e. the Systematic Mineralogy Database, also provides a didactic guideline for the user to digest the presented knowledge. The digital Koch Sándor Mineral Database includes images of all the 6000 minerals of the collection, and 3D rotating images of some of the most outstanding pieces, which are exhibited at the department in glass-cases. With a simple search one can gather those publications of the previous decades, which write about, or mention the chosen mineral. Further important information can be gained/ gathered by checking the places of occurrence and accessibility on maps covering the whole Carpathian Basin. Besides all these, the software can also provide a historical review on the life and work of famous scientists dealing with mineral collection.

[1] *Department of Mineralogy, Geochemistry and Petrology, University of Szeged, P.O. Box 651, H-6701 Szeged, Hungary; palm@geo.u-szeged.hu*
[2] *Department of Mathematics, Eötvös Lóránd University, H-1117 Budapest Pázmány Péter sétány 1/C, Hungary*

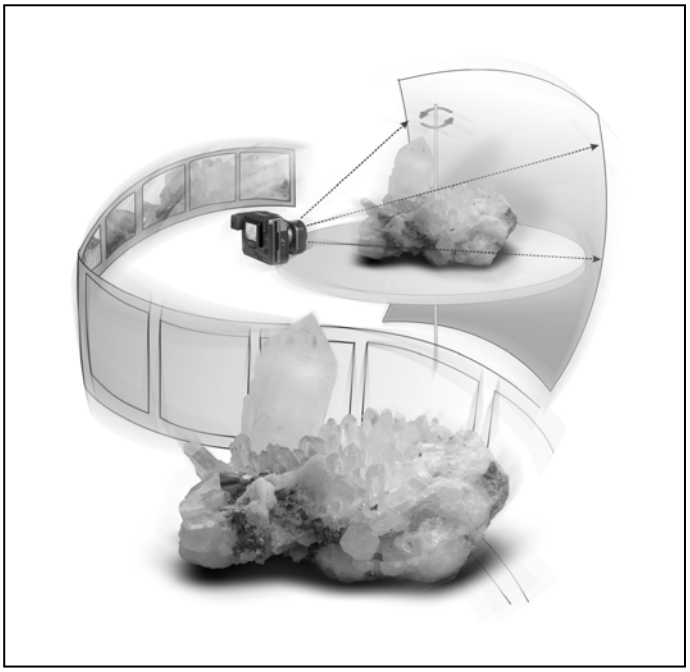

Fig. 1. Photographs were taken in the Koch Sándor Mineralogical Collection in front of a homogeneous background at the light of four 100 W lamps with adjustable filters. From the high resolution raw images each mineral was cropped and shaded aesthetically. No adjustments were made concerning the shape and colour of the minerals. 3D images are the results of special panoramic photographs. Minerals were put on a turntable and photographs with a nearly 30% overlap were taken of the rotating objects, pictures were then mosaiced and transformed into a cylindrical projection. The image created this way can be rotated, which provides a spectacular, realistic 3D view of the mineral.

CONCLUSIONS

In all we have produced software called Lapidator which is ready to be applied by people of any age, both with a professional or non-professional background and either for research or simply for studying the wonders of minerals.

REFERENCES

PÁL-MOLNÁR E., KÓBOR B., 2000: University of Szeged, the "Sándor Koch Mineral Collection". Acta Mineral. Petrogr. Suppl. Szeged, 41: 84.

PÁL-MOLNÁR E., JÁNOSI T., 2005: A Szegedi Tudományegyetem Ásványtani, Geokémiai és Kőzettani Tanszék "Koch Sándor ásványgyűjteményének" digitális feldolgozása. VII. Székelyföldi Geológus Találkozó, Csíkszereda, 47-48.

PÁL-MOLNÁR E., JÁNOSI T., 2006: The Lapidator Project, Department of Mineralogy, Geochemistry And Petrology, University of Szeged. Acta Mineral. Petrogr. Abstract Series Szeged, 5: 89.

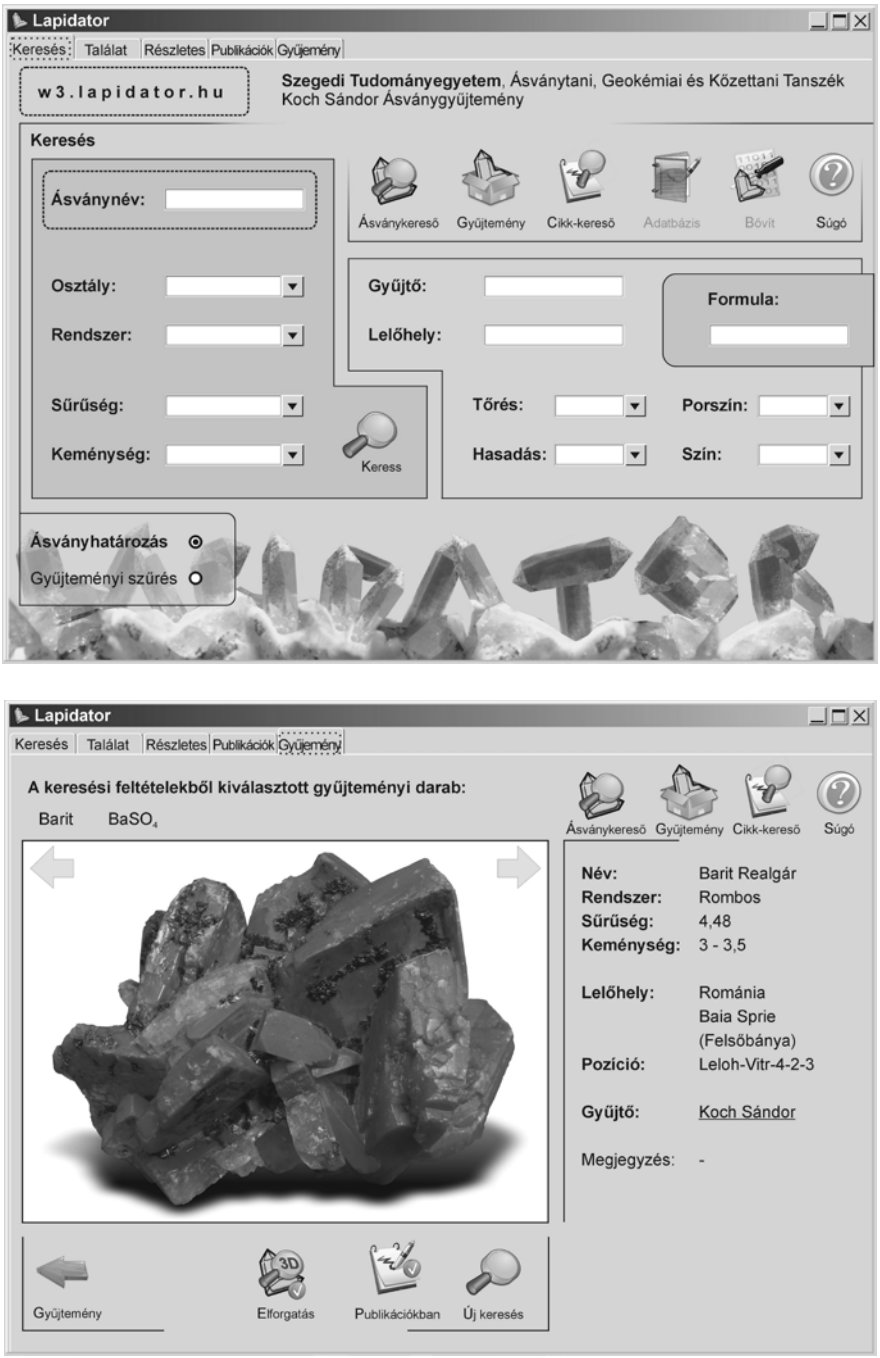

Fig. 2. Some picture about the screen of the software.

MINERALOGIA POLONICA - SPECIAL PAPERS
Volume 28 - 2006

Maciej PAWLIKOWSKI[1], *Jakub BAZARNIK*[1]

RESULTS OF THE MINERALOGICAL INVESTIGATION OF THE POTTERY FROM PITTEN (AUSTRIA)

INTRODUCTION

Pottery artefacts are significant because of their priority in the reflecting of the skills of an ancient man. Therefore the study of the archaeological pottery helps to understand better the earliest tradition and culture, technologies of production. Similarity of pottery present at various sites is an indicator of ruts of transport i.e. contacts between human groups.

The fragments of pottery were founded in Pitten – Austria. The pieces of pottery were discovered during technical works at private land. Graves from Bronze Age with rich furnishings were found as well as Slavic grave fields form the early 9th century were documented. Pitten was a main town of a county form 11th to 17th century. There was also some evidence of ore deposits mining since 1607.

METHODS

The thin-section of a pottery was obtained by cutting and polishing of fragments of pottery up to thickness 0.02 mm. Material prepared was subjected to examination under the polarizing light microscope Nicon 120. A slice of the thin-scetion was taken from standarized place i.e. from the wall of the vessel belly.

Observed phenomenons were documented with microphotographs.

The research comprised planimetric and granulometric analyses of the fabric. In each case about 1000 grains were counted for determination of mineral composition and 1000 grains for determination of grain size composition. The countings as well as generally methods of analyzes were standard. Results of investigations were stated in percentage.

All obtained datas were collected using POTTERY computer programme created by M.SC Adam Gaweł at AGH University of Science and Technology – Krakow. Moreover POTTERY computer programe was used for determination of similarity of tested pottery. All 35 features of each fragment collected in the tables were compared with the same features of the rest of analized samples. Obtained data of comparison were given as the percents of similarity wher 100 % means identity. All similarities above 60% were printed at separate chapter: Results of the comparative analysis of obtained data with the use of POTTERY computer programme.

RESULTS

Computer analyses of similarity of tested fragments of pottery were performed for all i.e. macroscopic and microscopic features of tested pottery.

[1] *University of Science and Technology, Department of Mineralogy, Petrography and Geochemistry, al. Mickiewicza 30, 30-059 Krakow, Poland; jbazarnik@poczta.fm*

Only similarities of tested ceramic masses above 45 % were collected in the list. This limit is determined as confirming real similarity of tested parameters.

Results of computer tests of similarity are collected in the lists (Tab. 1). The symbol of analized sample i.e. sample compared to all other samples is present at the right side of the list. It has for example no: compared sample => A-Pit-p1. At the left side are collected no. of samples compared to standard sample. It has for example no.: A-Pit-P5. Samples are collected starting from the highest percents of similarity to the lowest one. Between both datas is collected list of similarity of tested features marked for example as: LCZ = 61 %. Samples absent in the list show similarity of their features to features of other samples less than 45 %.

Mineralogical investigation (Fig. 1-4.) showed that tested pottery is generally produced of similar ceramic mass. Samples 1, 2, 4, 5, 6 are done using clay deposited as secondary products of weathering of metamorphic rocks. These primary metamorphic rocks are represented at the area by phyllites and granites composed mainly of flakes of micas. Muscovite is dominating mica present in clay. Flakes of this mineral are altered and contain colouring brown-redish iron oxides. Thermally changed clay minerals and micas create major part of ceramic mass. Together with these minerals are observed grains of metamorphic quartz and fragments of metamorphic rocks. These rocks under microscope are seen as rounded grains of microgranites, metamorphic schists and quartzites of metamorphozed quartz. Ocassionally small fragments of older pottery, charcoal (black opaque grains), rare heavy minerals and grains of feldpsars are observed. These compositions of ceramic mass confirm that raw material for production of tested pottery was obtained at the region of presence of metamorphic rocks.

Sample No. 4 is slightly different (Tab. 1.). Ceramic mass of this pottery contains highest amount of clay minerals where flakes of muscovite are also present. The colour of this pottery (after firing) is not as brown as in ealier described samples. This is because of lower amount of iron oxides in this mass or atmosphere of firing is not enough oxidated. Pottery is the only one containing admixture of fragments of older pottery.

Generally tested pottery was fired at temperature about 800 °C. Atmosphere of firing was oxidated (Cultrone et al. 2001). On internal wall of pottery one can see relicts of organic substance primary present in the vessel.

Production technology of pottery, high temperatures of firing as well as glassy coating of the vessel surface suggest that tested pottery is young, most probably not older than XVIII-XIX century. This suggestion have to be confirmed by archaeologist specialized in young pottery (see also Ghegari et al. 2006).

The datas obtained from POTTERY programme confirmed that most of samples is composed of similar raw material. Only sample no A-Pit-P3 has different mineral and grain composition.

REFERENCES

CULTRONE G., RODRIGUEZ-NAVARRO C., SEBASTIAN E., CAZALLA O., DE LA TORRE M. J., 2001: Carbonate and silicate phase reactions during ceramic firing. Eur. J. Mineral., 13: 621-634.

MINERALOGIA POLONICA - SPECIAL PAPERS
Volume 28 - 2006

GHERGARI L., LAZAR C., IONESCU C., 2006: Mineralogical and petrographic characteristics of the XVIIth century ceramic ware found in the Oradea fortress (Romania). Acta Mineral. Petrogr., Abstr. Ser., Szeged, 5: 31.

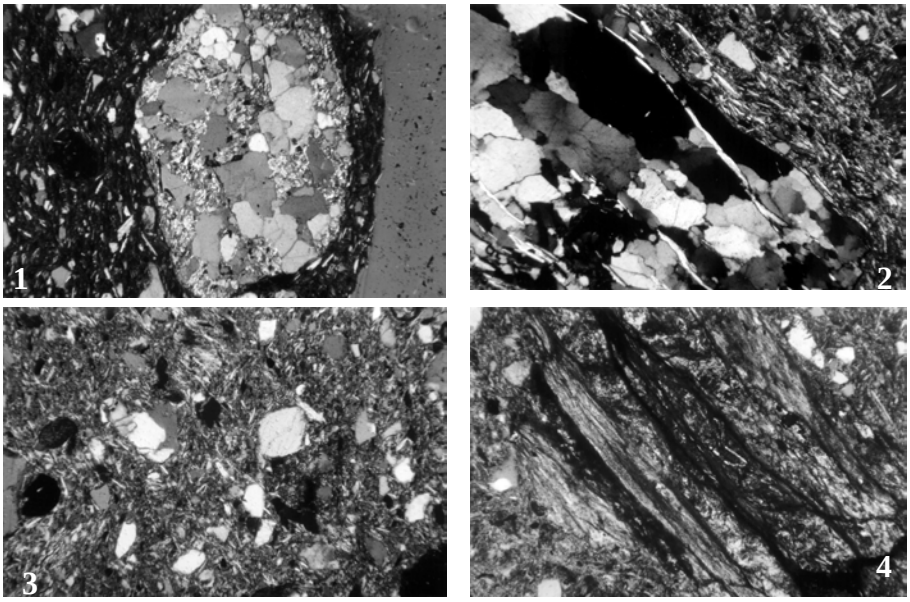

Fig. 1. Sample A-Pit-P1. Microscopic picture of ceramic mass near of external surface vessel. One can see rounded fragment of micaceous sandstone. Phot. 2. Sample A-Pit-P2. Contact of grain of gnais with cay thermally changed mass. Phot. 3. Sample A-Pit-P3. General microscopic picture of ceramic mass of the vessel. Phot. 4. Sample A-Pit-P4. Microscopic picture of relatively big fragment of metamorfhic shist present at thermally changed ceramic mass. (Polarizing light microscope, Polaroides X, magnification 45x.)

Table 1.

compared sample => A-Pit-P1		**compared sample => A-Pit-P5**	
A-Pit-P5	LCZ = 61 %	A-Pit-P1	LCZ = 61 %
A-Pit-P6	LCZ = 58 %	A-Pit-P6	LCZ = 61 %
A-Pit-P4	LCZ = 58 %	A-Pit-P3	LCZ = 58 %
A-Pit-P2	LCZ = 52 %	A-Pit-P4	LCZ = 55 %
A-Pit-P3	LCZ = 48 %	A-Pit-P2	LCZ = 52 %
compared sample => A-Pit-P2		**compared sample => A-Pit-P6**	
A-Pit-P6	LCZ = 61 %	A-Pit-P2	LCZ = 61 %
A-Pit-P3	LCZ = 55 %	A-Pit-P5	LCZ = 61 %
A-Pit-P4	LCZ = 55 %	A-Pit-P1	LCZ = 58 %
A-Pit-P1	LCZ = 52 %	A-Pit-P4	LCZ = 58 %
A-Pit-P5	LCZ = 52 %	A-Pit-P3	LCZ = 52 %
compared sample => A-Pit-P3		**compared sample => A-Pit-P4**	
A-Pit-P5	LCZ = 58 %	A-Pit-P1	LCZ = 58 %
A-Pit-P2	LCZ = 55 %	A-Pit-P6	LCZ = 58 %
A-Pit-P6	LCZ = 52 %	A-Pit-P2	LCZ = 55 %
A-Pit-P1	LCZ = 48 %	A-Pit-P5	LCZ = 55 %
A-Pit-P4	LCZ = 45 %	A-Pit-P3	LCZ = 45 %

MINERALOGIA POLONICA - SPECIAL PAPERS
Volume 28 - 2006

Adam PIECZKA[1], Bożena GOŁĘBIOWSKA[1], Jan PARAFINIUK[2]

THE STANNITE-GROUP MINERALS FROM RĘDZINY (LOWER SILESIA, POLAND)

INTRODUCTION

The Rędziny village is located in the middle part of the Rudawy Janowickie Range, within the eastern envelope of the Karkonosze granite intrusion known for occurrences of small ore deposits (Kowary, Czarnów, Wieściszowice, Miedzianka-Ciechanowice). About 1.5 km to W there is a large quarry emplaced in a dolostone lens, being only about 200 m away from the granite outcrops. Amphibolites, mylonites and mica schists of the Kowary-Czarnów Unit surrounding the lens contain a dispersed ore mineralization composed of arsenopyrite, cassiterite, base-metal sulphides, many rare minerals belonging to Cu(Ag)-Pb-Bi(Sb)-sulphosalts, Bi-sulphotellurides, Bi-sulphoselenides (Pieczka et al. 2004, 2005), and also an extensive assemblage of hypergenic minerals (Gołębiowska 2003).

METHODS

Chemical compositions of the ore minerals were analysed at the Inter-Institute Analytical Complex for Minerals and Synthetic Substances of the Warsaw University with a Cameca SX100 electron microprobe operating in the WDS mode under the following conditions: excitation voltage 15 kV, beam current 20 nA, peak count-time 20 s, background time10 s.

RESULTS AND DISCUSSION

At Rędziny, the stannite-group minerals have been found within:

- the sphalerite–ferrokesterite–Zn-enriched chalcopyrite assemblage occurring in fragments of quartz–chlorite–arsenopyrite veins;
- aggregates of Ag-bearing galena, as inclusions of kesterite and černỳite coexisting with Ag-bearing tetrahedrite and chalcopyrite;
- a schist belt cross-cutting the dolostone lens, as dispersed grains of stannite, stannoidite, mawsonite and unknown Sn-bearing sulphides coexisting with cassiterite, chalcopyrite, bornite, malayaite and an unknown $CuFeSn(OH)_8$ phase.

The sphalerite–ferrokesterite–chalcopyrite assemblage

This paragenetic assemblage was encountered in fragments of the quartz-arsenopyrite-chlorite veins containing dark brownish sphalerite accompanied by chalcopyrite, galena and Cu(Ag)-Pb-Bi(Sb)-sulphosalts. In the grains of sphalerite, both chalcopyrite and ferrokesterite usually occur as bleb inclusions. Only

[1] *Department of Mineralogy, Petrography and Geochemistry, AGH University of Science and Technology, al. Mickiewicza 30, 30-059 Kraków, Poland; pieczka@uci.agh.edu.pl*

[2] *Institute of Geochemistry, Mineralogy and Petrology, University of Warsaw, Żwirki i Wigury 93, 02-089 Warszawa, Poland*

exceptionally were observed large euhedral crystals of ferrokesterite reaching 250-300 μm, more commonly disseminated blebs or „clouds" of very fine drop-like inclusions with sizes of single micrometers and smaller. All the three coexisting phases are not homogeneous. Ferrokesterite shows compositions with an almost constant content of Sn (26.4 to 26.9 wt. %), only slightly varying Cu (27.8-29.1 wt. %), Cd (0.2-0.8 wt. %) and Zn (4.1-5.4 wt. %), and the most variable Fe (11.5-8.1 wt. %). In traces, it contains Se (about 0.1 wt. %), In (0.10-0.15 wt. %), whereas Ag is almost absent. The Zn/(Fe+Zn) ratio varying between 0.24 and 0.35 allows to classify this stannite as ferrokesterite. The host Sn-free sphalerite usually contains 58.9-60.5 wt. % Zn, 6.3-5.0 wt. % Fe, 1.3-1.6 wt.% Cd as well as traces of Mn (0.1-0.2 wt. %) and Cu (up to 0.1 wt. %). However, even within the sphalerite without visible exsolutions of stannite and chalcopyrite, Sn-free and Sn-rich zones have been observed. The latter contain up to 3.2 wt. % Sn, 3.3 wt. % Cu and 5.6 wt. % Fe, and their Sn/Cu ratio is close to 1:2, typical of stannite. The molar composition of the ferrokesterite: 88-63 mol. % Cu_2FeSnS_4, 6-34 mol. % Cu_2ZnSnS_4, 6-3 mol. % (Zn,Cd,Cu,Sn)S, and also the presence of Zn in chalcopyrite from blebs (up to 1.5 wt. %) suggest that all these phases are products of exsolution from a high-temperature (Zn,Cd,Cu,Fe,Sn)-sulphide broken down on cooling into Zn-enriched stannite (ferrokesterite), Zn-enriched chalcopyrite, and (Fe,Cd,Cu,Sn)-enriched sphalerite. The formation conditions of the assemblage were estimated at 320-290 °C and $\log f(S_2) \approx -9.5 \pm 0.5$ (Pieczka et al. 2004).

The kesterite–černỳite– tetrahedrite–chalcopyrite–Ag-bearing galena assemblage

Within aggregates of Ag-bearing galena (0.3-0.8 wt. % Ag), the stannite-group minerals are rare and occur as very fine inclusions, only sometimes exceeding 10 μm across. Usually they are associated with Ag-bearing tetrahedrite (10.7-2.6 wt.% Ag) overgrowing stannite, whereas chalcopyrite is exceptionally rare. Representative compositions of these stannite-group members are following: 12.2 wt. % Zn, 1.7 wt. % Fe and only 0.2 wt. % Cd for kesterite; 11.8 wt. % Cd, 3.5 wt. % Fe and 3.0 wt. % Zn for černỳite; 10.0 wt. %. Fe, 2.0 wt. % Zn and 1.8 wt. % Cd for (Zn,Cd)-bearing stannite.

The cassiterite–tin-bearing sulphides–chalcopyrite–bornite assemblage

The assemblage has been encountered within the schist belt cross-cutting the dolostone lens. In the western part, small rare inclusions of stannite coexist with chalcopyrite, cubanite, pavonite, gustavite, gold, pyrite, bismuthinite, tetradymite, arsenopyrite and pyrrhotite relics. In the eastern part, tin sulphides commonly represented by stannite, stannoidite, mawsonite and some unknown Sn-bearing phases coexist with chalcopyrite and Ag-enriched bornite (up to 0.5 wt. % Ag), and numerous inclusions of acanthite, matildite, pavonite, Ag,Bi-bearing tetrahedrite (up to 12.5 wt. % Ag and 16.0 wt. % Bi), Ag-bearing wittichenite (up to 1.3 wt. % Ag), Ag-bearing galena (up to 1.1 wt. % Ag), bismuthinite and native Bi, mostly 20 μm in size. The most common chalcopyrite forms partly altered grains up to 2-3 mm across, whereas grains of the tin sulphides are commonly smaller and attain mostly 0.2-0.3 mm in size. In such aggregates of Sn-sulphides, cassiterite very often forms a core, around which crystallized stannite, stannoidite and mawsonite. These sulphides very often form also thin rims around the grains of chalcopyrite, or

myrmeckite exsolutions within them. The compositions of stannite, stannoidite and mawsonite are commonly close to the stoichiometric formulas, except for some stannoidite crystals in which the content of Zn increases from typical 0.1-0.6 wt. % to almost 3.0 wt. %. In contrast, Ag concentrates in some grains of Zn-poor stannite (up to 0.8 wt. %), stannoidite (up to 2.0 wt. %) and mawsonite (up to 1.3 wt. %).

Beside the tin sulphides disscussed above, two important cases of their occurrences were noted. The first is a grain composed of Sn sulphides overgrowing a cassiterite core. An internal sulphide zone being in contact with the core is not homogeneous and contains, in relation to stannoidite, elevated amount of Sn, ranging from 20 to 25 wt. %, but too low for stannite. These compositions fit neither stannoidite, nor stannite, chatkalite or even volfsonite. However, in the triangle (Fe,Mn,Zn,Cg)–(Sn,In)–(Cu,Ag) they plot next to chatkalite and probably represent relics of an earlier, metastable, Sn-bearing, chatkalite-like sulphide phase.

Finding of some fine (up to 0.2 mm in size), poorly zoned grains of Sn-bearing sulphides with unknown compositions was a surprise. The cores of the grains usually correspond to $Cu_4Fe_3SnS_8$, to the rims the amounts of Cu increase and of Fe decrease according to the $2Cu^{+}(Fe^{2+})_{-1}$ and $Cu^{+}Cu^{2+}(Fe^{3+})_{-1}$ substitutions, and in the outermost zone were observed compositions close to $Cu_{10}SnS_8$. Both end-members can be connected with mawsonite by a reaction $3Cu_6Fe_2SnS_8 = 2Cu_4Fe_3SnS_8 + Cu_{10}SnS_8$, and could have been products of its destabilization. In the system (Cu,Ag)–(Fe,Mn,Zn,Cd)–(Sn,In), the Cu content within the $Cu_4Fe_3SnS_8$–$Cu_{10}SnS_8$ series changes between 50-61 and 72-89 at. %, whereas the Fe contents between 38-28 and 18-1 at. %, respectively. Compositions corresponding to mawsonite or close to it were not observed in the grains. The intervals of the Cu, Fe and Sn content correspond well to two subseries: $Cu_4Fe_3SnS_8$–$Cu_{16}Fe_7Sn_3S_{24}$ and $Cu_{20}Fe_5Sn_3S_{24}$ –$Cu_{10}SnS_8$.

ACKNOWLEDGEMENTS: These studies were supported by the AGH - University of Science and Technology grant no. 11.11.140.158 and the Ministry of Education and Science grant no. 5 T12B 043 24.

REFERENCES

GOŁĘBIOWSKA B., 2003: Okruszcowanie w złożu dolomitu „Rędziny" ze szczególnym uwzględnieniem minerałów strefy hipergenicznej. Ph.D. thesis, AGH - University of Science and Technology, unpublished, 1-249. (in Polish)

PIECZKA A., GOŁĘBIOWSKA B., PARAFINIUK J., 2004: Sphalerite-chalcopyrite-stannite assemblage from a mineralization zone in Rędziny and its significance in ore-genesis explanation. Pol. Tow. Mineral. Prace Spec., 24: 315-318.

PIECZKA A., GOŁĘBIOWSKA B., PARAFINIUK J., 2005: Formation conditions of sulphide mineralization in the Rędziny area (West Sudetes, Poland). Pol. Tow. Mineral. Prace Spec., 25: 167-171.

MINERALOGIA POLONICA - SPECIAL PAPERS
Volume 28 - 2006

Adam Pieczka[1]

AN UNUSUAL MANGANOAN APATITE FROM THE SZKLARY PEGMATITE (LOWER SILESIA, POLAND)

INTRODUCTION

Manganoan apatite is a typical component of many granitic pegmatites. As the apatite richest in Mn is considered fluorapatite from the Cross Lake granitic pegmatite #22, with the MnO content attaining 18.6 wt. % (Černý et al. 1998). In Poland, Mn-bearing apatite coexisting with beusite is known from a pegmatite occurring within serpentinites of the Szklary massif, but the mineral has not been studied in details. Recently completed electron microprobe studies of various phosphats from the pegmatite have shown that this apatite with the composition corresponding to $Mn_3Ca_2(PO_4)_3(Cl,F,OH)$ is much more enriched in Mn than that from Cross Lake.

GEOLOGICAL SETTING

The Szklary massif is situated about 60 km to S of Wrocław, in the southern part of the Early-Carboniferous Niemcza shear zone that extends along the eastern edge of the Góry Sowie Mountains block in the northeastern part of the Bohemian Massif (Central Sudetes and the Fore-Sudetic Block, southwestern Poland). It represents one of several small bodies of serpentinized ultrabasic and basic rocks rimming the Góry Sowie Mountains gneissic complex, considered parts of the tectonically fragmented ophiolite suite, about 420 Ma old (Oliver et al. 1993). The Szkłary massif is composed of weakly serpentinized harzburgites, lherzolites and pyroxenites containing enclaves of amphibolites and, in the middle part, of rodingites. In its northern and middle parts, the serpentinites are cut by numerous aplite veins and, less common, veins of lamprophyre. The pegmatite is subordinate; only a single dike has been known for over a hundred years in one of the open pits of the abandoned mine of silicate nickel ores in the northern part of the massif.

DESCRIPTION OF THE PEGMATITE

The pegmatite represents a poorly zoned dike, up to 1 m thick, composed of the two feldspars, quartz, micas and tourmaline. Saccharoidal aplite abuts the dike from NW, whereas amphibolite is in contact to SE. The wall zone consists of graphic intergrowths of plagioclase (Ab-Ol) and quartz, with small accumulations of altered biotite and less common clinochlore. Toward the middle of the dike, plagioclase is gradually replaced by microcline perthite, and there is a gradation into the coarsely-crystalline intermediate zone with accumulations of more common muscovite and black tourmaline. Both feldspars are enriched in phosphorus (0.57 and 0.53 wt. % P_2O_5, respectively). The amount of Rb in K-

[1] *Department of Mineralogy, Petrography and Geochemistry, AGH - University of Science and Technology, al. Mickiewicza 30, 30-059 Kraków, Poland; pieczka@uci.agh.edu.pl*

feldspars varies between 0.13 and 0.19 wt. %, and the K/Rb ratio changes from about 90 to 60. The tourmaline crystals from the wall zone are enriched in Mg, whereas those from the intermediate zone in Fe and slightly in Mn, but both represent Fe^{3+}-bearing, Li-free transitional members of the schörl-dravite series. Many rare minerals like spessartine, chrysoberyl, manganocolumbite-manganotantalite, fersmite, stibiocolumbite-stibiotantalite, various pyrochlore-group minerals (pyrochlore, microlite and betafite enriched in Sb, Pb, Bi and U), holtite, Hf-enriched zircon, Dy-bearing xenotime, uraninite, paradocrasite and stibarsen (inclusions within zircon crystals), Mn-rich beusite, Mn-rich apatite and also Mn-bearing oxides can be found within the pegmatite.

RESULTS

The earliest generation of manganoan **fluorapatite** is represented by dark green to almost black euhedral crystals, 2-3 cm long, and less commonly by small, black to brownish nest-like aggregates, 1-2 mm in size. Both the crystals and the aggregates are not homogeneous. Their matrix reveals compositional patchy zones or a network of thin veinlets formed by a younger apatite. Within the matrix of the crystals as well as within the veinlets are often present tiny inclusions of (Ba,Ca,Bi)-enriched Mn-bearing oxides (romanéchite, ranciéite, and an unknown, Bi-enriched phase).

The apatite matrix is strongly enriched in Mn. It usually contains about 16.0-16.5 wt. % MnO (1.17-1.21 Mn *apfu*), 0.7-0.8 wt. % FeO (0.05-0.06 Fe *apfu*), and traces of Mg (0.05-0.09 wt. % MgO) and Bi (up to 0.12 wt.% Bi_2O_3). In the dark-tingled aggregate, Mn concentrates reaching 19.3 wt. % MnO (1.43 Mn *apfu*), i.e. more than in fluorapatite from the Cross Like pegmatite. The content of F sometimes exceeds 3 wt. %, whereas the Cl content changes from amounts lower than the detection level in the WDS mode (~0.02 wt. %) to 0.X wt. %.

The younger generations of fluorapatite show progressive decreasing of Mn, with MnO contents varying from about 12.5-11.7 wt. % in the greenish fluorapatite and the brownish portions of the aggregate, to about 8.5-7.5 wt. % in the brownish, and from 5.0 to about 1.5 wt. % MnO in the bluish and white portions. In relation to the earliest fluorapatite, the younger generations of the apatite are reduced in Fe (usually below 0.1 wt. % FeO), and contain 2.9-2.4 wt. % F and 0.3-0.8 wt. % Cl. The compositions of the younger apatite normalized in relation to twelve oxygen atoms and one (F,Cl,OH) per formula unit, display the Σ*Me*/P ratio exceeding the ideal value 5:3 and indicating depletion of phosphorus as a result of the presence of carbonte ion identified in their IR spectra.

Manganoan **chlorapatite** is less frequent than fluorapatite, but is usually extremely enriched in Mn. The apatite with the highest Mn content has been found close to beusite in the form of few homogeneous relics (around 100 μm in size) of a greater crystal divided by alteration proccesses into separated grains surrounded by a mixture of secondary Mn-oxides. Additionally, chlorapatite-oxide aggregates intergrown with K-feldspar have also been encountered.

The chlorapatite occuring close to beusite contains 31.5 wt. % MnO (2.43 Mn *apfu*) and 3.1 wt. % FeO (0.23 Fe *apfu*) as mean values giving the Mn/(Mn+Fe)

ratio about 0.91. The content of Cl (2.89 wt. %, 0.48 *apfu*) exceeds that of F (1.11 wt. %, 0.32 *apfu*). Chlorapatite from the dark brownish aggregates is composed of a matrix with a relatively low MnO content of 12.3 wt. % (0.91 Mn *apfu*) and FeO of 0.25 wt.% (0.02 Fe *apfu*), and small relics, about 10 μm in size, after an earlier apatite crystal. Within the relics the content of MnO is high (21.0-25.5 wt. %, 1.58-1.94 Mn *apfu*), whereas FeO is only subordinate (0.7-0.9 wt. %, 0.05-0.07 Fe *apfu*). The Mn/(Mn+Fe) ratios in the relics and the matrix (0.97-0.98) are higher than that in the chlorapatite coexisting with beusite (0.91). The amounts of Cl are slightly higher in the relics (2.6-3.3 wt. %, 0.40-0.51 *apfu*) than in the matrix (2.5 wt. %, 0.37 *apfu*), whereas the F contents range between 0.6 and 1.2 wt. % (0.16-0.35 *apfu*). The youngest chlorapatite forming the white aggregate coexisting with Mn-bearing oxide is enriched in Na_2O (0.6 wt. %), Cl (3.1 wt. %) and CO_2 (up to 1.0 wt. %), poor in Mn and Fe (0.1 wt. % or less), and F (only 0.2 wt. %).

CONCLUSIONS

The chlorapatite from the Szklary pegmatite containing up to 35 wt. % MnO is currently the apatite richest in Mn worldwide, with the composition close to $Mn_3Ca_2(PO_4)_2(Cl,F,OH)$. Similarly, in the dark-tingled aggregate of fluorapatite from the pegmatite Mn concentrates, reaching 19.3 wt. % MnO, the content also higher than that determined at the Canadian fluorapatite. The reasons of such atypically high enrichment in Mn are following:

- an initial extraction of Mn from melts into F-bearing fluids,
- a decrease of F and Fe activities due to crystallization of tourmaline and fluorapatite that enabled Mn/Fe fractionation, and favoured the subsequent crystallization of beusite,
- a liberation of the hydrous phase, fractionation of Cl over F, and further extraction of Mn by later, Cl-enriched solutions,
- a dissolution of metastable beusite resulted from an aggressive action of late Cl-bearing hydrothermal fluids increasing concentration of Mn in the solutions.

ACKNOWLEDGEMENTS: These studies were supported by the Ministry of Education and Science grant No. 5 T12B 043 24 and the AGH - University of Science and Technology grant No. 11.11.140.158.

REFERENCES

ČERNÝ P., SELWAY J.B., ERCIT T.S., ANDERSON A.J., ANDERSON S.D., 1998: Graftonite – beusite in granitic pegmatites of the Superior Province: a study in contrast. Can. Mineral., 36: 367-376.

OLIVER G.J.H., CORFU F., KROGH T.E., 1993: U-Pb ages from SW Poland: evidence for a Caledonian suture zone between Baltica and Gondwana. J. Geol. of London, 150: 355-369.

MINERALOGIA POLONICA - SPECIAL PAPERS
Volume 28 - 2006

Jakub PLÁŠIL[1], Jiří SEJKORA[2], Radek ŠKODA[3], Viktor GOLIÁŠ[1]

SUPERGENE Y, REE MINERALS FROM THE MEDVĚDÍN DEPOSIT, THE KRKONOŠE (GIANT) MTS., CZECH REPUBLIC

INTRODUCTION

The Medvědín deposit (also known as Horní Mísečky) is situated approximately 3 km to the west from Špindlerův Mlýn in the Krkonoše (Giant) Mts. (Czech Republic)**.** The deposit was discovered by surface gamma survey in 1953. It was opened by three adits. Over 25 t of uranium was worked-out there during 1953-1959. The Medvědín deposit is the largest uranium deposit of the Czech part of the Krkonoše-Jizera crystalline complex. It is situated close to exocontact of the Krkonoše-Jizera granite pluton. Host rocks are metapelites of the Velká Úpa group, contactly metamorphosed onto cordieritic and andalusitic hornfels. Uranium mineralization is related to the tectonic structures (veins) of NW direction, SW dip with 2-20 cm thickness. Majority of the ore mineralization was connected with veins M3, M4, M5, M11, M12 and especially M18. Three generation of quartz and tectonic clay are predominant in the vein composition (Veselý 1982). Uranium supergene minerals with uraninite relics are the main ore minerals in whole mining levels, but till now have not been studied.

METHODS

The surface morphology of samples was studied by the optical microscope Nikon SMZ1500 (National Museum, Prague) and scanning electron microscope Jeol JSM-6380 (Faculty of Science, Charles University, Prague). Phase analysis was done by powder diffractometer PANalytical X´Pert Pro with secondary monochromator and detector X´Cellerator (Faculty of Science, Charles University, Prague). Quantitative chemical data were collected with the electron microprobe Cameca SX100 in wavelength dispersive mode (Joint laboratory of Masaryk University and Czech Geological Survey, Brno) at polished samples in the epoxy resin.

SUPERGENE MINERAL ASSOCIATIONS

Supergene mineral associations were studied as part of our research of this deposit especially in the M7 and M18 veins. Their origin is bonded on weathering of supergene zone *in-situ*. So far no mineral phases of a recent or subrecent character were discovered. Besides below described REE minerals phases, we identified here occurrences of autunite, bismutite, kasolite, metaautunite,

[1] *Institute of Geochemistry, Mineralogy and Mineral resources, Faculty of Science, Charles University, Albertov 6, 128 43 Praha 2, Czech Republic; sir.plaschan@volny.cz*
[2] *Department of Mineralogy and Petrology, National Museum, Václavské nám. 68, 115 79 Praha 1, Czech Republic*
[3] *Institute of Earth Sciences, Faculty of Science, Masaryk University, Kotlářská 2, 611 37 Brno, Czech Republic*

metatorbernite (also Ca-rich varieties), parsonsite (also As-rich varieties), phosphuranylite (also Pb-rich varieties), pseudomalachite, pyromorphite, saleéite and uranophane.

Y, REE MINERAL PHASES

Agardite-(Y) was found as brightly light-green crystalline coatings on a surface up to 1.5 x 2 cm and spherical aggregates up to 1 mm, formed by needle-like crystals. Individual crystals having length 0.1-0.3 mm and thickness only 3-5 μm are light-green, transparent to translucent and intensively glassy bright. In association with agardite-(Y) were observed churchite-(Y), pseudomalachite and metatorbernite. Chemical composition of agardite-(Y) sample studied may be expressed with its empirical formula (mean 3 points): $(Ca_{0.23}Pb_{0.20}Y_{0.20}Bi_{0.09}Ce_{0.07}La_{0.06}Nd_{0.05}Fe_{0.03}Sm_{0.02}Dy_{0.02}Gd_{0.01}Pr_{0.01}Al_{0.01})_{1.00}Cu_{6.40}[(AsO_4)_{1.95}(PO_4)_{0.75}(SiO_4)_{0.30}]_{3.00}(OH)_6 \cdot 3H_2O$.

Churchite-(Y) was observed as coatings on gangue with area up to several tens cm^2**.** These coatings are composed by spherical aggregates up to 0.5 to 0.8 mm, rarely up to 1 mm; the surface of the aggregates consists of fine prismatic needles up to 10 μm. It has grey to rubbish-white colour and vitreous lustre. Aggregates of churchite-(Y) usually growth on older coatings of unnamed $Pb(Ce,REE)_3(PO_4)_3(OH)_2 \cdot nH_2O$ and are covered by younger crystals and aggregates of parsonsite. Metatorbernite, pyromorphite, saleéite and rarely younger pseudomalachite and agardite-(Y) were also observed in association with churchite-(Y). Chemical composition of churchite-(Y) sample studied may be expressed with its empirical formula inferred on the basis of 2 *apfu* (mean 11 points): $(Y_{0.60}Nd_{0.06}Gd_{0.06}Ca_{0.06}Dy_{0.05}Sm_{0.04}Ce_{0.04}Eu_{0.03}Yb_{0.03}Er_{0.02}Ho_{0.01}Pb_{0.01}Tb_{0.01}Pr_{0.01})_{1.01}[(PO_4)_{0.96}(AsO_4)_{0.01}]_{0.97} \cdot 2H_2O$. Chondrite normalized REE pattern shows depletion of LREE a HREE and enrichment in MREE and slight positive Eu anomaly. The tetrad effect is evident from the shape of REE curve (Fig. 1).

Unnamed mineral phase $Pb(Ce,REE)_3(PO_4)_3(OH)_2 \cdot nH_2O$ forms hemispherical to kidney-shaped aggregates having size up to 0.1 mm with uneven to finely crystalline surface. These aggregates develop irregular coatings on a surface to several cm^2 and are mostly covered by younger coatings of churchite-(Y). Crystals and crystalline aggregates of parsonsite growth on coatings of churchite-(Y). This unnamed phase studied has reddish brown colour, dark reddish slightly transparent in small fragments, its lustre is waxy. From the results of chemical analyses an idealized formula of this unnamed mineral phase may be expressed as $A^{2+}B^{3+}{}_3(PO_4)_3(OH)_2 \cdot nH_2O$, in which A-site = Pb and Ca; B-site = besides REE and Y also Al, U a Fe are observed and therefore included. Ce is the dominant element in the Y+REE group. Chemical analyses (15 points) a BSE images enable to infer that aggregates of this unnamed phase are formed by two chemical varieties distinctly differing especially in minority contents of Fe a Si.

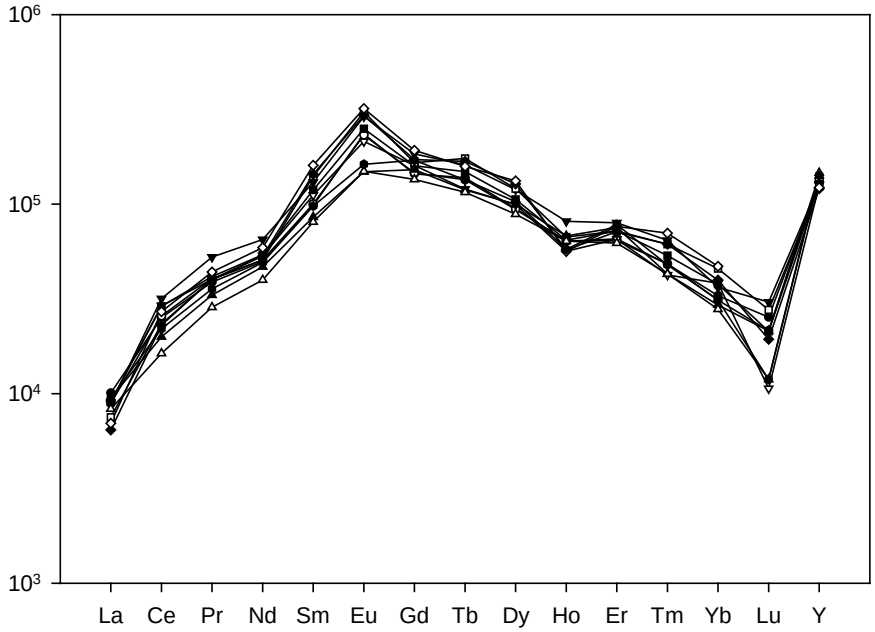

Fig. 1. REE pattern of churchite-(Y) normalized by chondrite (Taylor, McLennan 1985).

Chemical composition of the older (centres of aggregates) variety may be characterized by empirical formula $(Pb_{0.98}Ca_{0.12})_{1.10}(Fe_{0.97}Ce_{0.51}Y_{0.41}Al_{0.38}Nd_{0.33}Gd_{0.12}Sm_{0.10}U_{0.08}Pr_{0.07}La_{0.06}Dy_{0.03}Eu_{0.02}Er_{0.02}Ho_{0.01}Yb_{0.01})_{3.11}[(PO_4)_{2.29}(SiO_4)_{0.61}(AsO_4)_{0.10}]_{3.00}(OH)_2 \cdot nH_2O$, younger variety (rims of aggregates) corresponds to an empirical formula $(Pb_{1.13}Ca_{0.10})_{\Sigma 1.23}(Ce_{0.61}Nd_{0.43}Y_{0.34}Gd_{0.15}Sm_{0.12}U_{0.12}Fe_{0.12}Pr_{0.09}La_{0.09}Al_{0.04}Eu_{0.04}Dy_{0.04}Er_{0.02}Tb_{0.01}Ho_{0.01}Yb_{0.01})_{2.23}[(PO_4)_{2.84}(AsO_4)_{0.13}(SiO_4)_{0.03}]_{3.00}(OH)_2 \cdot nH_2O$.

ACKNOWLEDGEMENTS: We thank to M. Mazuch and O. Fatka (Faculty of Science, Charles University, Prague) for their kind cooperation. This work was supported by the grants MK00002327201 and A3407401.

REFERENCES

VESELÝ T., 1982: Small uranium deposits of crystalline complexes of the Czech Massif. Part III: Area of northwestern and northern Bohemia. Geol. Hydrometalur. uranu, 6, 3: 3-46. (in Czech)

TAYLOR S., R., MCLENNAN S., M., 1985: The continental crust: its composition and evolution. Blackwell Scientific Publ., Oxford, 1-321.

MINERALOGIA POLONICA - SPECIAL PAPERS
Volume 28 - 2006

Jaroslav PRŠEK[1], Daniel OZDÍN[1], Martin CHOVAN[1],

CHEMICAL COMPOSITION OF TETRAHEDRITE-TENNANTITE SOLID SOLUTION AS THE INDICATOR OF TYPE OF THE HYDROTHERMAL MINERALIZATION: EXAMPLES FROM THE WESTERN CARPATHIANS

INTRODUCTION

Minerals of tetrahedrite group are common at the various hydrothermal sulphide mineralizations. Chemical formula for tetrahedrite $Cu_{12}Sb_4S_{13}$ was postulated by Pauling, Neuman (1934). Natural tetrahedrite contains substantial amounts of minor elements e.g. Fe, Zn, Ag, Hg, As, Bi in the solid solution, and the general formula is more nearly $(Cu,Ag)_{10}(Fe,Zn..)_2(Sb,As..)_4S_{13}$ (Takéuchi 1971). By study of crystal chemistry of synthetic tetrahedrites and by isomorphism some atypical elements in tetrahedrites (for example Cr, Pb, V, Ni etc.) going into Makovicky, Karup-Møller (1994). Chemical composition of tetrahedrite from sulphide mineralization in the Western Carpathians was studied by many authors as a part of mineralogical investigations of ore deposits. Tetrahedrite as a minor ore mineral in the stibnite mineralization in the Tatric Unit was studied by Chovan et al. (1998) and tetrahedrite from siderite mineralization was studied in the Tatric Unit by Ozdín & Chovan (1999). All these authors published several microprobe analyses of tetrahedrite investigated by mineralogical revision of ore deposits.

METHODS

Minerals from tetrahedrite group were examined under reflected polarized light. Wavelenght microprobe analyses were performed with JEOL Superprobe 733 and CAMECA SX100, with standards ZnS (ZnKα), Cu_3AsS_4 (CuKα, AsLα, SKα), Cu_3SbS_4 (SbLα), $CuFeS_2$ (FeKα), pure Ag (AgLα), Bi_2S_3 (BiLα), HgS (HgMα) CdS (CdLα), under analytical conditions: accelerating voltage 20 kV, current beam 20nA at the Geologisk Institut University of Copenhagen, Denmark and State geological Institute of Dionýz Štúr, Bratislava.

RESULTS

We studied chemical composition of the minerals from the tetrahedrite-tenanntite solid solution, mainly the contents of Sb, As, Bi, Fe, Zn, Cu and Ag as the main elements. Due to the metalogenic aspect of view the relations between Cu vs. Ag, Sb vs. As and Fe vs. Zn were examined.

Two fields of analyses could be distinguished in the Sb vs. Sb/(Sb+As+Bi) diagram. The first one contains very high content of Sb. The second one is with the contents of Sb 10 at. % and As 2 at. %. The field of tennantite is also characteristic.

[1] *Department of Mineralogy and Petrology, Faculty of Natural Sciences, Comenius University, Mlynská dolina, 842 15 Bratislava, Slovak Republic; prsek@yahoo.com*

Analyses of the tetrahedrites from the stibnite and base-metal mineralization fall into the first field. Tetrahedrites from the siderite type of mineralization fall into the second field. Small overlap of these two fields could be seen. The tennatite was identified only at the few localities with another As minerals.

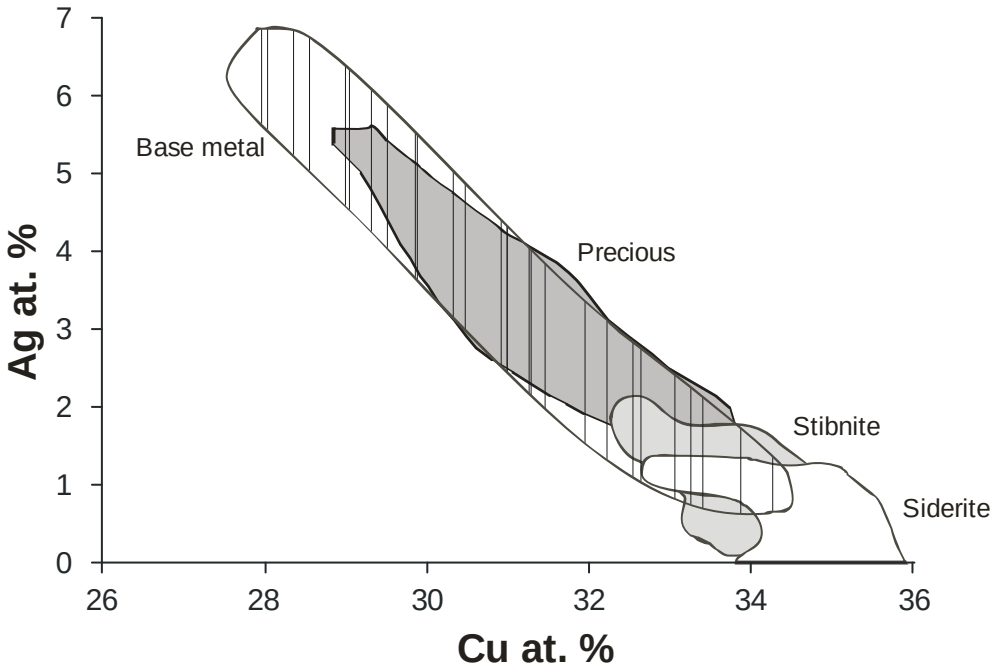

Fig. 1. Substitution of Ag and Cu in tetrahedrites from various type of mineralization.

Three fields of analyses could be distinguished in the Ag vs. Cu diagram (Fig. 1), but generally content of Ag in the microprobe analyses is very low. Analyses of the freibergite from the base–metal mineralization fall into the first field. The second one with the contents of silver from 1.5 up to 7 at. % is typical for tetrahedrite from base-metal and precious metal mineralizations. The biggest group of analyses is concentrated in the lower part of the diagram with low contents of Ag. It could be divided into two subgroups. Analyses from the siderite mineralization take place in the first subgroup with minimal content of silver. Analyses from the stibnite type mineralization take place in the second subgroup with contents of silver from 0.5 up to 1 at. %. Small overlap could be seen again.
Three fields of analyses could be distinguished in the Zn vs. Fe diagram. The first one is the field of the Fe tennantite with minimal content of Zn. The second one is the field of the Zn rich tetrahedrite, typical for the stibnite type of mineralization and partly for precious type of mineralization. Analyses of the tetrahedrites from the siderite type of the mineralization are concentrated in the field limited by the content of Zn from 2 up to 4 at. % and Fe from 3 up to 4.5 at. %. The analyses of base-metal tetrahedrites range in the broad interval in the all fields.

Tetrahedrites could be divided into some groups due to type of the mineralization which they come from. The tetrahedrite from the individual types of mineralization could be isolated use the general chemical compostion. The tetrahedrites differ mainly in the content of Sb, As, Fe, Zn, Cu and Ag; sometimes they contain other elements which could help to classify the tetrahedrites to the certain mineralization type.

CONCLUSIONS

Tetrahedrite from the siderite type is typical by higher As contents, low Ag contents and Fe prevail to Zn, from the stibnite type by high Sb, low Ag contents and Zn prevail Fe, from the base-metal type by higher to high Ag content, Sb prevail As, Fe and Zn with broad ranges and that from precious type by higher Ag content, Sb prevail As, Fe and Zn approximately the same.

ACKNOWLEDGEMENTS: Financial support of research was provided by the project of VEGA No. V-374-05-00 and by the project No. 0503 “Source of ore-bearing fluids in the metallogeny of Western Carpathians”.

REFERENCES

OZDÍN D., CHOVAN M., 1999: New mineralogical and paragenetical knowledge about siderite veins in the vicinity of Vyšná Boca, Nízke Tatry Mts. Slovak Geol. Mag., 5, 4: 255-271.

CHOVAN M., MAJZLAN J., RAGAN M., SIMAN P., KRIŠTÍN J., 1998: Pb-Sb and Pb-Sb-Bi sulfosalts and associated sulphides from Dúbrava antimony deposit, Nízke Tatry Mts. Acta Geol. Univ. Comen., 53: 37-49.

MAKOVICKÝ E., KARUP-MØLLER S., 1994: Exploratory studies on substitution of the minor elements in synthetic tetrahedrite. Part I. Substitution by Fe, Zn, Co, Ni, Cr, V and Pb. Unit-cell parameter changes on substitution and the structural role of “Cu^{2+}” N. Jb. Miner. Abh., 167: 89-123.

PAULING L., NEUMAN E-W., 1934: The crystal structure of binnite, $(Cu,Fe)_{12}As_4S_{13}$ and the chemical composition and the structure of the tetrahedrite group. Z. Kristallogr., 88: 54-62.

TAKÉUCHI Y., 1971**:** On the crystal chemistry of sulphides and sulfosalts. In: T. Tatsumi T. (ed.): Volcanism and Ore Genesis. Univ. Tokyo Press, 395-420.

MINERALOGIA POLONICA - SPECIAL PAPERS
Volume 28 - 2006

Grzegorz RZEPA[1], Jakub BAZARNIK[1], Adam GAWEŁ[1], Marek MUSZYŃSKI[1]

MINERAL COMPOSITION OF BOXWORK-LIKE CONCRETIONS FROM BRZĄCZOWICE (DOBCZYCE REGION, THE POLISH FLYSCH CARPATHIANS)

INTRODUCTION

In the northern edge of the Dobczyce retention reservoir near Brzączowice (*ca*. 30 km S of Kraków), the Istebna Beds crop out. Sandstones, mudstones and shales build them up. Their more fine-grained and thin-bedded parts contain rusty, brown or yellow layers enriched in Fe compounds. On the basis of hand specimen features, various types of Fe-rich concentrations were distinguished. They include: sandstones impregnated with Fe oxyhydroxides, incrustations on the surfaces of sandstones, sulphate-oxide concentrations, phosphate-oxide aggregates and boxwork-like concretions (Rzepa et al. 2006). The most interesting are the latter and they were studied in detail.

METHODS

Mineral composition was investigated using light microscopy, X-ray diffractometry and scanning electron microscopy. The contents of HCl-soluble Fe and Mn were also determined using a Philips PY9100X atomic absorption spectrometer. The XRD analyses were carried out on powdered samples using a Philips X'Pert diffractometer with a graphite monochromator under the following operating conditions: CuK_{α} radiation, scanning speed 0,05°(2Θ)/1sec., range 3-73°(2Θ). The mean crystal dimensions (MCD) were calculated according to the Scherrer formula (Schulze, Schwertmann 1984). Widths of the X-ray peaks at their half heights were determined using Winfit program by *S. Krumm*. As the standard, showing only instrumental line broadening, quartz from Jegłowa was selected. SEM-EDS analyses were performed using a FEI QUANTA 200F microscope coupled with an energy dispersive spectrometer (EDAX) at the Department of Mineralogy, Petrography and Geochemistry, AGH – University of Science and Technology, Kraków.

RESULTS AND DISCUSSION

The ferruginous concentrations studied exhibit characteristic structure resembling boxes – empty or filled up. Their dimensions vary from several mm up to several cm. The boxes are almost square, rectangular, trapezoidal or triangular (Fig. 1). Very often concentric, "ring-like" structure, resembling Liesegang rings, can be seen within the infillings (Fig. 1, 2). Their inner rings are usually enriched in Fe oxyhydroxides in comparison to the outer ones (Fig. 2). The latter may gradually pass into an adjacent, sometimes altered rock (sandstone or mudstone).

[1] *AGH – University of Science and Technology, Department of Mineralogy, Petrography and Geochemistry; al. Mickiewicza 30, 30-059 Kraków, Poland; grzesio@geol.agh.edu.pl*

Within the “boxes” infillings, primary, non-ferruginous minerals (quartz, alkali feldspars, micas, apatite and clay minerals) are dispersed or form more discoloured bands and zones. They are often affected by chemical corrosion and weathering processes.

Fig. 1. Macroscopic view of a boxwork-like concretion.

Fig. 2. Thin section image (25 mm width) and Fe contents determined by SEM-EDS. Explanations: W – wall, Gt – goethite, L – lepidocrocite, Ap – apatite, Q – quartz, Mn – Mn oxides, Mds – mudstone, im – isotropic material, Cl – clay material.

The dominating Fe mineral is cryptocrystalline goethite. It builds walls as well as infillings of the “boxes”. It is characteristic that the Fe content in the walls exceeds 60 wt.% and is usually higher than that in the infillings. Moreover, goethite in the walls is more crystalline in comparison to the infillings (MCD_{110} reaches ca. 19 nm and 12 nm, respectively).

Goethite usually builds up cryptocrystalline masses. But it can also form characteristic “palisades” and fan-shaped aggregates of elongated crystals, lining the walls of pores and fractures, in that case, the oxyhydroxide contain less impurities and can be associated with lepidocrocite.

In almost every “box”, manganese oxides are present. They can be dispersed but usually fill up pores, veins and cracks, form incrustations, irregular concentrations, spots or dendrites (Fig. 2). Micromorphology of Mn oxide aggregates observed on the SEM images resembles birnessite.

CONCLUSIONS

The origin of the boxwork-like concretions studied is probably related to weathering under oxidizing conditions of primary Fe-bearing minerals (silicates, sulphides, carbonates) that must have been present in the surrounding rocks. The accompanying of sulphate-rich concretions, rich in jarosite strongly implies weathering of sulphides (Dutrizac, Jambor 2000). Goethite, the main Fe component of boxwork-like concentrations, can be formed in different weathering environments characterized by a wide spectrum of physicochemical conditions (pH, Eh, foreign ions; Cornell, Schwertmann, 1996). Variations of these parameters may have controlled the forms of occurrence and the degree of crystallinity of goethite. Its presence in different forms suggests several stages and/or mechanisms of weathering, various Fe sources, etc. The boxwork-like structures were probably formed by precipitation of goethite from the solutions that penetrated cracks in sandstones and progressively replaced the primary rock with the iron oxyhydroxide (Rukhin 1953). However, Gucwa and Wieser (1978) studied similar concentrations from the Lower Variegated Shales and suggested that they originated from metasomatic veinlets connected with contractional fractures in formerly oligonite nodules.

ACKNOWLEDGEMENTS: The investigations were supported by the AGH-UST research project no. 11.11.140.158.

REFERENCES

CORNELL R. M., SCHWERTMANN U., 1996: The iron oxides. Structures, properties, occurrences, characterization and uses. VCH, Weinheim. 1-573.

DUTRIZAC J.E., JAMBOR, J.L,. 2000: Jarosites and their application in hydrometallurgy In: ALPERS C.N., JAMBOR J.L., NORDSTROM D.K. (Eds.) Sulfate minerals – crystallography, geochemistry and environmental significance. Rev. Mineral. Geochem., 40: 405–452.

GUCWA I., WIESER T., 1978: Ferromanganese nodules in the Western Carpathian Flysch deposits of Poland. Roczn. Pol Tow. Geol., 48: 147–182.

RUKHIN L.B., 1953: Osnovy litologii. Moskwa: Gostoptekhizdat, 1-671 (in Russian).

RZEPA G., BAZARNIK J., MUSZYŃSKI M., GAWEŁ A., 2006: Ferruginous concentrations in sandstones near Dobczyce (Silesian Unit, the Western Polish Carpathians). Acta Mineral. Petrogr. Abstr. Ser. Szeged, 5: 105.

SCHULZE D.G., SCHWERTMANN U., 1984: The influence of aluminium on iron oxides. X. Properties of Al-substituted goethites. Clay Miner., 19: 521-539.

MINERALOGIA POLONICA - SPECIAL PAPERS
Volume 28 - 2006

Grzegorz RZEPA[1], Bartosz BUDZYŃ[2], Tomasz BAJDA[1]

IRON OXIDES IN THE WEATHERING ZONE OF SERPENTINITES FROM THE SZKLARY MASSIF (LOWER SILESIA) – PRELIMINARY MINERALOGICAL DESCRIPTION

INTRODUCTION

Previous investigations of the serpentinite regoliths from the Szklary massif were focused on the genesis of the Ni deposit, as well as mineralogy and geochemistry of ore minerals (e.g. Ostrowicki 1965, Niśkiewicz 1967, Dubińska 1984). There is less data on the Fe oxides in weathered parts of the massif (Salamon 1975).

In this paper characteristic of Fe oxides occurring in the weathering cover of serpentinites is presented. Fe rich nodules were found within the cover. Their presence has not been reported before.

MATERIALS AND METHODS

Samples of the brownish red saprolite, soil, and the Fe oxide nodules were collected in the central part of the Szklary massif. Chemical composition was determined by wet classic methods. Minerals have been identified using optical microscopy, X-ray diffractometry (Philips X'PERT), thermal analysis (Derivatograph C), and scanning electron microscopy (HITACHI S-4700 microscope coupled with a NORAN Vantage EDS and FEI QUANTA 200 FEG microscope coupled with EDX and EBSD).

RESULTS AND DISCUSSION

The chemical composition of the brownish red saprolite (samples S/III/3, S/III/4) and soil (sample S/III/5), occurring in the profile of the serpentinite regolith is presented in Table 1. The saprolite is composed mainly of phyllosilicates (chlorite and talc), accompanied by Fe oxides (goethite, occasionally hematite and maghemite), Fe-Cr spinels, quartz and different varieties of chalcedony and opal (Bajda 2000). Insignificant amount of oxalate-soluble Fe indicates the absence of ferrihydrite (Rzepa et al. 2002). The dominating Fe oxide mineral and main colouring agent is goethite. Cryptocrystalline masses of this mineral are dispersed in thin sections. Goethite is also responsible for strong endothermic effects observed on DTA curves in temperature range of 295-305 °C.

Selective chemical extractions of regoliths and soils from Szklary indicate that Fe oxides are important carriers of Cr (Bajda 2000) as well as Ni and Zn (Karczewska, Bogda 2006, Rzepa et al. 2006).

[1] *AGH-UST, Department of Mineralogy, Petrography and Geochemistry, Mickiewicza 30, 30-059 Kraków, Poland; grzesio@geol.agh.edu.pl*

[2] *Jagiellonian University, Institute of Geological Sciences; Oleandry 2a, 30-063 Kraków, Poland*

Table 1. Chemical composition of the saprolite and soil samples (wt. % d. w.)

sample	SiO_2	Al_2O_3	Fe_2O_3	Cr_2O_3	CaO	MgO	MnO	NiO	Na_2O	K_2O	H_2O^+	LOI
S/III/3	37.20	5.00	29.62	1.37	1.51	14.22	0.57	2.18	1.25	0.19	5.48	1.42
S/III/4	45.63	6.03	24.51	1.44	0.82	12.46	0.35	0.88	1.71	0.35	5.49	1.05
S/III/5	55.78	7.94	9.80	0.43	1.67	13.47	0.18	0.59	1.74	1.42	5.83	0.96

Fe oxides also concentrate in the form of nodules. Their position in the profile is unclear because of their displacement downwards along the slope. It is probable, however, that they had occurred within the brownish red saprolite. As was mentioned above, the presence of these nodules has not been reported before.

Fig. 1. Macroscopic view of Fe oxide nodule.

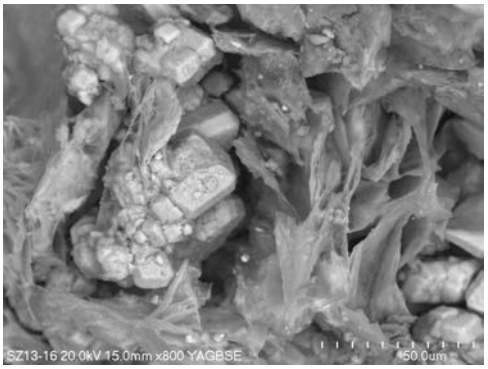

Fig. 2. Fe (large crystals) and Mn (flakes) oxides. SE image.

The nodules are a few centimeters in size and exhibit oval or irregular shapes (Fig. 1). They are non-uniformly coloured, what might be observed as concentric zones. Usually the inner parts are yellow. The intermediate and the outermost ones may be brown, orange or almost black. Black spots and dendrite-like structures are common. XRD patterns indicate that all zones are composed of goethite, whereas the black parts additionally contain Mn oxide minerals. Mn oxides also form silver aggregates, from fractions of mm up to ca 1 cm in size. Sometimes they fill up veins. SEM observations revealed that these manganese accumulations are composed of grassy aggregates (Fig. 2) or thin plates and lamellas several dozen micrometers in diameter and up to 2-3 μm thick. Weak EBSD patterns suggest that these plates are pyrolusitic in composition. In most cases Mn oxides contain impurities - mainly Fe, Ca, Ba, K, occasionally Si, Al, Mg, Na and Ni.

Goethite is the sole constituent of yellow and brown voids infillings and zones. Despite of relatively well-defined crystal structure, goethite crystals usually are not apparent in the SEM images; it forms compact aggregates and masses. However, locally, concentrations of bipyramidal and diamond-shaped crystals up to 30-40 μm in size are observed (Fig. 2). Similar habits were noted for some synthetic goethites (Cornell, Schwertmann 1996) as well as goethites from soil (Arocena et

al. 1994). They usually contain some Ca, Si, and P, and are often partially covered by very fine Mn-oxide particles.

White and yellowish calcite crystals up to 1-2 mm in size were observed in some nodules on the inner surface of voids. During SEM analyses, scarce quartz and mica, as well as chlorite crystals were found. Occasionally, barite was encountered too.

ACKNOWLEDGEMENTS: This work was supported by the AGH-UST as the projects Nos. 10.10.140.305 and 11.11.140.158, and JU research fund. The authors acknowledge Dr. B. Gołębiowska, Dr. A. Pieczka and A. Gaweł M.Sc. for their contribution to this work.

REFERENCES

AROCENA J.M., PAWLUK S., DUDAS M.J., 1994: Iron oxides in iron-rich nodules of sandy soils from Alberta (Canada). In: Ringrose-Voase A.J., Humphreys G.S. (eds.) Soil micromorphology: studies in management and genesis. Developments in Soil Science 22, Elsevier, Amsterdam: 83-97.

BAJDA T., 2000: Mineralogy and geochemistry of chromium compounds of the weathering zone of serpentinites from the Szklary Massif (Lower Silesia). Pol. Tow. Mineral. Prace Spec. 17: 111-113.

CORNELL R. M., SCHWERTMANN U., 1996: The iron oxides. Structures, properties, occurrences, characterization and uses. VCH, Weinheim. 573 p.

DUBIŃSKA E., 1984: Interstratified minerals with chlorite layers from Szklary near Ząbkowice Śląskie (Lower Silesia). Arch. Miner., 39, 2: 5-24.

KARCZEWSKA A., BOGDA A., 2006: Heavy metals in soils of former mining areas in the Sudety Mountains – their forms and solubility. Pol. J. Env. Stud. 15, 2A: 104-110.

NIŚKIEWICZ J., 1967: Budowa geologiczna masywu Szklar. Rocz. Pol. Tow. Geol., 37: 387-414. (in Polish)

OSTROWICKI B., 1965: Minerały niklu strefy wietrzenia serpentynitów w Szklarach. Pr. Miner., 1: 1-92. (in Polish)

RZEPA G., BAJDA T., KRACZKOWSKA I., GOŁĘBIOWSKA B., 2002: Comparison of iron oxides from different hipergenic formations using the methods of selective chemical extraction. Miner. Slov., Geovestnik 34, 1: 10-11

RZEPA G., BAJDA T., SIKORA M., 2006: Speciation and concentration of trace elements in the ferruginous sediments of Poland. Pol. J. Env. Stud. 15, 2A (*in press*).

SALAMON S., 1975: Tlenkowe minerały żelaza i manganu w złożu niklu Szklary. Spraw. z Pos. Kom. Nauk. PAN Oddz. w Krakowie, 18/1. (in Polish)

MINERALOGIA POLONICA - SPECIAL PAPERS
Volume 28 - 2006

Marcus SCHREINER[1], Alistair W.G. PIKE[2], Gavin L. FOSTER[3], Ernst PERNICKA[1]

ARCHAEOMETALLURGY AND LEAD ISOTOPES IN SLOVAKIA

INTRODUCTION

For prehistoric archaeology metal artefacts have always been of great interest. In Europe the first implements were made of copper and they were found in the south-eastern regions (e.g. Bulgaria and Serbia, Gale et al. 2000, Pernicka et al. 1993, Pernicka et al. 1997). Only slightly later they also occurred in Slovakia (see e.g. Novotná 1970).

For many years attempts have been made to relate those objects to specific ore sources in order to reconstruct the production as well as the trade of such valuable goods. Geological sciences have contributed a great deal by developing the application of isotope analyses to ores and consequently also artefacts.

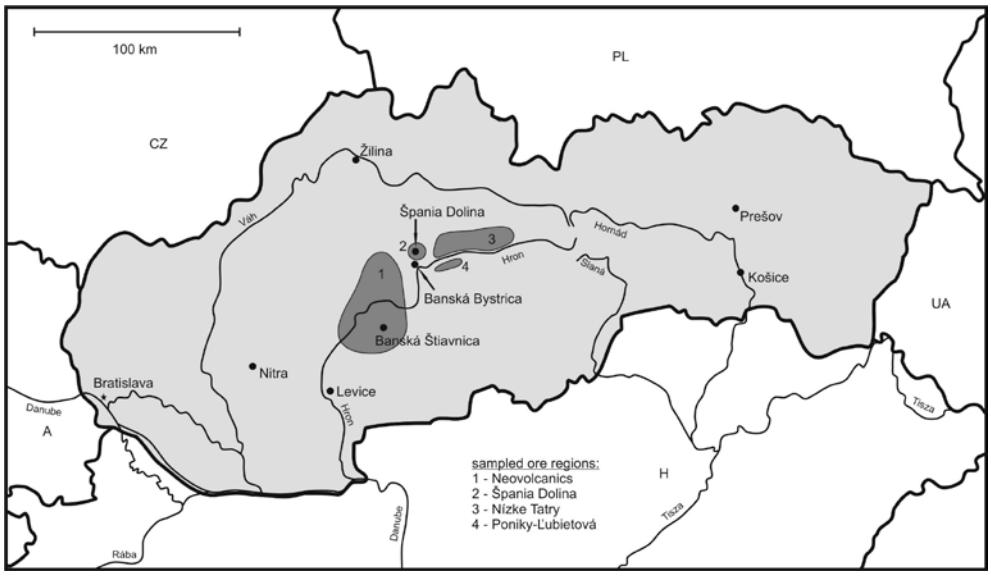

Figure 1: Mining regions investigated in this work

In our work we applied the analysis of lead isotopes to ores from copper sources on both sides of the river Hron as well as to archaeological artefacts. Additionally, trace elements were analysed in order to have a broader analytical base.

[1] *Curt-Engelhorn-Zentrum für Archäometrie gGmbH, D6, 68159 Mannheim, Germany; schreine@merkur.hrz.tu-freiberg.de*

[2] *Department of Archaeology and Anthropology, University of Bristol, 43 Woodland Road, Bristol BS8 1UU, UK*

[3] *Department of Earth Sciences, University of Bristol, Wills Memorial Building, Queens Road, Bristol BS8 1RJ, UK*

SAMPLES

The artefacts derive from a large range of contexts and cover the whole time span of the Eneolithic, from Early Eneolithic heavy implements to objects from the beginning of the Bronze Age. They also represent the full range of metal objects (weapons through ornaments). Their provenance is centred on the south-west-Slovakian plain with occasional finds from the more distant Carpathian basin.

The copper ore samples were taken from deposits in the mountains along the river Hron, covering the Nízke Tatry Mts., the area around Banská Bystrica and the mountains of Kremnica and Banská Štiavnica.

METHODS

The analytical programme was divided into four parts: the chemistry and isotopy of the artefacts and the chemistry and isotopy of the ore samples. Chemical analyses on the artefacts were carried out using energy-dispersive XRF (Lutz and Pernicka 1996). The ore samples were analysed with the same XRF (pressed pellets) and with a Quadrupole-ICP-MS (HF solution). For the isotopes two different methods were applied: solution MC-ICP-MS and also the relative novelty of laser ablation MC-ICP-MS. For the laser ablation no preparation other than some mounting for better handling was necessary, whereas for the solution measurements the usual preparation process was used (see Niederschlag et al. 2003).

RESULTS

There are several results of our work. First, it is possible to analyse ores with LA-MC-ICP-MS to a degree of accuracy and precision that is comparable to methods used so far. Problematic are samples with too little Pb as well as samples with too much Hg, as here interferences can render some results unusable. Whereas the determination of the chemical composition of the artefact samples was very straightforward, the analysis of the ores proved very difficult.

CONCLUSIONS

The results of the analyses have shown that there is a strong case for a local provenance of the artefacts. The isotopic as well as the chemical signature of copper ores especially from the areas of Špania Dolina and Poniky/Ľubietová correspond quite well with those of the analysed artefacts. As this work was intended to be a general overview, more work could possibly resolve the questions in much more detail, especially concerning the use of ores in specific periods.

REFERENCES

GALE N.H., STOS-GALE Z., RADOUNCHEVA. A., IVANOV I., LILOV P., TODOROV T., PANAYOTOV I., 2000: Early Metallurgy in Bulgaria. Annuary of Department of Arhaeology – NBU/IAM IV-V: 102-168.

LUTZ J., PERNICKA E., 1996: Energy dispersive X-ray fluorescence analysis of ancient copper alloys: empirical values for precision and accuracy. Archaeometry 38, 2: 313-323.

NIEDERSCHLAG E., PERNICKA E., SEIFERT Th., BARTELHEIM M., 2003: Determination of Lead Isotope ratios by Multiple Collector ICP-MS: A case study of Early Bronze Age Artefacts and their possible relation with ore deposits of the Erzgebirge. Archaeometry 45, 1: 61-100.

NOVOTNÁ M, 1970: Die Äxte und Beile in der Slowakei. München: C.H. Beck'sche Verlagsbuchhandlung.

PERNICKA E., BEGEMANN F., SCHMITT-STRECKER S., WAGNER G.A., 1993: Eneolithic and Early Bronze Age copper artefacts from the Balkans and their relation to Serbian copper ores. Prähistorische Zeitschrift, 68, 1: 1-54.

PERNICKA E., BEGEMANN F., SCHMITT-STRECKER S., TODOROVA H., KULEFF I., 1997: Prehistoric copper in Bulgaria. Eurasia Antiqua, 3: 41-180.

MINERALOGIA POLONICA - SPECIAL PAPERS
Volume 28 - 2006

Jiří SEJKORA[1], Radek ŠKODA[2], Petr PAULIŠ[3]

SELENIUM MINERALIZATION OF THE URANIUM DEPOSIT ZÁLESÍ, THE RYCHLEBSKÉ HORY MTS., CZECH REPUBLIC

INTRODUCTION

The small uranium deposit Zálesí is situated at the southern margin of settlement Zálesí, about 6.5 km SW of Javorník at the Rychlebské hory Mts., northern Moravia, Czech Republic. The deposit was discovered during the regional uranium exploration and opens from the shaft Pavel and mined from Galleries I. - III. in five levels at vertical intervals 50 m. Over 400 t of uranium was worked-out there during 11 years (1958-1968). The samples studied were collected on the mine dumps of the shaft Pavel during several past years.

GEOLOGY

Thirty hydrothermal veins and two stockworks are hosted by the folded and metamorphosed Paleozoic sequence of the Strónia Group belonging to the Orlice-Snieznik crystalline complex. The primary mineralization of the deposit originated in three mineralization stages - uraninite, arsenide and sulphide and may be classified as close to the so-called "five-elements" formation (U-Ni-Co-As-Ag). Majority of primary Se mineralization is related to uraninite stage, the occurrence of Bi selenides (ikunolite-laitakarite) in bismuth of arsenide stage was found only sporadically (Fojt et al. 2005). The first results of the present research of primary and supergene Se mineralization of the deposit were published by Sejkora et al. (2004) and Fojt, Škoda (2005).

METHODS

The surface morphology of samples was studied with optical microscope Nikon SMZ1500 (National Museum, Prague) and scanning electron microscope Jeol JSM-6380 (Faculty of Science, Charles University, Prague). X-ray powder patterns of studied phases were obtained by X-ray powder diffractometer HZG4/AREM-Seifert (National Museum, Prague) and proceeded by ZD - software (by P. Ondruš), unit-cell parameters were refined by a least-squares method. Quantitative chemical data were collected with the electron microprobe Cameca SX100 in wavelength dispersive mode (Joint laboratory of Masaryk University and Czech Geological Survey, Brno) at polished samples mounted in the epoxy resin.

RESULTS - PRIMARY MINERALS

[1] *Department of Mineralogy and Petrology, National Museum, Václavské nám. 68, 115 79 Praha 1, Czech Republic; jiri.sejkora@nm.cz*
[2] *Institute of Earth Sciences, Faculty of Science, Masaryk University, Kotlářská 2, 611 37 Brno, Czech Republic*
[3] *Smíškova 564, 284 01 Kutná Hora, Czech Republic*

Clausthalite is the most abundant selenide at the deposit; it forms (in intergrowths with quartz) fine-grained aggregates up to 4 cm; in association, chalcopyrite, uraninite and other selenides were observed. At a part of samples, clausthalite is intensively replaced by supergene molybdomenite or rarely demesmaekerite. Clausthalite usually contains minority contents of Bi (up to 0.04) and Ag (up to 0.02 *apfu*). Empirical formula: $(Pb_{0.98}Bi_{0.02}Ag_{0.01})_{1.01}(Se_{0.95}S_{0.04})_{0.99}$.

Naumannite usually forms only tiny (up to 10-20 μm) anhedral grains in association with clausthalite and Bi-selenides. The finds of its grains up to 1 mm in association of clausthalite and crystals up to 0.5 mm in altered quartz are exceptional. Empirical formula: $Ag_{2.03}Se_{0.96}$.

Bohdanowiczite was identified as anhedral grains up to 40 x 40 μm in association with Bi-selenides and clausthalite. It is very rare, only few grains were observed. Empirical formula: $Ag_{1.00}(Bi_{0.97}As_{0.01})_{0.98}(Se_{1.98}S_{0.02})_{2.00}$.

Bi sulfoselenides of the series ikunolite - laitakarite form irregular grains up to 50 μm in aggregates of bismuth of the arsenide stage. The determined chemical composition varies in the range of empirical formulas: $(Bi_{3.92}Pb_{0.08}Sn_{0.01})_{4.02}(S_{2.03}Se_{0.94}As_{0.03})_{3.00}$ - $(Bi_{3.85}Pb_{0.11}Cd_{0.05}Sn_{0.01})_{4.02}(S_{1.29}Se_{1.70}As_{0.01})_{3.00}$.

Unnamed Bi_4Se_3 was determined as lathy and needle-like crystals up to 100 μm; it is usually overgrown with clausthalite. This phase is slightly nonstoichiometric with small excess of cations $(Bi_{3.94\text{-}4.08}Pb_{0.12\text{-}0.15}Sn_{0.01})_{4.11\text{-}4.22}(Se_{2.83\text{-}2.93}S_{0.07\text{-}0.07}Te_{0.01})_{\Sigma 3.00}$.

SUPERGENE MINERALS

Selenium was determined as rich irregular or spherical aggregates (up to 10-30 μm) in molybdomenite in association with unnamed $(BiO)_2(SeO_3)\cdot nH_2O$ and with relics of Bi-selenides. Chemical composition of selenium is simple, only minority contents of S (up to 0.003 *apfu*) and Pb (up to 0.001 *apfu*) were determined.

Naumannite forms irregular indistinct aggregates up to 10 μm in molybdomenite grains in association with pyromorphite and cerussite. Empirical formula: $(Ag_{2.01}Pb_{0.05})_{2.06}(Se_{0.92}S_{0.01})_{0.93}$; the content of Pb may be influenced by an occurrence of molybdomenite around naumannite.

Chalcomenite was found as relatively abundant crystalline coatings (up to 1x1.5 cm) and more rarely as well-developed prismatic crystals up to 2-3 mm. It is transparent to translucent and has characteristic bright to dark blue colour with green tint. Empirical formula: $(Cu_{0.98}Al_{0.02})_{1.00}(SeO_3)_{1.00}\cdot 2H_2O$. Unit-cell parameters: a = 6.6724(9), b = 9.165(1), c = 7.371(1) Å.

Molybdomenite is the most abundant supergene Se mineral at this deposit, usually to a large extent replaced primary clausthalite. It was also found as tiny fibrous aggregates, rarely it forms well-developed tabular crystals up to 1-2 mm. Aggregates has white to grey colour, crystals are colourless and transparent. Empirical formula: $(Pb_{0.98}Al_{0.02})_{1.00}[(SeO_3)_{0.98}(SO_4)_{0.01}]_{0.99}$. Unit-cell parameters: a = 4.5311(7), b = 5.5126(7), c = 6.602(1) Å, β = 106.42(1).

Schmiederite was found only very rarely as translucent aggregates (up to 1.5 mm) and transparent acicular crystals (up to 0.5 mm in the length). It has light sky-blue colour and vitreous to silky lustre. Empirical formula: $(Pb_{1.91}Al_{0.02})_{1.93}$

$(Cu_{1.97}Fe_{0.01})_{1.98}(SeO_3)_{1.00}[(SeO_4)_{0.82}(SO_4)_{0.26}]_{1.08}(OH)_4$. Unit-cell parameters: a = 9.904(6), b = 5.702(4), c = 9.352(6) Å, β = 101.99(5).

Demesmaekerite was identified only very rarely. It forms irregular aggregates up to 0.6 mm replaced by chalcomenite; its aggregates contain abundant tiny relics of primary clausthalite. Empirical formula: $(Pb_{1.80}Al_{0.08}Fe_{0.05}Ca_{0.04}Bi_{0.01})_{1.98}Cu_{5.41}(UO_2)_{1.95}[(SeO_3)_{5.92}(SO_4)_{0.03}(SiO_4)_{0.03}(AsO_4)_{0.02}]_{6.00}(OH)_6 \cdot 2H_2O$.

Unnamed $(BiO)_2(SeO_3)\cdot nH_2O$ mineral phase was found as irregular aggregates up to 20-100 μm, which are intensively replaced Bi-selenides; relics of Bi-selenides, molybdomenite and selenium were identified in the mineral association. Empirical formula: $(Bi_{1.82}Pb_{0.13}Fe_{0.02}Ca_{0.01})_{1.98}O_2[(SeO_3)_{0.94}(SO_4)_{0.01}]_{0.95} \cdot nH_2O$, n=1.5 for total of microprobe analyses about 100 wt. %.

ACKNOWLEDGEMENTS: The authors thank to J. Plášil and M. Mazuch (Faculty of Science, Charles University, Prague) and B. Fojt (Faculty of Science, Masaryk University) for their kind cooperation. This work was supported by the grants MK00002327201 and 205/03/D004.

REFERENCES

FOJT B., DOLNÍČEK Z., KOPA D., SULOVSKÝ P., ŠKODA R., 2005: Paragenesis of the hypogene associations from the uranium deposit at Zálesí near Rychlebské hory Mts., Czech Republic. Čas. Slez. Muz. Opava (A), 54: 223-280. (in Czech)

FOJT B., ŠKODA R., 2005: Bi_4Se_3 and ikunolite-laitakarite from the uranium deposit Zálesí near Javorník, the Rychlebské hory Mts. Acta Mus. Moraviae, Sci. geol., 90: 99-107. (in Czech)

SEJKORA J., PAULIŠ P., MALEC J., 2004: The supergene selenium mineralization at the uranium deposit Zálesí, the Rychlebské hory Mts. (Czech Republic). Bull. mineral.-petrolog. Odd. Nár. Muz. (Praha), 12: 174-179. (in Czech)

MINERALOGIA POLONICA - SPECIAL PAPERS
Volume 28 - 2006

Elena P. SHCHERBAKOVA[1], Tatyana N. MOROZ[2], Vera L. LYUBIMOVA[3], Kadriya G. ALEXANDROVA[3]

TWO REMARKABLE CZECH MINERALS FROM THE COLLECTIONS OF NATURAL SCIENCE MUSEUM OF THE ILMEN STATE RESERVE (SOUTH URAL, RUSSIA)

INTRODUCTION

The relatively small mineralogical collection of the Natural Science Museum of the Ilmen State Reserve (South Ural, Russia) includes about 800 mineral species. 10% of them represent the mineral species from the countries of central Europe. In most cases, the samples have been passed to the museum in the beginning of 1990th, when our mineralogists began to take part at the international conferences, exhibitions, mineral shows, and field trips. Besides, a series of samples from various deposits of Czech Republic and Slovakia was presented to the museum by Marek Kotrlý (Czech Republic). There were fifteen mineral species such as kobellite $Pb_{22}Cu_4(Bi,Sb)_{30}S_{69}$, heyrovskýite $AgPb_{10}Bi_5S_{18}$, kaňkite $Fe^{3+}(AsO_4)\cdot 3.5H_2O$, bukovskýite $Fe^{3+}{}_2(OH)(SO_4)(AsO_4)\cdot 3H_2O$, zeunerite $Cu^{2+}(UO_2)_2(AsO_4)_2\cdot 10\text{-}16H_2O$, kutnohorite $Ca(Mn^{2+},Mg,Fe^{2+})(CO_3)_2$, dawsonite $NaAl(OH)_2(CO_3)$, monohydrocalcite $Ca(CO_3)\cdot H_2O$, znucalite $CaZn_{11}(UO_2)(CO_3)_3(OH)_{20}\cdot 4H_2O$, klebelsbergite $Sb^{3+}{}_4O_4(OH)_2(SO_4)$, libethenite $Cu_2(PO_4)(OH)$, etc. At the time, Marek Kotrlý presented the small collection of minerals from the burnt waste heaps of Kladno (Czech Republic) to the head of laboratory of mineralogy of technogenesis of the Institute of Mineralogy of Ural Branch RAS Dr. Boris Chesnokov. The collection included the samples of rare sulfates (millosevichite $(Al,Fe)_2(SO_4)_3$, godovikovite $NH_4(Al,Fe)(SO_4)_2$, efremovite $(NH_4)_2Mg_2(SO_4)_3$, boussingaultite $(NH_4)_2Mg(SO_4)_2\cdot 6H_2O$ and organic minerals (kratochvilite $C_{13}H_{10}$, hoelite $C_{14}H_8O_2$, kladnoite $C_6H_4(CO)_2NH$); later it was passed to the museum also.

METHODS

The IR spectrum of the thin crystal of Czech hoelite was recorded on Fourier transform FT-IR spectrometer Vertex 70 with HYPERION microscope and N2 cold detector in the region 370 – 4000 cm^{-1}.

The IR spectra of different solid samples of kladnoite were recorded on a Bomem FTIR spectrophotometer using KBr disc technique. The Raman spectra were measured by the Bruker RFS 100/S FT Raman spectrometer with the use of

[1] *Institute of Mineralogy of Ural Branch of Russian Acad. Sci., Ilmen State Reserve, 456317 Miass, Russia; founds@ilmeny.ac.ru*

[2] *Institute of Geology and Mineralogy of Siberian Branch of Russian Acad. Sci., Prospect Acad. Koptyuga, 3, 630090 Novosibirsk, Russia*

[3] *Natural Science Museum of the Ilmen State Reserve of Ural Branch of Russian Acad. Sci., Ilmen State Reserve, 456317 Miass, Russia*

the 1064 nm line of NIR Nd^{3+}: YAG laser and Ramanor U1000 (514.5 nm Ar + laser).

RESULTS

Hoelite and kladnoite from these samples have been studied by X-ray diffractometry and vibrational (IR and Raman) spectroscopy. For comparison, the similar samples from the burnt waste heaps of Kopeisk (Russia) were used.

Hoelite $C_{14}H_8O_2$, natural analogue of 9.10-antraquinone, forms the acicular brightly-yellow transparent crystals with length of 1 - 10 mm or the radiated accumulations of these crystals (Fig. 1). X-ray diffraction patterns of Czech and Russian hoelite confirm their identity and correspondence to synthetic analogue (Žáček, 1989, Shcherbakova, Moroz, 2005).

Basic 9.10- antraquinone IR bands in solid phase such as the C-H bending modes (974, 1099, 1165 cm^{-1}), C-C stretching modes (1259, 1284, 1305, 1333, 1458 cm^{-1}), and C=O (1674 cm^{-1}) were observed on the spectrum (Fig. 2). Raman spectra were recorded on Labram spectrometer Jobin Yvon using 633 nm excitation of He-Ne laser. The antraquinone Raman lines with C=O vibration at 1672 cm^{-1} missed. Two intensive lines at 1350 and 1395 cm^{-1}, 982 cm^{-1} band and strong fluorescence with wide bands of composite contour were observed in spectra of different points of the sample with this laser line. Perhaps these lines were caused by numerous white inclusions (possible other aromatic compounds such as phenantrene or anthracene $C_{14}H_{10}$) presented in underlying rock. They have given the contribution to the observed Raman spectra and mask the hoelite Raman bands (Nasdala et al., 1993).

Kladnoite $C_6H_4(CO)_2NH$, natural analogue of phthalimide, usually forms the small friable accumulations of light silvery flakes (fig. 3). X-ray diffraction patterns of Czech and Russian kladnoite are similar and correspond to the above-mentioned synthetics (Rost, 1937, Žáček, 1988, Chesnokov, Shcherbakova 1991).

Main phthalimide vibrational modes are observed in the Fourier transformed (FT) IR and FT Raman spectra of kladnoite (fig. 4).

CONCLUSIONS

The study of the mineral samples from the museum collections by modern analytical methods gives favorable possibilities to make the interesting mineralogical findings up to discovery of quite new mineral species. As a result of our work, to compare the genetically similar samples from the burnt waste heaps of Kladno and Kopeisk, we would be able to find hoelite first in Russia and to suppose presence of new aromatic minerals both in Czech and in Russian samples. Future cooperative researches will allow testablishing true nature of these minerals.

ACKNOWLEDGEMENTS: We are very grateful to Russian Fund of Basic Research (RFBR) for support of this work (grant No. 06-05-64845) and to our Czech colleagues Vladimír Žáček and Jan Jehlička for constructive discussion of received results.

REFERENCES

CHESNOKOV B.V., SHCHERBAKOVA E.P., 1991: Mineralogy of burnt waste heaps of the Chelyabinsk coal basin. Moscow, Nauka, 1-152. (in Russian).

NASDALA L., PEKOV I.V., WITZKE T., 1993: Raman Investigation of Naturally Occurring $C_{14}H_{10}$. Chem. Erde, 53: 59-69.

ROST R., 1937: The minerals formed on burning heaps in the coal basin of Kladno. Bull. Int. Acad. Sci. Bohem., 11: 1-7.

SHCHERBAKOVA E.P, MOROZ T.N., 2005: Hoelite $C_{14}H_8O_2$: New Data. Mineralogical Museums-220, St-Petersburg, 199-201.

ŽÁČEK V., 1988: Zonal association of secondary minerals from burning dumps of coal mines near Kladno, Central Bohemia, Chechoslovakia. Acta Univ. Carol. Geol., 3: 315-341. (in Czech)

ŽÁČEK V.1989: Hoelit (9,10-antrachinon, $C_{14}H_8O_2$) z kladenských hořících hald. Čas. Mineral. Geol., 4: 433-435. (in Czech)

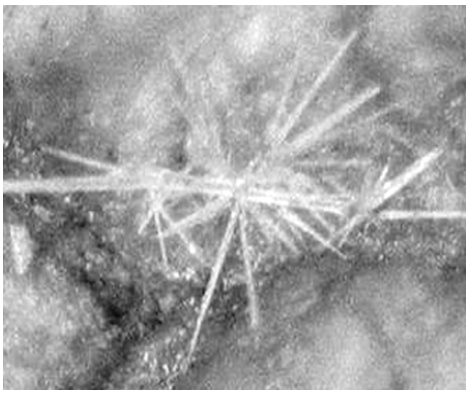

Fig. 1. Hoelite from Kladno, Czech Republic.

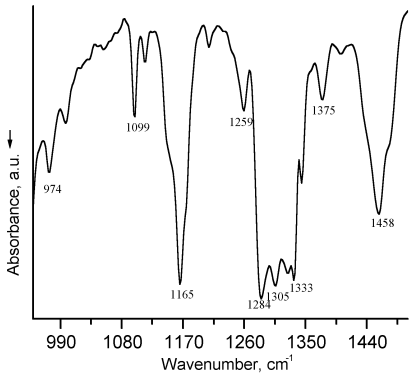

Fig. 2. IR-spectrum of Czech hoelite.

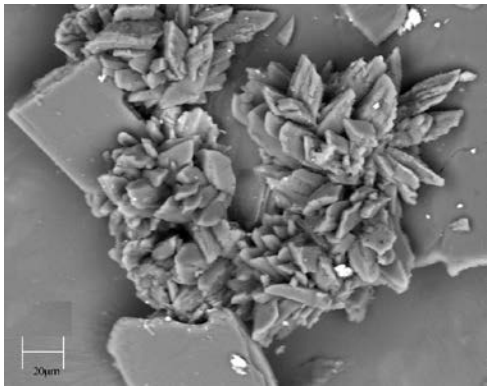

Fig. 3. SEM image of kladnoite, Kopeisk, Russia.

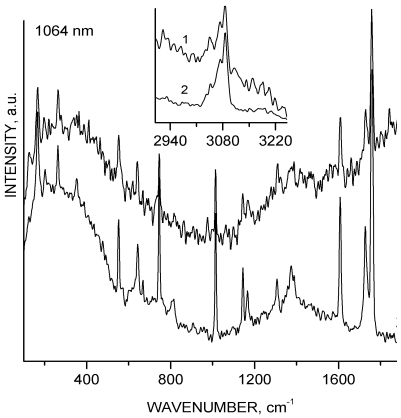

Fig. 4. Raman spectra of Czech (1) and Russian (2) kladnoites.

MINERALOGIA POLONICA - SPECIAL PAPERS
Volume 28 - 2006

Rafał SIUDA[1], Łukasz KRUSZEWSKI[1]

NEW DATA ON BAYLDONITE, CORNWALLITE, OLIVENITE AND PHILIPSBURGITE FROM MIEDZIANKA (RUDAWY JANOWICKIE MTS., SUDETES, POLAND)

INTRODUCTION

Miedzianka deposit is located about 12 km from Jelenia Góra in Rudawy Janowickie Mountains and belongs to a group of several ore deposits connected with Karkonosze pluton, which are situated in metamorphic rocks of the eastern cover of the Karkonosze granite. Deposit is built of metasomatic ore lens (lying on the contact between Karkonosze granite and amphibolites) and polymetallic veins which cut amphibolites and schists. Supragenic zone of Miedzianka deposit contains rich assemblage of secondary minerals (Holeczek, Janeczek 1991; Ciesielczuk, Bzowski 2003; Ciesielczuk et al. 2004).

METHODS

Samples of ores and rocks containing hipergenic parageneses were collected on old heaps east of Miedzianka. Further investigations were performed on samples formerly occurring in oxidated part of Blaugang vein, which was exploited in Adler and Neu Adler mines. Chemical composition of chosen mineral phases was obtained with CAMECA SX100 microprobe (Fac. of Geol., Warsaw University).

MINERALS OF THE SUPRAGENIC ZONE

In this study, a paragenesis of secondary minerals represented by Cu and Pb arsenates was recognized. Arsenates co-occur with chrysocolla and are represented by four mineral species. Bayldonite from Miedzianka was originally recognized by Ciesielczuk, Bzowski (2003) on the basis of X-ray diffraction, but without chemical data. This mineral occurs only in a form of very small (up to tens of μm) rounded aggregates which grow on surface of highly hydrated chrysocolla or, together with olivenite, fill up fissures cutting ore minerals and amphibolites. It is also present in botryoidal concentrations of philipsburgite, coexisting with cornwallite. According to chemical analyzes baydolnite from Miedzianka contains small amounts of Fe (up to 0.8 wt. %), Zn (up to 0.16 wt. %), P (up to 0.5 wt. %) and V (up to 0.15 wt. %). Following empirical formula was established: $Cu_{3.12}Pb_{1.00}Fe_{0.06}Ca_{0.01}[(AsO_4)_{1.92}(PO_4)_{0.05}(VO_4)_{0.01}]_{1.98}(OH)_{1.40}$.

Cornwallite is found as deep green, botryoidal concentrations in philipsburgite (Fig. 4). Chemical analyzes prove that Zn (up to 0.64 wt. %), Pb (up to 0.49 wt. %) and Fe (up to 0.10 wt. %) are present in this mineral. Characteristic feature of researched cornwallite is constant, small content of P (around 0.40 wt. %). Such low concentration confirms that mineral researched in this paper does not belong to cornwallite-pseudomalachite solid solution, what was suggested by Ciesielczuk,

[1] *Institute of Geochemistry, Mineralogy and Petrology, Faculty of Geology, Warsaw University, Al. Żwirki i Wigury 93, 02-089 Warsaw; siuda@uw.edu.pl*

Bzowski (2003). Chemical composition of investigated mineral sample corresponds to $Cu_{5.08}Zn_{0.03}Pb_{0.01}[(AsO_4)_{1.90}(PO_4)_{0.05}]_{1.95}(OH)_{3.68}$.

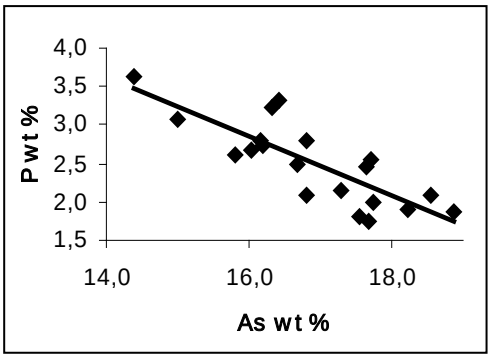

Fig. 1. Correlation between As and P concentration in olivenite. R^2= -0,82.

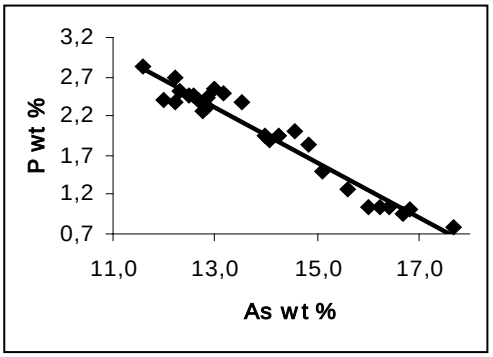

Fig. 2. Correlation between As and P concentration in philipsburgite. R^2= -0.97.

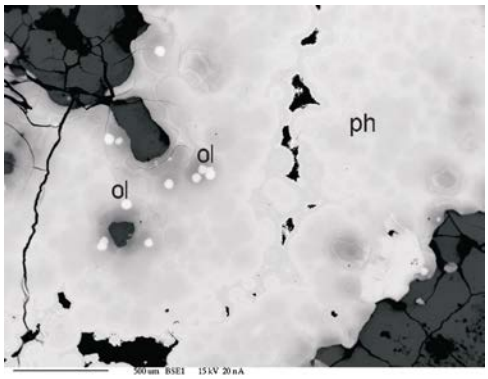

Fig. 3. Philipsburgite (ph) and olivenite (ol). BSE image.

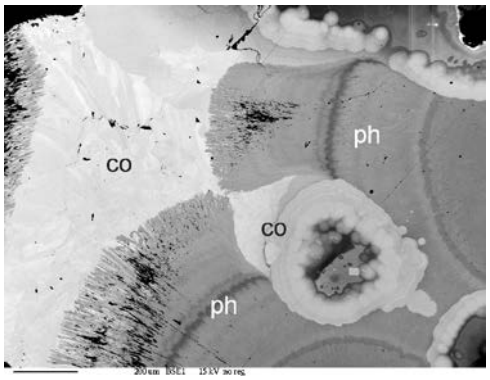

Fig. 4. Cornwallite (co) with philipsburgite (ph). BSE image.

Philipsburgite from Miedzianka was identified by Ciesielczuk, Bzowski (2003) basing on XRD data. In our samples this mineral occurs as massive, cryptocrystalline coatings and botryoidal accumulations on the surface of amphibolites, containing altering ore minerals (Fig. 3). Its thin tabular crystals are visible under high magnification. Macroscopically it is indistinguishable from olivenite and cornwallite. Contents of Zn in philipsburgite reaches 8.5 wt. %. The mineral contains also small amounts of Pb (up to 0.2 wt. %), Fe (up to 0.05 wt. %) and V (up to 0.1 wt. %). Contents of As and P varies from 11.6 to 17.7 wt. % and from 0.8 to 2.8 wt. %, respectively. Linear correlation between As and P contents in philipsburgite is observed (Fig. 2). Empirical formula is: $Cu_{5.04}Zn_{0.89}[(AsO_4)_{1.40}(PO_4)_{0.7}(VO_4)_{0.01}]_{1.88}(OH)_6 \cdot 1.29H_2O$.

Olivenite occurs in the mentioned accumulations of bayldonite and philipsburgite. It contains small amounts of Pb (up to 2.81 wt. %), Fe (up to 1.2 wt. %), Zn (up to 0.4 wt. %) and is distinctly enriched in P (up to 3,63 wt. %) (Fig.1). Calculated chemical formula of olivenite is: $Cu_{2.19}Fe_{0.02}Al_{0.01}$

$Zn_{0.01}Pb_{0.01}[(AsO_4)_{0.63}(PO_4)_{0.23}(SiO_4)_{0.05}]_{0.91}(OH)_{1.02}$. Distinct, linear correlation between contents of As and P suggests that the researched phase belongs to a continuous series of olivenite-libethenite solid solution.

CONDITIONS OF CU AND PB ARSENATES

Diversity of the paragenesis of Cu and Pb arsenates from Miedzianka is connected with mutability of its crystallization environment. Presence of cornwallite, olivenite, philipsburgite and bayldonite indicates high concentrations of Cu and As, as well as relatively low activity of Pb (confirmed by the absence of pyromorphite) in crystallization environment. Presence of essential Zn amount in philipsburgite points at participation of this metal in forming of the paragenesis. Admixture of PO_4^{3-} ion in the structure of the researched minerals bears witness to relatively high activity of P, however not as high as is required for pseudomalachite crystallization, which is absent in researched samples.

The presence of olivenite and absence of clinoclase suggest, that the paragenesis originated likely from low-acidic solution. At the same time, absence of hydrous sulphates (like brochantite) and carbonates (like malachite) indicates low concentrations of sulphate and carbonate ions in solution (Magalhaes et al. 1988).

Described paragenesis is supposed to be formed in a zone where two types of solutions were mixing. First type corresponds to ascending ground-waters, enriched in Cu, Pb, Zn and As by contact with altering ore minerals. Second type could be rainfall waters, migrating through soil strata to deeper parts of the oxidation zone and containing PO_4^{3-} ions. These ions could be released during decomposition of organic matter from the soil.

ACKNOWLEDGEMENTS: Researches were financially supported by Consultation Council on Students Affairs (Warsaw University, Poland).

REFERENCES

CIESIELCZUK J., BZOWSKI Z., 2003: Secondary (Cu, Zn)-oxyminerals from the Miedzianka copper deposit in Rudawy Janowickie, Sudetes Mts. Preliminary report. Min. Soc. of Poland Spec. Papers, 23: 54-55.

CIESIELCZUK J., SZALEG E., KUŹNIARSKI M., BYLINA P., 2004: Preliminary data of erythrine from Ciechanowice (Miedzianka deposit, Sudety Mts.), Min. Soc. of Poland Spec. Papers, 24: 123-125.

HOLECZEK J., JANECZEK J., 1991: Pseudomalachite from Radzimowice and some comments on its occurrence in Miedzianka (Sudetes Mts.). Min. Pol., 22: 17-25.

MAGALHAES M.C.F., PEDROSA DE JESUS J.D., WILLIAMS P.A., 1988: The chemistry of formation of some secondary arsenate minerals of Cu(II), Zn(II) and Pb(II). Min. Mag., 52: 679-690.

MINERALOGIA POLONICA - SPECIAL PAPERS
Volume 28 - 2006

Pavel ŠKÁCHA[1], Jiří SEJKORA[2], Jiří LITOCHLEB[2]

CHEMICAL COMPOSITION OF Ag-Sb MINERAL PHASES FROM THE PŘÍBRAM URANIUM ORE DISTRICT, CZECH REPUBLIC

INTRODUCTION

The uranium-polymetallic ore district Příbram with industrial accumulations of uranium, polymetallic and silver ores is important part of the Central Bohemia metallogenic zone. The hydrothermal ore veins of the varisan age are developed in tectonically strongly stricken formation of rocks in the Barrandien Neoproterozoic at NW exocontact zone of the Central Bohemian pluton. Individual deposits of ore district ("vein clusters") are situated at area 1-2x25 km, what parallel follows exocontact zone in direction NE-SW with deep reach of ore mineralization up to 2 km. The mineral filling of hydrothermal veins originated during four main stages - gold-bearing-quartz, siderite-sulphide (polymetallic), uraninite-calcite and the youngest sulphide-calcite in eight mineralization periods at least. The mineral phases of Ag-Sb system were found at different types of ore mineralization, especially in gold-bearing, polymetallic and silver-bearings types.

METHODS

New quantitative chemical data (more than 100 point analyses) were collected with the electron microprobe Cameca SX100 in wavelength dispersive mode (Geologický ústav Dionýza Štúra, Bratislava) at polished samples in the epoxy resin. Results of the study are distinctly summarized and given in Figures 1 and 2.

RESULTS

Dyscrasite (type I) was found in the siderite-sulphide vein B128G5 of the deposit Brod (24th level of mine 15) and described by Litochleb et al. (1984). It forms aggregates up to 10 cm in size formed by anhedral to subhedral striated grains up to 4x8 mm. Rare crystals (up to 1 mm) were observed in cavities of these aggregates. Dyscrasite (type I) is associated with Ag-rich gold, gersdorffite, pyrrhotite, safflorite and nickeline; gangue minerals are represented by siderite, dolomite-ankerite and calcite. In BSE image mosaic zonality is evident caused by moderate changes of the ratio Ag/Sb (3.4-3.6). The Ag and Sb contents in dyscrasite (type I) varied in the ranges 75-77 and 21-23 at. %; regular contents of Hg reached only up to 0.2-0.5 at. %.

Dyscrasite (type II) was found in carbonate veins of the deposit Háje (mine 21). The first occurrence was described (Knížek et al. 1990) in the vein H14F (6th level); dyscrasite type II forms there columnar pseudohexagonal crystals of a length of 1-8 cm with thickness up to 1 cm and compound crystals of the so-called

[1] *Institute of Geochemistry, Mineralogy and Mineral resources, Faculty of Science, Charles University, Albertov 6, 128 43 Praha 2, Czech Republic*

[2] *Department of Mineralogy and Petrology, National Museum, Václavské nám. 68, 115 79 Praha 1, Czech Republic*

oleander type up to 3x6 cm. Later, this type of dyscrasite was also found in the vein H14F3 (7^{th}-8^{th} level), where it forms rich aggregates of columnar crystals

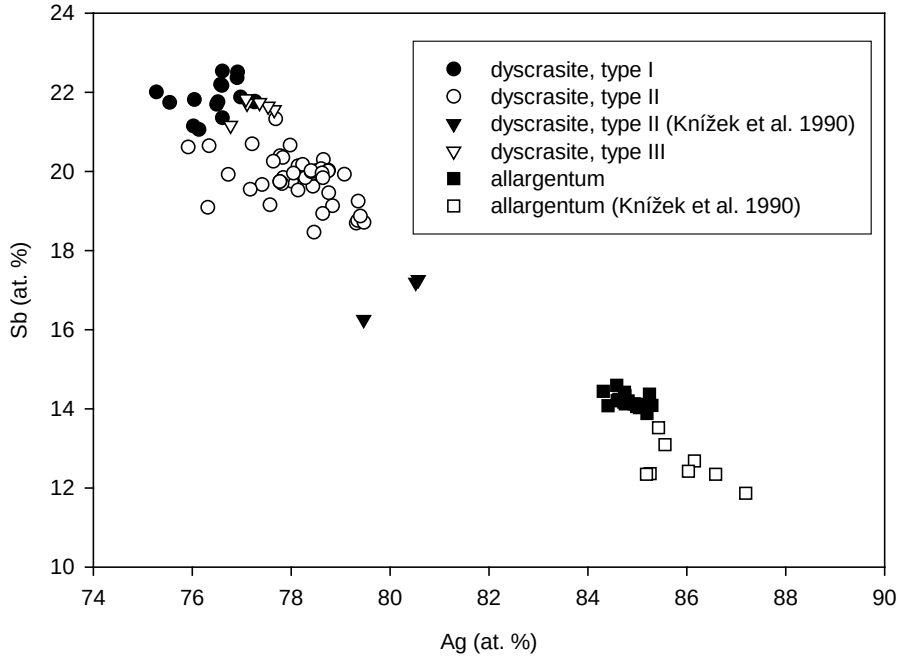

Fig. 1. Graph Ag vs. Sb (in at. %) for dyscrasite and allargentum from the Příbram uranium ore district.

up to some cm in length and rarely thin tabular crystals, too. At both described occurrences at Háje, columnar crystals of dyscrasite are always overgrown by younger native arsenic. In BSE image distinctly zoned crystals (mosaic zonality or zones parallel to elongation of crystals) were also observed beside completely homogeneous crystals; this zonality is caused especially by fluctuation of the Ag/Sb (3.6-4.2) ratio. Dyscrasite (II) is evidently chemically more variable (Fig. 1 and 2) and practically always contains higher Hg (up to 1.5 at. %) amounts. Ag contents are in the range 76.0-79.5 at. % and those of Sb in the range 18.5-21.3 at. %.

Dyscrasite (type III) was determined only in vein gangue from mine dumps of the mine 21, its occurrence may be probably possible to localize above the 7^{th} level in the vein H14F. It forms well-developed columnar crystals up to 5 mm and spherical aggregates up to some cm in size in calcite gangue or rarely in its cavities. Native silver, pyrargyrite, miargyrite and pyrrhotite were observed in this association. Zonality observed in BSE image is caused by moderate changes of Ag/Sb (3.5-3.6) ratio. Very low Hg contents (only up to 0.03 at. %) and Ag (77-78 at. %) and Sb (21-22 at. %) stable contents are characteristic for dyscrasite (III).

Allargentum was described by Knížek et al. (1990) as microscopic grains in outside parts of dyscrasite (II) crystals and as a part of polymineral Ag-Hg-Sb aggregates from the H14F (6^{th} level of mine 21, Háje) vein. It was found newly in the studied material from the veins H14F a H14F3 (mine 21, Háje) as separate phase in the form of up to several mm large aggregates or together with dyscrazite as an important part (more than 50 %) of columnar crystals. The BSE image proves that allargentum is usually always irregularly to mosaic zoned; beside high Hg (0-0.6 at. %) contents, zonality is caused particularly by moderate fluctuation of Ag/Sb ratio in the range 5.8-6.1.

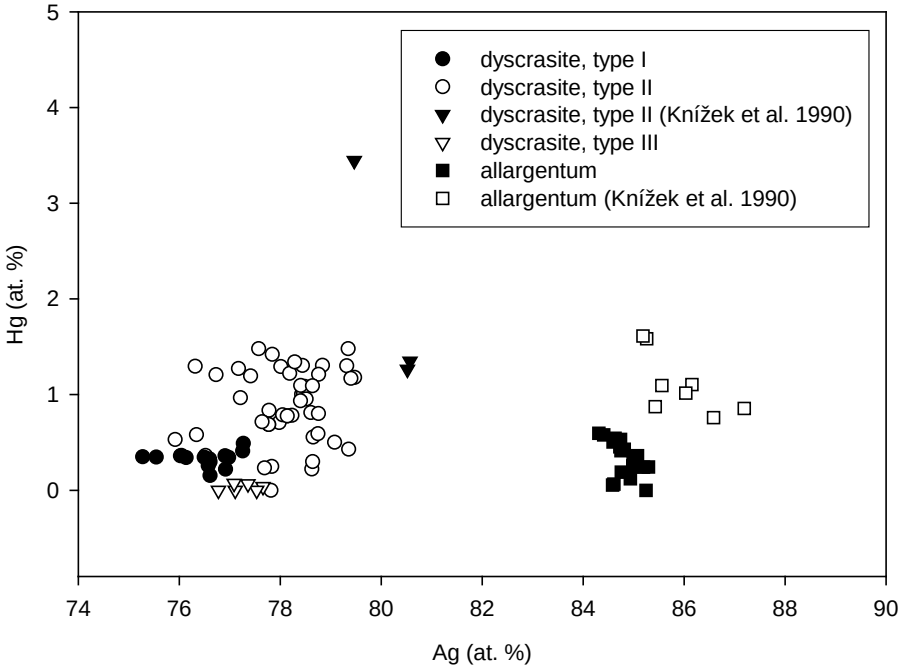

Fig. 2. Graph Ag vs. Hg (in at. %) for dyscrasite and allargentum from the Příbram uranium ore district.

ACKNOWLEDGEMENTS: We thank to D. Ozdín (Faculty of Science, Comenius University, Bratislava) for his kind cooperation. This work was supported by the grant MK00002327201.

KNÍŽEK F., LITOCHLEB J., ŠREIN V., 1990: Dyscrasite and allargentum from the Háje vein bundle of the Příbram uranium deposit. Bull. Geol. Survey, 65, 6: 321-328.

LITOCHLEB J., ČERNÝ P., RŮŽIČKA J., BURDA J., 1984: The mineralogical characteristic of the polymetallic vein with dyscrasite in the ore deposit at Brod near Příbram (central Bohemia). Vlastivěd. Sbor. Podbrdska, 26: 159-173. (in Czech)

MINERALOGIA POLONICA - SPECIAL PAPERS
Volume 28 - 2006

Radek ŠKODA[1], *Renata ČOPJAKOVÁ*[1]

AUTHIGENIC REE MINERALS FROM GREYWACKES OF THE DRAHANY UPLANDS, CZECH REPUBLIC AND THEIR SIGNIFICANCE FOR DIAGENETIC PROCESSES

INTRODUCTION

Rhabdophane-(Ce) and synchysite-(Ce) where found in hydrothermal veins cutting the Culm sediments (Zimák, Novotný 2002; Krmíček et al. 2005). Recently, we found rhabdophane-(Ce), OH-analogue of synchysite-(Ce) and thorogummite in the cement of the Culm greywackes from the Drahany Uplands, Czech Republic.

Rhabdophane is a hexagonal, hydrated phosphate of REE with ideal formula $LREEPO_4.nH_2O$, where *n* ranging from 0.5-1.0. Synchysite is a monoclinic fluorocarbonate REE and Ca with ideal formula $Ca(REE,Y)(CO_3)_2(F,OH)$ and thorogummite is hydrated Th silicate with ideal formula $(Th,U)(SiO_4)_{1-x}(OH)_{4x}$.

Drahany Uplands represent the southern part of the Moravo-Silesian Culm Basin. The sedimentation commenced about 340 Ma, and finished about 325 Ma ago. Franců et al. (1999) proposed diagenetic temperature at about 130-170 °C in the southern part of the basin and at about 170-200 °C in the northwestern part of the basin. The intensity of diagenetic overprint increases from SSE to NNW.

METHODS

REE minerals were examined in detail using a CAMECA SX 100 electron microprobe. Operating conditions were 15 kV an accelerating voltage, a beam current of 10-20 nA and a beam diameter of 5-10 μm. Peak counting times were 20 s for major elements, 30-100 s for minor elements.

RESULTS

Hydrated REE minerals occur at the majority of studied localities, but their participation increase at the NW part and decrease in the SE part of the Drahany Uplands. Rhabdophane-(Ce) and synchysite-(Ce) form aggregates (20-120 μm) of the fine needle-like to tabular crystals. The cavities among their crystals are filled by quartz, clay minerals, calcite, Ti-minerals, Fe-oxide-hydroxides and apatite. Rhabdophane and synchysite are considered as authigenic minerals growing together with other associated minerals during diagenetic processes. Thorogummite forms an individual, porous and inhomogeneous grains X0 μm in size or X μm inclusions in the rhabdophane-(Ce) or synchysite-(Ce). It is considered also as an authigenic mineral.

Rhabdophane-(Ce) is a REE phosphate with analytical totals from 91.5 to 94.8 wt. % of oxide, which correspond to approximately 0.5 to 1.0 apfu of H_2O.

[1] *Joint Laboratory of Electron Microscopy and Microanalysis, Masaryk University and Czech Geological Survey, Kotlářská 2, 611 37 Brno, Czech Republic; rskoda@sci.muni.cz*

Normalization based on 4 anions yields the deficit of the cations in the tetrahedral position (0.91-0.99 *apfu*) and the surplus of cations in the REE position (1.08-1.22). Ce is a dominant REE. Y content ranging from 1.4 to 2.7 wt.% Y_2O_3. Th (1.0-6.6 wt. % ThO_2) predominates over the U (max. 0.2 wt. % UO_2). The content of Ca (5.5-8.5 wt. % CaO) is high as well as Pb (0,2-0,5 wt. % PbO). REE pattern shows strong enrichment in LREE (Fig. 1a). The phosphorus is partially substituted by Si and S (bellow 0.08 *apfu* and 0.06 *apfu* respectively).

Chemical analyses of the Ca, REE fluorocarbonates yielded the synchysite-(Ce) composition. However, the content of F is low (0.38-0.43 *apfu*), and hence OH predominates over F. The REE pattern shows a strong enrichment in LREE (Fig. 1b). Ce is a dominant REE. Content of Y (0.9-2.3 wt. % Y_2O_3), Th (0.0-3.3 wt. % ThO_2) and U (<0.2 wt. % UO_2) are low.

Composition of the Th-rich phases corresponds to P-rich thorogummite (P is 0.32-0.42 *apfu*). Analyses normalized on 4 anions are stoichiometric or with slight surplus in the Th-site. U content is relatively high 0.9-3.3 wt.% UO_2 in comparison with other authigenic minerals. In the Th-site enters Y (up to 0.24 *apfu*), contents of REE do not exceed 0.09 *apfu*. The REE pattern shows enrichment in HREE (Fig. 1c). Low content of F enters instead of the OH (<0.1 *apfu*).

CONCLUSIONS

Rhabdophane-(Ce) shows a low variation of REE, Y, Th, and U and a similar shape of the REE pattern. Hence, we take in account origin in similar p-T-X conditions. The same stands for OH-analogue of synchysite-(Ce).

The REE pattern of rhabdophane-(Ce) is identical with a majority of the detrital monazite-(Ce) in comparison with the OH-analogue of synchysite-(Ce), which is more depleted in HREE (for detrital monazite composition see Čopjaková, Škoda, 2006). Content of U and Th in rhabdophane-(Ce) and OH-analogue of synchysite-(Ce) are lower than in monazite-(Ce). The U and Th preferentially enter the thorogummite forming frequent inclusions in rhabdophane-(Ce) and OH-analogue of synchysite-(Ce). Relatively high Pb and low U and Th content in the rhabdophane-(Ce) in comparison to the detrital monazite-(Ce) (Fig. 1d) suggest an incorporation of the Pb into the rhabdophane structure. Only traces of Pb can be radiogenic owing to low U, Th content in authigenic (<325 Ma) rhabdophane-(Ce).

The sources of the REE for authigenic REE minerals were REE bearing minerals unstable under sedimentary conditions. One of the important LREE source appears to be monazite-(Ce) (Čopjaková, Škoda 2006). Allanite-(Ce) occurs only scarcely in some of granitic pebbles. Part of the HREE can originate from the detrital garnet and biotite. Garnet is frequently conspicuously corroded, and the biotite is completely chloritized and both occur in large quantities. Detrital apatite appears to be stable under diagenetic conditions in the Culm sediment. Based on the chemical composition of the authigenic REE minerals, we consider diagenetic fluids relatively rich F, Ca, CO_2 a P. P was probably released from feldspars and phosphates. F can predominantly originate from altered biotite.

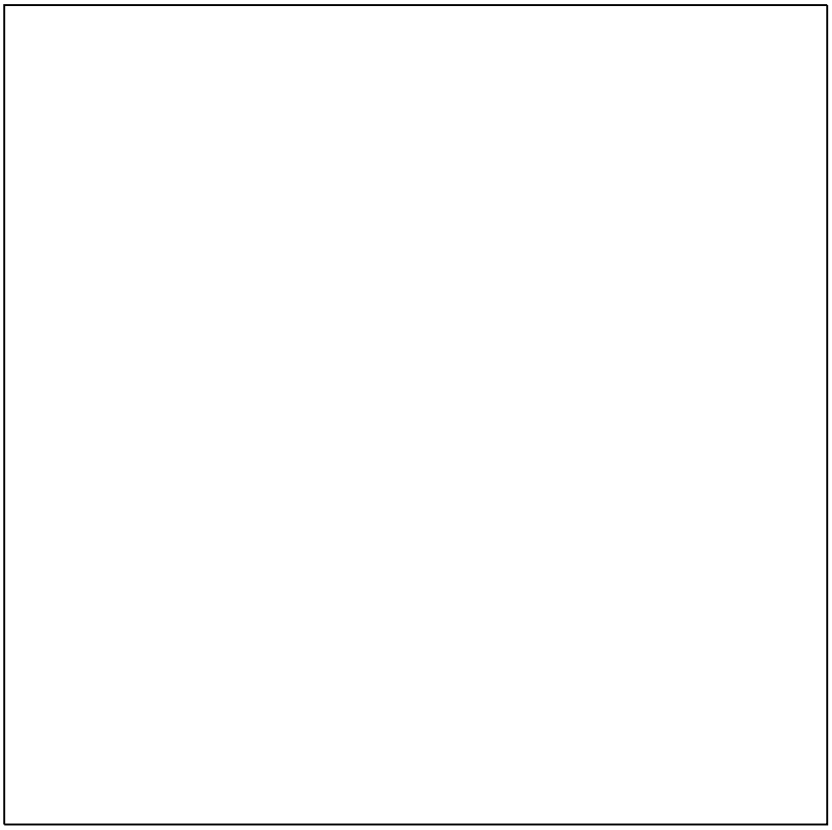

Fig. 1a-c. Chondrite normalized REE patterns. Grey area stands for values bellow detection limit of EMP; a) dark grey field – rhabdophane-(Ce) (short dashed area - field of monazite from greywackes is marked in a-c plots for comparison), b) dark grey field – OH-analogue of synchysite-(Ce); c) thorogummite; d) comparison of the average, minimal and maximal content of Th, U and Pb (apfu) from rhabdophane-(Ce) and detrital monazite-(Ce).

ACKNOWLEDGEMENTS: Financial support from the internal project of the CGS 3316 is gratefully acknowledged.

REFERENCES

ČOPJAKOVÁ R., ŠKODA R., 2006: Monazite hydrothermal alteration during high-temperature diagenesis of the greywackes from the Drahany Uplands (Bohemian Massif, Czech Republic). Miner. Polon., this volume.

FRANCŮ E., FRANCŮ J., KALVODA J., 1999: Illite crystalinity and vitrinite reflectance in Paleozoic siliciclastics in the Bohemian Massif as evidence of thermal history. Geol. Carpath., 50: 65-71.

KRMÍČEK L., SULOVSKÝ P., HALAVÍNOVÁ M., 2005: Výskyt minerálů vzácných zemin na hydrotermálních žílách Drahanské vrchoviny. Geol. Výzk., Mor. Slez. v R. 2004, 12: 64-68.

ZIMÁK J., NOVOTNÝ P., 2002: Minerály vzácných zemin na hydrotermálních žilách v kulmu Nízkého jeseníku a Oderských vrchů. Čas. Slez. Muz. Opava (A), 51: 179-182.

MINERALOGIA POLONICA - SPECIAL PAPERS
Volume 28 - 2006

Stanislav ŠOLTÉS[1], Otília LINTNEROVÁ[1], Peter ŠOTTNÍK[1]

COPIAPITE GROUP AND HALOTRICHITE IN OLD MINE HEAPS NEAR SMOLNÍK

INTRODUCTION

Old mining town Smolník (eastern Slovakia) and surrounding countryside is well known with its mining wastes and acid water accident in 1994. Pyrite-chalcopyrite mines were mined for centuries till 1991. There is also a lot of old mine heaps near Smolník. We can observe consequences of pyrite weathering and production of acid mine waters (AMD) in pyrite rich heaps. Secondary minerals formation is the result of these processes.

METHODS

Mineralogy of samples was determined by PXRD analysis on diffractometer PHILIPS PW 1710 (Geological Institute SAV, Bratislava). Analytical conditions are following: Cu radiation, scan step size 0.02° 2Θ, accelerating voltage 20 kV, current beam 40 mA. Morphology of gold coated samples was studied in backscattered-electrons (Faculty of Natural Sciences, Comenius University, Bratislava).

RESULTS

Secondary minerals occur on the surface of old mine heaps. Yellow and white coatings and their admixtures are the most frequent types in environs of abandoned Smolník mine.

Mainly aluminocopiapite $Al_{2/3}Fe^{3+}_4(SO_4)_6(OH)_2 \cdot 20H_2O$, copiapite $Fe^{2+}Fe^{3+}_4(SO_4)_6(OH)_2 \cdot 20H_2O$ and slavíkite $NaMg_2Fe^{3+}_5(SO_4)_7(OH)_6 \cdot 33H_2O$ were detected by XRD study in dominantly dark yellow samples (Fig. 1). In the white samples was detected only halotrichite $Fe^{2+}Al_2(SO_4)_4 \cdot 22H_2O$ (Fig. 3) with clear peaks at 4.77 and 3.47 Å.

Surface morphology of secondary minerals in white and yellow samples is different. Copiapite-aluminocopiapite forms tabular crystals (Fig. 2). Slavíkite forms long acicular crystals (Fig. 2). Halotrichite in white samples forms fibrous crystals often bounded together in groups (Fig. 4).

REFERENCES

Berry L.G. (ed.), 1974: Selected powder diffraction data for minerals, Philadelphia, JCPDS.

[1] *Department of Economic Geology, Faculty of Natural Science, Comenius University, Mlynská dolina G, 842 15 Bratislava, Slovak Republic; soltes@fns.uniba.sk*

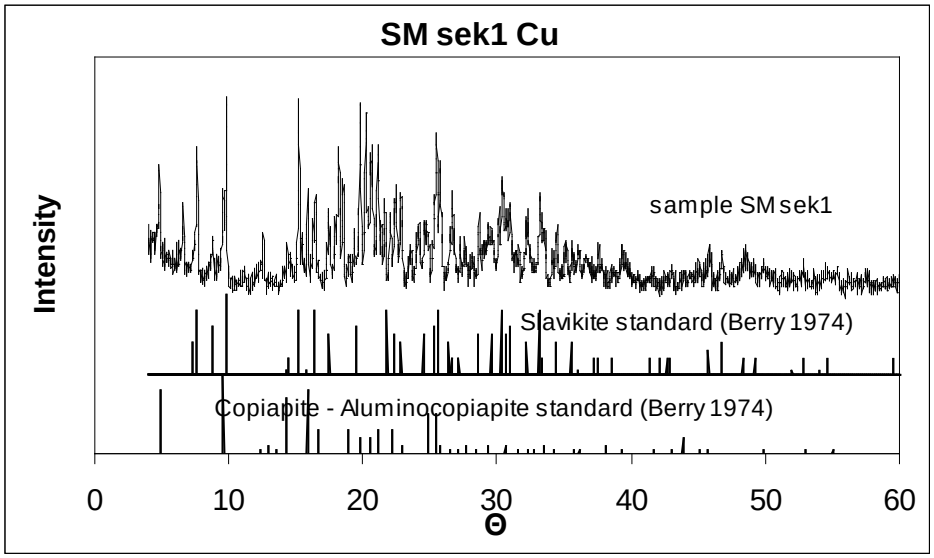

Fig. 1. XRD pattern from yellow sample SM sek1 and diffraction pattern of copiapite – aluminocopiapite (JCPDS 20.659) and slavikite (JCPDS 20.679) (standard Berry 1974).

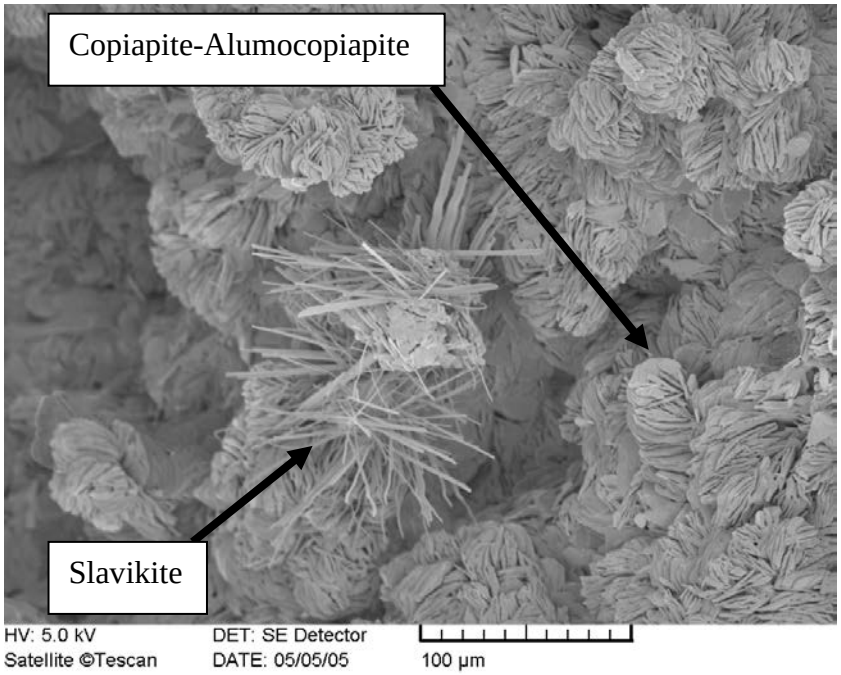

Fig. 2. Yellow sample SMsek1, copiapite-alumocopiapite and slavikite, backscattered-electron image.

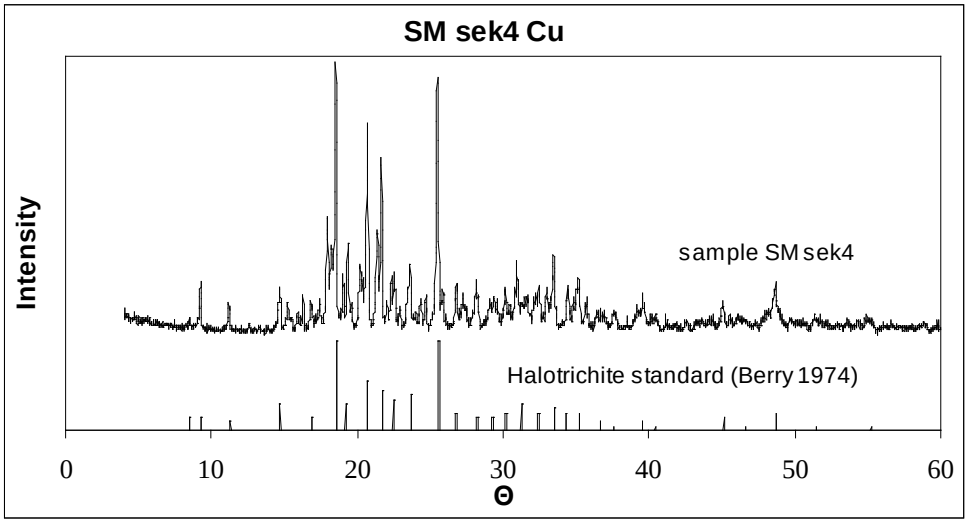

Fig. 3. XRD pattern from white sample SM sek4 and diffraction pattern of halotrichite (JCPDS 11.506) (standard Berry 1974).

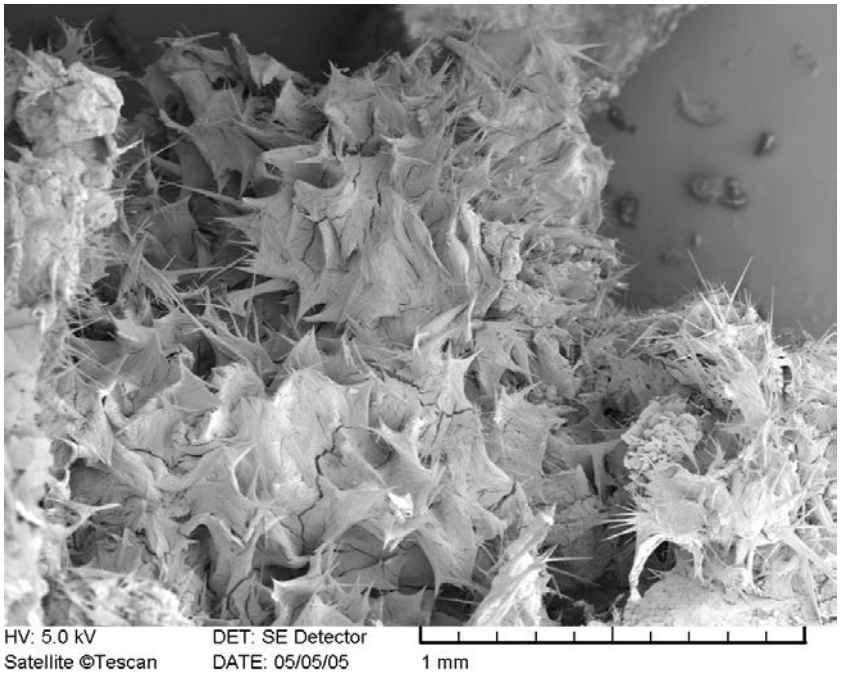

Fig. 4. White sample SMsek4, halotrichite, backscattered-electron image.

MINERALOGIA POLONICA - SPECIAL PAPERS
Volume 28 - 2006

Jana SUCHÁNKOVÁ[1], Jaromír LEICHMANN[1]

SUBSOLIDUS EVOLUTION OF JIHLAVA ULTRAPOTASSIC PLUTON, EVIDENCE FROM THE STUDY OF SECONDARY MINERALS

INTRODUCTION

Ultrapotassic rocks of the Jihlava pluton are geochemical similar to the durbachites (Holub 1997). The rocks of the Jihlava pluton (Bowes, Košler 1993, Kotková et al. 2003, Leichmann et al. 2005) are characteristic by high content of MgO (4 - 20 wt. %) and K_2O (2.5 - 6 wt. %). The K_2O/Na_2O ratio is usually higher than 2. The rocks are rich in Cr, Rb, Ba, Th and U. Rocks of the Jihlava pluton diverge from typical durbachites mainly by the structure and mineral composition. Rocks from Jihlava pluton are equigranular, whereas typical durbachites are porphyritic. Durbachites are Bt - Amf- bearing, whereas the rock from Jihlava pluton contain commonly Opx and Cpx, apart from biotite and amphibole. They could be classified as pyroxene-bearing monzogabbros, monzonites, melasyenites and melagranites. However syenites are most wide-spread. Jihlava pluton forms elongated body in NNW-SSE direction in the eastern Moldanubian Zone. The rocks of the Jihlava pluton were dated using U-Pb method on 335.2 ± 0.54 Ma (Kotková et al. 2003).

RESULTS

The studied samples come from Kosov quarry approximately 4 km southeast from the city of Jihlava. These rocks are dark, coarse-grained syenites, containing clinopyroxene, orthopyroxene, amphibole, biotite, perthitic K-feldspar, plagioclase and variable amount of quartz. Accessory minerals are represented by rutile, ilmenite, apatite, allanite, monazite, zircon and titanite. Rutile forms needle-like inclusion in both feldspar and Opx. Allanite-(Ce) is localy replaced by monazite-(Ce). Apatite, monazite-(Ce) and zircon form inclusion in mafic minerals mainly. Cathodoluminescence (CL) and electron-microscope study (EMS) were used to observed mineral reaction between the rock forming minerals.

Pyroxenes, K-fel dspar (Kfs), plagioclase are typical primary magmatic minerals. Perthitic Kfs are characterized by oscillatory zoning, nicely visible in CL. EMS study confirms that the zones of high CL intensity are enriched on BaO (up to 3.5 wt. %). The perthites in Kfs are An-rich (An_{35-42}). Plg display a normal continuous zoning, the core of plagioclase is An rich (An_{55}) and the rim is An poor (An_{40}). Clinopyroxene (Cpx) corresponds to augite, and exibit variable X_{Mg} = 0.70 to 0.84. Cpx contains admixtures of orthopyroxene (Opx). Orthopyroxene (X_{Mg} = 0.60) with Cpx admixtures is more seldom. Locally, Opx is hydrated and replaced by cumming-tonite. Farther reaction between Opx and Kfs forming biotite (Bt) and quartz (Qtz) is more common. Because of Opx contain admixtures of Cpx, and Kfs of Plg, small amount of amphibole originated during this reaction in addition. The

[1] *Institute of Geological Sciences, Masaryk University, Kotlářská 2, 611 37 Brno, Czech Republic; ja.su@mail.muni.cz*

contact between Opx and Kfs is locally rimmed by Qtz-Bt symplektites. Antophyllites appears as a later filling of the cracks in Opx.

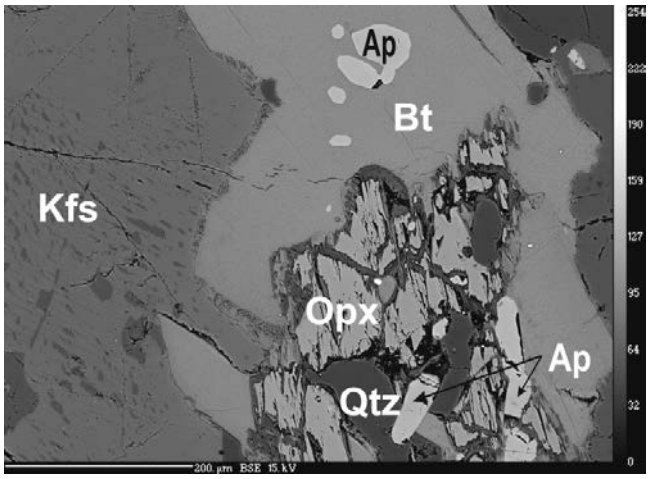

Fig.1. Reaction between Opx and Kfs (abbreviations see the text).

Cpx (X_{Mg} = 0.82 – 0.84) are replaced often by actinolithic hornblende (X_{Mg} 0.50-0.76) and Bt too. Bt is subhedral or lobate, X_{Mg} is variable (0.49-0.68). Bt appears mainly along the contact between Cpx and Kfs. Syenites are commonly intruded by leukogranitic veins. Mafic mineral in syenites are almost totally replaced by Bt along such contact. Tourmaline (uvite-dravite) forms a rim parallel with the contact on the granite site. Syenites are also penetrated by numerous very thin veins formed by Qtz+anthophyllite or Qtz+epidote. Biotite is locally replaced by chlorite and Plg by prehnite+albite.

CONCLUSIONS

Observed reactions indicate polyphase evolution of the Jihlava pluton. Four main phases could by define.

The first - magmatic phase is characterized by crystallization of primary magmatic minerals, such as perthitic Kfs, An rich Plg, Cpx, and Opx. This mineral assembly association is typical for dry granulite-facies conditions. Recaltulated composition of perthitic Kfs indicate temperatures around 1000-1100°C for the monzodiorites. The primary magma was probably dry and intruded in the lower crust conditions at 335.2 ± 0.54 Ma.

The second phase is characterized by the first hydration. Opx was replaced by Bt and cummingtonite, Cpx by actinolite and Bt. Pyroxene alteration is characterized by strong redistribution of Fe and Mg. High TiO_2 content in biotite indicates, that reaction was still relatively high temperature (Sengputa et al. 1999). The fluids responsible for the hydration could originate (i) during rapid exhumation

of the rock from granulite to amphibolite facies conditions or, (ii) were associated with intrusions of leucogranites.

For third phase is associated with intrusion of leucogranites. It is characterized by forming of tourmaline at the contact between leucogranite and syenite. Primary mafic minerals were replaced by Bt during this stage.

The fourth phase is followed by hydration again. Chlorite replaces biotite, prehnite plagioclase and antophylite Opx. The anthophylite-epidote-Qtz veins are related to this phase too. Infiltration of aqueous fluids in greenschist facies is high probably responsible for this stage.

Sequence of such reactions with common relics of the high temperature event could indicate rapid exhumation of Jihlava pluton as evidenced from kinzigite xenolites from the Jihlava pluton (Leichmann et al. 2006).

REFERENCES

BOWES D., KOŠLER J., 1993: Geochemical comparison of the subvolcanic appinite suite of the Central – European Hercynides – evidence for associated shoshonitic and granitic magmatism. Mineral. Petrol., 48: 47-63.

HOLUB F. V. 1997: Ultrapotassic plutonic rocks of the durbachite serie in the Bohemian Massif: Petrology, geochemistry and petrogenetic interpretetion.- Sbor. Geol. Věd Ložisk. Geol. Mineral., 31: 5-26.

KOTKOVÁ J., SCHALTEGGER U., LEICHMANN J., 2003: 338-335 Ma old intrusions in the E Bohemian massif - a relict of orogen - wide durbachitic magmatism in European Variscides. J. Czech Geol. Soc., 48: 80-81.

LEICHMANN J., NOVÁK M., BURIÁNEK D., BURGER, D., 2006: Garnet-sillimanite-cordierite kinzigite and garnet- migmatites from Petrovice, Jihlava pluton; Evidence for high temperature metamorphism related to durbachite intrusion.Geol. Carpath. (submitted).

SENGUPTA P. S. J., DASGUPTA S., RAITH M., BHUI U. E. J., 1999: Ultra-high temperature metamorphism of metapelitic granulites from Khondapalle, Eastern Ghats belt: Implications for the Indo-Antarctic correlation. J. Petrol., 40: 1065-1087.

MINERALOGIA POLONICA - SPECIAL PAPERS
Volume 28 - 2006

Petr SULOVSKÝ[1]

ALTERATION OF ALLANITE-(Ce) IN TŘEBÍČ PLUTON, BOHEMIAN MASSIF

INTRODUCTION

Allanite represents the principal primary host for LREE in weakly peraluminous granites of I- and S-type affinity. In many of its occurrences, allanite is metamict and/or altered. Depending on the timing of late magmatic or hydrothermal alteration and nature of fluids causing the allanite alteration textures are very variable (see e.g. Poitrasson 2002). A specific "onion-shell" type texture was first described in detail from the Třebíč durbachite pluton in SW Moravia.

METHODS

Allanite-(Ce) containing durbachite samples were taken from natural outcrops within a large study focused on the discrepancy of actinide distribution in rocks and heavy mineral assemblages in stream sediments (Sulovský 2002). The polished thin sections were first scanned for REE minerals using EDS and BSE imaging, and their detailed chemistry (including Th, U and Pb data for CHIME dating of monazite) was studied by WDS with electron microprobe Cameca SX100. More detailed images were obtained with FEG-SEM.

RESULTS

The onion-shell texture formed in allanites with all kinds of primary zoning – oscillatory, sectorial as well as patchy (Fig. 1). It consists of a series of alternating concentric zones with contrasting BSE signal (Fig. 2). A closer view shows that the brighter zones rim very thin fissures (Fig. 3); the former appear to be composed of submicroscopic crystals (Fig. 4). This texture often occurs across the whole grain - or it is confined just to a specific zone or sector with specific composition, probably originally richer in radiogenic elements. Its resemblance to the perlitic texture known from volcanic glass probably indicates that allanite during metamictization must have reached the glassy state; subsequent alteration hydrothermal fluids only served as a "developer" visualizing the perlitic texture.

In metamict minerals, the time necessary for accumulation of the radiation damage causing complete amorphisation is calculated from the equation

$D\alpha = 8N_{238U}(e^{\lambda 238Ut}-1) + 7N_{235U}(e^{\lambda 238Ut}-1) + 6N_{232Th}(e^{\lambda 232Tht}-1)$ (Murakami et al. 1993), where $D\alpha$ is the number of alpha disintegrations per miligram of mineral, N_x is the number of atoms of the isotope x and λ_x is the decay constant of isotope x. If we would suppose that the critical dose for complete metamictisation is the same for allanite as that for zircon ($7 – 13.10^{15}$ decay events per mg of mineral), for average Th (1.1 wt. %) and U (0.27 wt. %) contents in allanite from Třebíč Pluton durbachites, the time for accumulation of such a dose would be 60 ± 4 Ma.

[1] *Institute of Geological Science, Masaryk University, Kotlářská 2, 611 37 Brno, Czech Republic; sulovsky@sci.muni.cz*

Anyway, the occurrence of durbachite pebbles with allanite having perlitic texture in the nearby Drahany Culm basin agglomerates, known to sediment about 325 Ma (Gradstein, Ogg 1996), narrows the time span between the emplacement of durbachites of the Trebic Pluton (around 340 Ma – measured with CHIME method by the author) and their alteration to maximum 15 Ma. This interval strongly contrasts to the time needed for complete metamictization, mentioned above. This discrepancy might can be explained by the critical alpha dose necessary for allanite amorphisation being much lower than in zircon. The critical dose for amorphisation, calculated from this 15 Ma time interval is at least $2.2 \pm 0.2.10^{14}$ decay events per miligram, i.e. 55 times lower than in zircon.

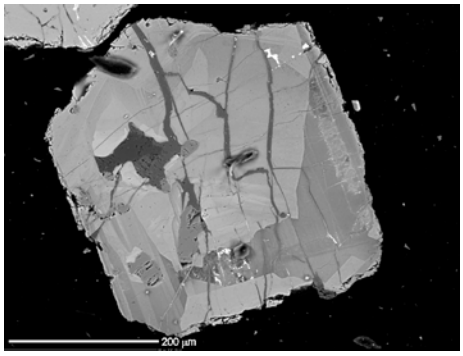

Fig. 1. Allanite-(Ce) grain with a combination of sectorial, growth, and patchy zoning. BSE, SX100.

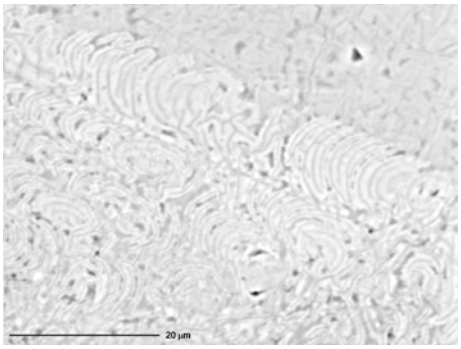

Fig.2. Subparallel perlitic parting in altered metamict allanite-(Ce). BSE, SX100.

Fig.3. Close-up of the perlitic texture, overprinted by alteration and recrystallization. FEG-SEM, Jeol.

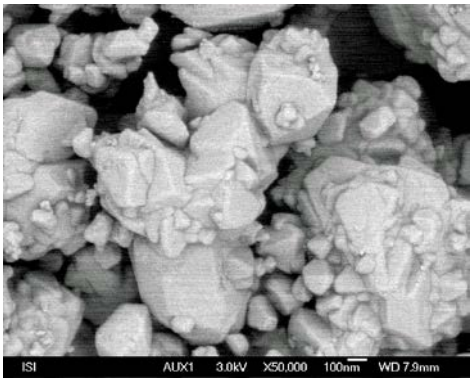

Fig.4. Microcrystalline nature of bright rims along perlitic fissures like those in Fig. 3. FEG-SEM, Jeol.

The (seldom occurring) portions of unaltered allanite can be characterized as Ce-dominant allanite. An example of a whole-grain analysis (obtained from a network of touching large-spot EMPA analyses) is presented in Table 1, together with average analyses of the dark and bright phases:

	SiO_2	TiO_2	Al_2O_3	Cr_2O_3	V_2O_3	FeO	MnO	CaO	MgO	Na_2O
Area	34.40	2.51	13.51	0.27	0.17	9.10	0.37	7.66	0.95	0.15
Dark	33.9	3.16	12.76	0.353	0.18	9.116	0.37	7.05	0.69	0.167
Bright	34.1	2.5	14.00	0.275	0.16	9.749	0.35	8.41	1.00	0.135
	La_2O_3	Ce_2O_3	Pr_2O_3	Nd_2O_3	Sm_2O_3	Gd_2O_3	ThO_2	UO_2	F	Total
Area	6.05	10.47	0.93	2.64	0.32	0.82	1.18	0.25	0.33	69.08
Dark	6.07	9.55	0.79	2.215	0.28	0.77	2.01	0.48	0.31	91.50
Bright	6.85	10.9	0.89	2.5	0.306	0.89	1.42	0.31	0.39	96.37

Compared with analyses of the brighter phase, the dark one has lower totals, higher Na, Th, and U contents and is depleted in REE, Al, Ca and Mg; Fe remains unchanged. The slope of REE patterns is very similar in both dark and bright phases and does not indicate substantial REE fractionation, although the REE fluorocarbonates associated with altered allanite have sometimes (esp. in samples where the alteration fluids were strongly oxidative, as evidenced by the occurrence of secondary CeO_2 and ThO_2) slight negative Ce anomaly. Allanite REE patterns do not differ in slope from those of jointly occurring primary, non-altered monazite.

CONCLUSIONS

The analogy with texturally similar parting in rhyolitic glass most probably indicates that in the course of metamictization, allanites with this “onion-shell” texture have reached glassy state. Further ageing of glassy allanite led to the development of concentric perlitic cracks. The expansion of the outer rind has further opened these fractures and made them migration paths for hydrothermal fluids. These have leached out many components, which have migrated and precipitated within the allanite grains as well as in substantial (mm- to cm- range) distance from their source. The fact that under the action of F-rich fluids U, Th and REE (as analogues to fissiogenic elements) can be mobilized and transported by percolating fluids represents an important aspect in the decision process considering the deep deposition of radioactive waste.

REFERENCES

GRADSTEIN F.M., OGG J.G., 1996: A Phanerozoic time scale. Episodes, 19: 3-19.

MURAKAMI T., CHAKOUMAKOS B.C., EWING R.C., LUMPKIN R.G., WEBER R.G.J., 1993: Alpha decay event damage in zircon. Am. Mineral., 76: 1510-1532.

POITRASSON F., 2002: In situ investigations of allanite hydrothermal alteration: examples from calc-alkaline and anorogenic granite sof Corsica (southeast France). Contrib. Mineral. Petrol., 142: 485-200.

SULOVSKÝ P., 2002: Accessory minerals of the Třebíč durbachite massif (SW Moravia). Miner. Slov., 33: 467-472.

MINERALOGIA POLONICA - SPECIAL PAPERS
Volume 28 - 2006

Eligiusz SZEŁĘG[1]

RUTILE-TITANITE MINERALIZATION FROM GŁUCHOŁAZY (EASTERN SUDETES, POLAND)

INTRODUCTION

Rejvíz and Vrbno are two metamorphic series occur in Głuchołazy region. They belong to Moravo-Silesian crystalline units and form NE cover of Děsná and Praděd crystalline massifs (Czech Republic) (Muszyńska 1989). Metabasites (matadiabases, amphibolites and greenstones) are present within those series (Souček 1978). In Polish part, metabasites occur in the Rejviz series (Muszyńska 1989). The Rejvíz series consists of fine-grained biotitic gneisses, biotitic paragneisses, quartzites and mica-schists (Sawicki 1970). Metabasites were produced as a consequence of metamorphism of volcanoclastic basic rocks (Majerowicz, Sawicki 1958; Sawicki 1972).

Muszyńska (1989) described the quartz-epidote rock, which forms lenses within fine-grained biotitic gneiss in old quarry in Biała Głuchołaska Valley. The rock was metamorphosed in amphibolite facies. Muszyńska reported on leucoxene forms irregular blasts with opaque core.

SAMPLE DESCRIPTION

Samples of amphibole bearing quartz-epidote rock were collected from a big lens (1 m in length) within fine-grained biotitic gneisses in old quarry in Biała Głuchołaska Valley, about 200 m to Polish-Czech boundary. White quartz, light-green epidote and dark-green amphibole are main rock-forming minerals. In accessory mineral group one can distinguish zoisite, apatite, rutile and titanite. The Ti-mineralization was found in core of amphibole bearing quartz-epidote lens.

METHODS

The images by secondary electrons (SE) were carried out using ESEM – XL 30 TMP (Philips/FEI) scanning electron microscope at the Faculty of Earth Sciences, University of Silesia, Sosnowiec, Poland. Electron-probe microanalyses in the wavelength-dispersive scans (WDS) mode were performed using a JEOL JXA-8600 Superprobe at the Department of Geology, Aarhus University, Denmark.

RESULTS

Back-scattered electron (BSE) images reveal complicated structure of rutile, differ in optical and chemical properties (Fig. 1). Chemical composition of rutile from Głuchołazy is given in Table 1. Number of atoms was calculated based on 1 cation. Pure rutile forms core of blasts, whereas Fe-bearing rutile with inclusions

[1] *Department of Geochemistry, Mineralogy and Petrography, Faculty of Earth Sciences, University of Silesia, Będzińska 60, 41-200 Sosnowiec, Poland; szeleg@wnoz.us.edu.pl*

of ilmenite forms rims (Fig. 1a, b). Both types of rutile form intergrowths in transitional zone. Small grains of Nb,Fe-bearing rutile were observed.

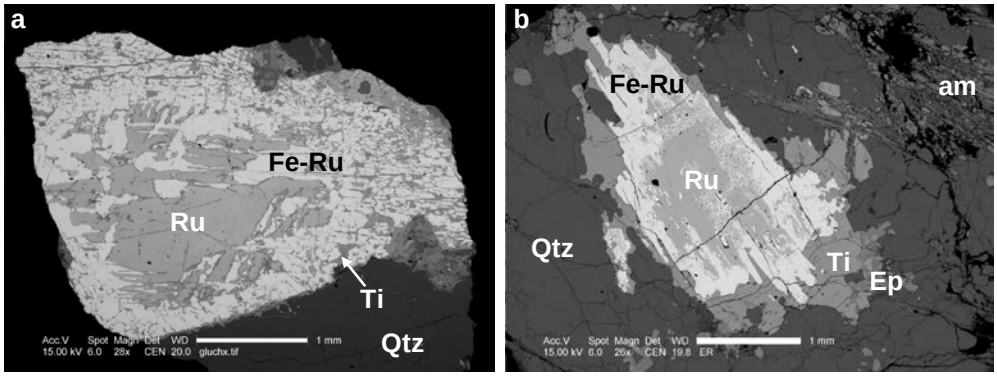

Fig. 1. **a:** intergrowths of pure rutile (Ru), Fe-bearing rutile (Fe-Ru), and titanite (Ti) in quartz (Qtz); **b:** secondary titanite rim (Ti) on pure rutile (Ru) and Fe-bearing rutile (Fe-Ru) with quartz (Qtz), epidote (Ep) and amphibole (am). BSE images.

Table 1. Chemical composition of rutile from Głuchołazy, wt. %.

	1	2	3	4
Nb_2O_5	6.49	4.20	1.60	0.30
Ta_2O_5	0.01	0.08	0.01	0.02
SiO_2	n.d.	n.d.	0.01	0.01
TiO_2	91.24	95.23	97.77	100.76
SnO_2	n.d.	0.02	0.02	0.02
Al_2O_3	0.03	0.03	0.02	0.02
Fe_2O_3*	3.17	2.15	1.34	0.79
Y_2O_3	0.01	0.01	n.d.	n.d.
CaO	0.01	n.d.	n.d.	0.01
Total	100.96	101.72	100.77	101.93
Ti	0.93	0.95	0.98	0.99
Nb	0.04	0.03	0.01	
Fe^{3+}	0.03	0.02	0.01	0.01

*Total iron content given as Fe_2O_3, 1-3 – Nb,Fe-bearing rutile, 4 – pure rutile

Titanite replaces rutile and forms rims on it (Fig. 1b). BSE images did not reveal compositional zoning in the titanite. Chemical composition of titanite is given in Table 2. Number of atoms was calculated based on 3 cations. The titanite contains medium concentrations of Al and Fe^{3+} (up to 0.08 and 0.03 apfu, respectively). Small concentration of Nb (up to 0.01 apfu) was measured only in the one point.

Table 2. Chemical compositions of titanite from Głuchołazy, wt. %.

	1	2	3	4	5	6	7	8
Nb_2O_5	0.27	0.09	0.31	0.06	n.d.	0.62	0.12	0.08
Ta_2O_5	0.10	0.17	0.18	0.13	0.14	0.18	0.15	0.12
SiO_2	30.13	30.75	29.92	30.42	29.98	30.14	30.93	30.55
TiO_2	38.00	37.34	37.58	36.73	37.71	37.21	37.28	37.28
SnO_2	n.d.	0.01	0.05	0.03	n.d.	0.03	n.d.	n.d.
Al_2O_3	1.34	1.90	1.81	2.16	1.48	1.81	1.85	1.98
$Fe_2O_3^*$	0.69	0.87	0.86	1.02	0.78	0.86	0.84	0.94
Y_2O_3	n.d.	n.d.	0.07	0.02	n.d.	0.01	n.d.	0.05
CaO	27.83	28.83	28.24	28.26	28.23	28.11	28.50	27.99
Na_2O	n.d.	0.01	n.d.	n.d.	0.01	n.d.	n.d.	n.d.
Total	98.36	99.97	99.02	98.83	98.33	98.96	99.68	98.99
Ca	0.99	1.00	0.99	0.99	1.00	0.99	0.99	0.98
Ti	0.94	0.91	0.93	0.90	0.94	0.92	0.91	0.92
Nb						0.01		
Al	0.05	0.07	0.07	0.08	0.06	0.07	0.07	0.08
Fe^{3+}	0.02	0.02	0.02	0.03	0.02	0.02	0.02	0.02
Si	1.00	0.99	0.98	1.00	0.99	0.99	1.00	1.00

*Total iron content given as Fe_2O_3

CONCLUSIONS

Nearly pure rutile, Fe-bearing rutile, Nb,Fe-bearing rutile and ilmenite are probably a product of recrystallization and two-partial replacement of primary homogeneous rutile. Titanite is a secondary mineral. The titanite rims on rutile is a common decompression texture in high-P rocks (Ghent et al. 1993). But in this case is more probably, that it is a product of Ca-metasomatism of the amphibole bearing quartz-epidote rock.

REFERENCES

GHENT E.D., STOUT M.Z., ERDMER P., 1993: Pressure-temperature evolution of lawsonite-bearing eclogites, Pinchi Lake, British Columbia. J. Metam. Geol. 11: 279-290.

MAJEROWICZ A., SAWICKI L., 1958: Wschodniosudeckie serie metamorficzne w rejonie Głuchołazów. Biul. Inst. Geol., 127: 37-121.

MUSZYŃSKA J., 1989: Petrografia metabazytów okolic Głuchołaz (Sudety Wschodnie). Acta Univ. Wratisl., Prace Geol. Miner., XV (1053): 63-90.

SAWICKI L., 1970: Mapa geologiczna 1:25 000, arkusz Podlesie. Wyd. Geol., Warszawa.

SAWICKI L., 1972: Objaśnienia do mapy geologicznej, arkusz Podlesie. Wyd. Geol., Warszawa.

SOUČEK J., 1978: Metabazity vrbenské a rejvizské serie, Hrubý Jeseník. Acta Univ. Carol. Geol., 3-4: 323-349.

MINERALOGIA POLONICA - SPECIAL PAPERS
Volume 28 - 2006

Agata SZWAKOPF [1,2], Jerzy CZERNY [1]; Maciej MANECKI [1]

THE AGE OF MONAZITES FROM THE DEILEGGA AND SOFIEBOGEN GROUP ROCKS, S PART OF WEDEL JARLSBERG LAND, SPITSBERGEN

INTRODUCTION

The Torellian unconformity (Birkenmajer 1975) separates the metamorphic complex of the N tectonic block of the S part of Wedel Jarlsberg Land on Spitsbergen into two structural stages (Czerny et al. 1993). A thick sequence of folded metasediments (phyllites, laminated quartzite schists and quartzites with single intercalations of carbonate rocks) occurring below this unconformity belong to the Deilegga Group. The series of metasediments (metaconglomerates, carbonate rocks, phyllites) and metavolcanites (greenstones) overlying discordantly by the unconformity have been included into the Sofiebogen Group. Rocks of both groups have been metamorphosed to greenschist facies (Czerny et al. 1993). The Ar/Ar age of muscovite from Sofiebogen Group (432 Ma) points to Caledonian metamorphism (Manecki et al. 1998).

To date, the age of the Torellian unconformity is undetermined. Monazite dating of Deilegga and Sofiebogen group rocks presented in this paper has shed light to this problem.

METHODS

Twenty four samples of metaconglomerates (Sofiebogen Group) and phyllites (Deilegga Group) were examined with petrographic microscope. After qualitative analyses performed with the use of scanning electron microscopy (HITACHI S4700 in the Institute of Geological Sciences of Jagiellonian University in Cracow, Poland), five samples were chosen for age determinations. The monazites were analysed using Cameca SX-100 electron microprobe in the Electron Micronalysis Department of Geological Survey of Slovak Republic in Bratislava, under analytical conditions: 20 kV, 130 nA, 2 μm, 100 seconds and with age calculation after Montel (1996) with the use of DAMON software (Konečný et al. 2004).

RESULTS

The age determinations were performed on monazite-(Ce) grains in the matrix of green, yellow and brown metaconglomerates of Sofiebogen Group (4 samples) and within phyllites of Deilegga and Sofiebogen groups (2 samples). 48 monazite grains were analyzed. Mostly, anhedral monazites are 10–40 μm in size and

[1] *AGH - University of Science and Technology, Faculty of Geology, Geophysics and Environmental Protection, Department of Mineralogy, Petrography and Geochemistry, Al. Mickiewicza 30, 30-059 Krakow, Poland; gatkasz@o2.pl*

[2] *Department of Mineralogy and Petrology, Faculty of Natural Sciences, Comenius University, Mlynská dolina, 842 15 Bratislava, Slovak Republic*

occasionally show irregular zonation. They contain 0,13 – 10,29 wt.% ThO_2 and 0,001–2,01 wt.% UO_2.

In all samples detrital monazites prevail. Younger, metamorphic ages were obtained from outer zones of detrital monazites or, rarely, from small individual grains. Detrital monazites from Deilegga Group phyllites represent wide age range: 2760-2360 Ma, 1680-980 Ma. Sparse detrital monazites from Sofiebogen Group rocks yielded 1880-1800 Ma, 1560-1480 Ma and 900-1180 Ma dates. However, metamorphic ages in all analysed rocks are similar and show two metamorphic events: Caledonian (540-420 Ma ages) and Kadomian/Baikalian (700-560 Ma; Fig. 1).

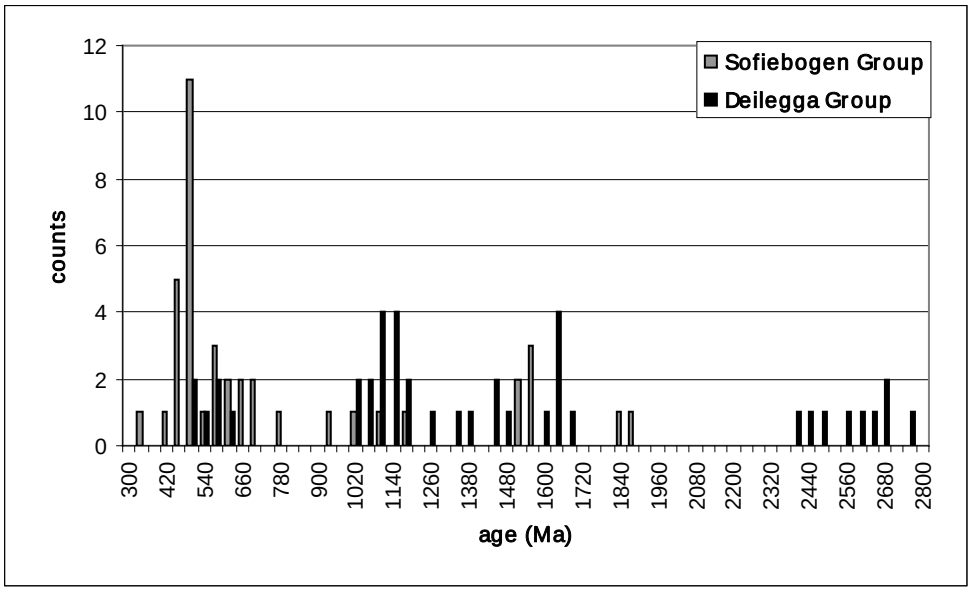

Fig. 1. Age histograms of ages yielded by monazites from Deilegga and Sofiebogen Groups.

CONCLUSIONS

Monazite ages determined in the Slyngfjellet metaconglomerates and the Deilegga phyllites indicate common metamorphic history of rocks on both sides of Torellian unconformity. There is no evidence for Grenvillian metamorphism of the Deilegga Group rocks, as suggested by Balashov et al. (1996). The Deilegga and Sofiebogen Group rocks were metamorphosed during Caledonian orogeny, as it is indicated by 540-420 Ma monazite dates. Ages ranging from 700 to 560 Ma may suggest a heating event corellated with metamorphism in the southern terrane of the S part of Wedel Jarlsberg Land (Manecki et al. 1998; Majka et al. 2006). This is in concordance with Birkenmajer (1990), that during Torellian diastrophism rocks of the Deilegga Group were only folded and then deeply eroded before deposition of the Sofiebogen Group sequence (Birkenmajer 1990). The age of the Torellian unconformity, formed during this event, was determined as ~750 Ma, which could be corellate with Rodinia break-down and Paleopacific opening.

ACKNOWLEDGEMENTS: The authors would like to thank Dr P. Konečný for the help with monazite data interpretation. This study was supported by grant project KBN no. 11.11.140.158.

REFERENCES

BALASHOV Y.A., PEUCAT J.J., TEBENKOV A.M., OHTA Y., LARIONOV A.N., SIROTKIN A.N., BJORNERUD M., 1996: Rb-Sr whole rock and U-Pb zircon dating of the granitic-gabbroic rocks from the Skålfjellet Subgroup, southwest Spitsbergen. Polar Res., 15: 153-165.

BIRKENMAJER K., 1975: Caledonides of Svalbard and plate tectonics. Bull. Geol. Pol., 22: 193-218.

BIRKENMAJER K., 1990: Geology of the Hornsund area, Spitsbergen. Explanations to the map 1:75000 scale. Uniwersytet Śląski, Katowice.

CZERNY J., KIERES A., MANECKI M., RAJCHEL J., MANECKI A. (Ed.) 1993: The geological map of the SW part of Wedel Jarlsberg Land, Spitsbergrn, 1:25 000. Institute of Geology and Mineral Deposits, University of Mining and Metallurgy, Cracow.

KONEČNÝ P., SIMAN P., HOLICKÝ I., JANÁK M., KOLLÁROVÁ V., 2004: Metodika datovania monazitu pomocou elektrónového mikroanalyzátora. Mineralia Slov., 36: 225-235.

MAJKA J., BUDZYN B., CZERNY J., MANECKI M., 2006: REE accessory minerals as regional metamorphic processes indicators: an example from Wedel Jarlsberg Land, Svalbard. GeoLines, 20: 88-89.

MANECKI M., HOLM D. K., CZERNY J., LUX D., 1998: Thermochronological evidence for late Proterozoic (Vendian) cooling in southwest Wedel Jarlsberg Land, Spitsbergen. Geol. Mag., 135: 63-69.

MONTEL J. M., FORET S., VESCHAMBRE M., NICOLLET CH., PROVOST A., 1996: Electron microprobe dating of monazite. Chem. Geol., 131: 37-53.

MINERALOGIA POLONICA - SPECIAL PAPERS
Volume 28 - 2006

Dan TOPA[1], *Emil MAKOVICKY*[2]

THE CRYSTAL STRUCTURE OF A NEW SYNTHETIC IN-BASED PHASE, $SN_{12}IN_{19}(S, SE)_{41}$, MODULAR DESCRIPTION AND PREDICTION OF SYNTHETIC IN-BASED PHASE FAMILIES

The new synthetic phase, $Sn_{12}In_{19}(Se, S)_{41}$, synthesized in a dry phase system Fe-Sn-Sb-In-S-Se at 600 °C, is monoclinic with *a* 56.23(2), *b* 3.920(1), *c* 15.888(5) Å, *ß* 102.770(6) º, space group *C2/m*, and Z= 2. It occurs as needle-like crystals together with chemically analyzed Fe_9S_{10}, $FeIn_2(S, Se)_4$, ~$SbSn_9(Se, S)_{10}$ and ~$Sn_4Sb_3In_2(S, Se)_{11}$. The crystal structure has been refined to a conventional *R*-factor R_1 of 6.29% for 2339 unique reflections with $F_o>4\sigma(F_o)$. There are 31 unique sites of Sn and In and 41 unique sites of Se and S, in one unit-cell. The crystal structure is presented below, projected along *b* axis. Circles in the order of decreasing size indicate (S, Se), Sn and In. Dark-grey and light-grey shading indicate two height levels, ~2 Å apart. The crystal structure consists of two alternating kinds of periodically sheared layers with a non-commensurate interface.

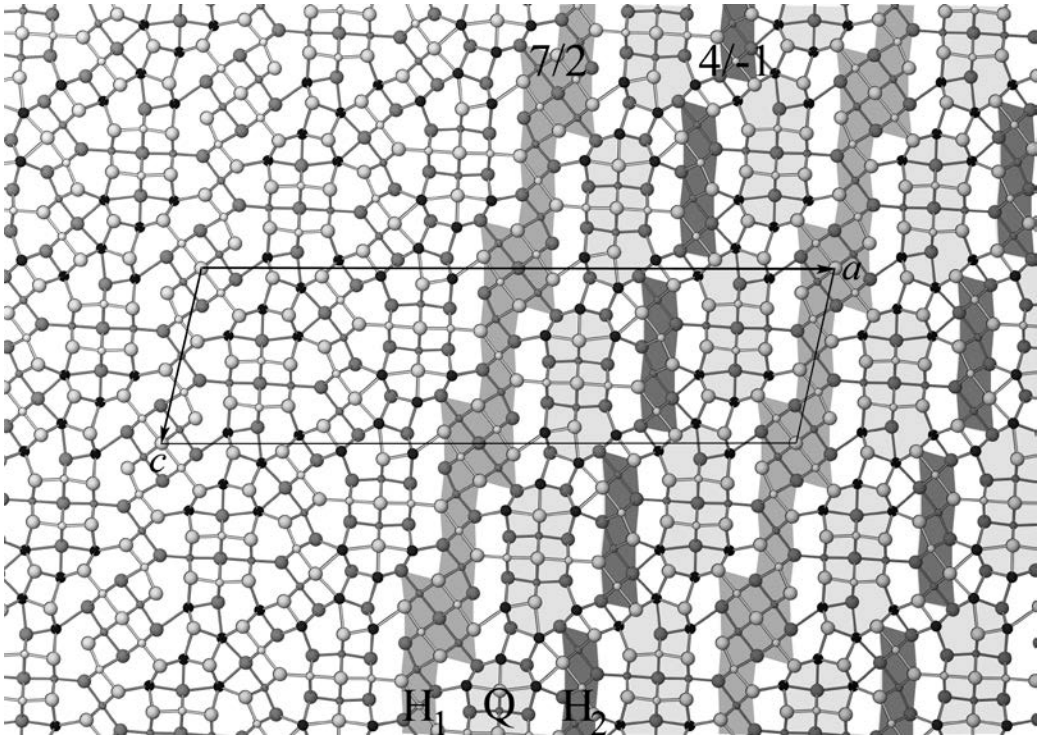

[1] *Department of Material Science, University of Salzburg, Hellbrunnerstr. 34, A*-5020 Salzburg, Austria
[2] *Geological Institute, University of Copenhagen, Østervoldgade 10, DK 1350 Copenhagen K, Denmark*

The pseudohexagonal layers (H_1 and H_2) are octahedral, In-based layers, doubled or not doubled in thickness in the step areas. The pseudohexagonal layers H_1 (7/2) are seven octahedra long with two octahedra that overlap, whereas the pseudohexagonal layers H_2 (4/-1) are four octahedra long with the octahedral layer altered into disjoint octahedral strips. The pseudotetragonal layers (Q) are three atomic planes thick, with four octahedra of In in the centre, surrounded by six coordination prisms of Sn, leading to a graphical "oval rods" of individual layer fragments.

The crystal structure of $Sn_6In_{10}S_{21}$ described by Likforman et al. (1990), with *a* 27.58, *b* 3.85, *c* 15.57 Å, *ß* 95.44º, space group *P2/m*, and Z= 2, consists from exactly the same pseudotetragonal layers Q and pseudohexagonal layers (*i.e.*, 7/2) as in the title compound, but the other type of pseudohexagonal 5/0 (*i.e.*, without overlapping).

A closer look at the spectrum of Pb, Sn, and Bi sulfosalts of indium (ICSDatabase) reveals the presence of other four synthetic In-based phases, which can be structurally described in terms of the same pseudotetragonal layers Q, and *only one* type of pseudohexagonal layers (H). Two of them, $Bi_4In_8Pb_{1.6}S_{19}$ described by Kraemer (1983) and $In^{3+}_6\ Sn^{2+}_4Sn^{4+}_2S_{19}$ described by Adenis *et al.* (1988) have similar unit cells (*a* 29.2, *b* 3.8, *c* 15.5 Å, *ß* 121.6º, space group *P2/m*, and Z= 2), similar pseudotetragonal layers Q and pseudohexagonal layers of type H_2 (*i.e.*, 4/-1). The phase $In_{10}Pb_6S_{21}$ described by Kraemer, Berroth (1980) (*a* 27.63, *b* 3.86, *c* 15.71 Å, *ß* 95.8º, space group C2/m) has pseudohexagonal layers six octahedra long with an overlap of one octahedron at both ends (*i.e.*, 6/1), whereas the phase $In_{11}Sn_{5.5}S_{22}$ described by Likforman et al. (1988) (*a* 15.64, *b* 3.85, *c* 14.63 Å, *ß* 97.4º, space group P2/m) has pseudohexagonal layers of type H_1 (*i.e.*, 7/2).

The $M_{15+N}S_{20+N}$ (or $Me^{2+}_{5+N}Me^{3+}_{10}S_{20+N}$) sliding series is the principal family of complex In-based sulfosalts presented here. The structures of this series consists of stepped (sheared) octahedral pseudohexagonal layers (H), one octahedron thick, in regular alternation with pseudotetragonal layers, which are three atomic layers thick and are individualized into an *en echelon* sequence "oval rods" as in the title compound. The order of a member of the sliding series may be defined as a number of overlapping octahedra in the “doubled” portions of the octahedral layer.

Thus, $In_{10}Pb_6S_{21}$ is the member N = 1 of the series, whereas $In_{11}Sn_{5.5}S_{22}$ has N = 2. This scheme can continue with hypothetical members N = 3 and, finally, up to N = 5 with a complete doubling of the octahedral layer, or up to N = 10 with a complete tripling of the octahedral layer.

This scheme inevitably leads to the N = 0 member, with sheared octahedral layers without overlap. A hypothetical pure N = 0 member is only known as a component of a combinatorial, N = 0, 2, 0, 2... structure of $In_{10}Sn_6S_{21}$ (Krämer, Berroth 1980). As an extreme, the N = -1 member occurs, with the octahedral layer altered into disjoint octahedral strips. This motif is present in $Bi_4In_8Pb_{1.6}S_{19}$ and $In_6Sn^{2+}_4Sn^{4+}_2S_{19}$, and in the combinatorial member $Sn_{12}\ In_{19}(S,\ Se)_{41}$ (Makovicky, Topa 2006), which has N = -1, 2, -1, 2, ... A natural occurrence of some of these phases can be expected, *e.g.* volcanic fumaroles.

REFERENCES

ADENIS C., OLIVIERFOURCADE J., JUMAS J.C., PHILIPPOT E., 1988: Structural study of $In_6Sn_8S_{19}$, a mixed-valence tin phase in the ternary-system In-Sn-S. Eur. J. Solid State Inorg. Chem., 25: 413-423.

KRAMER V., 1983: Lead indium bismuth chalcogenides .1. Structure of $Pb_{1.6}In_8Bi_4S_{19}$. Acta Crystallogr. Sect. C Cryst. Struct. Comm., 39: 1328-1329.

KRAMER V., BERROTH K., 1980: Phase investigations in the system PbS-In_2S_3 and the crystal-structures of $PbIn_2S_4$ and $Pb_6In_{10}S_{21}$. Mater. Res. Bull., 15: 299-308.

LIKFORMAN A., GUITTARD M., ROBERT F., 1990: Structure of indium tin sulfide. J. Solid State Chem., 89: 275-281.

LIKFORMAN A., 1988: Structure of indium tin sulfide $In_{11}Sn_{5.5}S_{22}$. Acta Crystallogr. Sect. C Cryst. Struct. Comm., 44: 1339-1342.

MAKOVICKY E., TOPA D., 2006: The crystal structure of $Sn_{12}In_{19}(S, Se)_{41}$ (in prep.).

MINERALOGIA POLONICA - SPECIAL PAPERS
Volume 28 - 2006

Marián URBAN[1], Jakub BUKOVINA[1], Tomáš KLIMKO[1], Vratislav HURAI[1], Martin CHOVAN[1]

FLUID INCLUSIONS IN STIBNITE FROM HYDROTHERMAL VEINS OF THE WESTERN CARPATHIANS – PRELIMINARY INFRARED MICROTHERMOMETRY DATA

INTRODUCTION

Campbell, Robinson-Cook (1987) introduced a novel infrared (IR) microthermometry technique as a tool for observation of fluid inclusions in opaque sulphides and sulphosalts, such as enargite (Mancano, Campbell 1995), stibnite, bournonite (Lüders 1996), and pyrite (e.g. Lüders, Ziemann 1999). Here we present preliminary results of IR-microscopic study on fluid inclusions in stibnite from hydrothermal veins of the Western Carpathians.

Economically important stibnite-bearing veins are located in Variscan granitoids of the Nízke Tatry Mountains, belonging to the Tatric tectonic unit. Stibnite usually post-dates arsenopyrite-pyrite, and predates polymetallic (tetrahedrite-sulphosalts) and barite stages. The Dúbrava deposit is the type locality, from which preliminary microthermometry data have been published by Chovan et al. (1999). Smaller quartz-stibnite veins occur in the Gemeric tectonic unit, within mylonitic shear zones in low-grade Lower Palaeozoic strata (black shales, lydites, carbonates, and porphyroids) intruded by Permian granites. The Čučma deposit near Rožňava town is the type locality, where stibnite accompanied by Sb-sulphosalts is predated by chalcopyrite and Cu-sulphosalts, and post-dated by calcite (Beňka, Caňo 1992). Quartz associated with tourmaline and stibnite contains primary superdense CO_2-rich metamorphogenic fluid inclusions coincidental with Alpine (Lower Cretaceous) overthrusts (Urban et al. 2006). Several small stibnite deposits occur in the Malé Karpaty Mts., belonging to the Tatric tectonic unit. The veins and lenses are located within shear zones in Lower Palaeozoic black shales, actinolite shales and amphibolites. Stibnite closely associated with gudmundite, native antimony and Sb-oxides is predated by pyrite, pyrrhotite and arsenopyrite (e.g. Chovan et al. 2002).

METHODS

Fluid inclusions were observed in 100-120 μm thick polished plates, using an OLYMPUS BX-51 IR microscope, and a HITACHI KP-161 CCD camera with spectral range up to 1.2 μm. Phase transitions were measured using a LINKAM THMSG-600 freezing-heating stage. Uncertainty was within ±0.1°C for the temperatures between -100 and 100 °C, and ±0.2 °C above 100 °C. The accuracy of the IR-microthermometry was checked using fluid inclusions in brown sphalerite, transparent in both visible and near-IR spectral ranges.

[1] *Department of Mineralogy and Petrology, Faculty of Natural Sciences, Comenius University, 842 15 Bratislava, Slovak Republic; majourban@gmail.com*

RESULTS

Stibnite from the veins hosted in the Tatric basement contains only aqueous inclusions with salinities between zero and 16 wt. % NaCl equivalents. Total homogenization temperatures are in the range of 120-173 °C, with most data clustering at 130-150 °C.

Polyphase aqueous fluid inclusions in stibnite from the Gemeric unit often contain one or several rounded unidentified solid phases. Gaseous bubble is composed either of aqueous vapour, CO_2-liquid, CO_2-vapour, or combination of both CO_2 phases. Partial homogenization takes place between 19.8 and 23 °C to liquid. The inclusions decrepitate prior to total homogenization. Salinity inferred

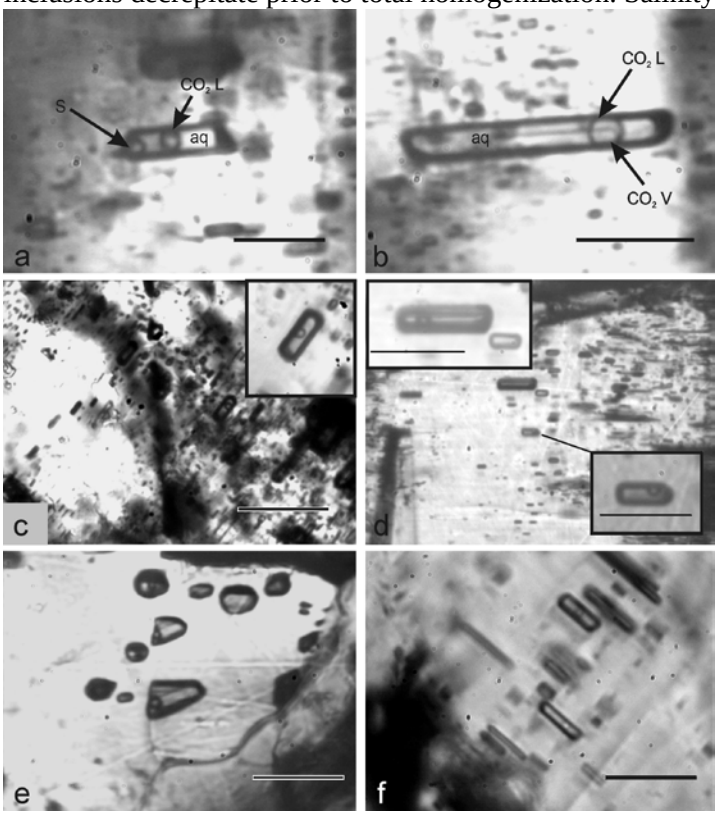

Fig. 1. Fluid inclusions in stibnite from hydrothermal veins of the Gemeric (a-c), and Tatric tectonic units (d-f). **a**) Fluid inclusion composed of aqueous liquid (aq), unknown solid daughter phase (s) and CO_2-liquid (CO_2 L), Čučma deposit, Klement vein. **b**) Three-phase aqueous inclusion with vapour bubble composed of CO_2-liquid (CO_2 L) and CO_2-vapour (CO_2 V) phases. Čučma deposit, Klement vein. **c**) Two-phase aqueous inclusion devoid of CO_2, Štofová dolina. **d**) Two-phase aqueous inclusions, Dúbrava. **e**) Group of monophase and two-phase aqueous inclusions, Pezinok. F) Two-phase aqueous inclusion, Pezinok. Bar scales correspond to 10 μm.

from temperature of CO_2-clathrate melting ranges between 3 and 6.5 wt. % NaCl eq., and bulk CO_2 concentration is within 2.6-5.4 mol. %.

At the Dúbrava deposit (Tatric unit), the IR-microthermometry data document difference in aqueous fluid salinities in stibnite and seemingly coexisting quartz, in which salinities up to 23 wt. % NaCl eq. are diagnostic. Similarly, CO_2-dominated inclusions hosted in quartz are absent in the coexisting stibnite from the Čučma deposit of the Gemeric unit, and salinities are lower (up to 6 wt. %), than those in the coexisting quartz (up to 23 wt. %). Obviously, precipitation of stibnite in the Variscan basement was triggered by influx of meteoric water into the vein system.

CONCLUSIONS

Preliminary IR-microthermometry data on stibnite from hydrothermal veins hosted in Variscan basement of the Western Carpathians reveals inconsistency of inclusion fluid parameters in stibnite and seemingly coexisting gangue minerals.

ACKNOWLEDGEMENTS: Financial support was provided by the VEGA grants 1/1027/04 and 1/1023/04.

REFERENCES

BEŇKA J., CAŇO F., 1992: Mineralogy, paragenesis and geochemistry of stibnite veins in the region of Betliar-Čučma-Volovec. Zapadné Karp. Mineral. Petrogr. Geochem. Metalog., 15: 61-69. (in Slovak)

CAMPBELL A.R., ROBINSON-COOK S., 1987: Infrared fluid inclusion microthermometry on coexisting wolframite and quartz. Econ. Geol., 82: 1640-1645.

CHOVAN M., LÜDERS V., HURAI, V., 1999: Fluid inclusions and C,O-isotope constraints on the origin of granodiorite-hosted Sb-As-Au-W deposit at Dúbrava (Nízke Tatry Mts, Western Carpathians). Terra Nostra, 99/6: 71-72.

CHOVAN M., TRTÍKOVÁ S., VILINOVIČ V., KHUN M., HANAS P., 2002: Ore mineralization in the Pezinok-Trojárová deposit in the Malé Karpaty Mts., Slovakia: mineralogical and geochemical characterization. Slov. Geol. Mag., 8: 179-193.

LÜDERS V., 1996: Contribution of infrared microscopy to fluid inclusion studies in some opaque minerals (wolframite, stibnite, bournonite); metallogenic implications. Econ. Geol., 91: 1462-1468.

LÜDERS V., ZIEMANN M., 1999: Possibilities and limits of infrared light microthermometry applied to studies of pyrite-hosted fluid inclusions. Chem. Geol., 154: 169-178.

MANCANO D.P., CAMPBELL A.R., 1995: Microthermometry of enargite-hosted fluid inclusions from Lepanto, Phillipines, high-sulfidation Cu-Au deposit. Geochim. Cosmochim. Acta, 59: 3909-3916.

URBAN M., THOMAS R., HURAI V., KONEČNÝ P., CHOVAN M., 2006: Superdense CO_2 inclusions in Cretaceous quartz-stibnite veins hosted in low-grade Variscan basement of the Western Carpathians, Slovakia. Mineral. Deposita, 40: 867-873.

MINERALOGIA POLONICA - SPECIAL PAPERS
Volume 28 - 2006

Jana VAVROVÁ[1], Adrian BIROŇ[2], Igor GALKO[3]

MANTIENNEITE – A NEW PHOSPHATE MINERAL FROM ALGINITE DEPOSIT (PINCINÁ, SLOVAKIA)

INTRODUCTION

Mantienneite is a phosphate mineral with idealized chemical formula $KMg_2Al_2Ti(PO_4)_4(OH)_3.15H_2O$. The first occurrence of this mineral was described from vivianite deposit of Anluoa, Cameroon. Associated with quartz, siderite and clay minerals (kaolinite, chlorite-montmorillonite mixed layer), mantienneite constitutes the matrix of sandy layers intercalated in black shale of lacustrine origin Fransolet et al. (1984).

Mantienneite was found at the alginite deposit near Pinciná village (Slovakia). The alginite is the sedimentary rock rich in algal organic matter and clay minerals. It was deposited in a maar lake which was formed during the Upper Miocene basalt volcanic activity (Pontian). Alginite is a raw material useful in agriculture because of their specific facilities. It protects crops and trees against drought (water absorption capacity), traps nutrients in soil and many others.

METHODS

The drill-hole samples of alginite were examined using XRD technique and total organic carbon (TOC) analyses. Whole-rock random powders as well as oriented <2μm fractions were analyzed. XRD analyses were performed on Philips PW 1710 difractometer under following conditions: 40 kV, 20 mA, CuKα, graphite monochromator, step size of 0.02° 2Θ, counting time 1.25s per step, scanning interval 2-50° 2Θ.

TOC analyses were determined on carbon analyzer C-MAT 5 500 Ströhnlein.

Chemical composition of mantienneite was determined by electron microprobe analyses on Cameca SX 100 at accelerating voltage 15 kV, beam current 15 - 20 nA, electron beam 5-20 μm in diameter.

RESULTS

The rock matrix consists of quartz, smectite (nontronite), kaolinite, illite, plagioclase, chlorite, siderite and pyrite. Mantienneite was found as an accessory mineral only in some horizons where clay minerals are represented by dominating smectite and kaolinite, while illite is present in subordinate amounts. It forms well-developed spheres of radiating crystals (ca 200 μm in diameter) growing in clayey matrix (Fig.1). The TOC content in these horizons is exceptionally high and ranges

[1] *State Geological Institute of Dionýz Štúr, Kynceľovská 10, 974 11 Banská Bystrica, Slovak Republic; vavrova@gssrbb.sk*

[2] *Geological Institute Slovak Academy of Sciences, Severná 5, 974 11 Banská Bystrica, Slovak Republic*

[3] *ENVIGEO, a.s., Kynceľová 2, 974 11 Banská Bystrica, Slovak Republic*

from 4.97 to 9.41 %. Mantienneite-bearing horizons are also enriched in secondary fissure-filling gypsum.

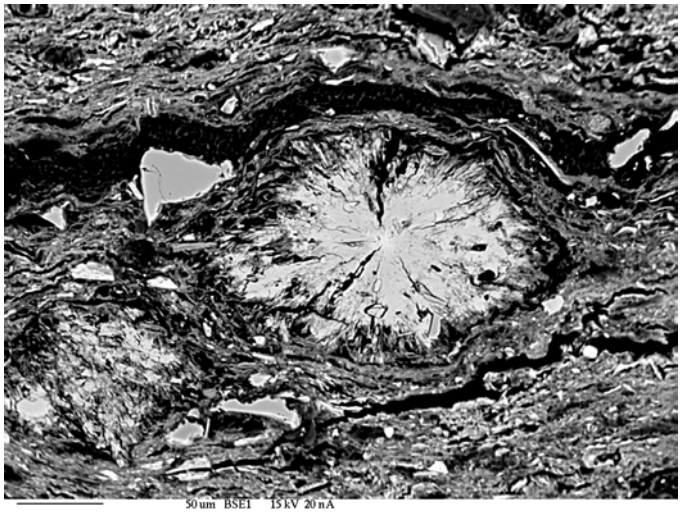

Fig. 1. The mantienneite spherolite from Pinciná (BSE image)

Chemical composition of mantienneite was determined by electron microprobe analyses. Average crystal-chemical formula calculated from 21 analyses on the basis of 4 (PO_4) is: $(\square_{0.45}K_{0.44}Ca_{0.09}Na_{0.02})_{1.00}(Mg_{1.99}Mn_{0.01})_{2.00}(Al_{1.38}Fe^{3+}_{0.33}Ti_{0.22})_{1.93}Ti_{1.00}(PO_4)_{4.00}(OH)_{2.56}\cdot 15H_2O$.

DISCUSSION AND CONCLUSIONS

In our best knowledge, the mantienneite from Pinciná was described for the first time from alginite deposit and it is only second occurrence of this mineral in the world. Its chemical composition is unique. The M^{1+} position is occupied by K (0.12-0.92 *apfu*) with only negligible Na content. Considering M^{2+} site occupancy, mantienneite from Pinciná is almost pure Mg end-member (Fig. 2). Its Mg content ranges between 1.91 and 2.27 *apfu*, which is much higher then in mantienneite from Anluoa (1.43 *apfu*; Fransolet et al. 1984). Figure 2 shows comparison of M^{2+} occupancy in minerals related to mantienneite. Paulkerrite from Arizona is also Mg dominant (1.10 *apfu*) but Mn content is high too (0.97 *apfu*; Peacor at al. 1984). Composition of "matveevite" is between paulkerrite and benyacarite (Mn 1.10 apfu, Mg 0.84 *apfu*; Kydryashova, Rozhdestvanskaya 1991) and benyacarite is markedly Mn dominant (1.60 *apfu* Demartin at al. 1997; 1.60-1.78 Sejkora et al. 2006). Al is dominating cation in M^{3+} site and its content is ranging from 1.06 to 1.87 *apfu*. The M^{4+} structural position is fully occupied with Ti, therefore its excess over 1 *apfu* is attributed to M^{3+} site.

Origin of mantienneite is probably related to fluid activity within sedimentary sequence containing alginite. Delicate habit of crystals suggests that this mineral precipitated probably directly from solution. The components required for

mantienneite crystallization may have been mobilized by hot fluids during post-volcanic stage of maar evolution. The gradual decomposition of algal organic matter may have served as source of P, while other elements (Al, Mg, Fe and Ti) were probably released during alteration of basalt pyroclastics. Direct precipitation of mantienneite from solution is also supported by close association with secondary gypsum.

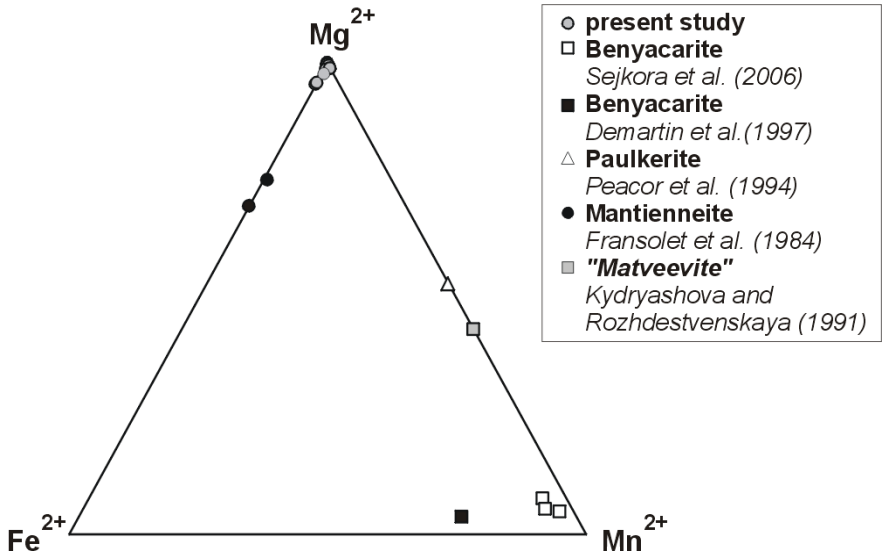

Fig. 2. Occupancy of M^{2+} structural position in mantienneite related minerals.

ACKNOWLEDGMENTS: Dr. J. Sejkora is thanked for its help with data processing and Dr. I. Holický for microprobe analysis.

REFERENCES

DEMARTIN F., GAY H.D., GRAMACCIOLI C.M., PILLATI T., 1997: Benyacarite, a new titanium-bearing phosphate mineral species from Cerro Blanco, Argentina. Can. Mineral., 35: 707-712.

FRANSOLET A. M., OUSTRIÉRE P., FONTAIN F., PILLARD F., 1984: La mantiennéite, une nouvelle espèce minérale du gisement de vivianite d'Anloua, Cameroun. Bulletin de Minéralogie, 107: 737-744.

KYDRYASHOVA V.I., ROZHDESTVENSKAYA I.V., 1991: New minerals XLV. Zapiski Vses. Mineral. Obshch., 120, 4: 100-115. (in Russian)

PEACOR, D.R., DUNN, P.J., SIMMONS W.B., 1984: Paulkerrite, a new titanium phosphate from Arizona. Min. Record. 5, Vol.25: 303-306.

SEJKORA J., ŠKODA, R., ONDRUŠ, P., BERAN P., SŰSSER, C., 2006: Mineralogy of phosphate accumulations in the Huber stock, Krásno ore district, Slavkovský les area, Czech Republic. J. Czech Geol. Soc., in press.

MINERALOGIA POLONICA - SPECIAL PAPERS
Volume 28 - 2006

Jiří ZACHARIÁŠ[1], Jiří ADAMOVIČ[2], Lucie DOLEŽALOVÁ[1]

LATE ALPINE SILICIFICATION AND ASSOCIATED MINERALIZATIONS IN THE VICINITY OF TEPLICE, NORTHWESTERN BOHEMIA, CZECH REPUBLIC

INTRODUCTION

Occurrences of silicified sandstones (quartzites) concentrate around Tertiary volcanic centres in the Eger Graben, northwestern Bohemia. Three principal genetic types of quartzites were distinguished: 1) horizontal bodies of large areal extent related to effects of Paleocene climate, mostly groundwater silcretes; 2) epithermal quartzites associated with silica redistribution along volcanic and intrusive bodies; and 3) epithermal quartzites associated with large-scale circulation of low-temperature geothermal fluids. Mineralogy of the last type is discussed in this paper.

In the quarry of Jeníkov, west of Teplice, mineralization formed by ascending geothermal fluids concentrated to Lower Turonian quartzose sandstones above the Carboniferous Teplice rhyolite body and beneath the sealing horizon of Middle Turonian marlstones. On the crest of Salesiova výšina, west of Dubí, silica cementation of Lower Miocene sands was related to fluid transport along the Krušné Hory Fault system limiting the Eger Graben. Two superimposed quartzite bodies were encountered by former drilling, the upper one of which locally exceeds 20 m in thickness. At both localities, silica cementation largely preceded the precipitation of other minerals, the succession of which was spatially and temporally controlled by movements on the Krušné Hory Fault.

Three mineralization phases were recognized by Čadek et al. (1963) in the Teplice area: (1) silicification phase, (2) sulphidic phase with pyrite, marcasite, sphalerite, and the youngest (3) barite–fluorite phase also characterized by Fe and U oxides, galena, sphalerite, pyrite etc. Čadek and Malkovský (1968) presumed, besides the older Paleogene silcretization, two phases of Neogene hydrothermal silicification, with Salesiova Výšina quartzites being products of the older stage and the ones at Jeníkov representing the younger stage.

METHODS

Polished thin sections were prepared from 35 quartzite samples. Paragenetic relationships were studied by transmitted and reflected light optical microscopy, electron microscopy (BSE, SE) and by electron microscopy cathodoluminescence (SEM-CL). Identification of some phases is based on ED microanalyses (CamScan S4 microscope, Link ISIS 300 ED system, operator R. Procházka, Charles University).

[1] *Institute of Geochemistry, Mineralogy and Mineral Resources, Faculty of Science, Charles University, Albertov 6, 128 43 Praha 2, Czech Republic; zachar@natur.cuni.cz*
[2] *Institute of Geology, Academy of Sciences CR, Rozvojová 269, 165 02 Praha 6, Czech Republic*

RESULTS

The mineralizations at Jeníkov and Salesiova Výšina are similar in their paragenetic relationships but differ significantly in relative abundance of individual mineral phases.

Up to four substages of silica precipitation can be distinguished. The process started with seldom precipitation of quartz microcrystals of scepter-like habit (Qtz-1) on the surfaces of quartz grains. This substage was followed by widespread formation of quartz overgrowths (Qtz-2) on quartz grains. Thick euhedral overgrowths predominate at Salesiova Výšina crest, while thin anhedral ones at Jeníkov. Next substage is characterized by the formation of mostly microcrystalline quartz (Qtz-3) in the pores of sandstones. Finally, the process diminished through the local development of megaquartz crystals in voids or late microfractures.

The formation of Qtz-2 and Qtz-3 is coeval with the onset of sulphidic mineralization, mostly in the form of pyrite framboids or microcrystals. Max. five or six generations of pyrite can be distinguished in total at Jeníkov, the youngest one being coeval with barite precipitation on late fractures. In contrast to Jeníkov, sulphides are rare at Salesiova Výšina.

Other, mostly minor phases, coeval with Qtz-3 or Qtz-4 comprise kaolinite, illite, jarosite, amorphous carbon, and various types of iron oxyhydroxides and uranium oxides.

CONCLUSIONS

Complex relationships were documented among late Alpine silicification and sulphidic and barite-fluorite mineralizations from the northwestern faulted margin of the Eger Graben. They all are associated with fossil geothermal discharges of the present Teplice Spa system and were probably controlled by tectonic movements on the Krušné Hory Fault.

ACKNOWLEDGEMENTS: This research was supported by the GA AS CR, project A3013302.

REFERENCES

ČADEK J., KAČURA G., MALKOVSKÝ M., 1963: Genetické vztahy mezi termami a neoidní mineralizací hornin v oblasti Teplic a Ústí nad Labem. Věst. Ústř. Úst. Geol., 38: 265-268. (in Czech)

ČADEK J., MALKOVSKÝ M., 1968: Silicifikace svrchnokřídových hornin v okolí Teplic. Sbor. Geol. Věd, Geol., 14: 71-91. (in Czech)

MINERALOGIA POLONICA - SPECIAL PAPERS
Volume 28 - 2006

Jiří ZACHARIÁŠ[1], Jiří ADAMOVIČ[2], Anna LANGROVÁ[2]

TRACE ELEMENT CHEMISTRY AND TEXTURES OF LOW-TEMPERATURE PYRITES ASSOCIATED WITH SHALLOW FOSSIL SUBSURFACE GEOTHERMAL DISCHARGE IN THE EGER GRABEN, NORTHWESTERN BOHEMIA

INTRODUCTION

Pyrite is the most common sulfide mineral on Earth. It is associated with high-temperature sulfidic ores as well as with low-temperature sediments. The latter occurrences often show framboidal pyrite textures. Pyrite is commonly a stoichiometric FeS_2 phase; however, significant amounts of As, Ni, Co and minor Au amounts were found in many natural samples. The extent of arsenic solubility and type of bonding in the pyrite structure (isomorphous $As_{+1}S_{-1}$ substitution vs. nanoinclusions of arsenopyrite) was recently discussed by Reich and Becker (2006).

The Eger Graben in NW Bohemian Massif is limited by the Krušné hory Fault in the NW and the České středohoří Fault in the SE. The oldest tectonic activity dates back to Oligo-Miocene, but the largest movements on the Krušné hory Fault are very young extending beyond the Pliocene/Pleistocene boundary (Adamovič, Coubal 1999). Late Alpine epithermal mineralization associated with the movements on the Krušné hory Fault is hosted by the Teplice rhyolite ignimbrite body (part of the Altenberg-Teplice Caldera), and by the overlying Cretaceous sediments. Three mineralization phases were recognized by Čadek et al. (1963): 1. silicification phase, 2. sulphidic phase with pyrite, marcasite, sphalerite, and the youngest 3. barite–fluorite phase also characterized by Fe and U oxides, galena, sphalerite, pyrite etc. Subrecent age of the last phase is indicated by the disequilibrium between the activity of ^{226}Ra and the parent uranium in barite (Ulrych et al. 2006, in print), and is compatible with the chemistry of present thermal springs.

In the quarry of Jeníkov, west of Teplice, mineralization by ascending fluids concentrates to Lower Turonian quartzose sandstones beneath the sealing horizon of Middle Turonian marlstones (Čech, Váně 1988).

METHODS

Polished thin sections were prepared from about 20 samples of silicified sandstone from the Jeníkov quarry. Sulfide textures and paragenetic relationships were studied by transmitted and reflected light optical microscopy and by the back-scattered electron mode (BSE) electron microscopy.

[1] *Institute of Geochemistry, Mineralogy and Mineral Resources, Faculty of Science, Charles University, Albertov 6, 128 43 Praha 2, Czech Republic; zachar@natur.cuni.cz*
[2] *Institute of Geology, Academy of Sciences CR, Rozvojová 269, 165 02 Praha 6, Czech Republic*

Chemistry of pyrites was studied by the microprobe WD system (Cameca SX 100, operator A. Langrová, Inst. Geol. AS CR). Elements measured: S (Ka), Fe (Ka), Co (Ka), Ni (Ka), Zn (Ka), As (La) and Tl (Mb). Spectrometers used: LTAP (As), LPET (Tl), PET (S), and LIF (Fe, Co, Ni). Standards used: marcasite (Fe, S), metallic Co (Co), metallic Ni (Ni), GaAs (As), ZnS (Zn) and TlBr (Tl).

PYRITE TYPES AND TEXTURES

Six generations of pyrite were recognized, referred to as Py-1 (oldest) through Py-6 (youngest). The oldest ones (Py-1, -2, ± -3) crystallized together with silica cement in pores of Turonian sandstones, while the younger ones (Py-4, -5) fill cavities in the silicified sandstones, or brittle joints and fractures in them (Py-5, -6).

Py-1 occurs as rare anhedral grains up to 50 μm in size, frequently exhibiting chemical corrosion features on its surfaces. It is always overgrown by younger pyrite growth zones (Py-3 and Py-4), and no individual Py-1 grains were found.

Py-2 forms framboids (~35 to ~10 μm in size), consisting of closely packed cubes, or octahedra (~0.5 to ~1 μm in size). We have noticed progressive increase in size of both framboids and individual framboids-forming pyrite grains, resulting in progressive "welding" of individual crystals within the framboids. Independently of this process, the framboids are frequently overgrown by Py-4 cubes (~ 5 μm in size). In contrast to Py-1, Py-2 lacks any corrosion and Py-3 overgrowth zones.

Py-3 forms well developed crystal-faced overgrowth zones containing 1 or 2 thin (~ 1-2 μm) As-rich growth bands.

Py-4 crystallized as numerous seeds on the Py-3 surfaces and consists of several thick As-rich zones separated by thin (~ 1-2 μm) As-low bands.

Py-5 forms As-rich grains up to 80 μm in size or massive pyrite coatings on fractures in the quartzites.

Py-6 forms numerous tiny (max. 10 μm) crystal inclusions in the barite crystals, filling very young fractures in quartzites. Pyrite inclusions are commonly coeval with individual barite growth zones, and some were associated with solid inclusions of amorphous carbon phase.

PYRITE CHEMISTRY

Individual pyrite generations/types differ significantly in arsenic content (average wt. % As content: 0.01, 0.15, 2.94, 3.91, 6.14 and 0.76 wt % As for Py-1 through Py-6, respectively) that gradually increases towards younger pyrite types (except for Py-6). Arsenic contents correlate well with sulfur deficit, suggesting $As_{+1}S_{-1}$ substitution mechanism. Arsenic content in most of the analyzed Py-1 and Py-2 grains was below the detection limits. No other trace elements were detected in Py-1 trough Py-5, except thallium (0.19±0.13 wt. % Tl in Py-5).

Several growth zones can be distinguished in barite; many of them are accompanied by contemporaneous tiny pyrite crystal (Py-6). The oldest generation of these pyrite inclusions is variably enriched in Ni (3.47 ± 2.09 wt. %), Co (8.86 ± 3.68 wt. %) with traces of As and Zn, while the younger ones are only slightly enriched in arsenic (0.76 wt. % As).

CONCLUSIONS

Evolution of pyrite textures from framboids (neglecting rare Py-1 anhedral grains) to individual crystals (mostly cubes), suggests oversaturation of early fluids with respect to pyrite and its rapid crystallization. This could by partly due to retaining of the fluids beneath the sealing horizon of Middle Turonian marlstones and to the role of contemporaneous silicification processes. The As contents in Py-3 and Py-4 correlate well with the theoretically predicted As solubility in FeS_2 at lower temperatures (Reich, Becker 2006), while those in Py-5 correspond likely to metastable arsenic solid solution. Sudden presence of nickel and cobalt in some of the Py-6 crystals most probably resulted from incorporation of weathering-related products of late Variscan hydrothermal mineralization, common in the Saxothuringian Zone.

ACKNOWLEDGEMENTS: This research was supported by the GA AS CR, project A3013302.

REFERENCES

ADAMOVIČ J., COUBAL, M., 1999: Intrusive geometries and Cenozoic stress history of the northern part of the Bohemian Massif. GeoLines, 9: 5-14.

ČADEK J., KAČURA G., MALKOVSKÝ M., 1963: Genetické vztahy mezi termami a neoidní mineralizací hornin v oblasti Teplic a Ústí nad Labem. Věst. Ústř. Úst. Geol., 38: 265-268. (In Czech).

ČECH S., VÁNĚ M., 1988. K otázkám vývoje cenomanu a spodního turonu v Podkrušnohoří. Čas. Mineral. Geol., 33: 395-410. (In Czech).

REICH M., BECKER U., 2006: First-principles calculations of the thermodynamic mixing properties of arsenic incorporation into pyrite and marcasite. Chem. Geol., 225: 278-290.

ULRYCH J., ADAMOVIČ J., ŽÁK K., FRÁNA J., ŘANDA Z., LANGROVÁ A., SKÁLA R., CHVÁTAL M., 2006 in print: Revision of the alleged "radiobarites" from the Ohře (Eger) Rift, Bohemian Massif. Chemie der Erde, 65.

MINERALOGIA POLONICA - SPECIAL PAPERS
Volume 28 - 2006

Jana ZAHRANÍKOVÁ [1]

FLUID INCLUSIONS STUDY FROM ĽUBIETOVÁ DEPOSIT

INTRODUCTION

Ľubietová is situated cca 10 km eastern from Banská Bystrica in the north-western part of Veporské vrchy Mts, in the orography area of Čiertaž. Geological setting of studied area is built by Ľubietová and Krakľov belt of the Northern Veporic Unit (Vozárová, Vozár, 1988). The area is built by sedimentary and magmatogenic metamorphosed Lower-Paleozoic complexes, Upper-Paleozoic formations and volcanics, and Triassic, sporadically Jurrassic and Lower-Cretacerous sediments, which are a part of cover sequence (Ilavský et al., 1994). Significant morpho-tectonic feature of Čierťaž Mts. is alpine-formed anticlinal structure of the Ľubietová belt. Its axial part is NE-SW oriented and is visible continously from Podbrezová to Ľubietová, where is separated by lateral fault tectonics (NNW – SSE orientation). This structure continues at SW as an isolated horsts, with structural and lithological features identical with main part of Ľubietová Belt (Kamenický, 1977).

Hydrothermal copper mineralization occur on three deposits (Podlipa, Svätodušná and Kolba). These three deposits, especially Podlipa deposit were the objects of mining from the bronze age, where native copper was explorated. Mining exploitation took place until the half of 19th century (Pauliš, Ďuďa, 2002). Mineralization of Svätodušná and Kolba deposits occurs in the rocks of Ľubietová crystalline complex and Cu-sulphidic mineralization in the Podlipa deposit is developed in Permian greywacke and arcose rocks.

Primary mineralization on the Podlipa deposit is poor and composed from chalcopyrite, tetrahedrite and pyrite disseminated in thin quartz veinlets. Primary mineralisation on the Svätodušná and Kolba deposit is more abundant as on Podlipa deposit. From these two deposits were described: albite, ankerite, arsenopyrite, barite, calcite, chalcopyrite, chamosite, cobaltite, dravite, galena, gersdorffite, hematite, monazite-(Ce), muscovite, pyrite, quartz, rutile, scutterudite, siderite, tennantite, tetrahedrite and zircon (Koděra ed., 1990 Pauliš, Ďuďa, 2002, Ozdín, 2001). Besides the primary mineralization is Ľubietová developed by rich association of secondary minerals with world famous specimens of libethenite, mrázekite, pseudomalachite, ludjibaite, reichenbachite, euchroite and parnauite (Chovan et al., 1996).

METHODS

Fluid inclusions have studied in polished plates 0.2 mm thick in the polarization microscope Olympus BX-51 with optics adapted to wavelenght 365-1200 nm, which cover the wavelenght of ultraviolet spectra, visible spectra (400-765 nm) and a part of infrared spectra of electromagnetic emission. Temperatures of phase

[1] *Department of Mineralogy and petrology, Faculty of Natural Sciences, Comenius University, Mlynská dolina G, 842 15 Bratislava; zahradnikova.jana@gmail.com*

transitions in inclusions were observed with microthermometric apparate Linkam THMSG-600 which operated in temperatures from -196 to 600 °C.

RESULTS

Fluid inclusions were observed and measured from polished plates from locality Ľubietová – Svätodušná and Ľubietová – Kolba. On Svätodušná deposit were fluid inclusions in white quartz associated with sulphidic mineralization (chalcopyrite, tetrahedrite). We observed two phase aqous fluid inclusions with low salinity (average 9.21 wt. % NaCl). Homogenization temperatures vary from 182 – 260 °C and ice melting temperatures (N = 15) vary from -3 to -8.6 °C.

On Ľubietová - Kolba deposit were fluid inclusions in white quartz associated with chalcopyrite and tetrahedrite. We observed two phase aqous fluid inclusions with average salinity 9.74 wt. % NaCl. Homogenization temperatures vary from 157 to 226 °C and ice melting temperatures vary from -3.9 to -10.7 °C. Histograms of homogenization temperatures of fluid inclusions from Ľubietová – Svätodušná and Kolba shows Figure 1 and 2.

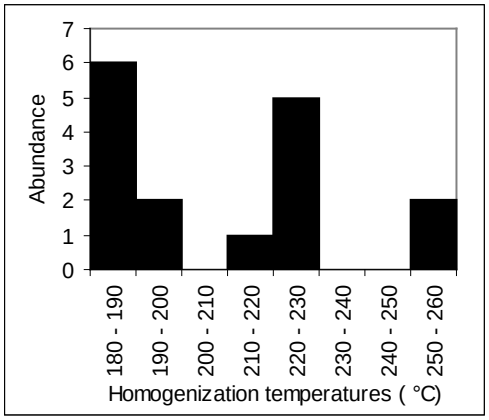

Fig. 1. Histogram of homogenization temperatures of fluid inclusions from Ľubietová – Svätodušná deposit

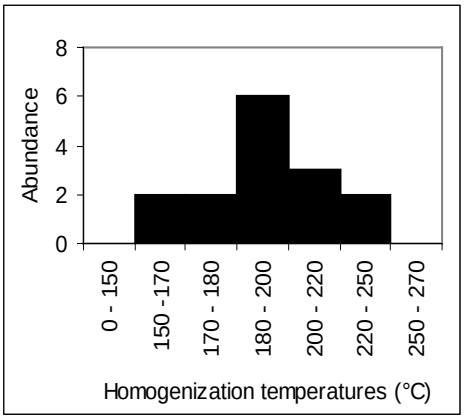

Fig. 2. Homogenization temperatures versus salinity diagram of fluid inclusions from Ľubietová – Kolba deposit.

One fluid inclusion from tourmaline was measured from Ľubietová - Podlipa. Black tourmaline (not analysed yet) form prismatic crystals in white quartz in Permian arcoses. Following data were measured: homogenization temperature 165.7 °C, ice-melting temperature -7.4 °C and salinity 10.98 wt. % NaCl.

CONCLUSIONS

Similar ore mineralization occur in the Northern Veporic also at Špania Dolina and Staré Hory Mts. Fluid inclusions from the locality Špania dolina – Piesky were studied. Two phase fluid inclusions occur in white quartz with sulphidic

mineralization (chalcopyrite and tetrahedrite). Homogenization temperatures vary from 117 to 123 °C, ice-melting temperatures from -9.2 to -13.8 °C. Fluid inculsions have higher salinity as on Ľubietová locality (from 13.08 to 17.43 wt. % NaCl with average salinity 15.54 wt. % NaCl).

Measured data from Ľubietová locality are comparable with hydrothermal carbonate-sulphidic mineralization near Bacúch village. Mineralization occurs mainly in Bacúch valley (Jánov grúň and Sokolová dolina), also on Vrbovica massif, Zadná Hola and Homôlka (Petro, 1973). Primary inclusions in quartz are two-phase, with ice-melting temperatures from -5.3 to -22.6 °C, salinity from 9.58 to 22 wt. % NaCl. Low concentration of KCl in solution is deduced from measured eutectic temperatures. Density of inclusions vary from 0.9 to 1.1 g/cm^3. Homogenization temperatures are in the range from 198 to 201 °C with the maximum 180 °C for Jánov grúň and 170 °C for Sokolová dolina.

ACKNOWLEDGEMENTS: This work was financed by the VEGA grants V-374-05-00 and by the project No. 0503 “Source of ore-bearing fluids in the metallogeny of Western Carpathians”.

REFERENCES

CHOVAN M., OZDÍN D., MIKO O., 1996: Ľubietová (Veporské vrchy Mts.). Excursion guide, field trip E2 West and Central Slovakia. Budapest, 20-22.

ILAVSKÝ J., VOZÁROVÁ A., VOZÁR J., 1994: Ľubietová - štruktúrno-vyhľadávacie vrty LU-1, LU-2 a LU-3. GÚDŠ, Bratislava, 1-77.

KAMENICKÝ J., 1977: Der geologishe Bau des NW Teiles des Vepor-Erzgebirges. Acta Geol. Geogr. Univ. Comen. Geologica, 32: 161-189.

KODĚRA M. (ED.), 1990: Topografická mineralógia Slovenska. I-III. Veda, Bratislava, 1-1592.

OZDÍN D., 2001: Metamorfno-hydrotermálne zrudnenie na výskyte Ľubietová-Predsvätodušná. Geol. Práce, Správy, 105: 77-82.

PAULIŠ P., ĎUĎA R.,2002: Nejznámejší mineralogická naleziště Slovenska. Kuttna, Kutná Hora, 1-136.

PETRO M., 1973: Nerastné suroviny na liste Polomka 1:25 000. Manuscript, ŠGÚDŠ, Bratislava, 1-82.

VOZÁROVÁ A., VOZÁR J., 1988: Late Paleozoic in Western Carpathians. Bratislava, Geol. Úst. D. Štúra, 1-314.

MINERALOGIA POLONICA - SPECIAL PAPERS
Volume 28 - 2006

Franc ZALEWSKI[1]

PATINA ON THE BEDROCKS AND MONUMENTAL BUILDINGS OF THE GIZA REGION, EGYPT

The term monumental buildings refers here to pyramids, temples with squares surrounding them and tombs.

Megaliths were built in the periods referred to by historians as pre-dynasty, early-dynasty and the Old Kingdom of Egypt (3500-2125 BC).

Nowadays the major part of these buildings is in a poor state. As a researcher, the Author was especially interested in the outer part of the buildings, as only on their surface the traces of the influence of the atmosphere and other factors had been preserved. Unfortunately, there are not many such places left.

The three pyramids at Giza are the best-known Egyptian megaliths. Until the 8th century they were covered by the facing and thus they constituted a smooth, polished surface.

The blocks of high quality were taken for the sake of building Cairo in the 8th-9th century as in those days the pyramids were treated as the source of building material.

Only seven blocks on the north side of the Cheops Pyramid, which constitued it's facing, are still to be analysed.

Also the squares surrounding Cheops and Chefren Pyramids are important research objects as well as the Red Pyramid in Dahszur with the small samples of facing tiles on the east side. Relatively numerous samples of facing has been preserved in the Bent Pyramid as it is located further from the developing urban agglomerations.

The samples of limestone taken from the above buildings were tested in the laboratories of AGH University of Science and Technology and Jagiellonian University in Cracow. The other rocks taken for the sake of research, such as granite or basalt, were weathered and thus did not preserve their outer layer.

The tests of limestone samples carried out in the crossing light using a polarization microscope indicated that they are micrinite-sparite and have an amorphous layer.

After testing the samples with the application of SEM with the EDS attachment it was detected that the transparent layer consists of carbon (C), which is covered by a thin layer of sulfates (to 20 μm).

It was also found that in some samples carbon is separated from the rock with a similar layer of sulfates.

After further detailed tests, in the layer of sulfates trapped between the calcite-dolomite rock and the carbon layer, 5 μm elements of iron (Fe) were found as well

[1] *AGH - University of Science and Technology, Department of Mineralogy Petrography and Geochemistry, al. Mickiewicza 30, 30-059 Kraków, Poland; franc.zalewski@poczta.onet.pl*

as the closed enclave of calcite-magnesium-silicate mixture with mircrogranules of nickel (Ni) was detected.

What is interesting here is that the carbon patina was also found on human bones, which were excavated from the early-dynasty cemetery in Teba. It was the burial with incomplete skeleton.

The occurrence of patina is connected with the fall of meteorites in this region in historic times.

MINERALOGIA POLONICA - SPECIAL PAPERS
Volume 28 - 2006

Jiří ZIMÁK[1], Kamil KROPÁČ[1]

MINERALOGY OF METAMANGANOLITES IN BIF OF THE DESNÁ GROUP

INTRODUCTION

The Desná Group is a part of Silesicum belonging to the northeastern margin of the Bohemian Massif. A typical rock of the Desná Group, the so-called Desná Gneiss (biotite paragneisses, partly chloritized) corresponds to the Proterozoic grey-wacke-pelitic protolith (e.g., Grygar and Vavro 1995). Zircon from orthogneiss from the Desná Group yielded a mean $^{207}Pb/^{206}Pb$ age of 506.7 ± 1.7 Ma, which is interpreted as the time of emplacement of the gneiss protolith (Kröner et al. 2000). Basic rocks of the Sobotín Amphibolite Massif which intrude to Desná gneisses are represented partly by dikes, sills or apophyses, and partly irregular injections and cumulates of hornblende in paragneisses; in place amphibolitization of gneisses can be observed (e.g., Pouba 1970).

Small bodies of banded magnetite ores (BIF) occur in Desná gneisses in the neigbourhood of Sobotín and Verníøovice (NE of the town Šumperk). A protolith of Desná gneisses and banded magnetite ores was affected with pre-Variscan regional metamorphism that reached the grade of amphibolite facies (the foliation seen in the Desná Gneiss must have formed between 507 and 502 Ma ago, i.e. during an early Palaeozoic event – see, Kröner et al. 2000) and polyphase retrograde metamorphism connected with the Variscan tectogenesis (e.g., Fojt 2002). Iron ore bodies in Desná gneisses were considered to be magmatic segregations, contact-metasomatic bodies, sedimentary ores with indirect influence of submarine-exhalation processes and submarine volcanism (see, Pouba 1970), product of filter-pressing effects connected with basic magmatites of the Sobotín Massif (Mücke, Losos 2000).

Banded magnetite ores of the Desná Group form one or two parallel horizons in biotite gneisses, few cm to 3 m thick, intensely folded and dissected into several segments attaining a total length of more than 20-25 km (Pouba 1970).

METHODS

Whole rock chemical analyses were performed in ACME laboratories (Vancouver, Canada). The garnet composition was determined by electron microprobes CAMSCAN (equipped with an EDX analyzer Link AN 10 000, analyst V. Vávra) and CAMECA SX-100 (in a WDX mode, analyst P. Sulovský, R. Èopjaková and R. Škoda), all at the Faculty of Science of the Masaryk University (Brno, Czech Republic).

[1] *Faculty of Sciences, Palacký University, Tø. Svobody 26, 771 46 Olomouc, Czech Republic; zimak@prfnw.upol.cz*

RESULTS AND DISCUSSION

The BIF horizons in the Desná Group show variation in mineral composition and in the proportion of the major constituents. Minerals include quartz, magnetite, feldspars (K-feldspar, albite to andesine), biotite, chlorite, muscovite, fluorapatite, Ca-amphibole, ilmenite, locally calcite, clizoisite-epidote, garnet, pyroxene of diopside-hedenbergite series, titanite, rutile, and pyrite are also present. Hematite appears to be a minor component occurring principally as small inclusions in quartz and as martite. Manganese-rich types of banded iron ores are specially enriched in Mn-garnet that either forms mesobands in the ore like magnetite, or magnetite and garnet microbands alternate with quartz microbands and often with microbands rich in calcium amphibole, biotite, chlorite, and clinozoisite-epidote. The thickness of the mesobands varies from 2-3 mm to as much as 1 to 1.5 cm.

Table 1. Chemical analyses of iron ore samples (1 to 4), garnet-rich mesobands (5 to 7) and metamanganolites (8 and 9), wt. %.

Sample No.	1	2	3	4	5	6	7	8	9
SiO_2	56.47	52.49	59.37	58.61	46.85	57.28	60.72	52.51	41.43
TiO_2	0.37	0.32	0.52	0.59	0.89	0.29	0.34	0.34	0.45
Cr_2O_3	-	0.006	0.005	-	-	-	0.003	0.001	-
Al_2O_3	3.49	5.84	8.35	7.17	13.50	12.14	10.53	10.57	16.06
Fe as Fe_2O_3	-	32.02	21.67	-	-	-	11.27	13.11	-
Fe_2O_3	21.67	n.d.	n.d.	13.57	6.36	3.19	n.d.	n.d.	4.65
FeO	10.29	n.d.	n.d.	9.86	7.66	9.68	n.d.	n.d.	12.53
MnO	0.39	1.03	2.59	3.19	13.21	10.23	9.83	5.95	10.49
MgO	1.55	2.56	2.53	1.37	2.68	1.26	1.06	2.00	1.96
CaO	4.20	4.95	3.16	3.19	3.76	3.88	4.85	9.43	8.20
Na_2O	0.20	0.30	0.61	0.91	0.93	0.03	0.01	0.01	0.06
K_2O	0.10	0.16	1.10	0.66	0.77	0.14	0.04	0.04	0.05
P_2O_5	0.88	0.67	0.45	0.55	1.01	0.38	0.41	0.70	0.65
CO_2	0.32	n.d.	n.d.	0.24	0.80	0.29	n.d.	n.d.	2.64
TOT/C	n.d.	0.08	0.04	n.d.	n.d.	n.d.	0.44	1.52	n.d.
TOT/S	trace	0.03	0.01	0.08	0.18	trace	0.20	0.02	-
LOI	n.d.	0.10	0.10	n.d.	n.d.	n.d.	1.10	5.50	n.d.
H_2O^-	0.10	n.d.	n.d.	-	0.18	0.13	n.d.	n.d.	0.11
H_2O^+	0.53	n.d.	n.d.	0.58	1.04	1.42	n.d.	n.d.	0.49
Total	100.56	100.26	100.18	100.57	99.82	100.34	100.16	100.15	99.77

Manganiferous mesobands and layers of metamanganolites in width to 30 cm are easily identified in the field by their pink to brownish colour. They are banded with alternate pinkish to redbrown garnet-rich mesobands, nearly black biotite and/or amphibole-rich mesobands, and grey quartz-rich mesobands.

The major element analyses in Table 1 for the first four samples (labeled 1 to 4) are for banded magnetite ores. The remaining five (labeled 5 to 9) are of garnet-

rich bands in quartz-magnetite banded ores (5 to 7) and metamanganolite layers without or poor in magnetite (8 and 9).

The main constituents of iron ores (Samples No. 1 to 4) are iron oxides and silica; the iron content seems to be antipathetic with the silica content. The data indicate that the manganese content in studied iron ores is relativelly high (from 1 to 3 wt. % MnO) which corresponds to the presence of manganese garnet. Very high manganese contents were found in metamanganolite bands in BIF and in metamanganolite intercalations and layers.

Chemistry of garnets in banded magnetite ores, metamanganolite intercalations in BIF, and metamanganolite layers in chloritized biotite gneisses with very poor magnetite mineralization is plotted in Fig. 1.

No direct evidence of precursor mineralogy and textures is available – the studied iron ores and metamanganolites are coarsely and thoroughly recrystallized.

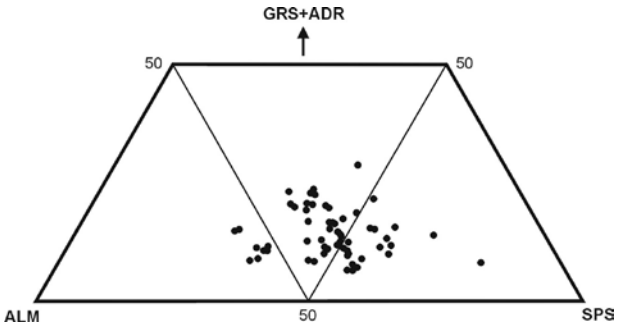

Fig. 1. Grs+Adr - Alm - Sps diagram demonstrating the composition of garnets.

REFERENCES

FOJT B., 2002: Páskované železné rudy v desenských rulách silezika: pøehled názorù na jejich vznik; souèasný stav poznatkù. Sborník „Mineralogie Èeského masivu a Západních Karpat“, 18-25. (in Czech)

GRYGAR R., VAVRO M., 1995: Evolution of Lugosilesian Orocline (North-eastern periphery of the Bohemian Massif): Kinematics of Variscan deformation. - J. Czech Geol. Soc., 40: 65-90.

KRÖNER A., ŠTÍPSKÁ P., SCHULMANN K., JAECKEL P., 2000: Chronological constraints on the pre-Variscan evolution of the northeastern margin of the Bohemian Massif, Czech Republic. In: Franke W., Haak V., Oncken O., Tanner D. (eds). Orogenetic Processes: Quantification and Modelling in the Variscan Belt. Geological Society. London. Special Publications, 179: 175-197.

MÜCKE A., LOSOS Z., 2000: Polymetamorfnì pøepracované, páskované a silicifikované magnetitové rudy v desenských rulách (silesikum, Èeská republika). - Acta Mus. Moraviae, Sci.geol., 85: 47-80. (in Czech)

POUBA Z. 1970: Pre-Cambrian banded magnetite ores of the Desná Dome. Sbor. geol. Vìd, Ø. L.G, 12: 7-64.